DEVELOPMENT AND PERFORMANCE EVALUATION OF A TRAY DRYER POWERED BY GENERATOR EXHAUST GAS WASTE HEAT

BY

ONONOGBO CHIBUIKE

REG. No: 20134877708

A THESIS SUBMITTED TO THE POSTGRADUATE SCHOOL

FEDERAL UNIVERSITY OF TECHNOLOGY, OWERRI

IN PARTIAL FULFILLMENT OF THE REQUIREMENTS FOR THE AWARD OF DOCTOR OF PHILOSOPHY (PH.D) IN ENERGY AND POWER ENGINEERING OF THE DEPARTMENT OF MECHANICAL ENGINEERING.

JANUARY, 2022

CERTIFICATION

This is to certify that this research work on "Development and Performance Evaluation of a Tray Dryer powered by Generator Exhaust Gas Waste Heat" carried out by **ONONOGBO CHIBUIKE (B.ENG, M.ENG)** with registration number, **20134877708,** is a thesis submitted to the Postgraduate School, Federal University of Technology, Owerri, in partial fulfilment for the award of Doctor of Philosophy in Energy and Power Engineering in the Department of Mechanical Engineering of the Federal University of Technology, Owerri.

Engr. Prof. E. E. Anyanwu (Principal Supervisor)	05/01/2022 Date
Engr. Dr. J. O. Igbokwe (Co- Supervisor)	05/01/2022 Date
Engr. Dr. C. A. Okoronkwo (Co- Supervisor)	05/01/22 Date
Engr. Dr. O. C. Nwufo (Co- Supervisor)	05/01/2022 Date
Engr. Dr. O.O. Obiukwu (HOD, MEE)	3/2/2022 Date
Engr. Prof. J. C. Ezeh (Dean, SEET)	07/02/2022 Date
Prof. C. C. Eze (Dean, Postgraduate School)	Date
External Examiner Engr. Prof. O. V. Ekechukwu	5 January, 2022 Date

DEDICATION

To the Virgin Mother of God, Mary most holy.

ACKNOWLEDGMENTS

I wish to use this page to express my sincere gratitude to Prof. E.E Anyanwu for his enormous contributions and unequalled support which in no small way helped for the achievement of success in the course of this research work. In a very special way, I convey my heartfelt appreciation to Engr. Dr. J. O. Igbokwe, Engr. Dr. C. A. Okoronkwo, Engr. Dr. O. C. Nwufo for their contributions to the success of this work. My gratitude also goes to Prof. J. C. Ezeh, Engr. Dr. Osueke G.O., Engr. Prof. Ogueke N. V., Engr. Dr. Nwakuba N. R. and Engr. Dr. Chukwuezi O. C., Engr. Dr. Godswill Nwaji and Engr. Adeyemo Oluwaseun for their wonderful encouragement. I also wish to thank the HOD, Engr. Dr. Obiukwu O. O. and the entire staff of the Department of Mechanical Engineering for all the support they rendered with a view to ensuring the successful conclusion of this work. I also in a very special way, extend my sincere gratitude to the Dean of Postgraduate School, Prof. C. C. Eze for the encouragement and support I received from him and the members of his staff. I wish to acknowledge the support I received from the Tertiary Education Trust Fund under the platform of Imo State Polytechnic, Umuagwo-Ohaji. I appreciate in a very special way, my beloved brother- Mr. Augustine Oguoma for his immense financial help and direction. My sincere gratitude also goes to my beloved wife, Mrs. Purity Ononogbo, and my beloved mother, Mrs. Eugenia Ononogbo for the overwhelming support they rendered to me during the period of this work. Finally, I wish to express my unalloyed appreciation to the former Rector of Imo State Polytechnic, Very Rev. Fr. Dr. Wenceslas Madu for his great assistance throughout the period within which these studies were carried out. I also thank Mr. Edebei Kenneth for his diligence during the construction of the test rig. I am also thankful to Mr. Colman C. Ibe for his encouragement during the period of this work. Finally, I wish to express my gratitude to Rev. Fr. Bede Nkamuke for his words of encouragement and prayers. I am indeed indebted to you all. May the holy name of the glorious Mother of God, Mary most holy be blessed and honored forever. Amen.

TABLE OF CONTENTS

LIST OF TABLES

LIST OF FIGURES

LIST OF PLATES

LIST OF APPENDICES

NOMENCLATURE

Symbols

A	=	Annulus area of turbine (m^2)
A_{he}	=	Area of heat exchanger (m^2)
A_{cf}	=	Area of drying chamber floor (m^2)
A_1	=	Area of heat exchanger (m^2)
A_2	=	Area of drying chamber (m^2)
A_w	=	Water activity
b	=	Blade height (m)
b^*	=	Empirical constant (s^{-1})
$\frac{b}{w}$	=	Blade height/width ratio
B_{hp}	=	Blower horsepower (Hp)
c	=	Absolute velocity of exhaust gas (m/s); Specific heat capacity of air (kJ/kgK)
c_a	=	Axial velocity of exhaust gas (m/s)
c_p	=	Specific heat of exhaust gas (kJ/kg°K)
c_c	=	Specific heat of corn above freezing point (kJ $kg^{-1}°C^{-1}$)
c_w	=	Whirl velocity (m/s)
ΔC_w	=	Change in the velocity of whirl (m/s)
D	=	Discharge or air flow rate ($m^3/secs$); Diffusivity (m^2/s) and airflow rate (cubic feet per minute)
D_o	=	Arrhenius constant (**t**) (m^2/s)
d_A	=	Average drying rate (g_{water}/min)
d_o	=	Outside diameter of heat exchanger (m)
D_b	=	Bulk density (kg/m^3)
D_e	=	Effective diffusivity ($m^2\ s^{-1}$)
d_R	=	Drying rate (g/min)
dt	=	Time interval (min)
d_T	=	Total drying time per batch (min)
d_s	=	Diameter of the turbine main shaft (m)
d_t	=	Drying time (min)
d_1	=	Diameter of the driver (m)
d_2	=	Diameter of the follower (m)
E_A	=	Activation energy (kJ/ mol)
EPC	=	Total electric power consumed (W-hr)
E_{th}	=	Thermal energy required (kW-hr)
g	=	Acceleration due to gravity (m/s^2)
gp_{sT}	=	Total static pressure (inches of water)
h	=	Heat transfer coefficient (W/m^2 °C); Enthalpies of the exhaust gas (kJ/kg)
h_o	=	Outside heat transfer coefficient ($W/m^2\,°C$)
H_{bs}	=	Bottom space (m)
H_c	=	Drying chamber height (m)
H_{hs}	=	Drying chamber head space (m)

h_{fg} = Latent heat of vaporisation of water (kJ/ kg)

h_i = Inside heat transfer coefficient ($W/m^2\ °C$)

H_t = Height of tray (m)

l = Dimensionless empirical constant

L_C = Length of drying chamber (m)

L_t = Length of tray (m)

k = Drying constant (s^{-1}) and thermal conductivity (W/mK)

k_m and k_t = shock and fatigue factors for bending and twisting

L = Latent heat of vaporization of water (kJ/kg); Half thickness of product (m)

L_{he} = of heat exchanger (m)

LMTD (θ_m) = Logarithmic mean temperature difference

L_{se} = Loss due to sudden enlargement ($m\ of\ water$)

M = Bending moment acting on the shaft (N mm); Moisture content (kg water/ kg solids) and Mach number

M_0 = Initial moisture content (kg water/ kg solids)

MC_{wb} = Moisture content (wet basis) in kg water/ kg solids

MC_{db} = Moisture content (dry basis) in kg water/ kg solids

M_d = Mass of dried grain (kg)

M_e = Equilibrium moisture content (kg water/ kg solids)

$MR_{pre,i}$ = ith predicted moisture ratio values

MR = Moisture ratio

M_f = Final moisture content (kg water/ kg solids)

$\dot{m}$ = Mass flow rate of the exhaust gas (kg/min)

$\dot{m}_g$ = Mass flow rate of exhaust gas (kg/s)

M_t = Moisture content at any time (kg water/ kg solids)

m_w = Mass of wet product (kg)

M_w = Mass of water to be removed from product sample (kg)

M_{t+dt} = Moisture content at $t + dt$ (kg water/ kg solids)

n = total number of constants in the drying model; Dimensionless empirical constant

N = Number of observations

N_b = Rotational speed of turbine wheel (rpm)

N_u = Nusselt number

N_1 = Speed of the driver (rpm)

N_2 = Speed of the follower (rpm)

P = Power transmitted and pressure (Watt); Loading density of sample (kg/ m^2)

P_{01} = Inlet pressure (kN/m^2)

$\frac{P_{01}}{P_{03}}$ = Pressure ratio

P_{hg} = Work done by the heat source per unit time (Watt)

P_{out} = Power output of turbine (kW)

p_{st} = Static pressure (inches of water)

P_r = Prandtle number

P_w = Partial pressure of water vapour (Nm^2)

P_{ws} = Equilibrium vapour pressure of water (Nm^2)

Q = Quantity of heat required for the removal of water from product (kJ)
Q_L = Total heal loss (Watt)
$\dot{Q}$ = Rate of heat transfer (kJ/min)
Q_r = Heat transfer rate (kW)
r = Radius of sample product (m)
R = Gas constant (J/mol K))
R_d = Degree of reaction
R_e = Reynolds number
RH = Relative humidity
r_m = Mean radius (m)
$RMSE$ = Root mean square error analysis
r_t/r_r = tip/root radius ratio
$r_1\ and\ r_2$ = Radii of the driving and driven pulleys (m)
R^2 = Coefficient of determination
s_b = Blade spacing (m)
S_a = Air space between trays and drying chamber walls (m)
S_t = Space between trays (m)
SEC = Specific energy consumption (kW-hr/kg)
SPC = Specific power consumption (W-hr/kg)
SSE = Sum of squares error
T = The torque transmitted by shaft (N/mm) and temperature in (K)
$\triangle T$ = The temperature difference (°K)
ΔT_{0s} = Temperature drop (K)
t_a = Inlet temperature of air into the heat exchanger (℃)
t_0 = the drying air temperature (℃)
T_{01} = Inlet temperature of exhaust gas to the stator (°C)
T_c = Centrifugal tension (N)
T_a = Assumed ambient temperature (°C)
t_b = Mean bulk temperature (℃)
T_e = Equivalent twisting moment (N mm)
T_g = Temperature of exhaust gas or of the drying product (°C)
T_{max} = Maximum (or total) tension in the belt (N)
t_s = Surface temperature of the heat exchanger tube (℃)
T_t = Tray thickness (m)
U = Overall heat transfer coefficient (W/m^2 ℃)
U_i = Linear velocity of air in the heat exchanger
U_m = Mean blade speed (m/s)
$\dot{V}$ = Exhaust gas flow (m^3/s)
v = Llinear velocity of belt (m/s)
V = Relative velocity (m/s)
v_a = Air speed (m/s)
V_t = Volume of tray (m^3)
W_C = Width of drying chamber (m)
W_t = Tray width (m)

W_T = Total vertical load acting on the pulley (N)

Greek Letters

α_i = Angle made by the absolute velocity with the axial direction (^{0})

β_i = Angle the relative velocity makes with the axial direction (^{0})

γ = Ratio of specific heats (c_p/c_v)

η_{th} = Thermal Efficiency of the drying process (%)

θ = Angle of lap (^{0})

μ_N = Nozzle loss coefficient

ξ_b = Blower efficiency (%)

ρ_a = Density of air (k/m^3)

σ_u = Ultimate tensile strength (MPa)

τ = Permissible shear stress ($\mathrm{N/mm^2}$)

$\emptyset$ = Flow coefficient

φ = Blade loading coefficient

ABSTRACT

Development and performance evaluation of a tray dryer powered by generator exhaust gas waste heat are presented. The test rig comprises a tray dryer, a turbine, a heat exchanger, an air blower, weight and temperature sensors and an Arduino driven control panel. The waste heat recovery equipment uses an axial flow turbine and a heat exchanger to extract the energy of the exhaust gas of a diesel engine generator for the purpose of drying. The system was assembled and subjected to no-load tests, and testing independently with indigenous variety of fresh maize grains of 1,500 g batch size, and yam slices of 2200g batch size. Samples of the white yam slices of different thicknesses (1.0, 1.5 and 2.0cm) were prepared for the study using blanching water of 80^0 C and 30 minutes soaking time. The maize grains and yam slices were dried from initial moisture contents of 35.6% and 69.5% (wet basis) to final moisture contents of 10% and 12% (wet basis), respectively. The studies focused on the impacts of the drying air temperature and velocity on the drying energy indices (specific energy consumption, specific power demand, and thermal energy), drying rate, thermal efficiency of the crop dryer, moisture diffusion coefficient, and activation energy of the studied samples. The tests were run at varying drying air temperatures (50, 55, and 60℃ for the maize grains, and 55, 65 and 75℃ for the yam slices); and air velocities of 1.0, 1.5, and 2.0m/s for both sample products. The results of the no-load tests revealed that the higher the speed of the inlet ambient air through the waste heat recovery equipment, the faster the rate of heating of the drying chamber. It was also noticed that the drying chamber, initially at 31℃, was heated to a maximum temperature of 116.1 ℃ after only a period of 39 mins. Furthermore, the results obtained for the drying of the crop samples showed that the drying parameters had noticeable influences on the moisture diffusion of both the maize and yam samples. The drying air temperature and velocity had a direct relationship with the diffusion coefficient and drying rate of the crop samples, but showed an inverse relationship with the drying time of the crops. The thermal efficiency increased as the drying air temperature increased; whereas its values decreased as the drying air velocity increased. The drying air temperature had an inverse effect on the values of the specific power consumption of the dryer at constant air velocity, whereas its values increased as the drying air velocity increased at constant air temperature. The results of the optimization of the drying process parameters using Surface Response Methodology showed that the optimum drying conditions were 60^0C and 1 m/s for the maize grains; and 75 ^{0}C, 1.0 m/s and 1.0 cm thickness for the yam slices. For testing with existing thin-layer drying models in the literature, the Aghbashlo model was observed to be the most suitable drying model for describing the thin-layer drying behavior of the maize grains and 1cm yam slices; whereas the Demir *et al* model was the most suitable for the 1.5cm and 2cm yam slices. With visual inspection of the dried samples after a period of six months storage, it was observed that the dried products did not experience any form of deterioration like any bacterial growth. Hence, it is concluded that the application of waste exhaust heat gases of diesel standby generators to the drying of food products, would be helpful in preserving a considerable amount of primary fuel, thus providing a viable means of cost saving and amelioration of environmental degradation. Prospects for commercial applications as well as recommendations for additional studies were stated.

Keywords: Waste heat recovery, thermal efficiency, drying, global warming, cost saving, activation energy, energy consumption.

CHAPTER ONE

INTRODUCTION

1.1 Background of the Study

There is high demand of fuel as a result of increases in population, urbanization and industrialization which have resulted to a rise in fuel costs. For this reason, efforts are being made to make energy use more efficient. Obviously, higher energy conversion translates to reduced cost of energy globally. One technique of improving energy efficiency is the use of waste heat recovery systems (Lee, Seo, Lee and Garud, 2020). Recently, huge efforts are directed to the reduction of the amount of energy that is wasted into the environment; and the ultimate aim is to help in the conservation of finite resources of fossil fuels, reduction of carbon footprint and climate change as well as the improvement of process economics (Jouhara *et al*., 2018; Nguyen, Lee, Garud and Lee, 2021).

To reduce dependence on fossil fuels in order to minimize the impact of fossil fuel-based pollutants on the environment, manufacturers should prioritize the use of renewable energy systems or the reduction of energy consumption by using waste heat recovery techniques (Woolley, Luo and Simeone, *et al*., 2018). According to Jouhara *et al*. (2018), waste heat recovery using available technologies can provide valuable energy sources and reduce the overall energy consumption. Waste heat is heat that is produced in a process as a result of fuel combustion or chemical reaction, and then discarded into the environment even though it could still be harnessed for some purposes that are useful and economic (Ali and Mohammad, 2015; Jouhara *et al*., 2018). Woolley *et al*. (2018) reported that up to one third of the global energy consumption is attributable to the industrial sector, with about fifty percent mainly wasted as heat. Thus, diminishing petroleum supplies and increasing fuel costs are causing governments and industries to look for ways to increase the power efficiency of engines (Jadhao and Thombare, 2013).

An internal combustion (IC) engine heat balance shows that the input energy is approximately split into three equal portions such as the energy put to useful work, energy lost to coolant and energy

lost to the environment with the exhaust gases. Hopefully, with the emerging discoveries on exhaust heat recovery to increase the efficiency of IC engines, world energy demand on the depleting fossil fuel reserves would be reduced and hence the impact of global warming (Saidur, 2012; Nadaf and Gangavati, 2014). It is widely believed that almost 70 % of the energy released from the fuel by an engine is lost, mostly in the form of heat. Pradip and Hole (2015) reported that approximately 25–30% of the energy generated by engines is dissipated in the form of energy loss through the exhaust gas. Waste heat produced from thermal combustion process in IC engines (which is lost to the environment through an exhaust pipe) could get as high as 30–40% (Hatazawa, Sugita, Ogawa and Seo, 2004; Stabler, 2002).

Basically, the direct dumping of exhaust gases into the surroundings, not only wastes energy but also contributes to the damage of the environment. However, several innovative cooling and exhaust heat recovery systems have been introduced to reduce cooling loss and regenerate the power by recovering the waste heat (Nadaf and Gangavati, 2014). In recent times, large efforts have been committed towards the recovery of waste thermal energy in vehicles and other waste heat generating industrial machines. It could be surmised from the foregoing that the energy released through the exhaust of IC engines is of the same magnitude as the mechanical power generated by the engine. Thus significant heat losses from combustion processes in IC engines such as large power generating sets are inevitable. Therefore, some facilities can be used to reduce these losses by either improving the equipment efficiency or by the installation of waste heat recovery technologies. The recovered energy could be used in preheating combustion air, space heating, electricity generation, etc.

Three essential components are required for waste heat recovery, namely: (i) a source of waste heat that is accessible (ii) a technique for its recovery, and (iii) an application for the recovered heat. The method required for the heat recovery partly depends on the temperature of the available waste heat and the economics involved. Generally, the higher the temperature of waste heat, the higher the quality which makes the heat recovery more cost effective. The temperatures of diesel exhaust gases immediately leaving the engine are as high as 450-600 ^{o}C; while their specific heats are in the range of 1.1-1.25 KJ/kg°K (Jadhao and Thombare, 2013). Table 1.1 shows the temperatures of waste

exhaust gases from some facilities whose processes are directly fired with range of temperatures at the medium level.

Table 1.1. Typical Waste Heat at Medium Temperature Range from Various Sources

Type of Device	Temperature, ^{o}C
Steam boiler exhausts	230-480
Gas turbine exhausts	370-540
Reciprocating engine exhausts	315-600
Reciprocating engine exhausts (turbo charged)	230- 370
Heat treating furnaces	425 - 650
Drying and baking ovens	230 - 600
Catalytic crackers	425 - 650
Annealing furnace cooling systems	425 - 650

(Bureau of Energy Efficiency, 2014)

Although technologies of energy recovery are available, there are still large potentials for their application, which according to Bergmeier (2003) have not yet been realized in industries. It has been reported that there are opportunities for waste heat recovery in the food industry (Feldman 1984). Food industry is the UK's fourth highest industrial energy user; and it accounts for about 26% of the EU's overall energy consumption (Carbon Trust, 2017). Most of the waste heat produced in the food industry is classified as low-medium temperature (Jouhara, 2018). It is noteworthy that there are numerous technologies used for waste heat recovery such as heat exchangers, thermoelectric devices, turbocompounds, etc. In this work, the source of waste heat energy to be accessed is the high temperature exhaust gas from a 250 kvA diesel generator. It involves recovery or conversion of energy of the exhaust gas to useful work. Captured and reused waste heat is an emission-free substitute for costly purchased fuels or electricity. By this recovery system, the impact of the pollutants to the environment is significantly reduced. The recovery technology to be employed is an axial flow turbine and a heat exchanger while the energy recovered is to be used for the drying of food products such as wet maize grains and yam slices.

Nigeria is blessed with a landmass of 98.3 million hectares with about 72% of it applicable to agricultural activities (Makanjuola, Abimbola and Anazodo, 1991). However, with this large expanse of land available, statistics still show a low growth rate of about 2.5 % annually in the area of food crops production (Aasa, Ajayi and Omotosho, 2012). According to Odigbo (1991), the poor growth is attributable to the poor level of food preservation in the country. However, efforts are being made with a view to achieving improvement in the production of agricultural products in a given number of ways such as drying. This encourages farmers to embark on large scale agricultural activities as long as ways of preserving their harvested crops are available. For instance, large amounts of maize grains perish yearly during post-harvest periods because of their relatively high moisture content, making them unsuitable for storage. The act of selling maize in its green form is oftentimes not economical to the farmer which causes him to hardly realize the cost of production of the maize from its sales. This is because at the period of harvest when maize is harvested green, it is usually readily available everywhere and experiences low demand and cost. Hence to reduce grain losses thereby increasing value and the profit margin of farmers, a grain dryer is necessary for the drying of wet grains. Many agricultural products require long drying times ranging from 5 minutes to 73 hours with optimum drying air temperatures requiring large quantity of energy that results in high overhead drying cost and high prices of dried food products (Tiwari, 2012; Antwi, 2007; Ehiem, Irtwange and Obetta, 2009). For most food products, it is best to use drying temperatures of 50°C to 55°C (Donald, 2012). This is because higher temperatures destroy nutrients contained in the food which causes the food to lose its dietary value. When higher temperatures are used, food cooks instead of drying which results in case hardening where the food dries on outside but moisture trapped inside allowing mould growth (Donald, 2012).

There are many types of dryers operated by different energy sources like solar energy, bioenergy, electrical energy, etc. Most of the energy sources involved in these operations have some associated setbacks in terms of their availability and costs. This makes the end products more expensive. There are more than 400 different dryers reported in the literature, among which the convective dryers are the most widely applied for agro-materials drying (Aghbashlo, Mobli, Rafiee and Madadlou, 2013).

Sun drying is the cheapest and oldest means of preserving food products, but the crop is often contaminated by dust, insect attack or infection by microbes and yet it is not always available. There are different artificial drying methods that are available to ensure continuous high quality food supply. The use of artificial means for products drying is such that the transfer of heat to the material to be dried may take place through convection, conduction, or radiation. The process of drying consumes a lot of energy due to the low energy efficiency of dryers as well as high latent heat of vaporization of water molecules (Syahrul, Hamdullahpur and Dincer, 2002; Beigi, 2016). Hence, the analysis of energy consumption is of paramount importance in drying processes in order to ensure that energy is effectively utilized and excessive products handling costs avoided.

In this work, a hot air tray dryer using exhust gas waste heat as energy source is considered for the drying of food crops. Tray dryers are widely used in agricultural products drying due to their capability to dry products irrespective of time and weather conditions (Katiyar and Sudhakar, 2013). Among all the drying techniques, the tray dryer is the most extensively used because of its simple and economic design (Katiyar and Sudhakar, 2013). The food product is spread out on trays at an acceptable thickness so that the product can be dried uniformly. Heating may be produced by hot air stream across the trays, conduction from heated trays, or radiation from heated surfaces. In a tray dryer, more products can be loaded as the trays are arranged at different levels. Tray dryers have the capability of drying products at high volume. The key to its successful operation is the uniform airflow distribution over the trays (Misha, Mat, Ruslan, Sopian and Salleh, 2013).

1.2 Statement of Problem

High demand of fuel and increased fuel costs are a direct impact of expansion in population, urbanization and industrialization. It is widely believed that energy conversions in most systems, particularly in thermal power plants barely attain 50% efficiency. About 30% of the total energy generated in an internal combustion engine is lost to the engine cooling system and another 30 to 40% is dumped into the environment through exhaust gases (Jadhao and Thombare, 2013). Therefore, there is great need to harness as much waste energy as possible from existing I.C engines

in order to preserve finite resources of fossil fuels and to combat climatic change globally. In food processing industries, reasonable amount of waste heat is dumped into the environment during production activities, which has a significant effect on both energy costs and the price of finished products. However, improved energy conversion and utilization in these plants will not only reduce the cost of energy utilization, but will also contribute immensely to the preservation of the environment from excessive pollution. One method of achieving this is by the use of a waste heat recovery dryer for the preservation of harvested agricultural products. Nigeria is considerably rich with regard to the landmass that is suitable for agricultural production, but the low rate of growth in the area of food production is attributable to the poor level of food preservation in the country due to high costs of energy utilization associated with drying processes (Odigboh, 1991; Syahrul *et al*., 2002; Aasa *et al*., 2012; Beigi, 2016). Consequently, many farmers are discouraged from going into large scale production of farm products, forcing many of them to live at the level of subsistence. However, to minimize losses of agricultural products after harvest and thereby increase value and the profit margin of the farmer, a dryer is necessary for the freshly harvested food crops. This will help the food materials to be adequately dried and stored to ensure availability and wholesomeness all year round. One way of achieving that is by the use of waste energy recovery technique. The concept in this work is geared towards recovery and utilization of the exhaust gas waste heat of a diesel electric generator engine for the drying of farm crops, instead of resorting to burning of fresh fuels to do the same work; thereby helping to save cost as well as reduce the quantity of pollutants released into the environment. It is believed that the application of the recovered waste energy (from the exhaust gas of a diesel electric generator) to drying of farm produce and processing of food products, would reduce the energy demand for the depleting fossil fuel reserves; help farmers to minimize the amount of agricultural product losses, improve the value and profit margin of both farmers and food processing industries, and hence the impact of global warming. There are many waste heat recovery technologies available, but there are still large potentials for their application which has not been realized industries. It is pertinent to note that the recovery of waste heat from exhaust gases exiting the tail pipe of heavy-duty electric generators has barely received any serious

attention by researchers. Yet, this enormous heat is directly released into the environment, even though it could still be extracted and applied meaningfully. In this work, the source of energy to be accessed is the high temperature exhaust gas from diesel electric generators. The process involves the capture of the energy of the exhaust gas and its application to useful work. Recovered waste heat is used as an emission-free substitute for expensive fossil fuels or use of electricity. By this recovery system, energy or fuel will be saved, and the impact of pollutants to the environment reduced.

1.3 Objectives of Study

The major objective of this work is the Development and Performance Evaluation of a Tray Dryer powered by Generator Exhaust Gas Waste Heat. The specific objectives are as follows:

i. Design of a tray dryer for food crops powered by generator exhaust gas waste heat
ii. Fabrication and assembly of a prototype of the hot air tray dryer
iii. Experimental investigation of the performances of the dryer in (ii) above
iv. Determination of the applicable drying model equations using the experimental data generated
v. Optimization of the drying process parameters using Surface Response Methodology

1.4 Justification of Study

In recent times, considerable efforts have been directed towards the reduction of the amount of energy that is wasted into the environment. And the ultimate aim of these efforts is to help in conserving the finite reserves of fossil fuels, to reduce the carbon footprint in order to mitigate the effects of global climate change, and to improve the process economics, even though it is seemingly a demanding task facing real thermodynamic barriers. Obviously, if some of the energy from the substantial amount of waste heat dumped into the environment from stationary diesel generators could be recaptured and reused, an appreciable quantity of primary fuel would be preserved, which is a viable means of achieving cost savings and remedying environmental degradation. In Nigeria, large amounts of food crops perish during postharvest periods (especially during rainy seasons) due to unavailability of or the high cost associated with the means of preserving agricultural products

such as the use of artificial drying equipment. This problem limits the activities and operations of a sizable number of farmers to a level of subsistence, which threatens food security. However, an inexpensive means of drying can encourage farmers to embark on large scale production such as the use of waste heat for crop drying. Furthermore, in food processing industries, huge quantities of thermal energy from power plants are discarded into the environment unutilized. This practice causes the energy required for food processing to be very high, thus impacting negatively on the prices of finished products. However, if a significant portion of this waste heat is recovered and reused by the system, the cost of energy for production will be lowered, which will in turn reduce the price of finished products. It is pertinent to note that the foregoing problem can be solved by the use of a waste heat recovery dryer using exhust gas waste heat as source of energy. It is hoped that this research work will certainly give rise to a viable means of cost saving in food crops processing and preservation; and will also serve as an antidote to excessive environmental pollution and degredation. However, the major beneficiaries of this work will be farmers and the drivers of food processing industries.

1.5 Scope of the Work

This work is focused on the development and performance evaluation of a tray dryer powered by generator exhaust gas waste heat. It involves the design and fabrication of the test rig waste heat recovery dryer with its ancillary components such as the heat exchanger and the axial flow turbine. The selection of the components of the test rig was actualized using some relevant governing laws and equations retrieved from standard literatures in textbooks and archival journals. Other components such as the solar panel and allied accessories as well as the air blower were sized and sourced from the market. The instruments such as the temperature, humidity, speed and weight-measuring devices were also sourced from various markets. The recovery technologies employed were an axial flow turbine and a heat exchanger while the energy recovered was used for drying agricultural crops. However, for much lower capacity generator engines such as 180 kVA, 150kVA generators, etc the use of the energy recovery turbines may not be feasible. This is because the low flow rates and pressures of their exhaust gases would not be sufficient to drive a turbine for the

production of the electricity needed to power the electrical components of the dryer. Therefore, when lower capacity generators are used, the turbine aspect of energy recovery should be eliminated and completely replaced by a solar panel for electricity generation. The study investigated the possibility of utilizing the waste heat from the exhaust gas of a diesel generator for the drying of some selected crops (maize grains and yam slices) using the proposed tray dryer.

CHAPTER TWO

LITERATURE REVIEW

2.1 Historical Background of Waste Heat Recovery

Energy recovery is considered an important method of achieving improvement in energy efficiency which is aimed at minimizing energy consumption and the emission of greenhouse gases (Minxing, 2011; Woolley *et al*.,2018). Historically, the origin and gradual development of waste energy recovery are traceable to the 19th century. However, applications and implementations of proven technologies of waste energy recovery are yet to be extensively achieved as a result of economic and political barriers (Bergmeier, 2003). The first move towards adapting a combustion engine to harness the energy released in the exhaust gas was recorded in the 1920s (Legros, Guillaume, Diny, Zaïdi and Lemort, 2014). At this time, the high price of coal compared to diesel, caused locomotive dealers to shift to the use of diesel engines whose exhaust lines were modified to use Rankine cycle engine for the purpose of waste heat recovery. The heat recovered was used to vaporize water to generate additional power to run the locomotive.

According to Toom (2007), the exhaust heat recovery system was able to produce between 15% to 30% of additional powerwhich was advantageous to the diesel engine, especially when the locomotive was starting and needed a high torque. Eventually, this development suffered a huge setback due to the sharp decline between the prices of diesel and coal. Hence, no economic advantage was derivable any longer in commercializing such a locomotive. Legros *et al*. (2014) reported that virtually no new thing in terms of waste heat recovery happened following this period until the oil crisis struck in the early 1970s which necessitated the implementation of the US Clean Air Act regulation. This motivated car manufacturers to research on ways that could help in reducing the fuel consumption of cars thus bringing the investigation of the Rankine cycle technology on the front burner. The first researches on the recovery of waste heat using Rankine cycles were conducted on trucks. Patel and Doyle (1976) reported the production of an additional 26 kW of mechanical

power at peak conditions where a mixture of water and trifluoroethanol in a three-stage axial turbine was mechanically coupled to the engine shaft. About this period, there were no records of literature showing works done on passenger cars (Legros *et al*., 2014). However, researches on passenger vehicles began with Oomori and Ogino (1993) where the cooling system of an engine was combined with a scroll expander to create a Rankine cycle using R123 as the working fluid and the fuel consumption of the car was reduced by 3%. Besides, it is pertinent to note that heat recovery from the high heat content exhaust gases exiting the tail pipe of diesel powered electric generators has barely received any meaningful attention by researchers. Yet, this enormous heat is directly dumped into the environment even though it could still be harnessed and transferred to a productive end-use. The reason behind the unavailability of research works done in this area could perhaps be due to the inability of researchers to identify any meaningful and beneficial application of the energy recoverable from these systems using available techniques.

2.2 Capture and Use of Waste Heat

Generated heat is used and dumped in virtually all industrial processes. Dumped waste heat can be recovered and used in other processes or applied to preheating of water and combustion air by way of process integration (Martin *et al*., 2000; Jouhara et al., 2018). Martin *et al*. (2000) also reported that energy savings (considered to be cost effective) of 5 to 40% through waste heat recovery were achieved through process integration analysis in nearly all industries. Devices such as pressure recovery turbines can be used to recover power for the purpose of electricity production. This is usually applied to blast furnaces of iron and steel industries. The turbines depressurize blast furnace gas from a top pressure furnace to produce electricity by the use of a generator. Cao, Tan and Zhang (2004) posited that the power output of the top gas pressure recovery turbine is capable of taking care of about 30% of electricity required for all equipment attached to the blast furnace. Other industrial production processes where energy recovery also finds application are in a fluid catalytic cracker, natural gas grids, etc, (Siddiqui, Marnay, Firestone and Zhou, 2007). However, in the case of a combined heat and power (cogeneration) system, both useful heat and electricity are produced. Cogeneration systems have some appealing and interesting features, apart from its capability of

producing heat and power. The attributes include increase in efficiency, waste reduction and reduction in the emission of unwanted substances into the environment. Cogeneration facilities utilize the waste heat emanating from power production for the purpose of district heating and other industrial applications. This improves the overall efficiency of the facility, thereby producing more useful energy per unit of the burnt fuel. In addition, the overall emission of greenhouse gases (GHG) and other harmful pollutants into the environment is reduced.

2.3. Technologies and Options of Waste Heat Recovery

There are a given number of methods of recovering waste energy; and these include the transfer of heat between fluids, production of mechanical power or electricity, the use of heat pumps which utilize waste heat to produce heating or cooling effects in some facilities, etc,. Many technologies of energy recovery are in existence, but still there are large potentials for their application, which have not yet been achieved in industries (Bergmeier, 2003). Useful technologies for waste heat recovery techniques are considered below.

2.3.1. Heat Exchangers

Woolley *et al*. (2018) noted that heat exchangers have been proposed as one of the best systems for recovering waste heat from available sources. Heat exchangers are heat transfer devices used for the transfer of heat from hot exhaust gases to air entering the furnace during a combustion process. It is noteworthy that significantly lower quantity of heat energy is required to be supplied by the fuel to the combustion air entering the furnace at a higher temperature which is previously preheated by the hot exhaust gases. Examples of technologies used for the preheating of air are: recuperators, regenerators and passive air preheating systems.

2.3.1.1. Recuperators

Recuperators are employed for recovery of waste heat from exhaust gases at medium to high temperatures. Their applications are found in areas such as after burners, radiant tube burners, melting furnaces, etc. (U.S. Department of Energy, 2008). Recuperators are broadly categorized into convection, radiation, or their combinations. A simple radiation type recuperator consists basically of two lengths of concentric ductwork. High temperature waste gases are made to pass through the

inner duct causing heat to be radiated to the wall as well as to the low temperature air entering the outer shell. The air that has been preheated in the shell is then routed to the furnace burners. The high temperature gases are channeled through very small diameter tubes placed in a bigger shell. The combustion air to be preheated enters the shell and is baffled around the hot gas tubes, causing heat to be picked up from the waste gas. An alternative aspect of recuperators which combines the benefits of both radiation type and convective recuperators has features that incorporate a part for radiation and that for convection so as to enhance the effectiveness of heat transfer. The material for the construction of recuperators is either metal or ceramics. In heat recovery applications where temperatures are below 1,093ºC, metallic recuperators are used, while for higher temperatures, ceramic recuperators are used. These are capable of operating with hot side temperatures as high as 1,538ºC and cold side temperatures of about 982ºC (Turner and Doty, 2006).

2.3.1.2. Regenerator

A regenerator is a heat exchanger which provides the means of intermittently storing the heat from a hot fluid in a thermal storage medium prior to its transfer to a cold fluid. A furnace regenerator is designed in such a way that hot and cold air alternately flow through two chambers that are made of bricks. The temperature of the bricks increases as they absorb the heat from the hot combustion gases passing through one of the chambers. The adjustment of air flow is then made so as to ensure that the incoming combustion air passes through the hot checker-work, thus causing the transfer of heat to the combustion air distributed to the furnace. This is achieved by the use of two chambers so that while one chamber absorbs heat from the hot exhaust gas, the other transfers heat to the combustion air. The direction of flow of air is altered periodically. The application of regenerators is predominant with glass furnaces and coke ovens. Regenerators were applied historically to steel open hearth furnaces before the replacement of the furnaces by more efficient designs. In iron making, regenerators are also used to preheat the hot blast provided to blast stoves, even though regenerators in blast stoves are not considered to be a heat recovery application, but rather a means of transferring the heat of the combustion gas to the hot blast air. Regenerative systems are used for

high temperature applications with dirty exhausts. However, the main disadvantage of regenerators is their large size which presupposes higher capital costs than recuperators (Turner and Doty, 2006). A rotary regenerator (Heat Wheel) uses a disc made of a high thermal capacity material which spins between the two ducts and causes heat transfer from the hot gas duct to the cold gas duct. Heat wheels are mainly suited or restricted to low and medium temperature applications as a result of the thermal stresses experienced in high temperature applications. Basically, high temperature gradients between the hot and cold ducts are capable of causing differential expansion and huge deformations, which compromise the integrity of the air seals of the duct wheel. However, in situations where high temperature applications are inevitable, ceramic wheels are used instead. Another problem with the use of heat wheels is that of averting cross contamination between the two gas streams, since the transport of contaminants in the wheel's porous material is possible (U.S. Department of Energy, 2008). Apart from the application of heat wheels to air conditioning processes and space heating, they are also viable, although to a limited degree in medium temperature applications, etc.

2.3.1.3. Passive Air Preheaters

A passive air preheater is a heat recovery device where heat is exchanged between two gases for low to medium temperature applications. The device does not entertain any form of cross-contamination between gas streams, thus finding application in steam boilers, gas turbine exhaust, ovens, etc. Passive air preheaters are categorized into– the plate-type and the heat pipe. The plate-type as seen in Figure 2.1 is made up of multiple plates that are parallel. The plates produce separate channels for both hot and cold gas streams. The flows of hot and cold fluids alternate between the plates and allow appreciable areas for heat transfer. The advantage which the device has over heat wheels is that of its less susceptibility to contamination. However, the device is more bulky, more expensive and more prone to fouling problems (U.S. Department of Energy, 2008).

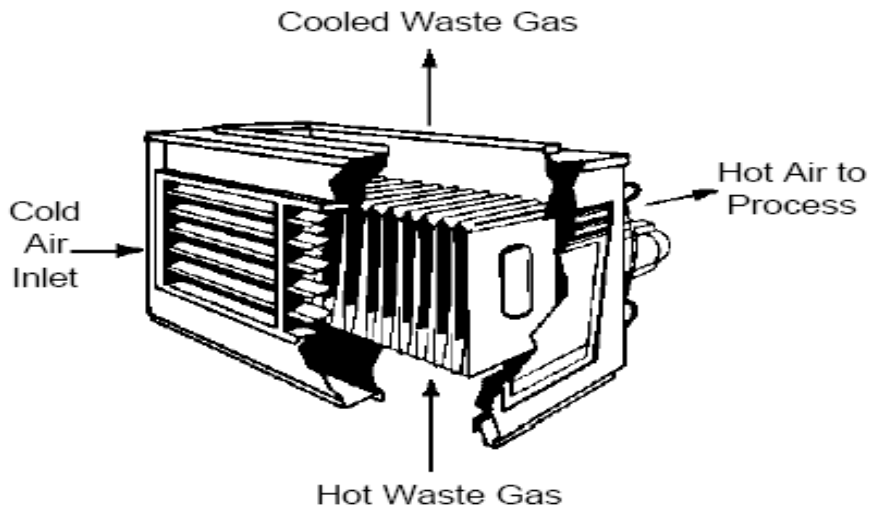

Figure 2.1. Passive Gas to Gas Air Preheater- plate-type
(Source: U.S. Department of Energy, 2008).

2.3.1.4. Regenerative/Recuperative Burners

Interestingly, some burners have been designed to integrate regenerative or recuperative systems. These systems are simpler and more compact in terms of design and construction when compared to a standalone regenerative furnaces or recuperators. They generate higher energy efficiency in comparison to burners operating with ambient air. A self-recuperative burner incorporates heat exchange surfaces as part of the design for the body of the burner so as to extract energy from the exiting flue gas, which passes back through the body. Burners that are self-regenerative allow the passage of exhaust gases through the body of the burner into a refractory media case, operating in pairs in a way that is the same as a regenerative furnace. Recuperative burners are mostly associated with lower area of heat exchange compared to regenerative burners, which have less mass than standalone units do. Therefore, their capacity in energy recovery is lower, but they have an advantage of lower costs and better adaptability to modification, thus making them a viable option for waste heat recovery.

2.3.1.5. Economizers, Waste Heat Boilers and Heat Pumps

A finned tube heat exchangers or economizer is another heat exchange device used for low to medium temperature applications. It is made of a circular tube lined with fins so as to increase the surface area for enhanced rate of heat transfer. A finned tube heat exchanger recovers heat from

exhaust gases and uses it to heat liquids in applications such as hot process liquid, home hot water, hot water for process heat, etc. The hot gases flowing across the tubes heat up the liquid flowing through the tubes (U.S. Department of Energy, 2008). A waste heat boiler is a two-pass boiler (a water tube boiler) that is employed in medium to high temperature applications. Waste heat boilers make use of the temperature of exhaust gases to raise steam. However, in situations where the available waste energy is insufficient for generating the desired steam output, provision of auxiliary burners is made to achieve the desired goal (Bureau of Energy Efficiency, 2014). The raised steam may be used for the generation of power or for process heating.

In most waste heat applications, heat is continuously transferred from a high temperature fluid to a cold fluid. As the heat is repeatedly transferred, its viability reduces and over time becomes unfit for the performance of any meaningful function. For waste heat recovery in industrial applications, there is a general rule of thumb that considers fluids with temperatures below 120^{o}C as limit for waste heat recovery due to the risk of condensation of corrosive liquids (Bureau of Energy Efficiency, 2014). However, the continuous rise in the price of fuels has necessitated the consideration of the use of such low temperature waste heat for space heating and other low temperature applications. Heat pumps are used to change the direction of heat flow and mostly operate on the principle of the vapour compression cycle (VCC). In VCC, the circulating fluid is physically separated from the source (waste heat) and user (heat to be used in the process) streams, and is re-used in a cyclical way. Heat pump as shown in Figure 2.2 is used for space heating where low temperature energy from the ambient air, water, etc is increased to heating system temperatures by doing work on the fluid using a compressor.

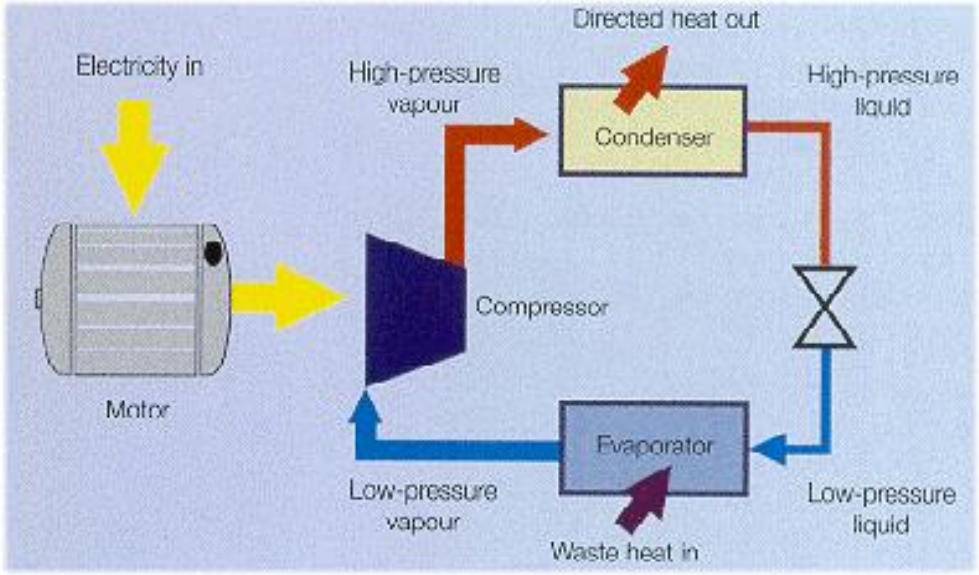

Figure 2.2. Heat pump (Source: Bureau of Energy Efficiency, 2014).

Heat pumps are capable of upgrading the quality of heat to a value that is more than twice the energy consumed by the device. According to the Bureau of Energy Efficiency, (2014), potentials in respect of the application of heat pumps, especially in industries are increasing considerably as they recover low grade waste heat and upgrade it for process steam purposes. Heat pumps also find application in cases where both heating and cooling are required at the same time. A typical example of this is found in plastics factory where cold water emanating from a heat pump is used for cooling injection-moulding machines while the output heat of the heat pump is used for office heating. Heat pumps are also applied to products drying, compressed air drying, and to the maintenance of dry atmosphere for storage.

2.3.2. The Rankine Cycle

The Rankine cycle as invented by William Rankine in 1859, is a model of an ideal steam-power cycle. The cycle makes use of a heat source to vaporize a working fluid under high pressure and then allows the fluid to expand in turbine. The power generated by the turbine is used to drive a generator for the production of electricity (Turner and Doty, 2006). Rankine cycles that make use of steam as a working fluid are employed in the majority of modern power plants. A Rankine cycle that uses waste heat for its operation recovers waste heat generated in some primary process such as from facilities that make use of combustion of fuel. The power produced may be used to augment

the propulsion system of vehicles or to generate electricity to operate the electrical components of the vehicle (Gunnar, 2013).

2.3.2.1. The Kalina cycle

The Kalina cycle in principle, is a modified Rankine cycle. It is also referred to as a reversed absorption cycle (Valdimarsson, 2003). One of the differences between it and the Rankine cycle is that it makes use of a mixture as the working fluid, rather than a pure fluid like water. The mixture consists of two or more different components, usually water and ammonia (Chen, 2011). The disadvantages of a Kalina cycle are:

(i) It requires a high vapour fraction in the boiler which results in lower overall heat transfer coefficients and a larger area for heat exchange.

(ii) It is susceptible to corrosion. Carbon dioxide or air are impurities in liquid ammonia, and are capable of causing stress corrosion cracking of mild steel. In addition, ammonia is also a highly corrosive substance towards copper and zinc (Chen, 2011).

Many designs of the Kalina cycle have similarities with the Rankine cycle. Each of the designs has a specific application for different heat sources as seen in combined cycles of gas turbine or low temperature geothermal plants (Mlcak, 1996). The references of Kalina cycles are listed by (Valdimarsson, 2003) as seen in the following plants:

- Demonstration plant of 3 – 6 MW- Canoga Park, USA
- Incineration plant, 4.5 MW- Fukuoka, Japan
- Waste heat recovery from a steel plant of 3.1 MW- Sumitomo, Japan
- Geothermal plant of 2.0 MW - Husavik, Iceland Valdimarsson (2003) reported that the net electrical efficiency for the Husavik plant was11 %; and also gave a budget of USD 720,000 for the 500 kW Kalina unit, which is equivalent to 1440 USD/kW.

2.3.2.2. Goswami Cycle

Goswami cycle is a new thermodynamic cycle suggested by Yogi Goswami in 1998. The cycle makes use of a binary mixture to cause a simultaneous production of power and refrigeration just in one loop. The cycle integrates a Rankine power cycle with an absorption cooling cycle. The

advantages of the cycle are as follows (i) Simultaneous production of power and cooling effect in the same cycle during operation (ii) Flexibility of design in the production of any combination of power and refrigeration (iii) Efficient conversion of low grade temperature waste heat, and (iv) Possibility of improved resource utilization in comparison to separate power and cooling systems (Vijayaraghavan and Goswami, 2006).

This thermodynamic cycle is still at the stage of research. The test rig for its experimentation was built in the University of Florida in the late 90's.

2.3.2.3. Organic Rankine Cycle

Most conventional techniques for heat recovery are inefficient for the conversion of the low-grade temperature waste heat (from exhaust gases) to electrical energy. However, the Organic Rankine Cycle (ORC) is a device that has proven to be viable for low-grade temperature waste heat applications. For thermodynamic cycles used for the conversion of low-grade heat to power, the ORC is the one that is most commercially developed for both small and large scale power plants (Chen, 2011). The ORC employs the principle of the steam Rankine cycle, but makes use of organic working fluids that have low boiling points in place of steam, in order to extract heat energy from a lower temperature heat source. The ORC is composed of a pump, a turbine for expansion, a boiler, and a condenser. However, the provision of a superheater is made where superheat is needed. The cycle has been extensively studied and compared for some years now; and according to Saidur *et al*. (2012), interests in Rankine bottoming cycles motivated some automotive manufacturing industries to carry out the investigation of its potentials for waste heat recovery. Many researchers have demonstrated how ORC has been used to achieve more than 10% reduction in fuel consumption for passenger cars and commercial trucks. Gambarotta (2010) researched on the operational performance of a stationary IC engine using ORC as a working fluid and recorded a 12% improvement in its efficiency. Mojtaba (2013) researched on two different configurations of the ORC capable of recovering waste heat simultaneously from exhaust gas and coolant of a 12L diesel engine. And the aim was to optimize the process for the improvement of power production and heat utilization factor of the cycle.

2.3.2.4. Trilateral Flash Cycle

Another important thermodynamic cycle using a mixture of ammonia and water as a working fluid is the Trilateral Flash Cycle (TFC). Its expansion process commences from the liquid at the saturated state instead of the vapor phase. The transfer of heat from a source of waste heat to the working fluid (liquid) is done using temperature matching that is near perfect as a result of the avoidance of the boiling part. The mixture of ammonia and water gives a better match with the heat sink- temperature profiles. For TFCs, the potential for the recovery of heat depends so much on the two-phase expansion process efficiency (Chen, 2011; Zamfirescu and Dincer, 2008). However, the major drawback as a result of which TFCs are not yet a success is the fact that appropriate two-phase expanders with high adiabatic efficiencies are not available. Extensive studies were carried out in the 1970s; and adiabatic efficiencies within the neighborhood of 50% were recorded for Lysholm type twin screw expanders (Chen, 2011). However, studies have shown the possibility of design and construction of twin screw expanders with predicted adiabatic efficiencies that are over 80%. The evaluation of some screw machines under test revealed adiabatic efficiencies that are over 70% for two-phase fluid expansion. According to Chen (2011), no TFC power plants are yet in operations. The demonstrations that have been carried out so far are pilot-oriented.

2.3.2.5. Supercritical CO2 Rankine cycle

Another power cycle that exhibits relatively high potential for the recovery of low-grade waste heat is the supercritical CO_2 Rankine cycle (Wang and Wu, 2006). This power cycle makes use of CO_2 (R-744) as a working fluid. Yamaguchi *et al*. (2006) reported that CO_2 has the advantages of being cheap, non-toxic, non-explosive and nonflammable. According to Wang and Wu (2006), another advantage of CO_2 is its critical pressure and temperature of 73.8 bar and 31.1ºC, respectively. Working fluids that are associated with low critical pressure and temperature are capable of being directly compressed to their supercritical pressures, and can also be heated to their supercritical temperature state preceding expansion. According to Chen (2011), the process of heating this cycle does not pass through a distinct two-phase region as is seen in a conventional steam Rankine cycle,

hence realizing a better thermal match in the boiler with less irreversibility. A supercritical CO_2 Rankine cycle was proposed by Yamaguchi, Zhang, Fujima, Enomoto, and Sawada (2006) for the production of electricity using solar energy. The device brings about the conversion of CO_2 into a high temperature supercritical state using evacuated solar collectors.

2.3.2.6. Absorption Refrigeration System

The recovery of heat from automotive engines has been applied majorly to turbo-charging or for the heating of the cabin with the absorption chillers application. Experimental investigations on the system have proved the feasibility of the concept regarding its capability of enhancing appreciably the performance of the system depending on part-load of the engine. According to Hugues and Talom (2009), the method could be employed for air conditioning and refrigeration of transportation vehicles. An experimental investigation on the adsorption air-conditioning unit incorporated in an IC engine for the cooling of the driver cabin in a locomotive has been conducted. The system makes use of zeolite-water as working pairs and is powered by the exhaust gas waste heat of an IC engine. Then the provision of refrigeration can be continuously made to the locomotive driver cabin for space cooling rather than the use of an electric vapor compression air-conditioning system. The single absorber with regenerator locomotive driver cabin air-conditioning system based on experiments conducted exhibits structural simplicity as well as operational reliability; and is convenient to control (Jiangzhou *et al*., 2003). The unit of absorption refrigeration connected to a Caterpillar diesel engine has found applications in cooling the charge air before ingestion to the engine cylinder as well as in air conditioning processes. Available results show that a diesel absorption combined cycle with pre-inter cooling feature will have a higher power output and a thermal efficiency than the other configurations. However, Talbi and Agnew (2002) reports that the overall efficiency of a pre-inter cooled cycle is lower than that of the inter-cooler.

2.3.3. Direct Electrical Conversion Devices

Traditional power plants convert the heat energy supplied to them into mechanical energy which may be used to produce electrical energy. However, new technologies such as thermoelectric, thermionic, and piezoelectric devices are developed which involve the direct generation of

electricity from heat. There has not been any evidence that these devices have been tested using industrial waste heat recovery applications, although a few have undergone some prototype testing in applications involving heat recovery in automotive vehicles (U.S. Department of Energy, 2008).

2.3.3.1. Thermoelectric Generator

A thermoelectric generator (TEG) relies on the Seebeck effect, which was named after Thomas Johann Seebeck who discovered it in 1823. This effect refers to the electrical potential generated when a temperature gradient is applied across the junctions of two dissimilar conductors (Rowe, 1996). Thermoelectric devices for power generation usually make use of p- and n-type semiconductor elements as the dissimilar conductors because it increases the potential output of the device (Stobart, Wijewardane and Allen, 2010). Figure 2.3 shows how thermoelectric materials are used to generate electricity.

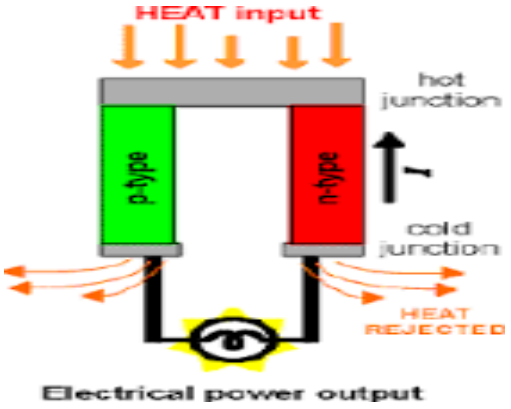

Figure 2.3. Schematic of a thermoelectric generator.

Thermoelectric generators are the most convenient and promising technologies that convert waste heat into electrical energy, as they do so without degrading the environment nor generating noise (Jin, 2014; Ma, Fang and Zhang, 2017). But they are associated with low conversion efficiency which has posed to be a challenge in their globalization (Patil, Seo and Lee, 2018). A thermoelectric device which generated about 58 W at peak conditions using FeSi2 elements was developed in the late 80s by Birkholz *et al*. (1988). However, subsequent studies were conducted on thermoelectric generators for passenger car applications. And in the 90s, the results of researches carried out showed improvements in the level of power produced as a record of up to 200 W was achieved in passenger cars or about 1 kW for a small truck application (Mori, Yamagami, Oda and Hattori,

2009). In heat recovery systems for combustion engines, the temperature difference applied across the junction of the device comes from the difference between the temperature of the hot exhaust gas and that of a cooling fluid. The factor, ZT (figure of merit), which is a dimensionless term is a characteristic constant for the two conducting materials used in the TEG. Together with the heat source and sink temperature, it is one of the major determinants of the performance of thermoelectric materials (Rowe, 1996). Thermoelectric devices rely on the ZT for electrical performance. According to Hussain (2009), modern commercial TEGs are incapable of realizing ZT factors of more than 1, giving a maximum realistic efficiency of around 5 % for the conversion of exhaust gas waste heat in automotive applications. Gunnar (2013) shows that an investigation carried out by the Ford Motor Company in 2009 examined the potential of thermoelectric heat recovery systems in gas-electric hybrid vehicles. It was found that 2.4 % of the waste energy in the exhaust gas could be recovered for a city cycle. And the value increased to 5.7 % for the highway cycle, as a result of the higher loads and exhaust gas temperatures that occur under these driving conditions. Baker and Shi (2012) reported that a study conducted in 2009 by Honda revealed that the use of a system in a 2.0 l gasoline engine would reduce overall fuel consumption by less than 1 %, while Stobart *et al*. (2010) made a prediction yearly fuel-saving potentials of 3.9 % to 4.7 % for a passenger car and up to 7.4 % for a transit bus.

2.3.3.2. Piezoelectric Power Generation

Piezoelectric Power Generation (PEPG) is an option that involves the conversion of low temperature waste heat (100-150°C) to electrical energy (BCS, 2006). Piezoelectric devices convert mechanical energy in the form of ambient vibrations into electrical energy. A piezoelectric thin film membrane takes advantage of oscillatory gas expansion to create a voltage output. However, there are technical challenges associated with Piezoelectric Power Generation technologies such as low efficiency of only about 1%; high internal impedance, complex oscillatory fluid dynamics within the liquid/vapor chamber, need for long term reliability and durability, and high costs. Although the conversion efficiency of piezoelectric technology is presently very low (1%), it is hoped that there may still be

opportunities to use a cascading of PEPG, wherein efficiencies could be improved to about 10%. Other drawbacks are the costs of manufacturing piezoelectric devices, as well as the design of heat exchangers to facilitate enough heat transfer rates across a very low temperature difference (BCS, 2006).

2.3.3.3. Thermionic Generation

A thermionic device functions in a similar way as the thermoelectric device but using thermionic emission for its operation. In the device, a temperature gradient initiates the flow of electrons through a vacuum from a metal to a metal oxide surface. A drawback in the use of these devices is the fact that they are limited to applications with high temperatures above 1,000°C. However, some studies have enabled their use at about 100-300°C (U.S. Department of Energy, 2008).

2.3.3.4. Thermo Photo Voltaic Generators

Thermo Photo Voltaic (TPV) Generators are used to convert radiant energy into electricity. The device consists of a heat source, an emitter, a radiation filter, and a PV cell similar to ones used in solar panels. The act of heating of the emitter causes the emission of electromagnetic radiation which the PV cell converts into electrical energy. The filter does the job of passing radiation at wavelengths that match the PV cell, while reflecting remaining energy back to the emitter. These systems have the potential of enabling new methods for waste heat recovery. However, a small number of prototypes of this technology have been built for small burner applications and in a helicopter gas turbine.

2.3.4. Turbocompounds

The turbocompound is a device that is used to recover energy from the exhaust gas by using an additional turbine in the exhaust system. The device is located downstream of the turbocharger turbine. The expansion of the exhaust gas in the turbine reduces the enthalpy of the exhaust gas. When multiplied by the turbine's efficiency, this enthalpy decrease represents the maximum work that can be obtained from the device. The difference between the device and turbochargers is that in turbochargers, the energy recovered is used to power a compressor; while the output energy of turbocompounds is used directly to augment the propulsion of the vehicle. However, in some cases,

the output of the device is used to drive a generator that produces electricity for the vehicle. Hence, there are two types of turbocompounds, viz: mechanical and electrical.

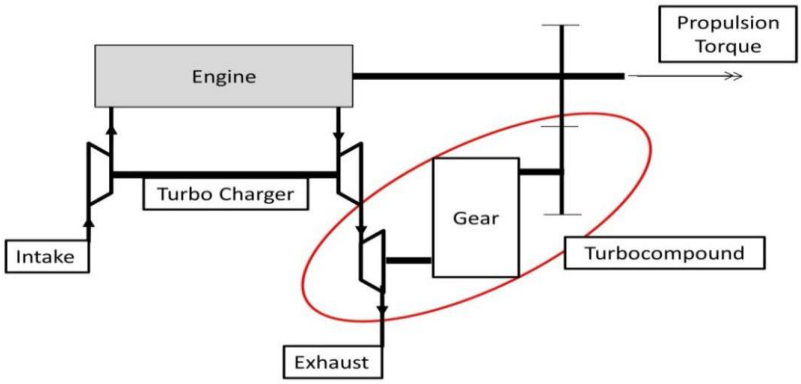

Figure 2.4: Configuration of a mechanical turbocompound system in a combustion engine (Source: Gunnar, 2013).

Figure 2.4 shows one possible configuration for a combustion engine with a mechanical turbocompound. In turbocompounds for the generation of mechanical energy, the reduction of the output speed of the turbine is achieved by the use of gears in order for the speed to match with the engine's crankshaft speed. Also, a fluid coupling is employed ultimately for the separation of the compound turbine from crankshaft's torsional vibrations in order to preserve the turbine and the high-speed gear set from being damaged (Ismail, Durrieu, Menegazzi, Chesse and Chalet, 2012). However, the fact that an electrical turbocompound is not connected to the vehicle's propulsion system is a huge advantage as their speed can be controlled independently of the engine's speed, thus avoiding the danger of having to operate the turbine inefficiently under off-design conditions (Greszler, 2008). Turbocompounds find application mostly in aircraft and heavy duty engines, where they have caused the reduction of fuel consumption by 3 to 5 %, even though the reduction was achieved under varying operating conditions. For low engine loads, turbocompounds may even have a negative impact as they can cause a slight increase in fuel consumption. This happens due to the increase in the exhaust backpressure caused by the turbine, which results in increased pumping losses during gas exchange in the combustion engine. However, it is interesting to note that the increased exhaust back pressure helps to improve the rate of Exhaust Gas Recirculation (EGR) for a short route EGR system. This is because the pressure gradient between the intake and the exhaust manifold increases.

2.3.5. The Availability of Waste Heat from IC Engines

The quantity of waste heat in an exhaust gas depends largely on its temperature and mass flow rate and, is expressed as seen in Eqn 2.1 (Jadhao and Thombare, 2013):

$$\dot{Q} = \dot{m} \times c_p \times \triangle T \qquad (2.1)$$

where, $\dot{Q}$ is the rate of heat loss (kJ/min); $\dot{m}$ is the mass flow rate of the exhaust gas (kg/min); c_p is the specific heat of exhaust gas (kJ/kg°K); and $\triangle T$ is the temperature difference in °K. For heat transfer and recovery to take place, it is necessary that the temperature of waste heat source is higher than the temperature of heat sink. Moreover, the magnitude of the temperature difference between the heat source and sink is an essential determinant of the quality of waste heat. The rate of heat transfer per unit surface area of the recovery system is influenced by the temperature gradient between the source and sink used (Heywood, 2011). In addition, the temperature range plays an important role in the type of waste heat recovery technology to be selected (Patel and Doyle, 1976). Table 2.1 shows a survey of exhaust temperatures from various internal combustion engines of vehicles and stationary engines.

Table 2.1. Temperature Range for Diesel Engines

S/ N	Engine	Temperature (^{0}C)
1	Single Cylinder Four Stroke Diesel Engine	456
2	Four Cylinder Four Stroke Diesel Engine (Tata Indica)	448
3	Six Cylinder Four Stroke Diesel Engine (TATA Truck)	336
4	Four Cylinder Four Stroke Diesel Engine (Mahindra arjun 605 DI)	310
5	Genset (Kirloskar) at power 198hp	383
6	Genset (Cummims) at power 200hp	396

(Source: Jadhao and Thombare, 2013).

2.4. Historical Development of Drying Processes

The drying of food products began in those ages when man first realized the need to preserve his food materials from decay by ensuring the removal of the required amount of moisture from the items. Early men relied so much on solar energy for the drying of their food items. However, as the practice of drying with the sun became commonplace, overtime, its limitations such as insufficiency of solar heating, especially during the rainy season necessitated the use of alternative sources of heat

for drying. Thus drying with solid fuels such as wood or coal as a source of heat was developed. About 3500 BC, the American Indians produced dry mashed potatoes; and fruits were dried in Mesopotamian about 1700 B.C as recorded in their tablets (Singham and Birwal, 2012). In the year 1780 AD, the very first patent recorded on vegetable drying was won in America. The vegetables previously boiled in salt water were kept for about 30 hours; while in France during the middle of the 1790s, the drying of sliced vegetables was achieved using air at 40°C, and the dried product was pressed and packaged in foils (Singham and Birwal, 2012; Sablani, 2006). Due to technological revolution during and after the First World War, appreciable improvements have been recorded in the area of drying; hence the space programme from 1950 to 1990 helped to bring technologies that have become widely accepted in our food industries (Adzimah and Seckley, 2009; Henry, 1997). Thus techniques in manufacturing have to a large extent enhanced the rates of production as the problem of bottle-necks due to long drying times formerly experienced in production lines as a result of the use of old drying methods have been drastically reduced. Archaic drying methods such as hot rooms under natural conditions, hot hearths, etc involving prolonged drying periods, and which were operated with little or no control have been completely phased out. Advancements in drying from the old methods to what is seen in present day drying practices were been gradually achieved through concerted research efforts (Carl, 1967). And continuous moves are still being made to develop dryers for better-quality dried products (Sablani, 2006). The process of drying could be expedited and at the same time improved using some mechanical techniques. For instance, the Arabs observed very early the possibility of preserving apricots for a very long time by first of all softening them, and thereafter boiling and drying them on broad sheets. Basically, the desire to have new categories of food products as well as interests in developing better performing drying equipment are the major reasons for unending research efforts. The drying of agricultural materials in order to improve their shelf life using artificial drying has expanded tremendously. This has necessitated the requirement for more rapid and economical drying techniques that will help minimize the amount of energy used in drying processes. Thus, various innovative techniques have been put in place to improve both the rates of drying and the quality of dried products.

2.5. Methods used for the Drying of Foodstuff

The methods used for the drying of foodstuff may be classified as follows:

(i) Direct contact drying with a heated surface. In this method, heat supplied to the product is mainly by conduction heat transfer.

(ii) Freeze drying: This method involves the freezing of the moisture in the food, followed by its sublimation to vapour usually achieved by heating under considerably low conditions of pressure.

(iii) Convective hot air drying: The food material to be dried is kept in contact with the heated air; and heat is transferred to the product usually by convection.

(iv) Drying using energy from microwaves or electricity, which is achieved especially by radiation source.

2.6. Drying Techniques

Even though drying improves the shelf life of food materials, it however reduces their quality and nutritional value. Hence it is necessary to minimize such detrimental effect by designing and developing dryers that will allow for sufficient drying rates as well as quality maintenance. The major techniques employed in drying are as presented below.

2.6.1. Solar Drying

According to Van Arsdel and Copley (1963), the use of artificial drying in place of sun drying became pronounced towards the end of the 1800s. The first and second world wars initiated improvements on dehydration processes for commercial operation. An improved form of sun drying using a mechanical means which was employed in the drying of vegetables was first recorded in the 18^{th} century (Van Arsdel and Copley, 1963). The solar dryer is an efficiently controlled dryer using solar energy in its operation; and has the capability of delivering higher air temperatures and lower relative humidity (Singham and Birwal, 2012).

2.6.2. Tray Dryers

Tray dryers find extensive application in the drying of agricultural products due to their simple and economic design, as well as their capability of drying items irrespective of weather conditions and time (Katiyar and Sudhakar, 2013). The item to be dried is outspread on the trays at a suitable thickness so as to ensure evenness of drying of the product. The application of heat to the drying product may be achieved in three ways, namely: by a stream of hot air moving across the trays, by heated trays through conduction, or from heated surfaces through radiation. Tray dryers accommodate the loading of more products because of the arrangement of the trays at different levels. They are the most widely used dryers in the small scale industries for the drying grains. Tray dryers are used for the drying of a wide variety of grains and are affordable in terms of purchase and maintenance in comparison to other techniques of drying. They mostly work on batch drying principles where a given amount of grain undergoes drying at a time. The amount of grain to be dried to the required moisture is determined by the dryer's holding capacity. However, drying of the next batch of grains can then be carried out as soon as the dried grains are unloaded. Thus loading and unloading time is considered in batch drying unlike in continuous drying where the drying product flows steadily without stop through the dryer. Tray dryers consist of trays fixed along the height of a drying chamber that is linked to a stream of hot air emanating from a heating source such as heating elements, gas, biomass, etc. The temperature of the hot air is usually regulated in order to maintain the optimum temperature range suitable for the food item to be dried. During operation they enable even distribution of airflow across the trays; and this has made them to be highly viable in the drying of agricultural products (Misha *et al*., 2013). This helps to improve the uniformity of drying products, and hence the efficiency of the dryer.

2.6.3. Cabinet Dryers

Cabinet dryers are highly simplified solar drying systems which exhibit very low holding capacity and are majorly used for the drying of vegetables and fruits (Mujumdar, 2004). Basically, between the 1870s and 1890s, the first steam heated radiator was invented in New York and was applied

extensively for drying various fruits such as grapes, dates, apples, etc and vegetables such as onion and cabbage. However, the drying equipment was inexpensive, but its operating cost such as labour was high.

2.6.4. Tunnel Dryers

The invention of tunnel dryers ushered in enormous changes and advantages into the food industry (Earle, 1992). They are seen as improvements of the tray dryer in which the trays are made to be mobile. The trays resting on trolleys move through an insulated tunnel where the application of heat and the removal of moisture take place (Brennan, 2006). It operates on the principles of continuous drying. The product to be dried is loaded from one end of the tunnel and unloaded from the other end. *It was introduced as a heated forced air dryer and a substitute for sun drying of prunes (Ratti and Crapiste, 1992).*

2.6.5. Drum Dryers

Drum drying was proposed during the beginning of the 1900s. In 1902, Hatmaker Just developed the first drum drying equipment starting with the double drum dryer type with material flowing into the nip. However, the fact that it was not quite suitable for viscous fluids led to the development of single drum with top feed to handle viscous products in 1945 (Singham and Birwal, 2012). The application of feed in single drum dryers was dipping, splashing, spraying and bottom feed roll. Feeding method is usually based on the viscosity of the feed. The particle size, bulk density, moisture content, and solubility of drum-dried foods are influenced by the following factors: drying temperature, feed rate, rotation speed, feed concentration, and surrounding air condition (Pua *et al*.,2010).

2.6.6. Spray Drying Technique

Spray drying methods developed from the 1870s through the earliest part of the twentieth century. According to Cal and Solohub (2009), the application of this drying technique was first introduced in 1860, and was patented in 1872 by Percy for the improvement it brought in drying processes as it caused the concentration of liquid substances by atomization. The centrifugal spray drier was proposed by George Krauss in 1912, while the conical spray drier was introduced in 1913 by Grey

and Jensen (Singham and Birwal, 2012). In the early 1950s the production of powder of fruits and vegetables was handled using spray drying techniques; and in the late 1950s, the food industry had commenced the use of spray drying encapsulation. In 1970, Kraftco Corp Company began its use for tomato juice dehydration, and spray dried tomato products were produced (Singham and Birwal, 2012). According to Mujumdar (2004), the first known spray dryers made use of nozzle atomizers, while the introduction of rotary atomizers was achieved some decades later.

2.6.7. Fluidized Bed Dryers

Fluidized Bed Dryer was developed after the 1960s to solve the problem of migration of soluble substances associated with belt trough dyers. It makes use of hot air below the bed to lift the material and then sends it outside. This dryer is widely applied for the dehydration of moist particulate, pastes, slurries, suspensions and granular materials that are easily fluidized in beds of inert solids (Singham and Birwal, 2012; Law and Mujumdar, 2006.). This drying technique is predominantly employed for the drying of vegetables such as: peas, carrots, green beans, onion, etc. Fluidized bed drying systems have become so advanced to the extent that there are more than 30 recorded versions that differ in some respect, making them preferable to other drying methods for the drying of particulate due to their relatively high heat and mass transfer possibilities.

2.6.8. Freeze Drying Technique

The practice of freeze drying is traced to the ancient Indian tribes of Peru in South America some of whose food materials were preserved by freezing in mountainous areas during a period of winter (Singham and Birwal, 2012). The frozen moisture is eventually extracted via the low vapour pressure of the water below in the surrounding air at very high altitude sun around 3500 B.C (Maharjan, 1995). This technique was used in the preservation of potatoes (Timothy, 1990). Vacuum freeze drying of foods was first applied by Flosdorf in 1945. But the process was very slow, even though the quality of the food was preserved as a result of its frozen state (Claussen, Ustad, Strommen, and Walde, 2007). Freeze dried orange juice was supplied to troops during WW II, and its commercialization came after 1960 (Singham and Birwal, 2012). In the beginning of the 1950s, many researches were conducted on freeze drying in the United Kingdom which paved way for

accelerated freeze drying techniques; and this led to the production of freeze-dried instant coffee in 1960 (Oetjen and Haseley, 2004). Interestingly, as a result of successful research efforts, foods are now processed mechanically by freezing them at about −20°C, followed by the application of a regulated quantity of heat energy under vacuum to bring about the sublimation of ice, and allowing the ice to condense on a refrigeration coil at about −55◦C (Barbosa-Cánovas and Vega-Mercado, 1996). However, the application of freeze drying on industrial scale is all-encompassing in terms of the drying of vegetables, fruits and fruit juices (Caparino et.al 2012; Kushwaha, 2012; Marques, Silveira, and José, 2006).

2.6.9. Vacuum Drying

Vacuum drying is a mass transfer process in which the water molecules contained in a substance are removed by the creation of a vacuum. In this method of drying, it is assumed that the partial pressure is zero because of the absence of air, hence absolute pressure is considered to be the vapour pressure of water. Vacuum drying was first patented in Sweden for wood drying in the year 1922; and subsequently a combination of vacuum and freeze drying was used for the drying of some food products (Singham and Birwal, 2012). In vacuum drying, pressure is the dominant transport factor that influences moisture migration (Cenkowski, Arntfield, and Scalon, 2008). This is achieved at a pressure that is below 101 kPa but higher than 0.6 kPa, in which the mode of transfer of heat is conduction (Maharjan, 1995). Creation of vacuum helps to decrease the drying chamber pressure below the vapour of the water, causing it to boil at low temperature, thus improving the drying rate and decreasing the drying time. In addition, the circulation of heat within the product increases, thereby resulting in high mass transfer.

2.6.10. Osmotic dehydration

This is a phenomenon that involves the partial removal of moisture from food products by the immersion of the food in a salt or sugar solution of high osmotic pressure before the actual drying takes place. The driving force for the removal of water is actually the intracellular fluid and the chemical solution. In addition, water removal is mainly by diffusion and capillary flow whereas uptake is achieved only by diffusion (Singham and Birwal, 2012; Rahman, 2006). The research on

osmotic dehydration of food materials was pioneered by Pointing and co-workers in the second half of the 1960s, and many publications came into sight thereafter (Rastogi, Raghavarao, Niranjan and Knorr, 2002). The subjection of fruit such as apple to osmotic drying, caused it to lose almost 50% of its initial weight before it was made to undergo freeze or vacuum drying (Farkas and Lazar, 1969).

2.7. Drying of Food Crops

Many food products are often harvested at moisture content that is very high, thus making their storage impossible except drying is embarked upon to improve their shelf life. Drying inhibits microbial growth in products as it reduces the degree of water activity that takes place in them, thus extending the period of their usage. Drying of food materials involves the removal of moisture from the product to moisture content that is in equilibrium with the surrounding air or to such moisture content that does not support the action of mould growth or infestation of insects(Fashina, Akande, Ibrahim and Sanusi, 2013). The main purpose of drying food materials is to boost their storability, transportability, texture and retainability (Adzimah and Seckley, 2009). In other words, dried products are stable micro-biologically and physio-chemically, and their cost of handling, storage and transportation is relatively small compared to that of wet products. . The process of drying makes use of high energy in comparison to other production processes as a result of low energy efficiency of dryers and high latent heat of evaporation of water (Syahrul *et al*., 2002; Beigi, 2016). Thus in countries like France, the USA and Canada, drying processes consume between 10 and 15% of the total national industrial energy demand, while in Germany and Denmark the range is 20-25% (Beigi, 2016). Basically, successful drying demands adequate heat transfer in order to provide the required latent heat of vaporization (Aminu, 2013). It is expected that the entire moisture from the exposed surfaces of the product must be lost to the drying air; hence the relative humidity of the drying air is a critical factor. The manner by which the food materials are is handled during drying (i.e. the degree to which potentially exposed surfaces are covered by contact with other food particles, trays, etc) is also a critical factor (Adzimah and Seckley, 2009).

2.7.1. Drying of Maize

Cereal grains such as maize, rice, millet, etc are prominent parts of most foods produced locally in West-Africa and other parts of the world (Adzimah and Seckley, 2009). The thickness of corn kernels (grains) is in the range of 3.24 to 5.05 mm (Eran and Yalçin, 2007; Karthik, Mahesh, Sumanth, and Tanmay, 2017). The radius of corn kernels range from 3.36 to 3.94 mm (Doymaz and Pala, 2003; Babiæ *et al*., 2013; Abasi, Minaei and Khoshtaghaza, 2017). Grains of maize are daily processed in a variety of ways to prepare maize meal which is a principal food for a vast cross-section of people living in Africa. Maize is an energy-rich food that provides sufficiently great quantities of nutrients, especially calories and protein. FAO (1992) reports that among 145 developing countries, it was discovered that 22 consumed more than 100 g of maize per person every day. However, in countries that are highly industrialized, maize is predominantly used as a source for livestock feed and as a raw material for a sizeable number of industrial products. Maize harvest usually takes place during the peak periods of the rainy season which is typically between the months of July and September in Nigeria. This essentially makes preservation of the product hard thus causing most of these grains to go into wastes. Maize grains harvested early usually have high moisture content, making it impossible for them to be immediately stored (Fashina *et al*, 2013). Generally, when maize is harvested green, a considerably high loss of grains accompanies it. About this time of harvest, natural drying in the field is ineffective as a result of the prevailing low temperature and high relative humidity conditions of the atmosphere. However, if the maize is left unharvested and allowed to stay much longer in the fields to dry, they soon become exposed to attacks from insects and rodents. Farmers are moved to embark on early harvest of maize at higher moisture level due to undesirable rain (Wall, James and Donaldson, 1975; Herter and Burris, 1989; Elikhani, 1990). Maize harvested fresh is often sold cheap for immediate consumption which grossly decreases the income of farmers. Experience has shown that in some cases, farmers could hardly realize the cost of production from their sales. Consequently, many farmers who depend on natural sun drying are discouraged from going into large scale production of maize, forcing many of them to live at the level of subsistence. However, to minimize grain losses and thereby increase value and

the profit margin of the farmer, a grain dryer is necessary for freshly harvested grains. This helps these grains to be adequately dried and stored to ensure availability and wholesomeness all year round. To ensure the grains are preserved from the danger of being damaged, maize is mainly harvested between the moisture contents of 22% to 35% (wet basis). According to Gürsoy, Choudhary and Watson, (2013), maize harvested at high moisture content needs quick drying for safe storage to prevent respiration, germination, mold damage and insect infestation. Artificial drying is essential to farmers since it is not weather-dependent and ensures effective drying of cereal crops (Gürsoy, *et al*., 2013). In artificial grain drying operation, heat transfer to grains may occur through the following modes: convection (hot air), conduction (solids), or radiation (high frequency electromagnetic energy). In drying processes that are achieved by conduction, heat flows from outside to inside of the grain with a gradual increase in temperature within the produce (Gürsoy, *et al*., 2013). Maize is an important source of food for human consumption and raw material for many industrial products for which reason its quality during drying has become a serious concern. If maize kernels are exposed to excessive heat during drying, they are usually affected by reduced germination, denaturation of protein and gelatinization of starch, all of which are harmful effects taking place at the following temperature ranges: 43-46°C, 55-65°C and 64-72°C, respectively (Gürsoy *et al*., 2013). These effects become more acute when the moisture content of the drying grains is high (Paulsen *et al*.,1996). According to Paulsen *et al*. (1996), stress cracks have been used reliably as an indirect measure to indicate the degree of protein denaturation and starch gelatinization; and the germination percentage denotes denaturation of protein and recovery of starch. Stress cracks are an essential quality index used in determining the seriousness of damage of grains taking place during drying since it is capable of increasing the number of broken grains and fine materials during further handling, thus resulting in a decrease in corn dry milling performance (Montross *et al*., 1999). Generally speaking, the formation of stress cracks is attributable to rapid drying of grains at high temperatures. Watkins and Maier (1997) reported that drying temperature significantly influences the development of stress cracks. Plate 2.1 shows a picture of dried grains of yellow maize.

Plate 2.1. Picture of dried maize grains.

Maize grains that are intended to be used as seeds for planting should be dried in a way that preserves their viability, hence high temperatures should be avoided (Ekechukwu, 1999). This is because of the fact that seed embryos are destroyed at temperatures well above 40-42°C, necessitating low temperature drying (Adzimah and Seckley, 2009). Basically, numerous farm products require long drying times ranging from 5 minutes to 73 hours with optimum drying air temperatures that make the process energy intensive. This leads to high overhead drying cost and high prices of dried food products (Tiwari, 2012; Ehiem *et al*., 2009 and Antwi, 2007). The optimum range of drying temperatures for the majority of food products is 50°C to 55°C (Donald, 2012). This is because considerably high drying temperatures destroy nutrients contained in the product which causes it to lose its dietary value. When higher temperatures are used, food cooks instead of drying which often results in case hardening, where the food dries externally but moisture trapped inside allowing the growth of mould (Donald, 2012). However, maize is dried over a temperature range of 30-110°C (Nazmi and Esref, 2013; Zahra, Mohammad, Seyyed and Mohammad, 2014; Dagde and Iminabo (2018). Danilo (2003) reported the drying of maize grains from 35 percent to 15 percent for a period of 12 hours, at a drying temperature of 60°C. The final moisture contents depicting the shelf life of different cereal grains are as shown in Table 2.2.

Table 2.2. Moisture contents for various grains

Cereal	Maximum moisture during harvest (%)	Optimum moisture at harvest (%)	Usual moisture at harvest (%)	Required moisture for safe storage	
				1 year	5 years
Barley	30	18-20	10-18	13	11
Corn	35	28-32	14-30	13	10-11
Oats	32	15-20	10-18	14	11
Rice	30	25-27	16-25	12-14	10-12
Rye	25	16-20	12-18	13	11
Sorghum	35	30-35	10-20	12-13	10-11
Wheat	38	18-20	9-17	13-14	11-12

(Source: Brooker, 1973)

Drying of seed grains may be carried out using any drying technique as long as the dryer is operated at an acceptable range of temperatures and good air flow. However, for the grain to attain safe moisture content, a large quantity of moisture must be removed from the wet grain, thus reducing the level of activities of bacteria and fungi on the grains. The shelf life (length of time for safe storage) of grains is determined using the value of the final moisture content of the crop sample.

2.7.1.1. Gross chemical composition of Maize

There is numerous information in the literature on the gross chemical composition of maize. However, the disparity of each of the main nutrient components is wide, and Cortez and Wild-Altamirano (1972) gave a summary of the data on different types of maize grains taken from several publications as seen in Table 2.3.

Table 2.3 - Gross chemical composition of different types of maize (%)

Maize type	Moisture	Ash	Protein	Crude fibre	Ether extract	Carbohydrate
Salpor	12.2	1.2	5.8	0.8	4.1	75.9
Crystalline	10.5	1.7	10.3	2.2	5.0	70.3
Floury	9.6	1.7	10.7	2.2	5.4	70.4
Starchy	11.2	2.9	9.1	1.8	2.2	72.8
Sweet	9.5	1.5	12.9	2.9	3.9	69.3
Pop	10.4	1.7	13.7	2.5	5.7	66.0
Black	12.3	1.2	5.2	1.0	4.4	75.9

Source: Cortez and Wild-Altamirano, (1972).

The disparity on the nutrients was both genetic and environmental which may likely have an effect on the distribution of weight and individual chemical composition of the germ, endosperm, and hull of the grains (Cortez and Wild-Altamirano, 1972). The investigation conducted by Sule *et al*. (2014) on the nutritional and chemical values of maize and maize products gotten from some different markets in different locations of Kaduna State in Nigeria showed the proximate composition as seen in Table 2.4.

Table 2.4. Proximate composition of maize and maize products

Moisture (%)	Ash (%)	Protein (%)	Crude fibre (%)	Fat (%)	Carbohydrate (%)
11.6-20	1.1-2.95	4.5-9.87	2.10-26.77	2.17-4.43	44.8-69.6

Source: Sule *et al*., (2014)

2.7.2. Drying of Yam

Yam (*Dioscorea spp*) is considered the third most essential tropical root crop after cassava and potato (Ojediran *et al*., 2020). In terms of its dietary sources, starch is the major nutrient, among others such as lipids, proteins, vitamin C, some essential minerals, fertility promotion and anti-aging substances. There are various species of *Dioscorea* whose tubers make up one of the basic staple carbohydrate foods used in many tropical countries. Over 600 species are available that likely differ in nutritional values and composition (Bhandari *et al*., 2003). Fresh yam is highly perishable due to the fact that it is associated with very high moisture content in the range of 50–80% (wet basis) and high rates of respiration (Abano and Amoah, 2015; Kouadio, Ghislaine, Assoi, Kouamé, and Kamenan, 2017). It is estimated that more than 10 % of yam tubers are lost during postharvest periods, and this is mainly due to rot caused by fungus (Ajala, Ngoddy and Olajide, 2015; Abano and Amoah, 2015). Losses during postharvest periods significantly affect the income of both farmers and traders with attendant negative effects on food security. Consequently, harvested tubers of yam should be consumed in a short period or be adequately processed into flour through peeling, slicing, blanching, drying and milling (Abano and Amoah, 2015). Yam slices are usually dried to an average moisture content of 12 % (w.b) for safe storage (Oyewole and Olaoye, 2013; Abano and Amoah, 2015).

Yam flour is produced from yam tuber. The tuber is first peeled and cut into the required thickness before drying and milling in order to obtain uniform texture. In most third world countries, especially in Africa, yam slices are mainly preserved by drying in the sun because of its low cost. Although sun drying is the cheapest and oldest method of food preservation known, it however, exposes the crop to contamination by dust, insect attack and infection by microbes; and yet it is not always available. Other limitations of sun drying are: the difficulty in controlling the drying process parameters, uncertainties of weather, high costs of labour and the need for a sizable drying area (Sankat and Mujaffar, 2004). Hence to achieve product quality improvement, a controlled environment is required. Hot air drying is one of the most predominantly applied methods for the drying of food crops (Adejumo, Okundare, Afolayan and Balogun, 2013). It is very suitable for the drying of yam slices; and with the right choice of appropriate techniques and conditions of drying, the final product quality can be controlled. Yam flour quality depends on blanching time and temperature (Adejumo *et al*., 2013). Blanching is a pre-treatment technique which involves scalding a food material in boiling water, and then removing it after a very short, timed interval, and finally cooling it to stop the cooking process. This cooking process is employed before drying yam slices to minimize quality loss over time. The preheating technique helps to inactivate enzymes, modify texture, preserve colour, flavour and nutritional value of the yam flour. Adejumo *et al*. (2013) recommended the combination of 40^{o}C blanching water temperature and 12hours soaking time for processing yam flour. Sanful, Addo, Oduro and Ellis (2015) blanched yam slabs before drying with blanching temperature and time of 100°C and 10mins. Oyewole and Olaoye (2013) blanched yam for 80, 90 and 100℃ at blanching times of 10, 20 and 30 minutes, respectively before drying. In fact, from literature, different blanching temperatures and times have been reported. Fresh yam slices have higher activation energies than boiled yam slices during drying for samples of the same thickness, indicating more ease of release of water in the boiled samples than in the fresh samples (Sanful *et al*., 2015). This was ascertained from an experiment where yam slices were previously boiled at 100^{o}C for 20 minutes before drying as against the drying of fresh yam slices . The food

quality of dried and stored yam products is usually preferred to that of fresh yam, for which reason it is often more expensive than fresh yam tubers in the market. This may be as a result of its perceived better food quality in terms of texture and taste (Otegbayo, Samuel, Kehinde, Sangoyomi and Okonkwo, 2010). Since the high moisture content of yam contributes largely to its perishability, then its preservation in terms of drying requires considerably high energy consumption which is usually costly. In general, factors such as pretreatment technique, drying temperature, product sizes and relative humidity affect drying kinetics of food crops (Ade-Omowaye, Rastogi, Angersbach and Knorr, 2002). The picture of a typical Nigerian white yam tuber is as seen in Plate 2.2.

Plate 2.2. Picture of Nigerian white yam tuber

Many researchers such as Sanful *et al*. (2015), Adejumo *et al*. (2013), etc have investigated the air drying characteristics of different species of yam tubers using conventional dryers.

2.8. Theory of Food Crops Drying

Drying of food products involves the removal of free moisture from the surface and interior part of the products. The transfer of heat to the food material surface occurs upon its exposure to a stream of heated air; and moisture is lost from the material through evaporation due to latent heat of vaporization. Moisture diffuses through a boundary film of air, generating a lower vapour pressure region at the surface of the product which establishes a moisture difference from the innermost part of the product to the dry air (Adzimah and Seckley, 2009; Robert, 1997). This difference in moisture is the driving force for moisture removal from the food, thus during drying, moisture transfer to the surface from the interior takes place through the mechanisms listed below:

- Moisture movement by capillary force
- Moisture diffusion due to the concentration gradient of solutes at different parts of the food product
- Absorption of diffused moisture in a layer at the surface of solid components of the products

Diffusion of moisture in air spaces within the wet material is made possible by pressure difference. The established pressure difference is caused by temperature gradient. In the first phase (initial period) of drying, sensible heat is transferred to the product and the contained water molecules. The product is heated up from the inlet condition, enabling the subsequent processes to take place.

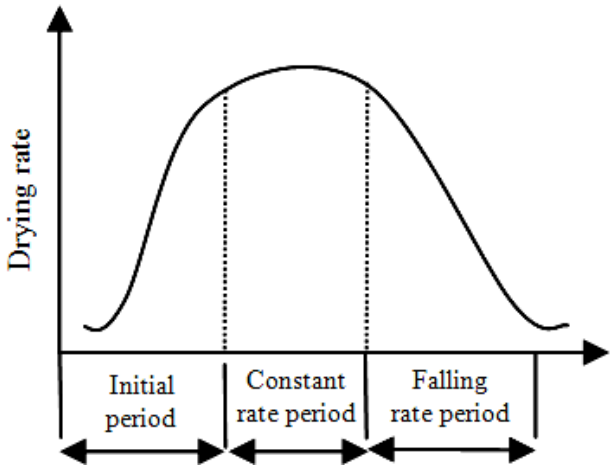

Figure 2.5: The drying curve (Brooker, 1973).

The second phase is the constant rate period within which drying is effected at the product's surface. This shares similarity with moisture evaporation from the surface of free water. The rate of evaporation of moisture is highly dependent upon the surroundings but is not so much influenced by the type of product. The constant rate period comes to an end at moisture content lower than that which is necessary to replace the product's surface moisture that is at the critical moisture content as seen in Figure. 2.5. During the second phase of drying, the air that is required for effective drying is characterized by low relative humidity, a fairly high dry bulb temperature and a high air velocity (Brooker, 1973; Adzimah and Seckley, 2009). The third phase of drying (falling rate period) refers to the period when moisture movement from inner interstices of the product to the external surface is considered to be the limiting factor that slows down the rate of drying. Hygroscopic food products

(i.e associated with bound water) such as grains, etc are characterized by two falling rate periods. The initial or first falling rate period occurs when the surface of the product no longer supplies enough moisture that can saturate the surrounding air. Drying rate within this period depends largely on the moisture transport mechanism from the product to the surface. At the end of this period, the surface of the material may be assumed dry. This is followed by the second falling rate period during which moisture gets to the surface by molecular diffusion. At this stage, the final rate of drying is influenced by forces controlling the diffusion of vapour; while the effect of the outside conditions is negligible. Thus drying involves the evaporation of moisture from the wet product due to heat transfer. Vaporization, capillary action, shrinkage, diffusion, gravity and vapour pressure are mechanisms that control moisture movement internally. Drying rate is dependent upon the following factors: the air velocity, proportion of air, surface heat transfer coefficient, the properties of food to be dried and the proportion of air in terms of dry bulb temperature, wet bulb temperature and relative humidity (Adzimah and Seckley, 2009). Determination of the time needed to attain the desired reduction in moisture content of any food product requires the calculation of the rate of moisture removed from the product (Brooker, 1973; Adzimah and Seckley, 2009). Drying rate is influenced by relative humidity of air, drying time, feed rate, moisture content of product, heat supply, depth of product, temperature of inlet and outlet air and drying operation.

2.8.1. Water activity (A_w)

This, as expressed in Eqn (2.2) is the ratio of the vapour pressure exerted by the food product to the saturated vapour pressure of moisture at the same temperature. It is the measure of the availability of water in chemical, microbiological and enzymatic reactions (Adzimah and Seckley, 2009). The moisture contained in a food product exerts a vapour pressure whose value depends on the quantity of water present as well as the temperature and composition of the food product.

$$A_w = \frac{\text{vapour pressure of water exerted by food}}{\text{saturated vapour pressure at the same temperature}} \qquad (2.2)$$

Water activity is related to relative humidity by the expression below:

$$A_w = \frac{\text{Relative Humidity } (RH)}{100} \tag{2.3}$$

Determination of A_w requires placing the food into a container that is sealed followed by the measurement of the relative humidity of the air in the container as soon as equilibrium is attained (Holman, 1998; Adzimah and Seckley, 2009).

2.8.2. Relative **humidity** ($\boldsymbol{RH}$)

This is defined as the ratio of the amount of water vapour in the air to the amount the air can hold when saturated at the same temperature. In other words, it is referred to as the ratio of the partial pressure of water vapour (P_w) to the equilibrium vapour pressure of water (P_{ws}) at a given temperature as expressed in Eqn 2.4:

$$RH = \frac{P_w}{P_{ws}} \times 100\% \tag{2.4}$$

2.8.3. Moisture Content (MC) of a Product sample

This is the amount of water contained in a moist product sample which is either measured in wet or dry basis (kg water/ kg solids). Moisture content (wet basis), MC_{wb} is the amount of water per unit mass of wet product sample. While moisture content (dry basis), MC_{db} refers to the amount of water per unit mass of product sample that is bone dry. Hence:

$$MC_{wb} = \frac{mass\ of\ water}{mass\ of\ moist\ product\ sample} \tag{2.5}$$

and

$$MC_{db} = \frac{mass\ of\ water}{mass\ of\ bone\ dry\ product\ sample} \tag{2.6}$$

2.8.3.1. Relationship between $\boldsymbol{MC_{wb}}$ and $\boldsymbol{MC_{db}}$

$$MC_{wb} = \frac{mass\ of\ water}{mass\ of\ moist\ product\ sample} \tag{2.7}$$

$$= \frac{mass\ of\ water}{mass\ of\ water + bone\ dry\ product\ sample}$$

Dividing both numerator and denominator by mass of bone dry product sample, we have:

$$MC_{wb} = \frac{mass\ of\ water/bone\ dry\ product\ sample}{\frac{mass\ of\ water}{bone\ dry\ product\ sample} + 1} \qquad (2.8)$$

Therefore,

$$MC_{wb} = \frac{MC_{db}}{MC_{db} + 1} \qquad (2.9)$$

And following the same method for MC_{db}, we have:

$$MC_{db} = \frac{MC_{wb}}{1 - MC_{wb}} \qquad (2.10)$$

2.8.3.2. **Equilibrium moisture content (M_e)**

This is defined as the moisture content of a moist material which is in equilibrium with air of given temperature and humidity. Materials that are exposed to air for a reasonable length of time at constant relative humidity and temperature will slowly arrive at a moisture content that is in equilibrium with the surrounding air. This trend does not depict that the moisture content of the sample product is the same as that of the surrounding air; rather, an equilibrium condition is established such that there is no net moisture exchange between the crop sample and the air (Wilhelm, Suter and Brusewitz, 2004).

2.8.4. Measurement of Moisture Content of a Product Sample

Determination of the moisture content of grains can be achieved using certain methods. These methods may be categorized into two, viz direct and indirect methods. Direct methods are used in determining the water content of samples by the removal of moisture. However, in indirect methods, it is required that the electrical property of the grain (either conductance or capacitance) be measured. According to Adzimah and Seckley (2009), direct methods are reputed for providing the true measurement of moisture content.

2.8.4.1. Direct methods:

- **Chemical reaction method:** This involves the extraction of moisture from grains chemically. Here, iodine reacts with water in the presence of sulphur (IV) oxide (Robert and Don, 1997).
- **Heating or oven method:** In this method, the determination of the moisture content is achieved by the subtraction of the dry mass of the sample from the initial mass.

2.8.4.2. Indirect methods:

- **Resistance method:** This consists of a moisture meter that gives the measurement of the electrical resistance of the sample product to an electrical current. The sample is placed between two electrodes in a compression cell where it is compressed to a known and constant value for accurate measurement (Adzimah and Seckley, 2009).
- **Capacitance:** This method involves the positioning of the sample product in an enclosure with some walls acting as condenser plates activated by high frequency current. Weighing with high precision and correction of temperature differing from 2.5°C are required for accurate measurement. Capacitance meters are found to be more reliable in terms of accuracy over a wider range of moisture than resistance meters (Adzimah and Seckley, 2009).

2.8.5. Moisture Diffusivity

The process of diffusion occurring in solid materials during drying is a highly complex one which may likely involve molecular diffusion, Knudsen flow, hydrodynamic flow, capillary flow, or surface diffusion. However, the use of a lumped parameter model concept entails the combination of all these phenomena in one term referred to as effective moisture diffusivity, D_e (Zafer and Filiz, 2009a). The description of moisture transport during drying is usually carried out by the solution term of the simplified second law of diffusion by Fick as shown in the third chapter of this work. D_e comes in handy as a useful tool in the description of the drying kinetics of food products

2.8.6. Determination of moisture ratio

The determination of the moisture ratio, MR usually goes with the assumption that the layer of the material is thin enough or the air velocity is appreciably high for constant drying air temperature and

humidity to be achieved throughout the material. The values of MR for the drying products is obtained using the initial, equilibrium moisture contents and the moisture content at the time considered. Thus,

$$MR = \frac{M_t - M_e}{M_0 - M_e} \tag{2.11}$$

where, M_t is the moisture content at the time considered; M_e is the moisture content when equilibrium is achieved; and M_0 is the moisture content at the initial time, all in $kg\ water/\ kg\ solids$; and with all the values in dry basis (Zafer and Filiz, 2009a). For food products, M_e is usually negligible in comparison to M_t and M_0, therefore, it is oftentimes ignored (Onu, Igbokwe and Nwabanne, 2017). Thus, MR is reduced to Eqn (2.12) below:

$$MR = \frac{M_t}{M_0} \tag{2.12}$$

2.8.7. Determination of Drying Rate

The value of the drying rate (which is usually influenced by drying time and temperature) is calculated using the following expression (Akpinar, Midilli and Bicer, 2003):

$$d_R = \frac{M_{t+dt} - M_t}{dt} \tag{2.13}$$

where d_R is the drying rate (g/min), and M_{t+dt} is the moisture content at $t + dt$ (kg water/kg dry matter), and dt is the time interval (min).

2.9. Mathematical Modelling of Food Drying

At the microscopic level, drying process is usually very complex and hard to understand due to the difficulties and deficiencies experienced in mathematical descriptions (Zafer and Filiz, 2009a). According to Yilbas, Hussain and Dincer, (2003), it has to do with simultaneous and often coupled and multiphase, heat, mass, and momentum transfer phenomena. Thin layer drying equations have been found to be very useful in mathematical modeling of drying processes; providing suitable results at the end. Drying-rate curves are required to be established before thin layer drying equations can be employed (Zafer and Filiz, 2009a). It is noteworthy that in practice, drying-rate curves are not calculated from fundamentals, instead they are measured experimentally (Baker, 1997).

2.9.1. Thin Layer Drying Equations

Basically, due to its thin structure, it is appropriate to assume a uniform temperature distribution in thin layer drying, thus making it suitable for lumped parameter models. The equations of thin layer drying are applied widely because of their ease of use when compared to models that are complex in terms of their distribution, for example phenomenological and coupling coefficients (O'zdemir and Devres, 1999). Equations of thin layer drying are categorized into (i) theoretical (ii) semi-theoretical and (iii) empirical models. Theoretical models only consider the internal resistance to moisture transfer (Parti, 1993), while semi-theoretical and empirical models only consider the external resistance to moisture transfer between the product sample and air (Zafer and Filiz , 2009a). Theoretical models give explanation to the drying patterns of the product and is suitable for use at all process conditions, while they make use of several assumptions leading to many errors. Most of the widely applied theoretical models in the field of drying are derived from the Fick's second law of diffusion (Zafer and Filiz, 2009a). Semi-theoretical models are also derived from Fick's second law and the modifications of its simplified forms as well as by analogues with Newton's law of cooling. They are more easy and need fewer assumptions as a result of the use of some experimental data but are only valid within the process conditions applied (Parry, 1985). Empirical models share similar characteristics with semi-theoretical models having strong dependence on the experimental conditions and provides limited information about the drying behaviors of the sample product (Keey, 1972).

2.9.2. Semi-Theoretical Models

The classification of semi-theoretical models is done in accordance with their derivation as seen in the following:

1. Models derived from the Newton's law of cooling:

These are the semi-theoretical models that are analogous to the Newton's law of cooling such as the Page model, Lewis model as well as their modified forms.

2. Models derived from the Fick's second law of diffusion:

Here, we consider the semi-theoretical models which are derivations from the Fick's second law of diffusion as seen in Eqn (2.14) below:

$$\frac{\delta M}{\delta t} = D\nabla^2 M \qquad (2.14)$$

where: M = moisture content (kg water/kg dry matter), t is the drying time (s), and D = diffusivity (m^2/s).

In most drying applications, the dominating stage is the falling-rate period (Amira, Saber and Fethi, 2014). Generally, there is an agreement that during the period of falling-rate, the moisture transfer mechanism within a solid that is hygroscopic could be represented using a phenomenon of diffusion according to the Fick's second law of diffusion (Amira *et al*., 2014). Fick's second law as shown in Eqn (2.14) expresses the unsteady state diffusion of moisture.

2.9.3 Models Derived from Newton's Law of Cooling

(i) Lewis Model

This model which is comparable in many respects to the Newton's law of cooling is referred to as Newton's model. In 1921, Lewis gave a suggestion that in drying porous materials that are hygroscopic in nature, the change of moisture content of the materials in the third phase of drying is proportional to the instantaneous difference between the moisture content and the expected moisture content when it comes into equilibrium with drying air. This very concept goes with the assumption that the material is significantly thin, or the air velocity is considerably high, and the drying conditions of air are made to be constant (Zafer and Filiz, 2009a). Therefore,

$$\frac{dM}{dt} = -k(M_t - M_e) \qquad (2.15)$$

where, k (s^{-1}) is the constant of drying. In the concept adopted for thin layer drying, k is the combination of mass coefficients and the transport properties of drying such as moisture diffusivity, interface heat and thermal conductivity (Marinos- Kouris and Maroulis, 1995). However, if k does not depend on M, then Eqn (2.15) can be rewritten as (Zafer and Filiz, 2009a):

$$MR = \frac{M_t - M_e}{M_0 - M_e} = \exp(-kt) \quad (2.16)$$

where, *k* is the drying constant (s^{-1}) that can be gotten from the experimental data and Eqn (2.16) is known as the Lewis (Newton) model.

(ii) Page Model

The Lewis model (Eqn 2.16) was modified by Page in 1949 to achieve a more correct and useful model by the addition of an empirical constant (*n*) which is dimensionless. Zafer and Filiz (2009a) reported a successful application of this model to the thin layer drying of shelled corns:

$$MR = \frac{M_t - M_e}{M_0 - M_e} = \exp(-kt^n) \quad (2.17)$$

(iii) Modified Page Models

The Page model was modified by Overhults, White, Hamilton, and Ross (1973), and was used for the description of the drying of soybeans (Zafer and Filiz, 2009a). This is as seen in Eqn (2.18). However, a few years later, another modification of the Page model referred to as the Modified Page-II Model was done by White, Bridges, Loewer, and Ross (1978) and the form is as seen in Eqn (2.19). This model was also applied in describing the drying of soyabeans (Zafer and Filiz, 2009a). These models are given below:

$$MR = \frac{M_t - M_e}{M_0 - M_e} = \exp(-kt)^n \quad (2.18)$$

and

$$MR = \frac{M_t - M_e}{M_0 - M_e} = \exp - k\left({}^{t}/_{l^2}\right)^n \quad (2.19)$$

where, *l* is a dimensionless empirical constant.

2.9.4. Models From Fick's Second Law of Diffusion

(i) Henderson and Pabis Model

An improvement of a model for drying using Fick's second law of diffusion was achieved by Henderson and Pabis (1961) as seen in Eqn (2.20) and was applied to the drying of corns (Zafer and Filiz, 2009a):

$$MR = \frac{M_t - M_e}{M_0 - M_e} = A_1 exp\left(-\frac{\pi^2 D_e t}{A_2}\right) \quad (2.20)$$

where D_e is the effective diffusivity ($m^2\ s^{-1}$). However, if D_e is considered to be constant during drying, then a drying constant *k* can be introduced by the rearrangement of Eqn (2.20) as:

$$MR = \frac{M_t - M_e}{M_0 - M_e} = aexp(-kt) \quad (2.21)$$

where the term *a* is dimensionless model constant given an indication of shape. These model constants are gotten from experimental data. Eqn (2.21) is generally known as the Henderson and Pabis Model or single term model.

(ii) Logarithmic Model

Chandra and Singh (1995) suggested a model which was a modification of the logarithmic form of the Henderson and Pabis model. In this model which is also referred to as asymptotic, an empirical term *c* was added. Yagcioglu *et al*. (1999) used this model (Eqn (2.22)) to describe the drying of laurel leaves:

$$MR = \frac{M_t - M_e}{M_0 - M_e} = aexp(-kt) + c \quad (2.22)$$

where, *c* is a dimensionless empirical constant.

(iii) Model derived by Midilli *et al* (2002)

A model was proposed by Midilli *et al*. (2002) from the Henderson and Pabis model where an additional empirical term t was included. This model combines a linear term and an exponential term, and was applied to the drying of pollen, mushroom, etc using different drying methods.

$$MR = \frac{M_t - M_e}{M_0 - M_e} = aexp(-kt) + b^* t \quad (2.23)$$

where, b^* is an empirical constant (s^{-1}). Other drying models from the reviews by Onwude *et al*. (2016) and Zafer and Filiz (2009a) are tabulated as seen in Table 2.5.

Table 2.5. Thin-layer models for the drying of fruits and vegetables.

Model name	Model	Reference
Two-term model	$MR = a\ exp(-k_1 t) + b\ \exp(-k_2 t)$	Sacilik (2007)
Two-term exponential	$MR = a\ exp(-k_0 t) + (1-a)\exp(-k_1 a t)$	Dash *et al*. (2013)
Hii *et al*. model	$MR = a\ exp(-k_1 t^n) + b\ exp(-k_2 t^n)$	Kumar *et al*., (2012)
Demir *et al*.	$MR = a\ exp(-kt)^n + b$	Demir *et al*. (2007)
Verma *et al*. model	$MR = a\ exp(-kt) + (1-a)\exp(-gt)$	Akpinar (2006)
Approximation of diffusion	$MR = a\ exp(-kt) + (1-a)\exp(-kbt)$	Yald´yz and Ertek´yn (2007)
Modified Midilli *et al*.	$MR = a\ exp(-kt) + b$	Gan and Poh (2014)
Aghbashlo *et al*. model	$MR = exp\left(\frac{k_1 t}{1 + k_2 t}\right)$	Aghbashlo *et al*. (2009)
Wang and Singh	$MR = 1 + at + bt^2$	Omolola *et al*. (2014)
Diamante *et al*. model	$In(-InMR) = a + b(In\ t) + c(In\ t)^2$	Diamante *et al*. (2010)
Weibull model	$MR = \alpha - bexp(-k_0 t^n)$	Tzempelikos *et al*. (2015)
Thompson model	$t = a\ In(MR) + b[In(MR)]^2$	Pardeshi (2009)
Silva *et al*. model	$MR = \exp(-at - b\sqrt{t})$	Pereira *et al*. (2014)
Peleg model	$MR = 1 - {}^{t}/_{(a+bt)}$	Da Silva *et al*. (2015)
Kaleemullah Model	$MR = exp - cT + t^{(pT+n)}$	Kaleemullah (2002)

2.10. Summary of Literature Review

Heat is produced, used and dumped virtually in all industrial productions. Obviously, from the literature about 70 % of the heat energy released from the fuel by an engine is lost to environment, mainly in the form of heat. Approximately 25–40% of the total energy generated by engines is dissipated in the form of energy loss through the exhaust gas with temperatures as high as 450-600°C. Thus direct discarding of exhaust gases into the surroundings, not only wastes energy but also contributes to the damage of the environment. Hence, the importance of waste heat recovery techniques. The dumped heat can be recovered and put to good use in other processes by process integration using some relevant technologies. The recovery of waste energy can be achieved using techniques such as the transfer of heat between fluids in preheating of combustion air or boiler feed

water; generation of mechanical energy or electricity, or using a heat pump to harness waste heat for the purpose of heating or cooling of facilities. There are available devices for transferring waste heat to productive end use such as turbocompounds, turbochargers, heat exchangers, thermoelectric devices, etc. Waste heat recovery methods have been used to achieve energy savings of 5% to 40% in many industries through process integration analysis. In the 1920s, the very first adaptation of a combustion engine to harness waste exhaust gas energy was actualized. In recent times, the moves to make energy use more efficient due to increase in fuel prices as well as moves to protect the environment from excessive damage have become trending issues globally. The incentives have now driven car manufacturers and other industrial equipment producers to reduce the consumption of fuel. A lot of researchers have conducted an investigation of the performance of different technologies and techniques to ensure an effective recovery of waste heat from industrial machines and automotive engines. And results show the production of about 26 kW power and fuel economy improved by up to 3%. In IC engines, turbochargers recover waste energy from exhaust gases and use it to drive compressors, while the output of a turbocompound is directly used to augment the propulsion of vehicles or for the production of electricity to be utilized by the vehicle. In turbocompounds, energy recovery is actualized by using the exhaust gas to generate electric or mechanical power while the rest of the heat content of the exhaust gas is dumped into the environment. However, it is the aim of this work to recover this enormous waste heat exiting the exhaust gas tail pipe of a diesel generator for the purpose of drying food crops. From the literature, it is evident that there are many types of dryers operated by different energy sources such as solar energy, electrical energy, etc. Most of these energy sources involved in these operations have some associated setbacks in terms of their availability and costs. This makes the end products more expensive. Obviously, there are many drying techniques used in the drying of materials; and the major ones are: solar drying, vacuum drying, freeze drying, tunnel drying, tray drying, drum drying, etc. Among all the drying techniques, the tray dryer is the most extensively used because of its simple and economic design as well as their capability of drying products irrespective of time and weather conditions. The key to their successful operation is the uniform airflow distribution over the

trays. Tray dryers have the capability of drying products at high volume, as more products can be loaded in trays arranged at different levels. They cover a wide range of grains and other food crops drying, and are relatively inexpensive to purchase as compared to other drying methods. They mostly work on batch drying principles where a given amount of an agricultural product undergoes drying at a time. The amount of grain to be dried to the required moisture content is determined by the dryer's holding capacity. In a conventional tray dryer, the fan (blower) required for its operation is attached to the dryer where it blows air across the heating source and supplies the resulting hot air to the trays holding the materials to be dried. However, the blower to be used in this work has no direct connection with the dryer. The blower is rather connected to the heat exchanger into which it draws in air to be heated by the exhaust gas passing through it and the heated air is then routed to the drying chamber of the dryer via a conically shaped section directly under the drying chamber. It is interesting that in this work, there are two stages of energy recovery.

In internal combustion engines, it is possible to recover energy from waste heat sources that otherwise would have been vented into the atmosphere using pressure recovery turbines, heat exchangers, etc. Gunnar (2013) notes that recovered waste heat can find application in areas such as the improvement of vehicle's propulsion system or electricity production for the vehicle's electrical systems. Other applications of heat recovery from automotive engines are seen in the area of turbo-charging or for cabin heating with application of absorption chillers. It is noteworthy that the act of identifying and assessing opportunities for the recovery of waste heat from facilities is quite a difficult task (Woolley *et al*., 2018). It was also noted by Woolley *et al*. (2018) that the task of selecting the most suitable technology for waste heat recovery from the wide range of options available is seemingly arduous. Obviously, there are numerous technologies and applications of energy recovery from exhaust gases of I.C. engines available. But there are still huge potentials for their application, which are yet to be realized. However, it is pertinent to note the following:

(i) Heat recovery from the high heat content exhaust gases exiting the tail pipe of diesel powered electric generators has barely received any meaningful attention by researchers. Yet, this enormous heat is directly dumped into the environment, even though it could still be harnessed and transferred

to a productive end-use. The reason behind the unavailability of research works done in this area could perhaps be due to the inability of researchers to identify any meaningful and beneficial application of the energy recoverable from these systems using available techniques. It is noteworthy that heat recovery from stationary diesel generators may be used effectively to power dryers for the preservation of agricultural crops. This can be achieved by an appropriate arrangement of the components of an energy recovery turbine, a solar panel and allied accessories, a heat exchanger and a hot air tray dryer as shown in this work.

(ii). From the literature, there is reasonable information on drying concerning moisture loss profiles, temperature variations and drying rates of crops such as tomato, yam, potato, etc., using conventional dryers. Hence, in this work, there is need to provide necessary information on the thermal efficiency and energy consumption of this novel drying system using fresh maize grains and yam slices.

CHAPTER THREE

RESEARCH METHODOLOGY

3.1. System Configuration

Figure 3.1 illustrates the configuration for the exhaust gas waste energy recovery dryer using a turbine and heat exchanger in a turbocharged 250kVA diesel generator. It comprises: waste energy recovery turbine, heat exchanger, solar panel, battery, dynamo, air blower, outlet fan, tray dryer, temperature and humidity sensors, weight sensors and arduino-based control panel.

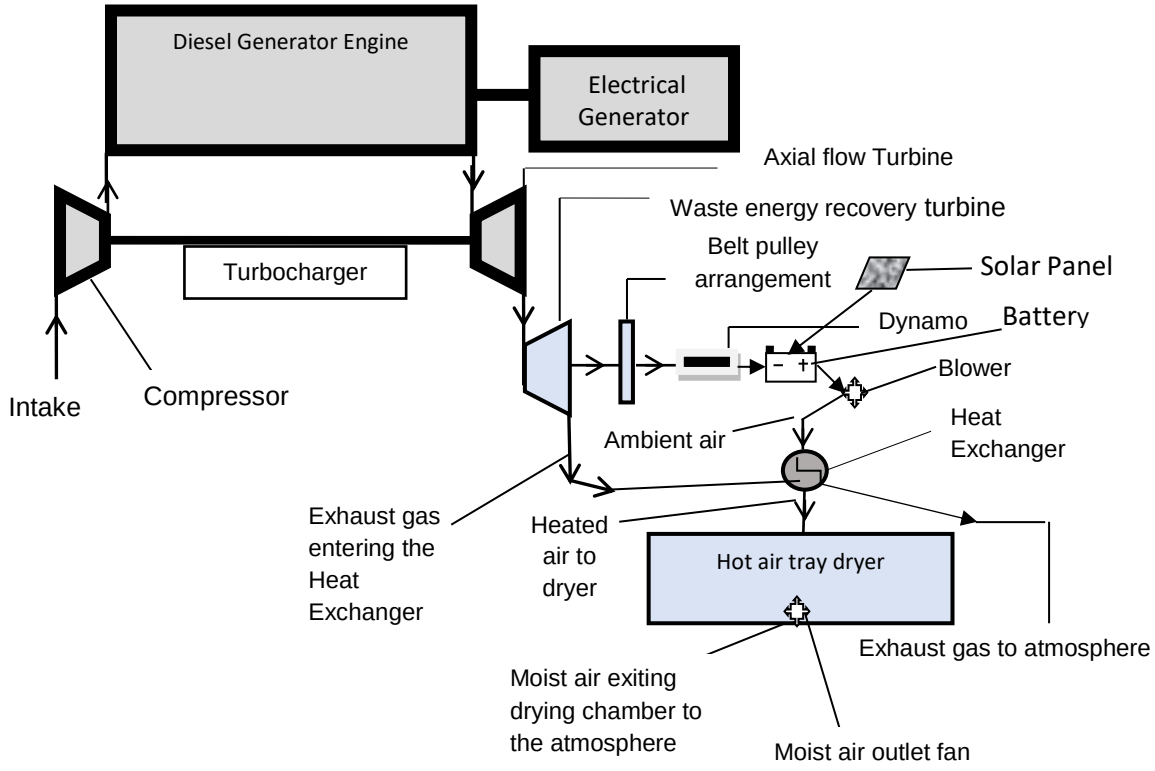

Figure 3.1: The System Configuration of the Waste Heat Recovery Dryer

3.1.1. The Waste Heat Recovery Dryer and its Mode of Operation

The waste heat recovery dryer operates by extracting the waste energy of electric generator exhaust gas for the purpose of drying crops. The generator exhaust gas at the point between its exit from the tail pipe and the atmosphere still exhibits high enthalpy; and this energy is usually what is discharged into the environment unharnessed. The temperature of the exhaust gas at the tail pipe of the generator was measured using a digital thermocouple thermometer and its reading was 382.7℃. In this work, the exhaust gas waste energy will at the first stage, be harnessed by the axial flow turbine to drive a

dynamo that will power the electrical components of the dryer such as the air blower, temperature and weight sensors. The second stage involves the heating of the ambient air (drawn into the shell of a heat exchanger) by the exhaust gas (passing through the tube of the heat exchanger) for the purpose of drying the selected agricultural products. One end of the turbine's housing is connected to the generator exhaust gas tail pipe, and the other end to a heat exchanger into which the exhaust gas leaving the energy recovery turbine flows. The turbine unit is connected to the exhaust gas tail pipe of the generator thus enabling the exhaust gases to impinge on the turbine blades in order to generate mechanical power. The mechanical power generated is used to drive a dynamo for the production of electricity to charge a battery. This battery supplies the electric power needed to drive the direct current (DC) low voltage electrical components such as the air blower, the microcontroller and other devices. A solar panel with its accessories was also employed as an alternative electric power source to help charge the same battery in a situation where the turbine-dynamo system malfunctions. The turbine is a secondary component of the whole arrangement employed to help achieve the primary purpose, which is the drying of food crops. For the solar panel to effectively serve its purpose as an alternative power supply unit, it must be kept at a position that has a large sunny space. However, for a constant supply of electricity to be achieved, battery charging by the solar panel must take place simultaneously as the battery powers the electrical components of the dryer during drying operation.

The turbine rotor is directly attached to the main shaft connected to the smaller pulley (driving-pulley), while the driven pulley of a larger diameter has a common shaft with the dynamo in order to drive it as it rotates. The driving and driven pulleys are linked via a belt arrangement and the electricity produced by this arrangement supplies electric power to the battery. The electric power supplied by the battery is then used to drive the air blower and other electrical components of the dryer. The second stage involves heat energy recovery. Here, the heat exchanger heats up the air (which is supplied by the blower), and then distributes it to the drying chamber of the hot air tray dryer. The exhaust gas exiting the turbine housing enters the tube(s) of the heat exchanger while the ambient air is driven into the shell where it is heated up. The heated air is then routed to the drying

chamber of the dryer where it is exposed to the wet product sample for the purpose of drying. The speed of the heated air entering the drying chamber is regulated by a blower (fan) controller connected to the Arduino platform; and an anemometer is used to measure the drying air velocity. The turbine unit has as its essential parts a row of aerodynamically shaped objects (stator) which are stationary and a row of blades (rotor) which rotate and supply the torque to the shaft; and the entire components are linked and placed in a housing as shown in the isometric view of the heat recovery system (Figure 3.16).

The different components that make up the waste heat recovery dryer are as shown in the exploded view of the test rig (Figure 3.17) while the orthographic view is shown in Figure 3.18. An array of these stator and rotor blades in turbomachinery is referred to as a stage. The whole unit is coupled to the exhaust gas tail pipe outlet in such a way that the rotor blades receive optimal results in terms of their spinning in the exhaust gas stream. During operation, the exhaust gas moving in the axial direction enters through an inlet cone (Figure 3.17), where the fluid slows down to interface with the blades of the stator. Thereafter, the blades of the stator place the speed and angle with which the exhaust gas enters the rotor. When the exhaust gas stream strikes the turbine rotor blades by virtue of its kinetic energy, the rotor blades spin, providing torque to the shaft which rotates the driving-pulley. The exhaust gas which is still at a high temperature exits the turbine housing and passes through the heat exchanger where it heats up the ambient air drawn in by the blower. Then, the hot air is routed to the drying chamber of a tray dryer for the purpose of drying food crops.

3.1.2. Description of the Hot air Tray Dryer

The Schematic diagram of the tray dryer is shown in Figure 3.2. The tray dryer consists of some important parts and components namely: the drying chamber, the trays, the chimney, the blower, the fan controller, the heat exchanger, the temperature and humidity sensors, the weight sensors, an Arduino based control unit and the moist air outlet fan. The dryer operates on the principle of batch drying where a given amount of a wet product undergoes drying at a time.

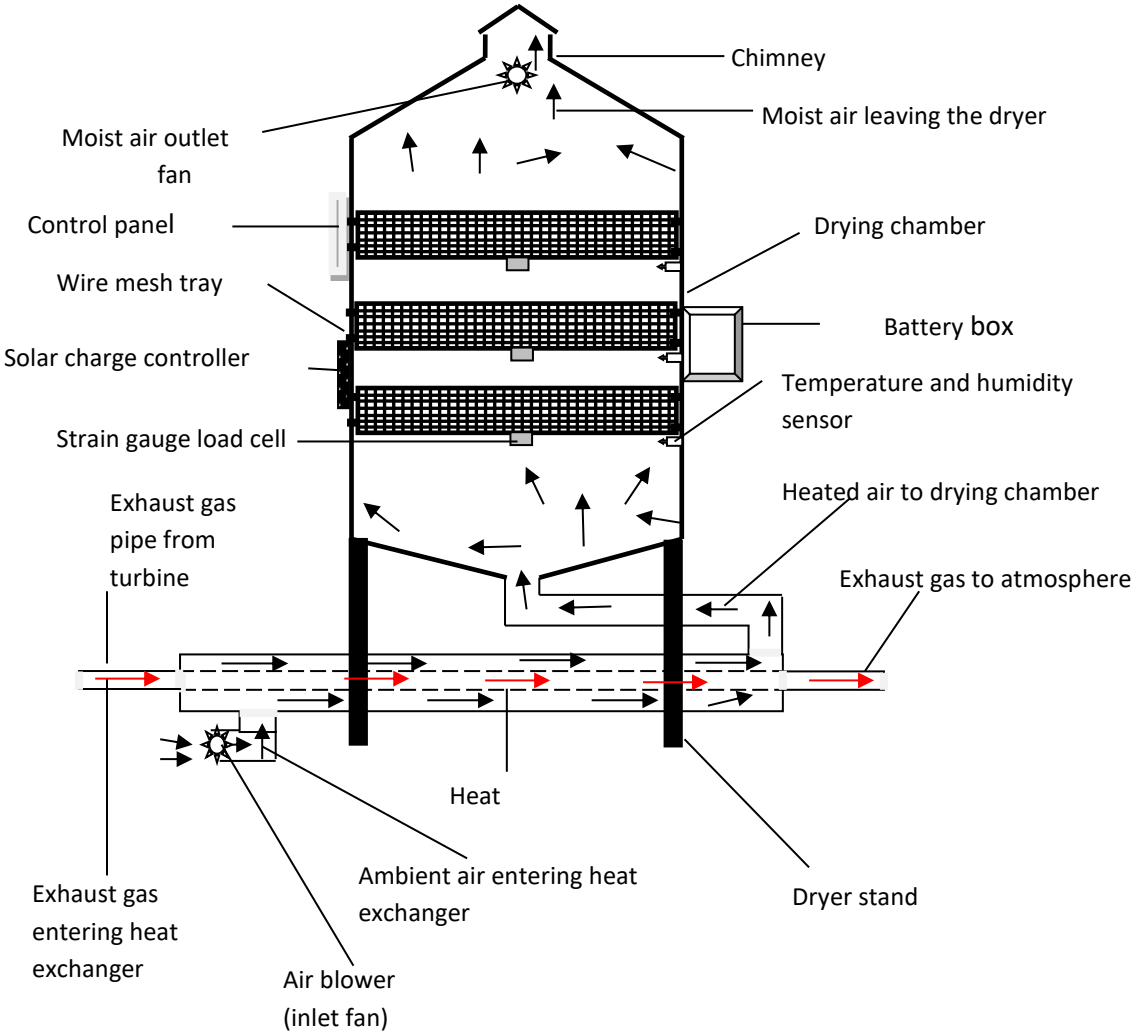

Figure 3.2: Schematic diagram of the tray dryer

The drying chamber is the space holding the trays wherein the products to be dried are fed before drying commences. Heat is supplied to the chamber by the hot air which is heated up by the exhaust gas passing through the heat exchanger. The heat energy supplied to the dryer is the main part of the heat recovery aspect of the hot exhaust gas from the diesel generator. The blower powered by the electrical energy from the dynamo or solar panel is connected to the heat exchanger into which it draws in ambient air to be heated up by the exhaust gas passing through the heat exchanger. The heated air passing through the heat exchanger expands and travels upwards into the drying chamber. The food crops to be dried are spread on wire gauze trays inside the drying chamber. As the warm air moves and circulates across the surfaces of the product samples, it picks up moisture. The air that has picked up moisture on its way through the drying chamber leaves the chamber through the chimney provided at the top of the dryer. The effectiveness of the evacuation of moist air through

the chimney is enhanced by the use of an outlet fan placed near the top of the dryer. To preserve the quality of food crops during drying, the temperature of the drying chamber is controlled so that it does not exceed desirable temperature ranges suitable for particular products to be dried. The temperature and humidity of the air in the drying chamber are monitored using DHT11 sensors connected to an arduino platform within the control unit (CU). This is structured in such a way that, if the temperature of the chamber goes above any of the preset temperatures: 50, 55, 60, 65 and 75 °C, the Arduino board receives the signal and controls the situation by reducing the rate of flow of heated air into the chamber or cutting it off entirely. This is achieved by the use of a speed controller connected to the Arduino platform which reduces the speed of the air blower or switches it off until the chamber temperature falls 2°C below the preset temperature before the operation of the blower is activated once again. Arduino is an open-source programme employed for building electronics projects. It is made up of a microcontroller and a piece of software referred to as Integrated Development Environment (IDE) which runs on the computer and used to write and upload computer codes to the physical board. In the test rig, the Arduino works as the heart of the controller unit. It receives signals from all sensors, processes them and saves their value. It also regulates the speed of the air blower which determines the velocity of the heated air within the drying chamber. The switching on or off of the inlet fan (blower) is achieved by the help of transistors based on the input temperature range. The Arduino microcontroller makes use of liquid crystal display (LCD) to display output values of the operating parameters such as temperature, humidity, speed and weight as they are measured by the sensors. The air speed to be delivered by the blower is selected by pressing the appropriate button on a keypad of the control unit to input the air speed needed for drying. The velocities of air within the drying chamber were measured by a hot wire anemometer (HWA) before their calibration with the Arduino based control panel. Strain gauge load cells on which the trays are suspended are used to measure the weights of the drying products. This is a weighing system that converts weights into analog output signals that can be further conditioned to indicate weight in digital meters, showing accurate real-time weight information displayed on the LCD screen. The control unit (CU) also measures and records the periodic energy consumption from

the battery; and the recorded values can be retrieved from the CU by the aid of a universal serial board (USB) port when connected to a Personal computer (PC). An Arduino software is employed in the CU to queue the readings obtained at intervals of 30 minutes in a database format; and the stored results can be retrieved when needed for analysis.

At the end of each batch of the drying experiment, the dried grains or yam slices removed from the dryer will be allowed to cool before they are packaged. The cooling will provide enough time for the moisture in the dried products to equilibrate and become uniform throughout the materials before packaging takes place. The dried products may "sweat" if they are packaged while still warm. This means that small amounts of moisture may still leave the dried materials and collect on the inside of the packaging material as tiny droplets of water which can then support mold growth.

3.2. Design of the Hot air Tray Dryer

The proposed dryer is one that will be suitable for drying different types of crops; but in this work, it will be used for the drying of maize grains and yam slices for the purpose of analysis. However, for the sizing of the dryer let it suffice to use the bulk density and other properties of maize. The drying chamber is composed of three (3) trays with each tray having the capacity to contain 10 kg of wet corn grains per batch with the total weight of corn per batch equal to 30 kg. However, from Fashina *et al*. (2013), the bulk density, D_b of the maize grain can be calculated using the relation:

$$D_b = 0.7019 + 0.01676M_{wb} - 0.0011598{M_{wb}}^2 + 000001824{M_{wb}}^3 \quad (3.1)$$

where M_{wb} is the moisture content of the grain (wet basis).

For maize harvested at maturity, the average moisture content is usually 32% (Fashina *et al*., 2013). Then, substituting 32 % into Eqn (3.1), yields:

$$D_b = 0.7019 + 0.01676(32) - 0.0011598(32)^2 + 0.00001824(32)^3$$

$$D_b = 0.6483\frac{g}{cm^3}\ Or \quad D_b = 648.3\frac{kg}{m^3}$$

This implies that 648.3 kg of freshly harvested maize occupies 1 m^3 by volume. Therefore, 1 kg of the fresh corn grains occupies 1/648.3 m^3; then the volume which the 30 kg of the corn grains will

occupy is 30 × 1/648.3 m^3 = 0.04628 m^3. And this is the holding capacity of the dryer. But there are three trays in the drying chamber in which the grains of corn to be dried will be filled. Hence each tray in the drying chamber has a volume of:

$$V_t = \frac{0.04628}{3} = 0.01543\ m^3$$

The trays are formed using wire gauze of galvanized steel material with a square steel pipe rectangular base. The volume of the tray is given by:

$$V_t = length \times width \times height$$

Assuming that the internal length and height of trays, L_t and H_t are 0.66 m and 0.05 m, then,

$$V_t = 0.01543 = 0.66 \times width \times 0.05$$

Therefore,

$$\text{Tray } width, W_t = \frac{0.01543}{0.66 \times 0.05} = 0.468\ m$$

However, assuming a tray thickness T_t of $0.005\ m$, then, the total width of tray, W_{Tt} is:

$$W_{Tt} = W_t + 2T_t = 0.468 + 2 \times 0.005 = 0.48\ m$$

And the total length of tray

$$L_{Tt} = L_t + 2T_t = 0.66 + 2 \times 0.005 = 0.67\ m$$

While the total height of tray

$$H_{Tt} = H_t + T_t = 0.05 + 0.005 = 0.055\ m$$

The trays are separated from each other by a distance of 0.12 m along the height of the chamber. To avoid unnecessary pressure build up within the chamber, a head space, H_{hs} of height 0.17 m was provided above the topmost tray to accommodate the wet air gradually exiting the cabinet to the atmosphere through the chimney. This height accommodates the chimney where the moist air outlet fan is fixed. While a bottom space, H_{bs} of 0.135 m is provided below the lowest tray. Hence, the height of the drying chamber, H_c is giving by Eqn (3.2):

$$H_c = 3 \times H_t + 3 \times T_t + 2 \times S_t + H_{hs} + H_{bs} \qquad (3.2)$$

where H_t is height of tray and S_t is space between trays. Therefore,

$$H_c = 3 \times 0.05 + 3 \times 0.005 + 2 \times 0.12 + 0.17 + 0.135 = 0.71\ m$$

To calculate the length and width of the drying chamber, L_C and W_C, we assume that there is an air space, S_a of $0.001\ m$ between either sides of the trays and the drying chamber walls . Then,

$$L_C = L_{Tt} + 2S_a = 0.67 + 2 \times 0.001 = 0.672\ m$$

And

$$W_C = W_{Tt} + 2S_a = 0.48 + 2 \times 0.001 = 0.482\ m$$

However, a door is meant to be installed at the front side of the chamber so as to ease the loading and unloading of the trays once it is opened. The drying chamber walls are made of mild steel sheets (gauge 16) due to its structural properties and weldability.

3.2.1. Mass of water to be removed from the maize grains

From Fashina *et al*. (2013), the average percentage moisture content of freshly harvested maize at maturity, M_o is 32% (wet basis), and the percentage final moisture content (M_f) for 5 years safe storage (Table 2.2), is 10% (wet basis). Weight loss from wet to dried grains is calculated from Ajala *et al*. (2015), as seen in Eqn (3.3). Therefore, the mass of dried grain is given by:

$$M_d = \frac{m_w(100 - M_o)}{100 - M_f} \tag{3.3}$$

$$M_d = \frac{30(100 - 32)}{100 - 10} = 22.67\ kg$$

where m_w is the mass of wet grain. Mass of water to be removed, M_w is given by:

$$M_w = m_w - M_d \tag{3.4}$$

Therefore,

$$M_w = 30 - 22.67 = 7.33\ kg$$

3.2.2. Quantity of Heat required for reduction of the Moisture Content

According to Ajala *et al*. (2015), the quantity of heat required for the removal of water from the maize grain is given by:

$$Q = m_w \times c_c(T_g - T_a) + M_w L \tag{3.5}$$

where: M_w = Mass of water to be removed, L = Latent heat of vaporization of water = 2256 kJ/kg, T_g = Temperature of the drying grains = 85 °C, T_a = Assumed ambient temperature = 31°C, m_w = Total mass of wet grain per batch = 30 kg.

From *ASHRAE Guide and Data Books*, specific heat of corn above freezing point, c_c is 3.35 kJ kg^{-1}°C^{-1} (see Appendix A),

Substituting this into Eqn (3.5), we have:

$$Q = 30 \times 3.35 \times (85 - 31) + 7.33 \times 2256 = 21971 \text{ kJ}$$

This is the quantity of heat to be supplied by the heat exchanger which is equivalent to the heat energy required from the exhaust gas in the heat exchanger to raise the temperature of the ambient air from 31^0 C to 85 ^{0}C. The rate of heat transfer, $\dot{Q}$ between the exhaust gas and the ambient air in the heat exchanger can be calculated using Eqn 3.6 (Azimah and Seckley, 2009):

$$\dot{Q} = \frac{Q}{time\ (secs)} \qquad (3.6)$$

Assuming the drying time of the grains in the dryer is 4.87 hours, then,

$$\dot{Q} = \frac{21971}{4.87 \times 3600} = 1.2523\ \frac{kJ}{s} = \ 1.2523\ kW$$

3.2.3. Sizing of the Heat Exchanger

A parallel flow heat exchanger is chosen in this work due to the convenience that will be experienced in allowing both the exhaust gas and the ambient air flowing through the heat exchanger to travel in the same direction as a result of the relative positions of the axial flow turbine and the tray dryer.

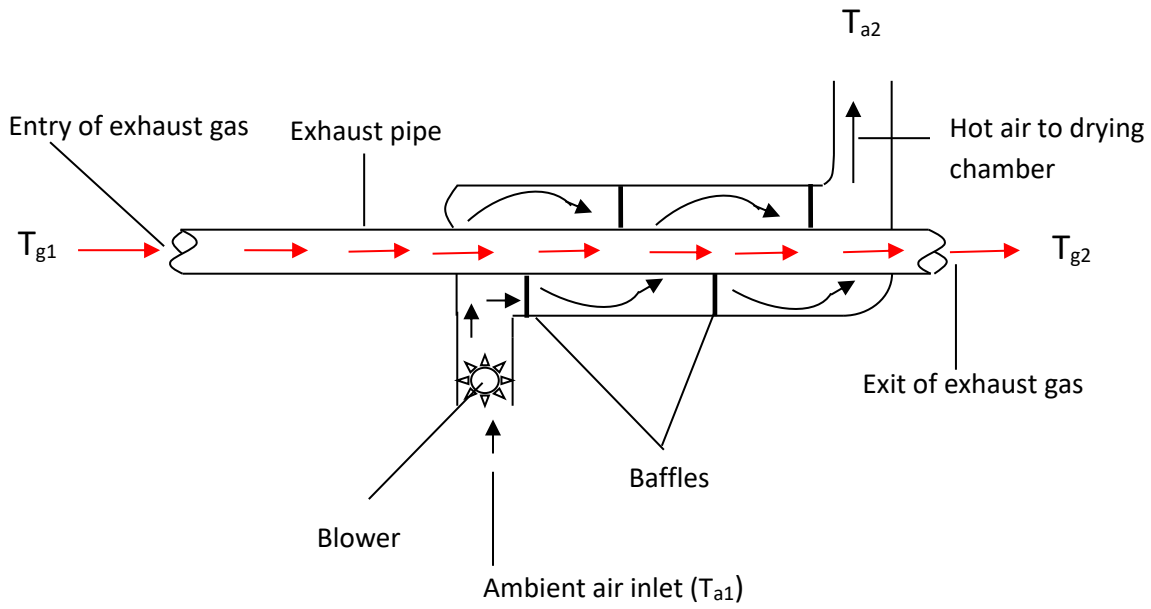

Figure 3.3: Schematic of the parallel flow Heat Exchanger.

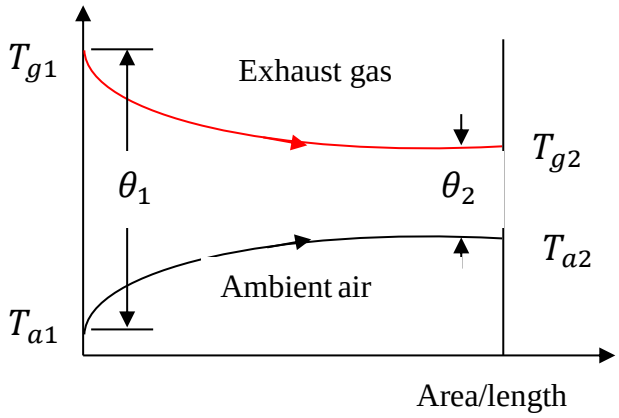

Figure 3.4: Temperature Distribution across the Heat Exchanger.

The flow arrangement and variation of the air and exhaust gas streams are shown in Figures 3.3 and 3.4. The two fluid streams enter at one end of the heat exchanger and leave at the other end as seen in Figure 3.3. It is evident from Figure 3.4 that the temperature difference between the hot and cold fluids goes on decreasing from inlet to outlet. The inlet temperature of the exhaust gas entering the heat exchanger depends largely on the length of the unlagged exhaust pipe conveying it from the generator to the turbine inlet. The longer the length of this pipe, the higher the amount of heat dissipated along the length of the pipe, hence the lower the temperature. This is because as the hot exhaust gas travels along the unlagged exhaust pipe, heat is dissipated as it heats up the pipe which

is exposed to ambient air. In addition to this, the energy expended in driving the turbine further reduces the exhaust gas temperature before it enters the heat exchanger. Thus the assumed inlet temperature of the exhaust gas into the heat exchanger, T_{g1} is $225\ °C$. However, given the following data for heat exchange between exhaust gas and air, for a parallel flow heat exchanger, the heat exchanger length, L_{he} and area, A_{he} can be estimated:

i. The rate of heat transfer, Q between the fluids $= 1.2523\ kJ/s$ (from previous calculation)
ii. Inside and outside heat transfer coefficients, $h_i = 25\ W/m^2\ °C$ (Rajput, 1999)
iii. Outside heat transfer coefficient, $h_o = 45\ W/m^2\ °C$ (Rajput, 1999)
iv. Inlet temperature of exhaust gas, $T_{g1} = 225\ °C$
v. Mass flow rate of exhaust gas $= 0.7022\ kg/s$ (see Eqn 3.45)
vi. Specific heat of exhaust gas at constant pressure, $c_{pg} = 1.15KJ/Kg\ K$ (Eastop and McConkey, 1993; Jadhao and Thombare, 2013).
vii. Inside and outside diameters of the tube $= 100\ and\ 110\ mm$, respectively.
viii. Inlet and outlet temperatures of ambient air, T_{a1} and $t_{a2} = 31\ and\ 85$ ℃, respectively.

The outlet temperature of air from the heat exchanger (85 ℃) is the maximum temperature of the air required in the drying chamber of the hot air dryer.

Let us first calculate the temperature of the exhaust gas at the exit of the heat exchanger, T_{g2}. The heat transfer rate, $\dot{Q}$ can also be expressed as follows (Eastop and McConkey, 1993):

$$\dot{Q} = \dot{m}_g c_{pg}\left(T_{g1} - T_{g2}\right) \qquad (3.7)$$

$$1.2523 = 0.7022 \times 1.15\left(225 - T_{g2}\right)$$

$$225 - T_{g2} = 1.5535\ \ Or\ \ T_{g2} = 225 - 1.5535 = 223.5\ ℃$$

The length can now be calculated using the logarithmic mean temperature difference (LMTD), θ_m (Rajput, 1999).

$$\theta_m = \frac{\theta_1 - \theta_2}{In\left(\frac{\theta_1}{\theta_2}\right)} = \frac{\left(T_{g1} - T_{a1}\right) - \left(T_{g2} - T_{a2}\right)}{In\left[\left(T_{g1} - T_{a1}\right)/\left(T_{g2} - T_{a2}\right)\right]} \qquad (3.8)$$

$$\theta_m = \frac{(225-31)-(223.5\ -85)}{In[(225-31)/(223.5\ -85)]} = 164.7\ ℃$$

However, according to Rajput (1999), the overall heat transfer coefficient, U is given by:

$$\frac{1}{U} = \frac{r_o}{r_i} \times \frac{1}{h_i} + \frac{1}{h_o} \tag{3.9}$$

$$= \frac{0.055}{0.050} \times \frac{1}{25} + \frac{1}{45} \quad Or \quad U = 15.1\ W\ /m^2\ ℃$$

From Rajput (1999), the total heat transfer rate is given by Eqn (10):

$$Q = UA_{he}\theta_m = U \times (\pi d_o L_{he}) \times \theta_m \tag{3.10}$$

$$A_{he} = \pi d_o L_{he} \tag{3.11}$$

$$\therefore \quad L_{he} = \frac{\dot{Q}}{U \times (\pi d_o \theta_m)} \tag{3.12}$$

Hence,

$$L_{he} = \frac{1.2523 \times 1000}{15.1 \times \pi(0.11) \times 164.7} = 1.4571\ m$$

Then the area, A_{he} from Eqn (3.11), $= \pi \times 0.11 \times 1.4571 \quad = 0.5036\ m^2$

3.2.4. The fan/blower selection

The blower does the job of drawing ambient air from the environment into the heat exchanger where it is heated up by the exhaust gas and then routed to the drying chamber for the purpose of drying product samples. In order to achieve effective distribution of heat, the selection of the fan to do the job should be done appropriately. Blowers must be sized based on volume of air delivery and static pressure. In this work, the blower is powered by the electricity produced by the dynamo or solar panel. The work done by the heat source is equivalent to the work done on the ambient air, P_a (Adzimah and Seckley, 2009); where the work done by the heat source per unit time, P_{hg} is 1.2523 kW. Thus:

$$P_{hg} = W_a = 1.2523\ kW \tag{3.13}$$

$$But \quad P_a = \dot{m}_a c_a \Delta T \tag{3.14}$$

where, $\dot{m}_a$ = Mass flow rate of air, and c = Specific heat capacity of air = 1.005 kJ/kgK. But the highest assumed chamber temperature is 85 ℃. Hence,

ΔT = Temperature difference = $85 - 31 = 54$ ℃

From Eqns (3.13 and 3.14), we have that:

$$1.2523 = \dot{m}_a \times 1.005 \times 54$$

$$\dot{m}_a = 0.0231\ kg/s$$

The density, ρ_a can be calculated using the relation (Naghavi, Moheb and Ziaei-Rad, 2010; Beigi, 2016):

$$\rho_a = \frac{101.325}{0.287 T_a} \qquad (3.15)$$

Hence,

$$\rho_a = \frac{101.325}{0.287(85 + 273)} = 0.9862 \text{ kg/m}^3$$

The specific volume of air, v_a at $85^0 C$ which is the reciprocal of its density at the same temperature is given by:

$$v_a = \frac{1}{\rho_a} = \frac{1}{0.9862} = 1.014\ m^3/kg$$

But from Adzimah and Seckley (2009), discharge of the heated air, D is given by:

$$D = \dot{m}_a v_a \qquad (3.16)$$

$$D = 0.0231 \times 1.014 = 0.02342\ m^3/secs$$

However, for standard fan specification, the discharge or air flow rate, D is converted to cubic feet per min (cfm). We know that

$$0.00047195\ m^3/secs = 1\ cfm$$

Therefore,

$$0.02342\ {}^{m^3}/_{secs} = \frac{0.02342 \times 1}{0.00047195} = 49.63\ cfm$$

From above, the length and width of the chamber, L_C and W_C are $0.672\ m$ and $0.482\ m$ respectively; while the area of the chamber floor,

$$A_{cf}\ or\ A_2 = L_C \times W_C = 0.672 \times 0.482 = 0.324\ m^2$$

The velocity of air, c_a required through the chamber or cabinet (Adzimah and Seckley, 2009), is calculated thus:

$$c_a = \frac{D}{A_{cf}} \qquad (3.17)$$

$$= \frac{0.02342}{0.324} = 0.0723\ m/s$$

The velocity obtained is now converted into cubic feet per minute / square foot. We know that

$$1\ m/s = 198.850394\ cfm\ /\ ft^2$$

Therefore, $0.0723\ m/s\ = 0.0723\ \times\ 198.850394 = 14.374\ cfm\ /\ ft^2$. Hence, $Velocity = 14.374\ cfm\ /\ ft^2$

From Adzimah and Seckley (2009), corn has a static pressure of 0.22 inch per foot of depth. However, to calculate the depth of grains in the cabinet, our interest should be on the height of trays wherein the grains are filled and not the entire drying cabinet. Hence, total depth of grains,

$$d_t = n_t \times H_t$$

where n_t is the number of trays and H_t is the height at which grains fill each tray.

$$d_t = 3 \times 0.05\ m = 0.15\ m = 0.492\ ft$$

The static pressure loss due to resistance to air flow is given by:

$$p_{sl} = total\ depths\ of\ grain \times static\ pressure\ per\ foot \qquad (3.18)$$

Hence, $p_{sl} = 0.492 \times 0.22 = 0.10824\ inc$h of water

Under field conditions, the grains may contain chaff and cracked kernels or foreign materials which increase the static pressures. Adzimah and Seckley (2009) reports that in the presence of foreign materials, the obtained value of static pressure should be multiplied by 1.3 to 1.5. So, assuming the corn grains contain these impurities; and choosing 1.5, the value of the static pressure, p_{sl} becomes:

$$p_{sl} = 0.10824 \text{ inch of water} \times 1.5 = 0.1624 \text{ inch of water.}$$

From Adzimah and Seckley (2009), another area of static pressure estimation is that of loss due to sudden enlargement, and is given by:

$$L_{se} = \frac{U_1^2}{2g(1 - \frac{A_2}{A_1})} \qquad (3.19)$$

where: U_1 = Linear velocity of air in the heat exchanger, g = Acceleration due to gravity, A_1 = Area of heat exchanger, and A_2 = Area of drying chamber. Also the mass flow rate of air, $\dot{m}_a$ is given by:

$$\dot{m}_a = \rho_1 A_1 U_1 = \rho_2 A_2 U_2 \qquad (3.20)$$

where: ρ_1 = Density of air in the heat exchanger, ρ_2 = Density of air in the drying chamber and U_2 = Linear velocity of air in the drying chamber.

But from above, $\dot{m}_a = 0.0231\ kg\ /\ s$; $A_1\ (A_{he}) = 0.5036\ m^2$ and area of drying chamber floor, $A_2(A_{cf}) = 0.324\ m^2$. The air density, ρ_{85} (ρ_1) obtained from previous calculation is 0.9862 kg/m^3. From, Eqn 3.20, $\dot{m}_a = \rho_1 A_1 U_1$. Hence,

$$0.0231 = 0.9862 \times 0.2283\ U_1 \quad or \quad U_1 = 0.1026\ m/s$$

Substituting all the values into Eqn (3.19), gives:

$$L_{se} = \frac{(0.1026\ )^2}{2 \times 9.81 \times (1 - \frac{0.324}{0.5036})} = 0.0015\ m\ of\ water$$

Converting $0.0015\ m$ of water column gives 0.059 inches of water column.

Then the total static pressure is:

$$gp_{sT} = p_{sl} + L_{se}$$

$$= 0.1624 \quad + 0.059 \quad = \ 0.223\ inches\ of\ water$$

But since the air blown into the heat exchanger shell is slightly obstructed by the heat exchanger tubes bearing the exhaust gas (i.e. the tubes pose some resistance to the flow of air through the heat exchanger), a static pressure of 2.0 inches of water column is chosen. However, according to Adzimah and Seckley (2009), the expression below gives the horsepower of the blower, B_{hp} required:

$$B_{hp} = \frac{D \times p_{st}}{6320 \times \xi_b} \qquad (3.21)$$

where $(6320 \times \xi_b)$ is called the conversion factor and ξ_b is the blower efficiency, D is the airflow rate (CFM) and p_{st} is the static pressure in inches of water. Choosing a blower of 50 % efficiency which moves ambient air into the heat exchanger, we have that:

$$B_{hp} = \frac{14.374 \times 2.0}{6320 \times 0.5} = 0.0091\ hp$$

But $1\ hp = 745.7\ watts$. Therefore,

$$0.0091\ hp = 0.0091 \times 745.7 = 6.786\ watts$$

Here, a blower of 10 watts and 2 inches of water static pressure is selected. Hence a DC fan of 10 W, 12 V was selected for the dryer. This is almost equivalent to the size of fan (3-7W, 12V) used by Nwakuba (2018) for thin-layer drying in a crop dryer. However, for effective evacuation of moist air, a smaller DC fan of 2.4 W is chosen.

3.2.5. Thermal Insulation of the Drying Chamber

The drying chamber is thermally insulated to avoid excessive heat loss through its walls. The thickness of the heat insulating (lagging) material will be determined using an analogy of heat transfer through a composite wall. The chamber wall is made of mild steel plates at the internal and external parts while the heat lagging material (fibreglass) is placed in-between the mild steel plates of the chamber walls as shown in Figure 3.5.

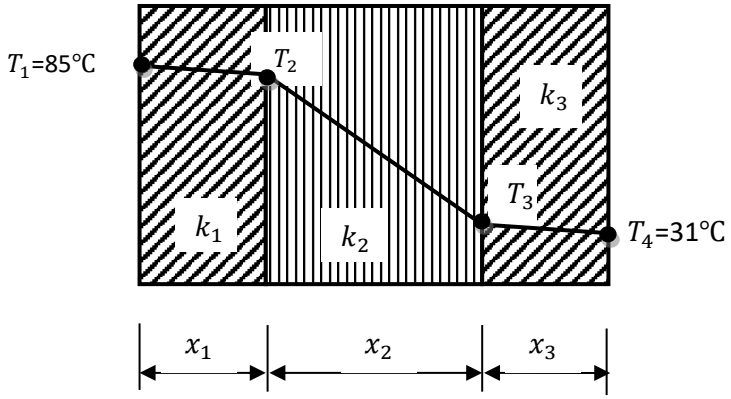

Figure 3.5: Heat Transfer through Composite Wall

The thermal conductivities of the three layers of the wall are: k_1, k_2 and k_3, while their thicknesses are: x_1, x_2 and x_3, respectively. The temperatures of the inner and outer surfaces of the drying chamber walls are T_1 and T_4 while the interface temperatures are T_2 and T_3, respectively. However, for continuity of flow to be achieved, the rate of heat transfer $\dot{Q}$ through the layers of the wall must be the same. Therefore, by Fourier's equation of heat transfer, we have:

$$\dot{Q} = \frac{k_1 A(T_1 - T_2)}{x_1} \qquad (3.22)$$

$$\dot{Q} = \frac{k_2 A(T_2 - T_3)}{x_2} \qquad (3.23)$$

$$\dot{Q} = \frac{k_3 A(T_3 - T_4)}{x_3} \tag{3.24}$$

The internal and external parts of the chamber are of the same material of thickness, 1 mm. Therefore, $k_1 = k_3$ and $x_1 = x_3$. Hence, Eqn (3.24) reduces to:

$$\dot{Q} = \frac{k_1 A(T_3 - T_4)}{x_1} \tag{3.25}$$

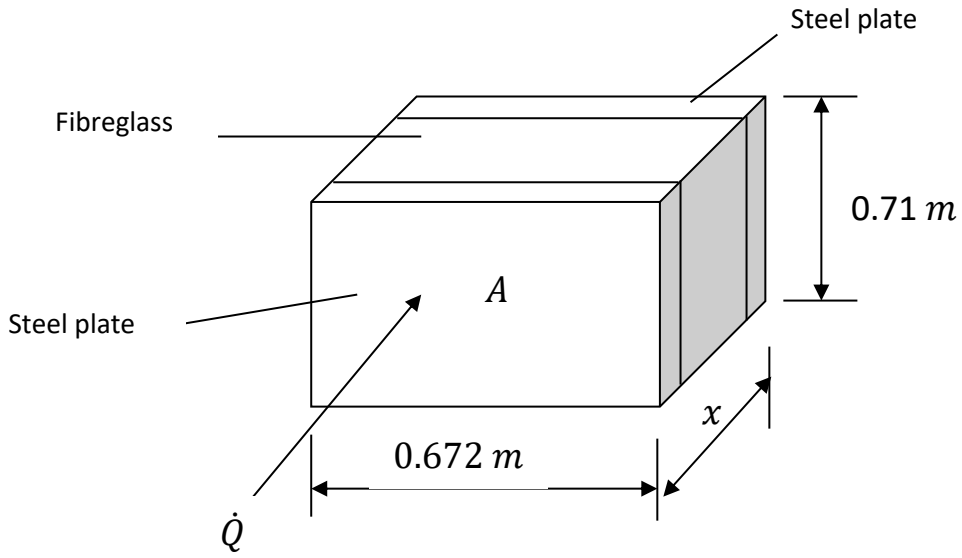

Figure 3.6: Area of the chamber wall.

From previous calculations, the length and height of the chamber wall are 0.672m and 0.71m. Thus, the area of heat transfer ($A = 0.47712\ m^2$) is as shown in Figure 3.6.

The quantity of heat per second required in the drying chamber to remove moisture from the maize grains was estimated in the previous calculations to be 1.2523 kW. However, assuming a total heal loss, Q_L of 5% is to be experienced through the chamber walls. Then,

$$Q_L = 5\% \times 1.2523\ kW = 62.62\ W$$

The thermal conductivities of mild steel and fibreglass are $43\ W/mK$ and $0.04\ W/mK$, respectively. The maximum chamber temperature, $T_1 = 85$℃ while T_4 is assumed to be 31℃. From Eqn (3.22), we have that:

$$\dot{Q} = 62.62 = \frac{43 \times 0.47712 \times (85 - T_2)}{0.001}$$

$$85 - T_2 = \frac{62.62 \times 0.001}{43 \times 0.47712}$$

$$T_2 = 84.997\ ℃$$

Also, from Eqn (3.23),

$$\dot{Q} = 62.62 = \frac{0.04 \times 0.47712 \times (84.997 - T_3)}{x_2}$$

$$62.62x_2 + 0.0191T_3 = 1.6222 \qquad (3.26)$$

From Eqn (3.25), we have that:

$$62.62 = \frac{43 \times 0.47712 \times (T_3 - 31)}{0.001}$$

$$20.5T_3 - 636 = 0.0062$$

$$T_3 = 31.03\ ℃$$

Substituting for t_3 into Eqn (3.26), we have:

$$62.62x_2 + 0.0191 \times 31.03 = 1.6222$$

$$\therefore \quad x_2 = 0.0164\ m \ \ or \ \ x_2 = 16.4\ mm$$

Hence, $20\ mm$ is chosen as the thickness of the thermal insulating material.

3.2.6. Sizing of the Axial Flow Turbine

The sequence of selecting the turbine to be used begins with the establishment of the turbine specifications which include the fluid to be used, the fluid stagnation temperature and pressure at inlet, either the fluid mass flow or the turbine power output required, and the shaft speed, the velocity diagrams at the mean diameter, the number of blades for the blade row, the temperature drop within the turbine stage, the flow and blade loading coefficients, the mean blade speed and the number of stages for the turbine. However, in this work,

i. A single stage axial reaction turbine is chosen.

ii. The degree of reaction, R_d is determined

iii. Exhaust gas flow, $\dot{V}$ = 44.5 m^3/min (see Table 3.1)

iv. Inlet temperature of exhaust gas to the stator, T_{01} = 382.7 ^{0}C = 655.7 K (measured value)

v. Gas constant, $R = 0.287 KJ/Kg\ K$

vi. Gas angles α_i and β_i are determined

vii. `Number of blades selected is 20 and the blade spacing is determined.

viii. Blade heights, b_i are determined

Note: i represents the different stations of the turbine, 1, 2 and 3. And α is the angle made by the absolute velocity with the axial direction, while β is the angle the relative velocity makes with the axial direction. Also, the specific heat at constant pressure of the exhaust gas, c_p is assumed to be $1.15 KJ/Kg\ K$ (Eastop and McConkey, 1993; Jadhao and Thombare, 2013).

The value of the exhaust gas flow rate for Perkins 250 kVA diesel generator is 44.5 m3/min as shown in Table 3.1.

Table 3.1: Perkins 250 kVA turbocharged diesel engine specification.

Engine brand	Perkins
Engine model	306A-E87TAG6
Cooling System	Water Cooled
Number of cylinders	6
Aspiration	Turbo and After-cooled
Displacement	8.7 Litres
Governor type	Electronic
Cooling system	Water cooled
Total coolant capacity	37.2 Litres
Total lub oil capacity	26.4 Litres
Cooling air flow	375 $m3^3$/min
Exhaust gas flow	44.5 m/min
Exhaust gas temperature	528 ºC
Combustion system	Direct injection
Fuel cons. @ 100% Standby	49.7 l/hr
Fuel cons. @ 100% Prime load	45.0 l/hr
Fuel cons. @ 75% Prime load	36.0 l/hr
Fuel cons. @ 50% Prime load	24.0 l/hr

3.2.6.2. **Blade Selection Assumptions**

In the selection of the turbine blades, some pertinent assumptions were made following Nagpurwala (2010) and Minasyan, Bradshaw, and Pesyridis (2018):

i. Flow coefficient, ∅ = 0.80

Note: For light weight applications, higher values of φ and ∅ are used; and the range is: $\varphi = 3\ to\ 5$ and $\emptyset = 0.8\ to\ 3.5$.

ii. For the determination of the blade loading coefficient, φ, it is assumed that the axial velocities, c_{a2} and c_{a3} are equal. And since it is a single stage axial turbine, α_1 is considered to be zero, and $c_1 = c_3$.

iii. For the determination of the degree of reaction, R_d, it is assumed that the absolute velocity at inlet of the rotor, c_2 is equal to the relative velocity at exit of the rotor, V_3; while the absolute velocity at exit of the rotor, c_3 is equal to the relative velocity at inlet of the rotor, V_2.

iv. A temperature drop, ΔT_{0s} of 3 K is selected since it is a small turbine arrangement; and the mean blade speed, U_m is so chosen that the value of the blade loading coefficient, φ does not fall outside its acceptable range of values as stated in assumption 1.

v. Pressure ratio, $\frac{P_{01}}{P_{03}} = 1.52$

vi. Inlet pressure, $P_{01} = 1.8$ bar

vii. Rotational speed of wheel, $N_b = 85$ rev/s (5,100 rpm)

viii. Mean blade speed, $U_m = 43$ m/s

ix. Nozzle loss coefficient, $\mu_N = 0.052$

x. Blade height/width ratio = $\frac{b}{w} = 1.1$

xi. Blade spacing, $s_b = 0.8w$. If the blade spacing/width ratio is in the neighbourhood of 0.25, it is considered to be rather low. A low value is desirable only to reduce the axial length and weight of the turbine.

Basically, the reaction turbine considers the use of both pure impulse and pure reaction principles. There are different stages of the reaction turbine where each stage consists of a fixed row of blades over the whole circumference of the annulus; and the same number of blades on a wheel (Eastop and McConkey, 1993). In this type of turbine, admission of the working fluid takes place over the entire area of annulus, hence there is full admission. The channels of the stator blades take the shape of a nozzle which paves way for a comparatively small drop in pressure followed by an appreciable

increase in fluid velocity (see Figure 3.9b). The exhaust gas passes through the rotor blades, causing a force to be exerted on the blades by the fluid. There is a further drop in pressure as the fluid passes through the rotor blades.

3.2.6.3. **Development of Velocity Diagrams**

Velocity diagram comes in handy as a tool used for the description of the velocity of the fluid flow inside the turbine blades at the inlet and at the outlet.

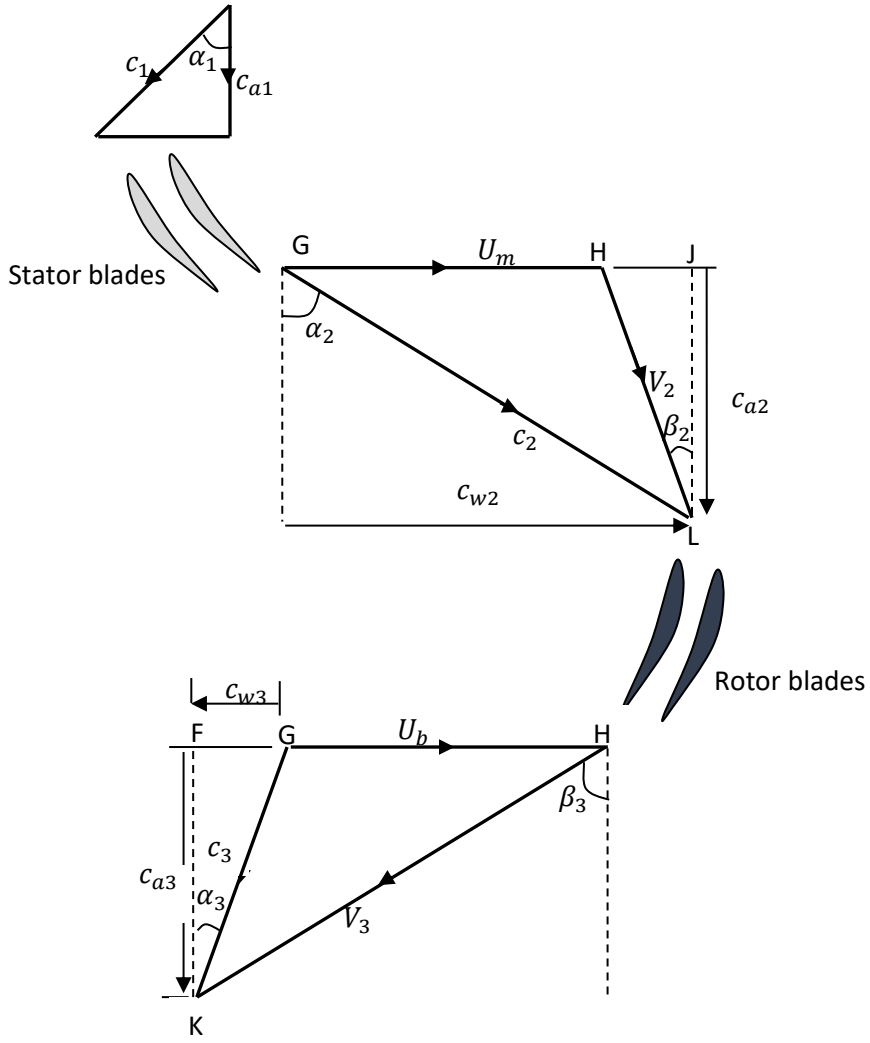

Figure 3.7: Velocities triangles at inlet and outlet of reaction turbine blades.

The arrows show the path through which the exhaust gas follows along the blades. According to Ingram (2009), the flow follows the blade angles. In other words, there is no deviation between the direction that the blades are pointing and the direction that the fluid travels in. The velocity diagram sets the speeds and loads at which the blades will work. Figure 3.7 shows the velocity triangles at

both the inlet and outlet for simple reaction turbine blades. The moving blade channels also exhibit the shape of a nozzle which paves way for an increase in the exhaust gas velocity relative to the blades as shown in the velocity diagram (Figure 3.8). The geometry of the velocity triangles is a symmetrical one as illustrated in the superimposed velocity diagram (Figure 3.8). It could be seen from this symmetrical velocity diagram that the axial (flow) velocities at the inlet, c_{a2} and at the exit, c_{a3} are equal. At both the inlet and exit, the horizontal components of the absolute velocities are referred to as the velocities of whirl, c_{w2} and c_{w3}.

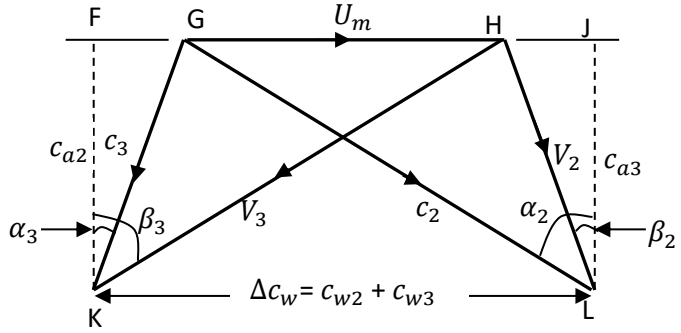

Figure 3.8: Superimposed Velocity diagram for simple reaction turbine blades.

3.2.6.4. **Determination of the Degree of Reaction**

The degree of reaction, R_d expresses the fraction of the stage expansion that occurs in the rotor and is usually defined in terms of the static temperature drop. The effect of reaction is one of degree since in reaction turbines; the impulse effect is always there. Hence, according to (Eastop and McConkey, 1999), the degree of reaction, R_d, is expressed as:

$$R_d = \frac{the\ enthalpy\ drop\ in\ the\ rotor}{the\ enthalpy\ drop\ in\ the\ stage} = \frac{h_2 - h_3}{h_1 - h_3} = \frac{T_2 - T_3}{T_1 - T_3} \quad (3.27)$$

where h_1, h_2 and h_3 are the enthalpies of the exhaust gas at inlet to the stator, at entry to the rotor, and at exit from the rotor respectively.

Applying the steady flow energy equation to the stator blades in Figure 3.9(b), neglecting changes in potential energy of the exhaust gas, the following expression is obtained:

$$h_1 + \frac{c_3^2}{2} = h_2 + \frac{c_2^2}{2}$$

$$Or \qquad h_1 - h_2 = \frac{c_2^2 - c_3^2}{2} \tag{3.28}$$

Note: $c_1 = c_3$

In a similar vein, if the steady-flow energy equation is applied to the rotor blades, we have (Eastop and McConkey, 1999):

$$h_2 - h_3 = \frac{V_3^2 - V_2^2}{2} \tag{3.29}$$

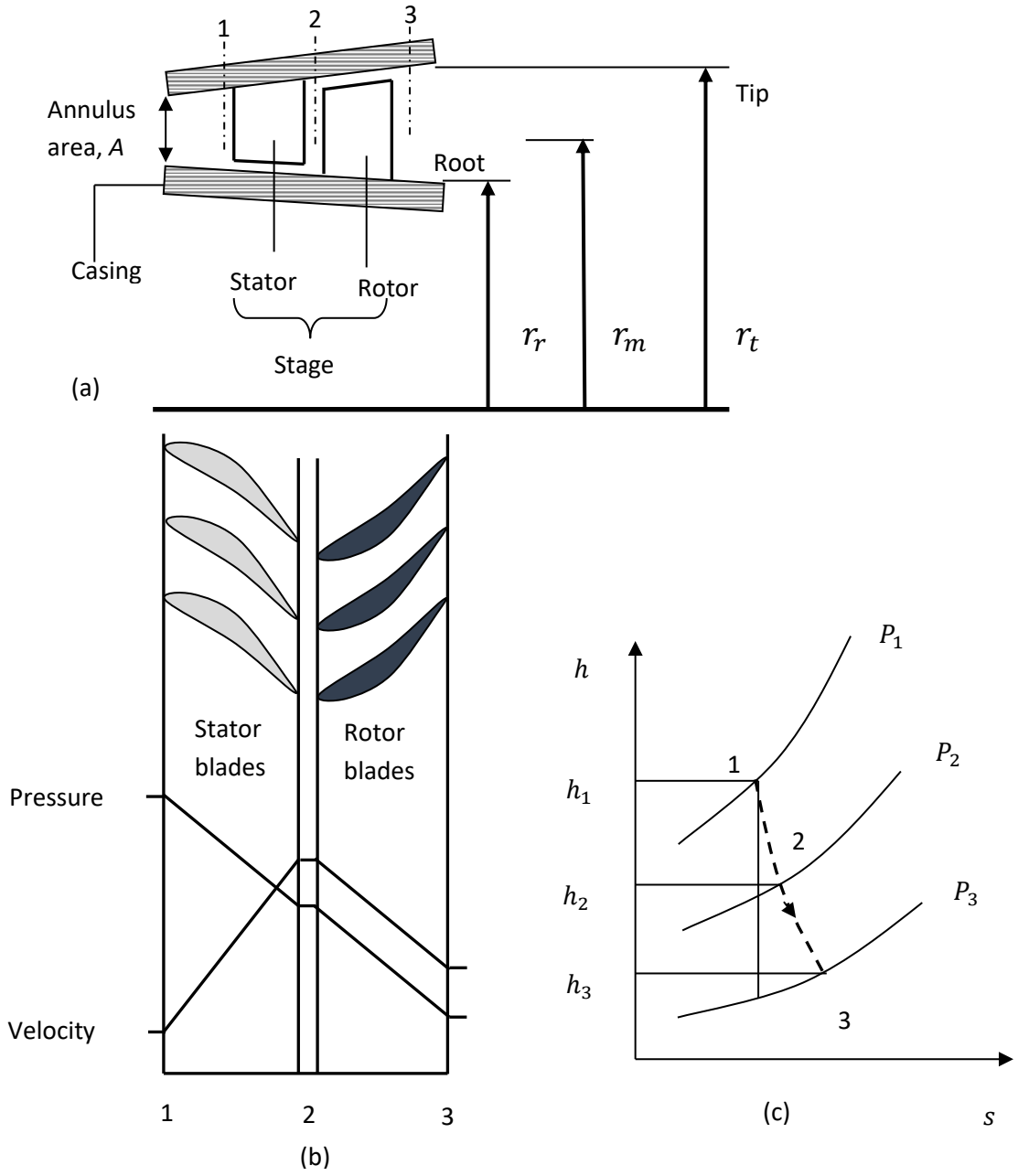

Figure 3.9 (a): Meridional view of an axial turbine stage

(b): Stator and rotor blades of a reaction turbine indicating variations in pressure

and velocity.

(c): Enthalpy-entropy diagram showing the process (Eastop and McConkey, 1999).

From the assumptions made, $c_2 = V_3$ and $c_3 = V_2$; so, substituting V_2 for c_3 and V_3 for c_2 in Eqn (3.8), causes Eqn (3.28) to be similar to Eqn (3.29). Hence,

$$h_1 - h_2 = h_2 - h_3 \qquad (3.30)$$

Making h_0 the subject of the equation from Eqn (3.30), we have that

$$h_1 = 2h_2 - h_3$$

However, subtracting h_3 from both sides of the above equation, we have that

$$h_1 - h_3 = 2(h_2 - h_3) \qquad (3.31)$$

Substituting for Eqn (3.30) and Eqn (3.31) into Eqn (3.1), we have that the degree of reaction,

$$R_d = \frac{h_2 - h_3}{h_1 - h_3} = \frac{h_2 - h_3}{2(h_2 - h_3)} = \frac{1}{2}$$

3.2.6.5. **Determination of the Blade Loading Coefficient**

From the assumption, $c_{a2} = c_{a3}$, and $c_1 = c_3$. And since the selection involves a single stage axial turbine, the inlet velocity will be axial; and for this reason, $\alpha_1 = 0$. The expression for the temperature drop (blade loading) coefficient, φ is given below (Minasyan, et al., 2018):

$$\varphi = \frac{2c_p \Delta T_{0s}}{U_m^2} \qquad (3.32)$$

$$\varphi = \frac{2 \times 1.15 \times 10^3 \times 3}{43^2} = 3.7253$$

The value of φ obtained is acceptable for the selection of the axial turbine since it falls within the acceptable range of values of φ which is from 3 to 5 (Nagpurwala, 2010).

3.2.6.6. **Determination of the Gas Angles**

The velocity diagram will be drawn with the values of the gas angles that will be obtained using known relations as seen in Nagpurwala (2010) and Minasyan *et al*., (2018). Thus,

$$\tan\beta_3 = \frac{1}{2\emptyset}\left(\frac{\varphi}{2} + 2R_d\right) \quad (3.33)$$

$$= \frac{1}{2 \times 0.8}\left(\frac{3.7253}{2} + 2 \times 0.5\right) = 1.7892$$

$$\beta_3 = \tan^{-1}(1.7892) = 60.8°$$

The expression for the gas angle β_2 is given by:

$$\tan\beta_2 = \frac{1}{2\emptyset}\left(\frac{\varphi}{2} - 2R_d\right) \quad (3.34)$$

$$= \frac{1}{2 \times 0.8}\left(\frac{3.7253}{2} - 2 \times 0.5\right) = 0.5392$$

$$\beta_2 = \tan^{-1} 0.5392 = 28.33°$$

For gas angle α_3,

$$\tan\alpha_3 = \tan\beta_3 - \frac{1}{\emptyset} \quad (3.35)$$

$$= 1.7892 - \frac{1}{0.8} = 0.5392$$

$$\alpha_3 = \tan^{-1}(0.5392) = 28.33°$$

For gas angle α_2,

$$\tan\alpha_2 = \tan\beta_2 + \frac{1}{\emptyset} \quad (3.36)$$

$$= 0.5392 + \frac{1}{0.8} = 1.7892$$

$$\alpha_2 = \tan^{-1}(1.6441) = 60.8°$$

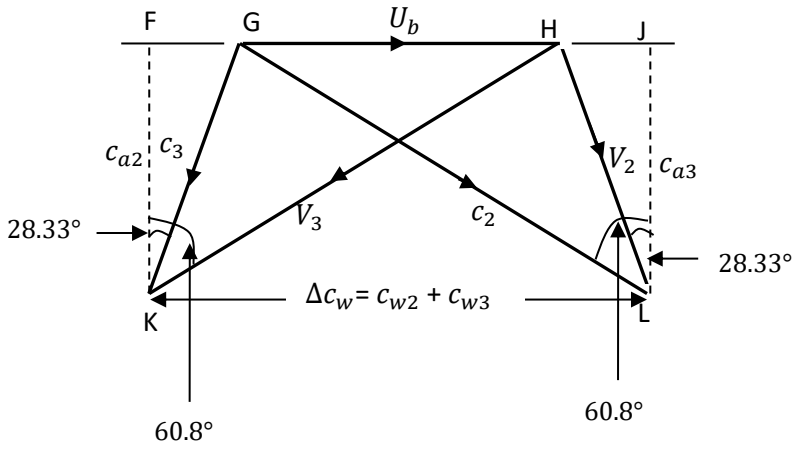

Figure 3.10: Superimposed velocity diagram based on the calculated gas angles

The next operation is to determine the density at stations 1,2 and 3 as shown in Figure. 3.9 (a). This will help for the estimation of the blade height, b, and $tip/root$ (r_t/r_r) radius ratio. It is worthwhile to start by first considering the second station (2) since some adjustments need to be made if the pressure ratio, P_{01}/P_2 along the convergent nozzles is well above the critical value, or if the Mach number relative to the rotor blades at inlet, M_{v2} is above 0.75 (Nagpurwala, 2010).

3.2.6.7. **Determination of Flow Parameters At Nozzle Exit**

Considering the geometry of the velocity diagram above,

$$c_{a2} = U_m \emptyset \qquad (3.37)$$

$$c_{a2} = c_{a3} = 43 \times 0.8 = 34.4\ m/s$$

$$c_2 = \frac{c_{a2}}{\cos \alpha_2} \qquad (3.38)$$

$$= \frac{34.4}{\cos 60.8} = 70.51\ m/s$$

The temperature equivalent of the outlet velocity is

$$T_{02} - T_2 = \frac{c_2^2}{2c_p} \qquad (3.39)$$

$$T_{02} - T_2 = \frac{70.51^2}{2 \times 1.15 \times 10^3} = 2.166K$$

3.2.6.8. **Choke Condition at Nozzle Exit**

$T_{02} = T_{01} = 655.7\ K$; then from above, $T_{02} - T_2 = 2.166\ K$, we then have

$$655.7 - T_2 = 2.166\ K$$

$$T_2 = 655.7 - 2.166K = 653.53\ K$$

$$T_2 - T_2^I = \mu_N \left(\frac{c_2^2}{2c_p}\right) \qquad (3.40)$$

$$T_2 - T_2^I = 0.052 \times \left(\frac{70.51^2}{2 \times 1.15 \times 10^3}\right) = 0.1126\ K$$

$$T_2^I = 653.53 - 0.1126 = 653.42\ K$$

P_2 is calculated from the isentropic relation below:

$$\frac{P_{01}}{P_2} = \left(\frac{T_{01}}{T_2^I}\right)^{\frac{\gamma}{\gamma-1}} \qquad (3.41)$$

$$\left(\frac{655.7}{653.42}\right)^{\frac{1.333}{1.333-1}} = \left(\frac{655.7}{653.42}\right)^4 = 1.0141$$

where $\gamma = 1.333$

$$P_{01} = 1.0141 P_2$$

$$P_2 = \frac{1.8}{1.0141} = 1.7751\ bar$$

Neglecting the influence of friction on the critical pressure ratio, then the following relation holds:

$$\frac{P_{01}}{P_c} = \left(\frac{\gamma+1}{2}\right)^{\frac{\gamma}{\gamma-1}} \qquad (3.42)$$

$$\left(\frac{1.333+1}{2}\right)^4 = 1.852$$

3.2.6.9. **Determination of Annulus Area at Nozzle Exit**

The actual pressure ratio is 1.02324 which is well below the critical value. Hence, the nozzles are not chocking, and the pressure in the plane of the throat is equal to P_2. The density at station 2 is given by (Minasyan *et al*., 2018):

$$\rho_2 = \frac{P_2}{RT_2} \qquad (3.43)$$

$$= \frac{1.7751 \times 10^5}{0.287 \times 10^3 \times 653.53} = 0.9464\ kg/m^3$$

The annulus area at plane 2 is given by:

$$A_2 = \frac{\dot{m}}{\rho_2 c_{a2}} \qquad (3.44)$$

But the exhaust gas the flow rate $\dot{V}$ is 44.5 m^3/min (0.742m^3/s). Therefore, the mass flow rate, $\dot{m}$ of the exhaust gas is given by:

$$\dot{m} = \dot{V} \times \rho_2 \qquad (3.45)$$

$$= 0.742 \times 0.9464 \ = 0.7022\ kg/s$$

$$A_2 = \frac{0.7022}{0.9464 \times 34.4} = 0.0216\ m^2$$

Throat area of the nozzle is required and is given by:

$$A_{2N} = \frac{\dot{m}}{\rho_2 c_2} \qquad (3.46)$$

$$= \frac{0.7022}{0.9464 \times 70.51} = 0.0105\ m^2$$

3.2.6.10. **Annulus Areas at Stations 1 And 3**

It is important to note that had the pressure ratio been slightly above the critical value, it would have been acceptable if a check on M_{V2} proved satisfactory. ρ_2 and A_2 would definitely remain unchanged, hence, $A_{2N} = \dot{m}/\rho_c c_c$, where ρ_c is obtained from P_c and T_c; and c_c assumes a Mach number of unity so that it can be found from $\sqrt{(\gamma R T_c)}$. However, the annulus area required in planes 1 and 3 can now be calculated. Because it is not a repeating stage, it is assumed that c_1 is axial, and this together with the assumptions that $c_1 = c_3$ and $c_{a3} = c_{a2}$, yields (Nagpurwala, 2010):

$$c_{a1} = c_1 = c_3 \ = \frac{c_{a3}}{\cos \alpha_3} \qquad (3.47)$$

$$= \frac{34.4}{\cos 28.33} = 39.081\ m/s$$

The temperature equivalent of the inlet and outlet kinetic energy is

$$T_{01} - T_1 = \frac{c_1^2}{2c_p} \tag{3.48}$$

$$T_{01} - T_1 = \frac{39.081^2}{2 \times 1.15 \times 10^3} = 0.6652\ K$$

But $T_{01} = T_{02}$. Hence,

$$T_1 = 655.7 - 0.6652 = 655.04\ K$$

$$\frac{P_1}{P_{01}} = \left(\frac{T_1}{T_{01}}\right)^{\frac{\gamma}{\gamma-1}} \tag{3.49}$$

$$\left(\frac{655.04}{655.7}\right)^{\frac{1.333}{1.333-1}} = \left(\frac{799.64}{801}\right)^4 = 0.9959$$

$$P_1 = P_{01} \times 0.9959 = 1.8 \times 0.9959 = 1.793\ bar$$

But

$$\rho_1 = \frac{P_1}{RT_1} \tag{3.50}$$

$$\rho_1 = \frac{1.793\ \times 10^5}{0.287 \times 10^3 \times 655.04} = 0.954\ kg/m^3$$

The annulus area at plane 1 is given by:

$$A_1 = \frac{\dot{m}}{\rho_1 c_{a1}} \tag{3.51}$$

$$= \frac{0.7022}{0.954 \times 39.081} = 0.01884\ m^2$$

Similarly, at the outlet from the stage, the following relation holds:

$$T_{03} = T_{01} - \Delta T_{0s} = 655.7 - 3 = 652.7\ K$$

And

$$T_3 = T_{03} - \frac{c_3^2}{2c_p} \tag{3.52}$$

$$T_3 = 652.7 - \frac{39.081^2}{2 \times 1.15 \times 10^3} = 652.04\ K$$

Isentropic relation at station 3 gives:

$$P_3 = P_{03}\left(\frac{T_3}{T_{03}}\right)^{\frac{\gamma}{\gamma-1}} \tag{3.53}$$

From data,

$$\frac{P_{01}}{P_{03}} = 1.52$$

But $P_{01} = 1.8\ bar$; hence,

$$P_{03} = \frac{1.8}{1.52} = 1.1842$$

Then from Eqn (3.53) above, we have that

$$P_3 = 1.1842 \times \left(\frac{652.04}{652.7}\right)^{\frac{1.333}{1.333-1}}$$

$$P_3 = 1.1842 \times \left(\frac{652.04}{652.7}\right)^{4} = 1.1794\ bar$$

The expression below is used to estimate the density at station 3:

$$\rho_3 = \frac{P_3}{RT_3} \qquad (3.54)$$

$$= \frac{1.1794 \times 10^5}{0.287 \times 10^3 \times 652.04} = 0.6302\ kg/m^3$$

The annulus area at plane 1 is given by:

$$A_3 = \frac{\dot{m}}{\rho_3 c_{a3}} \qquad (3.55)$$

$$A_3 = \frac{0.7022}{0.6302 \times 34.4} = 0.0324\ m^2$$

3.2.6.11. **Determination of the Blade Height**

The height of blade and radius ratio of the annulus at stations 1,2 and 3 can now be evaluated. At the mean diameter denoted by the subscript m, the mean blade speed is given by (Nagpurwala, 2010):

$$U_m = 2\pi N_b r_m \qquad (3.56)$$

$$r_m = \frac{U_m}{2\pi N_b} = \frac{43}{2\pi \times 85} = 0.0805\ m$$

The cross-sectional area of an axial tube as given in (Ingram, 2009) is:

$$A = \pi(r_t^2 - r_r^2) \tag{3.57}$$

where A is the area of annulus between the root radius r_r and tip radius r_t as seen in Figure 3.11.

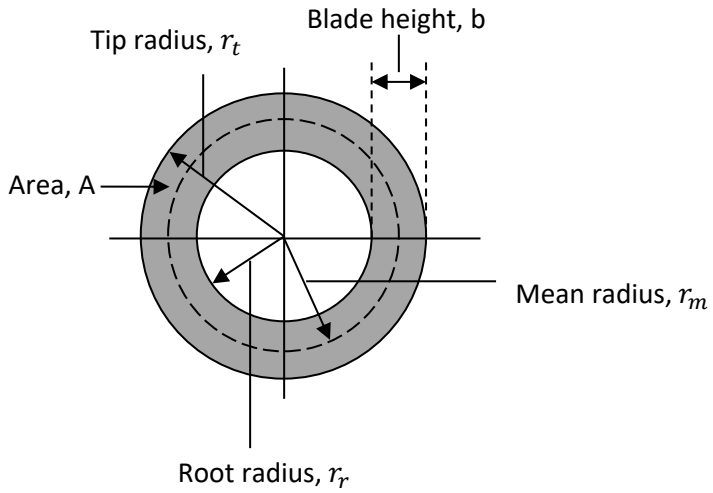

Figure 3.11: Turbine blading annulus.

For applications in turbomachinery, it is usually convenient to express the area in terms of the mean radius, r_m and blade height, b. From the meridional view of the turbine stage (Figure 3.9(a)),

$$r_m = \frac{r_t + r_r}{2}$$

$$\therefore \quad 2r_m = r_t + r_r \tag{3.58}$$

$$and \quad b = r_t - r_r \tag{3.59}$$

Rewriting Eqn (3.57) which has a difference of two squares term, the expression becomes:

$$A = \pi(r_t + r_r)(r_t - r_r) \tag{3.60}$$

Substituting Eqns (3.58) and (3.59) into Eqn (3.60), gives:

$$A = 2\pi r_m b \tag{3.61}$$

But from Eqn (3.56) above,

$$U_m = 2\pi N_b r_m$$

$$Or \qquad 2\pi r_m = \frac{U_m}{N_b}$$

Substituting $\frac{U_m}{N_b}$ for $2\pi r_m$ in Eqn (3.61), gives:

$$A = \frac{U_m b}{N_b}$$

Hence the blade height can be found at the various stations from the expression below:

$$b = \frac{AN_b}{U_m} \tag{3.62}$$

So, at station 1,

$$b_1 = \frac{A_1 N_b}{U_m} = \frac{0.01884 \times 85}{43} = 0.03724\ m$$

At station 2,

$$b_2 = \frac{A_2 N_b}{U_m} = \frac{0.0216 \times 85}{43} = 0.0427\ m$$

At station 3,

$$b_3 = \frac{A_3 N_b}{U_m} = \frac{0.0324 \times 85}{43} = 0.0641\ m$$

The annulus radius ratio can be calculated using:

$$\frac{r_t}{r_m} = \frac{r_m + \frac{b}{2}}{r_m - \frac{b}{2}} \tag{3.63}$$

So, at station 1, the following holds:

$$\left(\frac{r_t}{r_m}\right)_1 = \frac{0.0805 + \frac{0.03724}{2}}{0.0805 - \frac{0.03724}{2}} = 1.602$$

At station 2,

$$\left(\frac{r_t}{r_m}\right)_2 = \frac{0.0805 + \frac{0.0427}{2}}{0.0805 - \frac{0.0427}{2}} = 1.722$$

At station 3,

$$\left(\frac{r_t}{r_m}\right)_3 = \frac{0.0805 + \frac{0.0641}{2}}{0.0805 - \frac{0.0641}{2}} = 2.323$$

The dimensions of the annulus are presented in Table (3.2) below:

Table 3.2: Annulus Dimensions at various stations

Station	$A(m^2)$	$b(m)$	r_t/r_m
1	0.0189	0.03724	1.602
2	0.0216	0.0427	1.722
3	0.0324	0.0641	2.323

The meridional view of the turbine annulus is shown in Figure. 3.7. The letters S and R as seen in the diagram represent the stator (nozzle) and rotor of the turbine assembly; while s_b denotes inter-blade row spacing and w is the blade width.

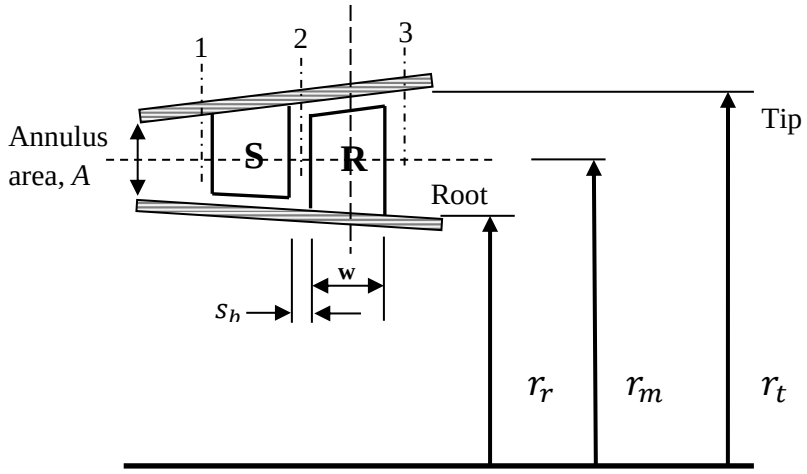

Figure 3.12: Meridional view of the turbine annulus.

3.2.6.12. **Check on Exit Mach Number**

It is important to check the value of the Mach number at exit of the stage, M_3. This is due the fact that if M_3 value is high, then the friction losses in the jet pipe will become unnecessarily large. For this case, we have:

$$M_3 = \frac{c_3}{\sqrt{\gamma R T_3}} \tag{3.64}$$

$$M_3 = \frac{39.081}{\sqrt{1.333 \times 0.287 \times 10^3 \times 652.04}} = 0.0783$$

The value so obtained is acceptable but if need be, it could be increased to reduce annulus flare. Annulus flare brings about a situation like separation of flow from the inner wall where the

acceleration and reaction are not high. This occurs when the angle of divergence of the end-walls is large.

3.2.6.13. **Power Output of the Turbine**

The power output of the turbine is obtained using the following relation:

$$P = \dot{m} c_{pg} (T_{02} - T_{03}) \tag{3.65}$$

$$0.7022 \times 1.15 \times (655.7 - 652.7) = 2.42\ kW$$

The power output calculated above can be verified using the whirl velocity formula. From Eastop and MacConkey (1999), the power output, P_{out} is given by:

$$P_{out} = \dot{m} \Delta C_w C_b \tag{3.66}$$

whereΔC_w, is the change in the velocity of whirl; and is given by:

$$\Delta c_w = c_{w2} + c_{w3} \tag{3.67}$$

The whirl velocities $c_{w2}\ and\ c_{w3}$ can be calculated from Figure 3.10. Here, the whirl velocity,

$$c_{w2} = \overline{GJ} \tag{3.68}$$

$Hence,$ $$c_{w2} = c_2 \sin \alpha_2 \tag{3.69}$$

$$c_{w2} = 70.51 \times \sin 60.8 \quad = 61.55\ m/s$$

$Also,$ $$c_{w3} = \overline{FG} \tag{3.70}$$

$Hence$ $$c_{w3} = c_3 \sin \alpha_3 \tag{3.71}$$

$$c_{w3} = 39.081 \times \sin 28.33 = 18.55\ m/s$$

$$\therefore\ \Delta c_w = 61.55 + 18.55 = 80.1\ m/s$$

But $$P_{out} = \dot{m} \Delta C_w U_m \tag{3.72}$$

$Hence,$ $$P_{out} = 0.7022 \times 80.1 \times 43 = 2418.5\ W \quad = 2.42\ kW$$

3.2.6.14. **Determination of the Blade Spacing**

The number of blades for the stator and the rotor is chosen to be the same. The blade number is selected to be ten (10), and the spacing can be calculated using the relation:

$$s = \frac{2\pi r_r}{n} \tag{3.73}$$

From the second station of the axial turbine,

$$\left(\frac{r_t}{r_m}\right)_2 = 1.722$$

But $r_m = 0.0805\ m$,

Therefore, r_t at station 2 is given by:

$$r_t = 1.722 \times 0.0805 = 0.1386\ m$$

Also, from Eqn (3.58), we have that,

$$2r_m = \ r_t + r_r$$

$$Hence, \quad r_r = \ 2r_m - r_t$$

$$Or \quad r_r = 2 \times 0.0805 - 0.1386 = 0.0224\ m$$

$$Therefore, \quad s = \frac{2\pi \times (0.0224)}{10} = 0.0141m$$

So, the blade spacing is approximately 14 mm.

3.2.6.15. **Sizing of the Cone**

The approach given by Gary *et al*. (2011) is followed in the sizing of the turbine nose-cone. Considering cases involving the aerodynamic structure of the nose cone section of anybody meant to travel through a compressible fluid medium or across which a compressible fluid travels, an important problem is the determination of the nose cone geometrical shape for optimum performance. For many applications, such a task requires the definition of a solid of revolution shape that experiences minimal resistance to constant flow of the fluid medium across the cone. A simple nose-cone shape is used. This shape is chosen for its ease of manufacture and drag characteristics.

3.2.6.15.1. **Dimensions of the Cone**

From Figure 3.13(a), (b) and (c), *L* is the overall length of the nose cone and R (which is the same as the root radius of the blade, r_r) is the radius of the base of the nose cone. In Figure 3.13 (a), *y* is the radius at any point *x*, as *x* varies from 0, at the tip of the nose cone, to *L*. The equations below define the 2-dimensional profile of the nose shape. The full body of revolution of the nose cone is formed by rotating the profile around the centreline *(C/L)*. For aerodynamic reasons, the apex of the cone (Figure 3.13(a)) is blunted to produce the shape of Figure 3.13(b); and this is achieved by capping the cone with a segment of a sphere as seen in Figure 3.13(c).

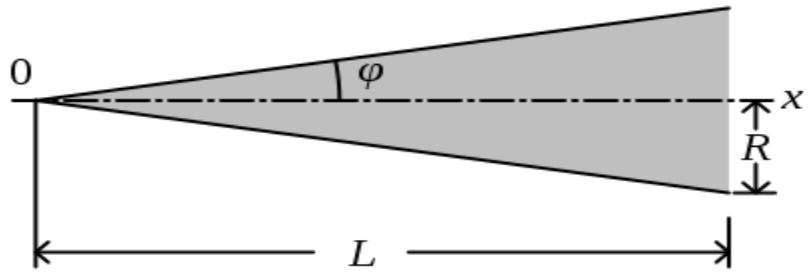

(a)

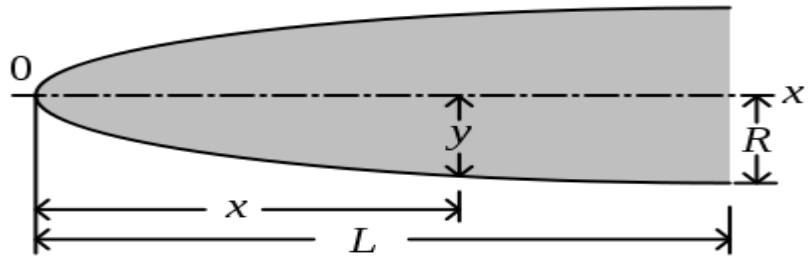

(b)

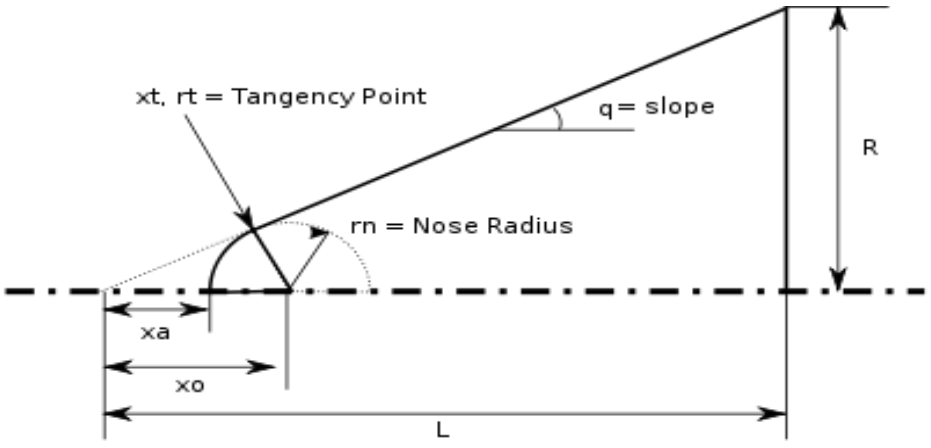

(c)

Figure 3.13: Nose cone profile of the turbine.

The sides of a conical profile are straight lines, and as a symmetrical geometry, the diameter equation (Figure 3.13 (b)) is given by:

$$y = \frac{xR}{L} \tag{3.74}$$

From Figure 3.13 (a),

$$\tan \emptyset = \frac{R}{L}$$

$$\emptyset = \tan^{-1}\left(\frac{R}{L}\right) \tag{3.75}$$

$$And \qquad y = x \tan \emptyset \tag{3.76}$$

where $\emptyset$ is the cone half angle. Assuming L to be 3 times the value of R,

$$i.e. \qquad L = 3r_r$$

$$L = 3 \times 0.0224 \ = 0.0672\ m$$

$$\emptyset = \tan^{-1}\left(\frac{0.0224}{0.0672}\right) = 18.44^0$$

Let $x = 0.04\ m$,

$$Then, \qquad y = \frac{0.04 \times 0.0224}{0.0672} = 0.01333\ m$$

The tangency point where the sphere meets the cone can be found from the equation:

$$x_t = \frac{L^2}{R}\sqrt{\frac{r_n^2}{R^2 + L^2}} \tag{3.77}$$

$$And \qquad y_t = \frac{x_t R}{L} \tag{3.78}$$

For a nose radius, r_n of 0.01 m,

$$x_t = \frac{0.0672^2}{0.0224}\sqrt{\frac{0.01^2}{0.0224^2 + 0.0672^2}} = 0.0285\ m$$

$$y_t = \frac{0.0285 \times 0.0224}{0.0672} = 0.0095\ m$$

where r_n is the nose cap radius of the sphere; and the centre of the spherical nose cap can be found from the equation:

$$x_0 = x_t + \sqrt{r_n^2 - y_t^2}$$

$$x_0 = 0.0285 + \sqrt{(0.01\ ^2 - 0.0095^2)} = 0.317\ m$$

And the apex point can be found from:

$$x_a = x_0 - r_n$$

$$x_a = 0.317 - 0.01 = 0.0217 \text{ m}.$$

3.2.6.16. **Shaft Selection**

The turbine shaft is driven by the rotor blades in the exhaust gas stream. This shaft is supported by a bearing at the centre of the head of the turbine housing as shown in Figure 3.16. At a distance along the length of the shaft beyond the bearing support (outside the turbine housing), a driving pulley of 70 mm diameter and 1kg (9.81 N) weight is connected to the shaft. The total length of the shaft is 350 mm; and at its end which is 50 mm (L_s) from the centre of the bearing attached to the centre of the turbine housing head (see Figure 3.14), the driving pulley is fixed.

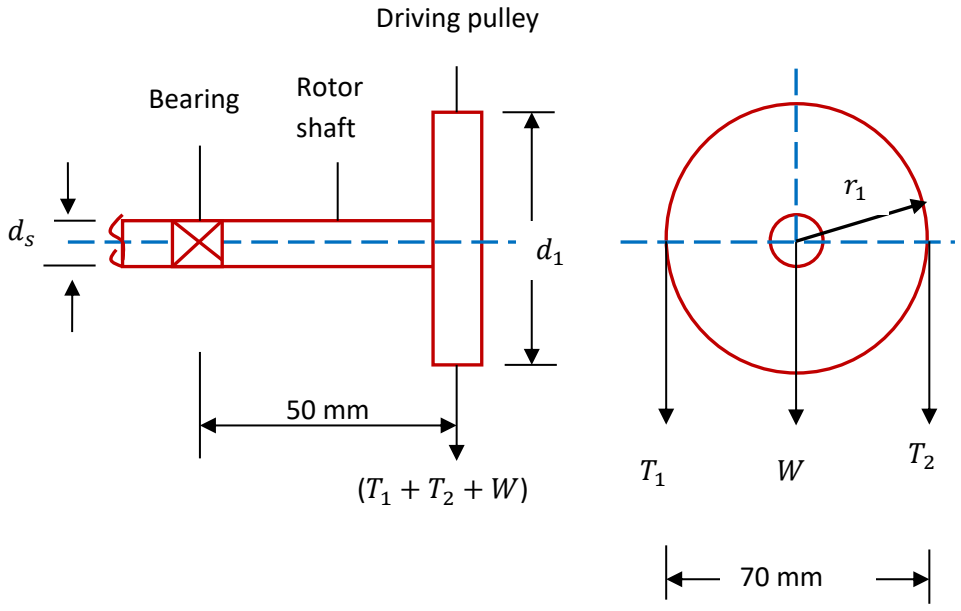

Figure 3.14. Link between the rotor shaft and the driving pulley (Khurmi and Gupta, 2005).

The driven pulley has a diameter of 100 mm and the distance, l between the centres of the two pulleys (driving and driven as seen in Figure 3.15) is 350 mm. The angle of lap or contact of the belt (θ) is to be calculated from Figure 3.15 while the coefficient of friction, (μ) between the belt and

the pulley is 0.3. The material used for the shaft is of specification 40 C 8 according to Indian Standard Designation, 1993 (Khurmi and Gupta, 2005). Assuming the system experiences a steady load, the shock and fatigue factors for bending (k_m) and twisting (k_t) are 1.5 and 1 respectively (Khurmi and Gupta, 2005). The speed of rotation of the shaft (N_b) is 5,100 rev/min and power output (P_{out}) is 2.42 kW as calculated above.

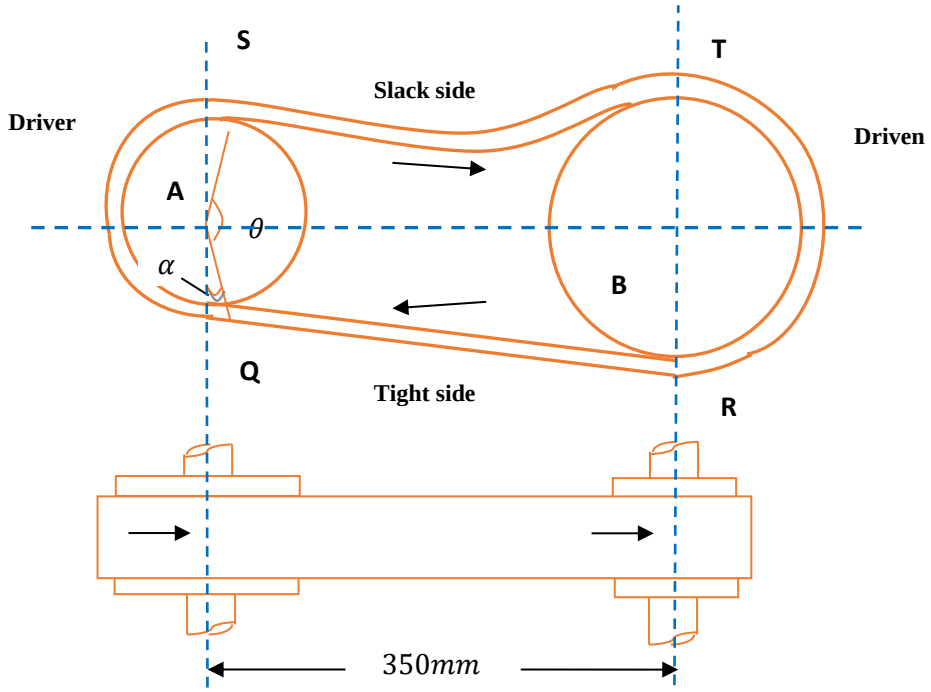

Figure 3.15. Open belt drive (Khurmi and Gupta, 2005).

3.2.6.16.1. **Torque Transmitted by the Shaft**

The torque transmitted by the shaft is given by:

$$T = \frac{P \times 60}{2\pi N} \qquad (3.79)$$

$$T = \frac{2.42 \times 10^3 \times 60}{2\pi \times 5100} = 4.53\ N\ m = 4.53 \times 10^3 N\ mm$$

3.2.6.16.2. **Determination of Shaft Diameter**

From Figure 3.14 above, T_1 and T_2 are the tensions in the tight and slack sides of the belt respectively in newton. Also, Torque transmitted,

$$T = (T_1 - T_2) \times r_1 \qquad (3.80)$$

where r_1 is the radius of the driving pulley, A.

$$Hence, \qquad 4.53 \times 10^3 = (T_1 - T_2) \times 35$$

$$(T_1 - T_2) = 129.5\ N \qquad (3.81)$$

From (Khurmi and Gupta, 2008), the following relation for the tensions T_1 and T_2 holds:

$$2.3\log\left(\frac{T_1}{T_2}\right) = \mu.\theta \qquad (3.82)$$

where μ is the coefficient of friction whose value is given above as 0.3, and $\theta$is the angle of lap. But from Figure 3.14, we have that

$$\sin\alpha = \frac{r_2 - r_1}{l} = \frac{50 - 35}{350} = 0.04286$$

$$Or \qquad \alpha = 2.46^0$$

where $r_1\ and\ r_2$ are the radii of the driving and driven pulleys (A and B). However, for an open belt, the angle of contact,

$$\theta = (180^0 - 2\alpha)$$

$$Hence, \qquad \theta = (180 - 2 \times 2.46^0) = 175.08^0$$

Converting the angle which is in degrees to radians, we have that:

$$\theta = 175.08 \times \frac{\pi}{180} = 3.056\ rad$$

Then, from Eqn (3.82),

$$2.3\log\left(\frac{T_1}{T_2}\right) = 0.3 \times 3.056\ rad$$

$$\log\left(\frac{T_1}{T_2}\right) = 0.3986$$

Taking the antilog of 0.3986, the above equation becomes,

$$\frac{T_1}{T_2} = 2.5036$$

Or

$$T_1 = 2.5036T_2 \qquad (3.83)$$

Substituting for T_1 in Eqn (3.83) into Eqn (3.47), we have

$$(2.5036T_2 - T_2) = 129.5\ \ N$$

$$Or \qquad T_2 = 86.11\ N$$

Substituting $86.11\ N$ for T_2 into Eqn (3.83), we have

$$T_1 = 2.5036 \times 86.11 = 215.6\ N$$

Total vertical load acting on the pulley,

$$W_T = T_1 + T_2 + W = 215.59 + 86.11 + 9.81 = 311.5\ N$$

Bending moment acting on the shaft,

$$M = W_T \times L_s \qquad (3.84)$$

$$M = 311.5 \times 50 = 15{,}575.5\ N\ mm$$

Let $d_s =$ diameter of the main shaft

The equivalent twisting moment is given by Khurmi and Gupta (2008) as:

$$T_e = \sqrt{(k_m \times M)^2 + (k_t \times T)^2} \qquad (3.85)$$

where T is the torque transmitted, and k_m and k_t are the shock and fatigue factors for bending and twisting, the values of which are 1.5 and 1.0.

$$T_e = \sqrt{(1.5 \times 15{,}575.5\ )^2 + (1 \times 4.53 \times 10^3)^2}$$

$$= 23{,}798.4\ N\ mm$$

Also, from Khurmi and Gupta (2008), the equivalent twisting moment,

$$T_e = \frac{\pi}{16} \times \tau \times d_s^3 \qquad (3.86)$$

And the relationship between ultimate tensile strength (σ_u) and permissible shear stress (τ) for a shaft is,

$$\tau = 0.18\sigma_u \qquad (3.87)$$

For an ordinary steel shaft material specification 40 C 8, according to Indian Standard Designation, the ultimate tensile strength is between 560 to 670 MPa. Selecting 570 MPa for σ_u, the permissible shear stress,

$$\tau = 0.18 \times 570 = 102.6\ \text{MPa} = 102.6\ \text{N/mm}^2$$

Substituting these values into Eqn (3.86) gives:

$$23{,}798.4 = \frac{\pi}{16} \times 102.6 \times d_s^3$$

$$d_s = \sqrt[3]{5{,}154.657} = 10.6\ mm$$

3.2.6.17. **Pulley-Belt Arrangement**

The power from the driving pulley, A to the driven pulley, B (or the follower) is transmitted by the use of a belt drive. In this work, an open belt drive is employed. An open belt drive, as shown in Figure 3.14, is used with shafts arranged parallel and rotating in the same direction. In this case, the driver A pulls the belt from one side (*i.e.* lower side *RQ*) and delivers it to the other side (*i.e.* upper side *ST*). Thus the tension in the lower side belt will be more than that in the upper side belt. The lower side belt (because of more tension) is known as tight side whereas the upper side belt (because of less tension) is known as slack side. The diameter of the driver which is made of cast iron material is 70 mm while the distance, *l* between the centres of the pulleys is 350. The belt used is of leather material which according to (Khurmi and Gupta, 2008) has a density, ρ of 1000 kg/m^3 and permissible stress, σ of 2.3 MPa; and the coefficient of friction between it and a cast iron pulley is 0.3.(Khurmi and Gupta, 2005).

3.2.6.18. **Calculation of the speed of the Driven Pulley using Velocity Ratio**

Velocity ratio is the ratio between the velocities of the driver and the follower. It may be expressed mathematically as seen below:

Let d_1 = Diameter of the driver,

d_2 = Diameter of the follower,

N_1 = Speed of the driver in r.p.m., and

N_2= Speed of the follower in r.p.m.

∴ Length of the belt that passes over the driver, in one minute

$$= \pi d_1 N_1$$

Similarly, length of the belt that passes over the follower, in one minute,

$$= \pi d_2 N_2$$

Since the length of belt that passes over the driver in one minute is equal to the length of belt that passes over the follower in one minute, therefore,

$$\pi d_1 N_1 = \pi d_2 N_2 \qquad (3.88)$$

$$\therefore \text{ Velocity ratio, } \quad \frac{N_2}{N_1} = \frac{d_1}{d_2} \qquad (3.89)$$

Here, the speed of the blower to be driven by the follower is given by:

$$\frac{N_2}{5100} = \frac{70}{100}$$

$$N_2 = 3570\ rev/min$$

$$Or \qquad N_2 = 60\ rev/secs$$

3.2.6.19. **Length of Belt Drive**

Let r_1 and r_2 = Radii of the smaller and larger pulleys,

l = Distance between the centres of the two pulleys, and

From Khurmi (2008), the total length of the belt is given by

$$L = \pi(r_1 + r_2) + 2l + \frac{(r_2 - r_1)^2}{l} \qquad (3.90)$$

$But\ r_1 = 35\ mm$; $r_2 = 50\ mm$ and $l = 350\ mm$. Substituting these into Eqn (3.90), we have

$$L = \pi(35 + 50) + 2 \times 350 + \frac{(50 - 35)^2}{350} = 967.68\ mm$$

3.2.6.19.1. **Velocity of Belt**

The linear velocity of belt is given by:

$$v = \frac{\pi d_1 N}{60} \qquad (3.91)$$

$$= \frac{\pi \times 0.07 \times 5100}{60} = 18.69\ m/s$$

3.2.6.19.2. **Width of Belt Drive**

When the velocity of belt is more than 10 m/s, the centrifugal tension must be taken into consideration. Assuming a leather belt, the density, ρ is 1000 kg/m^3 and permissible stress, σ is 2.3 MPa. Mass of the belt per meter length,

$$m = Area \times length \times density = (b \times t) \times L \times \rho \qquad (3.92)$$

where b is the width of belt and the length of belt, L obtained is 967.68 mm. Assuming a thickness, t of 4 mm (0.004 m),

$$m = b \times 0.004 \times 0.96768 \times 1000 = 3.871b\ kg/m$$

The centrifugal tension,

$$T_c = m.v^2 \qquad (3.93)$$

$$Or \qquad T_c = 3.871b(18.69)^2 = 1352.6\ b$$

From Khurmi and Gupta (2008), the maximum (or total) tension in the belt,

$$T_{max} = T_1 + T_c = Stress \times Area = \sigma.b.t \qquad (3.94)$$

$$or \qquad 215.6 + 1352.6\ b = 2.3 \times 10^6 \times b \times 0.004 = 9200b$$

$$9200b - 1352.6\ b = 215.6$$

$$or \qquad b = 0.028\ m$$

3.2.6.19.3. **Power Transmitted by the Belt**

The effective turning (driving) force at the circumference of the follower is the difference between the two tensions (*i.e.* $T_1 - T_2$).

$\therefore$ Work done per second = $(T_1 - T_2)\ v$ N-m/s

And power transmitted,

$$P = (T_1 - T_2)v \qquad (3.95)$$

$$= (215.6 - 86.11) \times 18.69 = 2420.16\ W = 2.42\ kW$$

The torque exerted on the driven pulley (*i.e.* follower),

$$T_f = (T_1 - T_2)r_2 \qquad (3.96)$$

$$= (215.6 - 86.11) \times 0.05 = 6.48\ Nm$$

The drawings of the exhaust gas heat recovery system as shown in Figures 3.16 to 3.18 were created using Autodesk Inventor 2019 program.

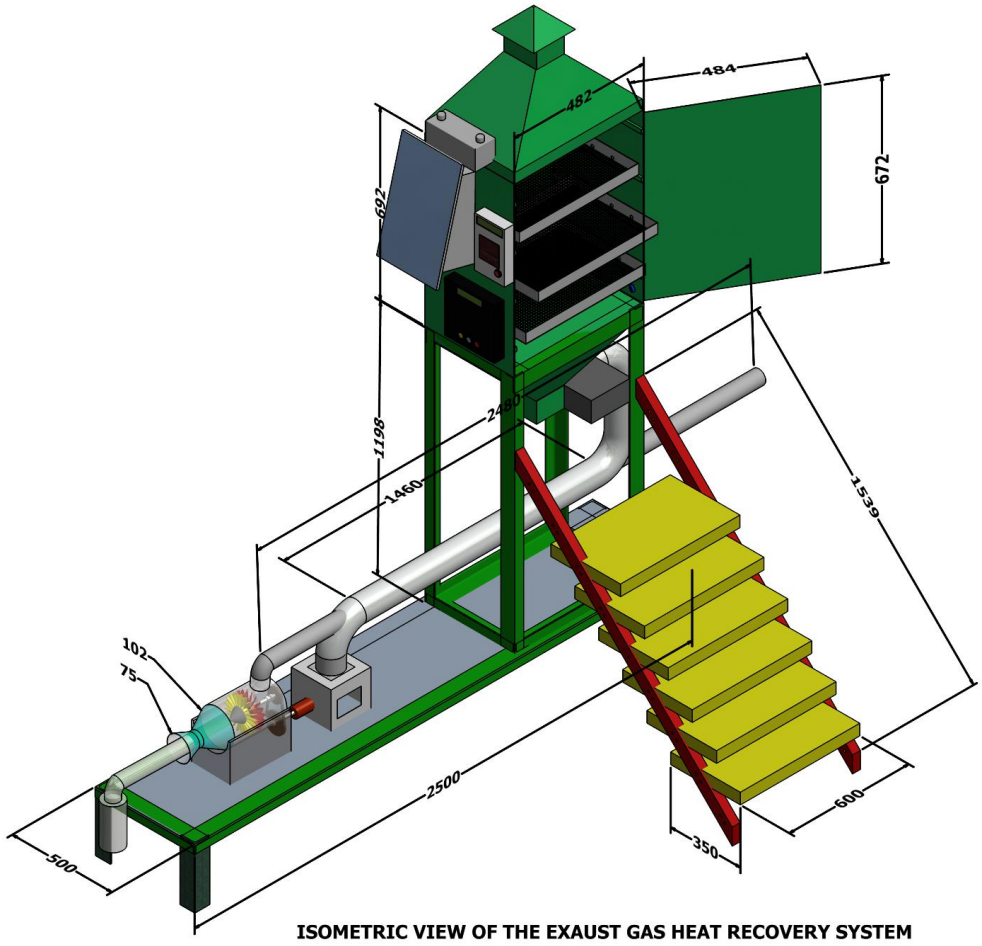

Figure 3.16: Isometric view of the exhaust gas heat recovery system

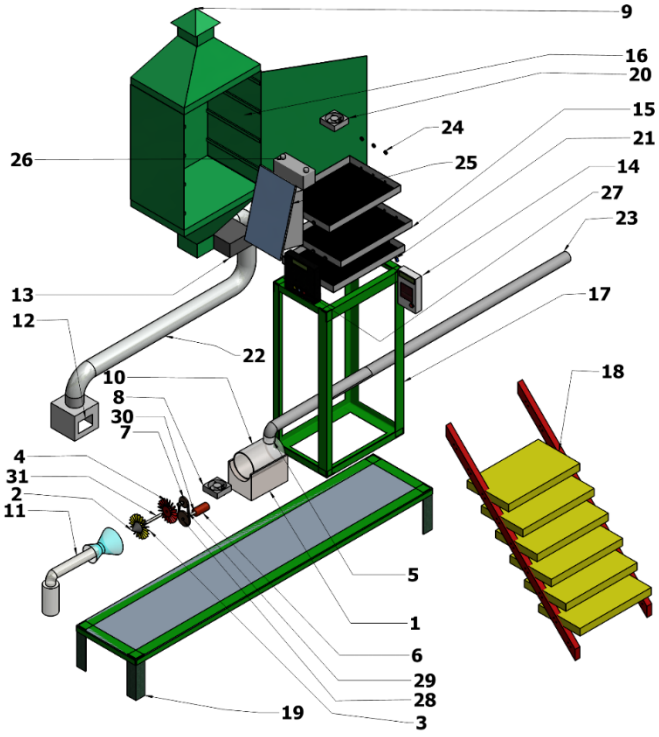

PARTS LIST	
ITEM	DESCRIPTION
1	Turbine support
2	Cone
3	Stator
4	Rotor
5	Exit of exhaust gas path
6	Dynamo
7	Driving Pulley
8	Inlet fan (Blower)
9	Chimney
10	Turbine Annulus
11	Exhaust pipe from generator
12	Air filter and inlet for dryer
13	Fan Controller
14	Arduino - based Electronic control panel
15	Drying tray
16	Drying chamber
17	Dryer stand
18	Stair case
19	Main stand
20	Outlet fan
21	Temperature/ humidity sensor
22	Heat Exchanger Shell
23	Heat Exchanger Tube
24	Weight Sensor
25	Solar Panel
26	Battery
27	Solar Charge Controller
28	Driven Pulley
29	Pulley Belt
30	Dynamo Shaft
31	Turbine Shaft

Figure 3.17: Exploded view of the waste energy recovery dryer

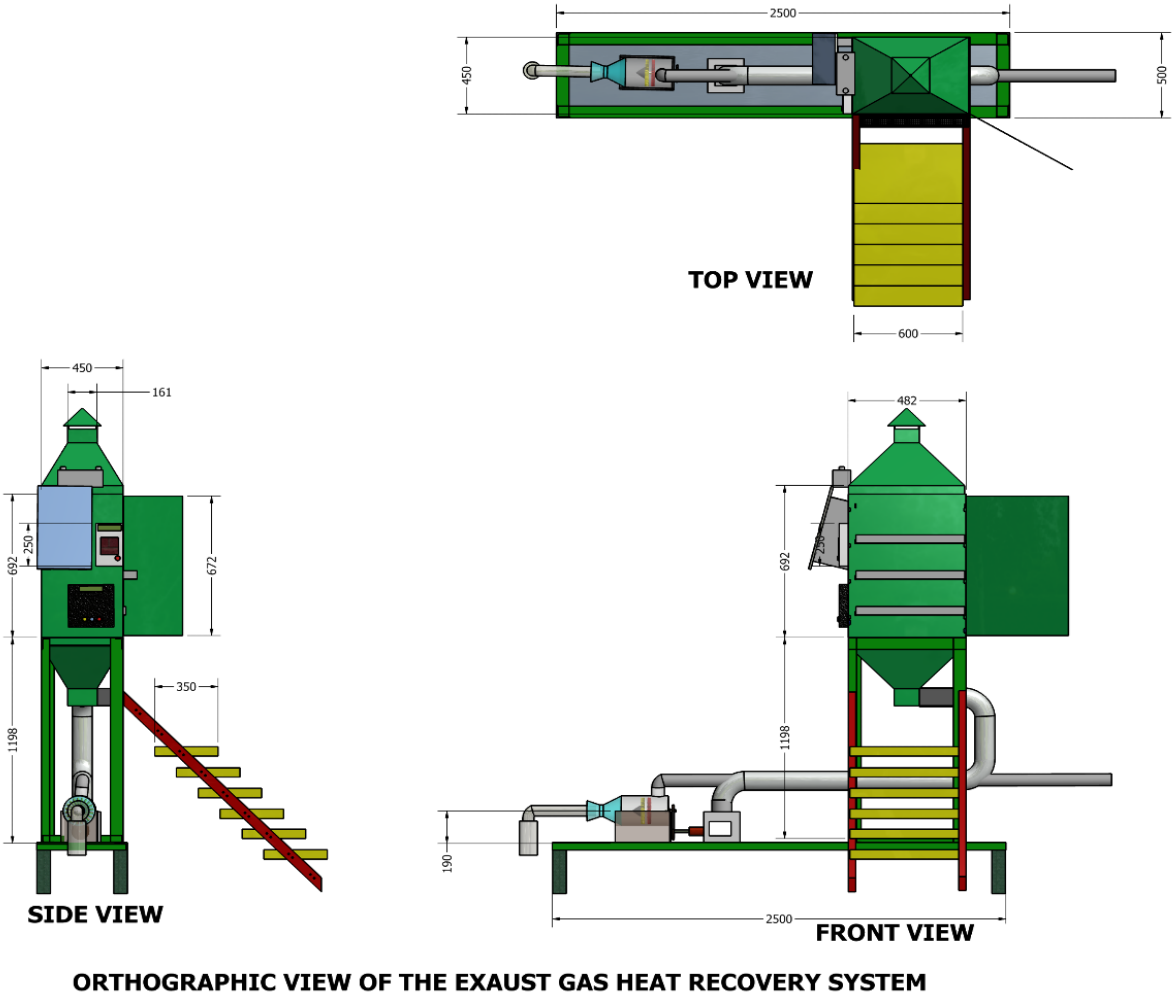

Figure 3.18: Orthographic view of the exhaust gas heat recovery system

3.2.7. Selection of the Solar Panel and the Battery

The size of the solar panel to be selected as an alternative source of power to the dryer depends on variables such as the power needed by the electrical components of the dryer, the length of time for its operation, and the intensity of sunshine prevalent at the time of the year. Hence the energy requirement of these components, the energy storing capacity of the battery, and the size of solar panel capable of replenishing the energy in the battery in line with the method of use must be determined. The power consumption of electrical components is measured in Watts. To estimate the energy (Wh) to be used over time, the power consumption (Watts) is multiplied by the time (h) of operation of the components. The electrical components of the dryer to be powered by the battery are: the blower (inlet fan), outlet fan, weight sensors, temperature, humidity sensors and the contents

of the control panel (CP). These components are to be operated for 6 hours daily (i.e. from 9.am to 3.pm). The electric power (load) demands of the components are as summarized below:

(i) From previous calculation on the sizing of the air blower, 10 W was selected as the capacity of the blower. Hence a blower (inlet fan) of 834 mA is chosen.

(ii) Outlet fan of 200 mA, 12V = 2.4 watts

(iii) Six (6) temperature and humidity sensors of 20 mA, 5V each = 0.6 watt

(iv) Three (3) weight sensors of 30 mA, 5 V each = 0.45 watt

(v) Contents of the control panel:Microcontroller of 80 mA, 5V = 0.4 watt

- LCD of 120mA, 5V = 0.6 watt
- Other contents of the CP- 100 mA, 5 V = 0.5 watt

Hence, the total connected load to the PV panel (total energy or load requirement) is 14.95 watts. Therefore, the total watt-hours rating of the system = Total connected load (watts) × Operating hours = 14.95 × 6 = 89.7 watt-hours.

3.2.7.1. **The Solar Panel Selection**

The rating of a solar panel in terms of power generation is also given in Watts. To calculate the energy the panel can supply to the battery, the power (watts) is multiplied by the time (hours) exposed to sunshine. Then the result is multiplied by an operating factor of 0.75 which is a factor that considers natural system losses. Assuming a PV panel of 40 watt. Then, the actual energy the panel can supply to the battery = Peak power rating × operating factor × hours per day = 40 × 0.75 × 6 = 180 Wh.

3.2.7.2. **Determination of the Battery Size**

The capacity of a battery is measured in Amp Hours (Ah). This is converted to Watt Hour by multiplying the Ah value by the voltage of the battery. For a 15 Ah, 12V battery, the capacity is 15 x 12 = 180 Wh. This shows that the battery can supply power to the components of the dryer (14.97 watts) for 12 hours uninterruptedly. However, the power going into the battery from the solar panel

is managed by a solar charge controller in order to avoid overcharging of the battery during the day or power drain back to the solar panel during night hours.

3.2.8. Important Materials Consideration in the Test Rig Fabrication

- Mild steel sheets of 1.5 mm was used for the construction of the turbine housing; heat exchanger shell; the internal and external walls of the drying chamber while galvanized steel pipes of 25 mm diameter was used in constructing the tubes of the heat exchanger.
- The test rig stand and the dryer frames was fabricated using angle iron, steel pipes of rectangular and circular cross-sections, respectively.
- The trays of the dryer was constructed using galvanized steel wire mesh (gauze). The aim of using galvanized steel wire mesh is to avoid rusting of the tray material and contamination of products to be dried; while the openings in the wire-mesh material will to help expose a large surface area of the grains to the drying air.
- To prevent the accumulation of moist air in the upper part of the dryer, a chimney was provided at the roof of the dryer to allow for an easy flow of moist air to the atmosphere. The chimney was constructed with an overhang attached to it in order to prevent rain and rodents from interfering with the drying chamber.
- To reduce heat losses due to conduction and to conserve heat energy within the drying space, the drying chamber was thermally insulated with fiberglass because of its low cost, effectiveness and availability.

3.2.9. Fabrication, Assembly and Installation of the Waste Heat Recovery Equipment

The hot air tray dryer and heat exchanger were fabricated in line with the results obtained in the materials sizing section. The rotating blades of the turbine were initially intended to be procured on the grounds of the difficulty envisaged in getting the right materials as well as experienced personnel for its fabrication. However, the turbine blades were eventually fabricated after series of attempts to procure one failed. Other components of the dryer such as the air blower, weight and temperature sensors, the moist air outlet fan, the Arduino primed control panel, the solar panel and its allied

accessories, etc, were procured from various markets in the South-eastern part of Nigeria. After the assembly of the fabricated and procured parts, the test rig of the waste heat recovery equipment was installed at the plant house of Imo State Polytechnic, Umuagwo-Ohaji; and thereafter, subjected to experimental investigation. The pictures of some component parts of the waste heat recovery dryer, the assembled test rig and samples of the selected crops for drying are shown in Plates 3.1 to 3.9, while the Bill of Engineering Measurement and Evaluation (BEME) is shown in Appendix C.

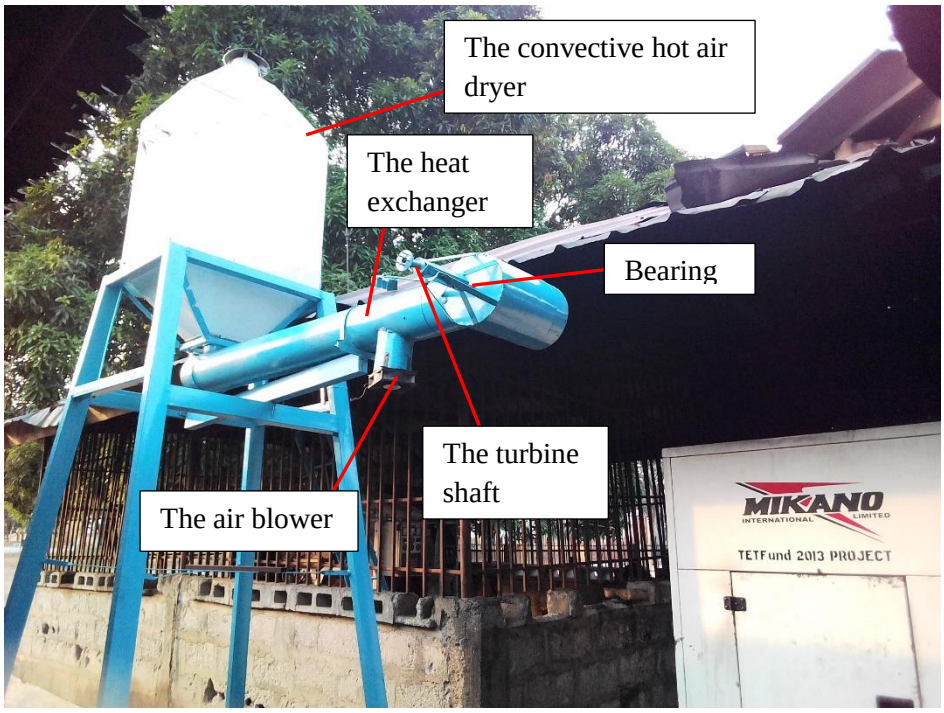

Plate 3.1: The test rig installed at the 250kVA generator set at the plant house of Imo State Polytechnic, Umuagwo.

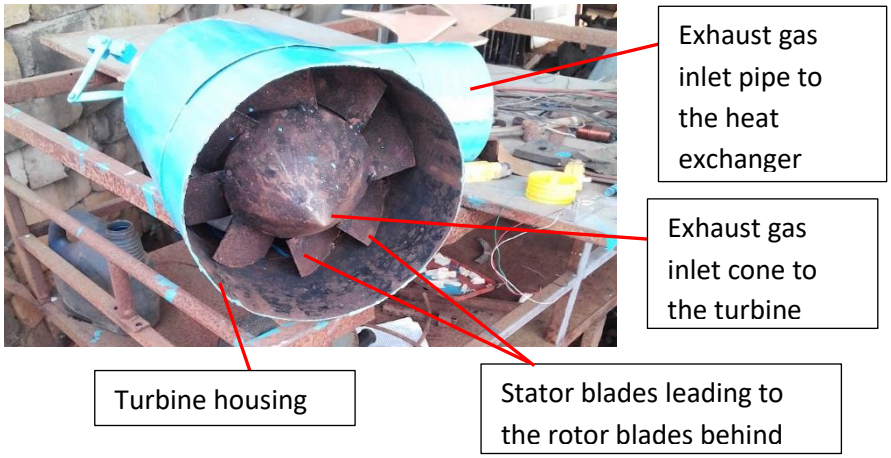

Plate 3.2: Some components of the turbine

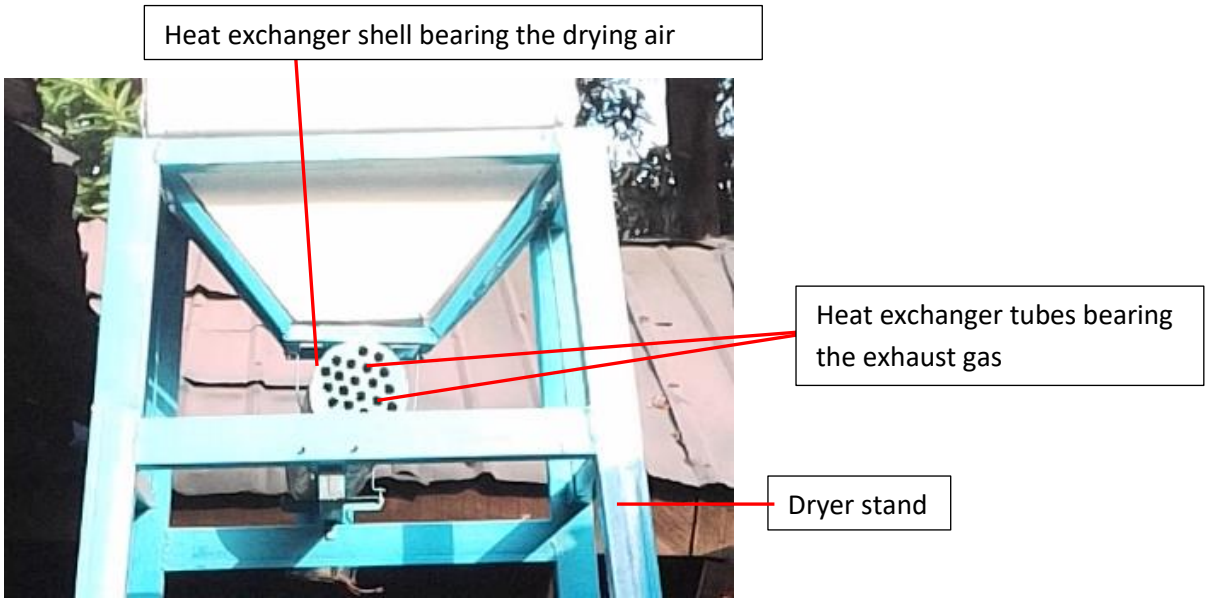

Plate 3.3: The features of the heat exchanger

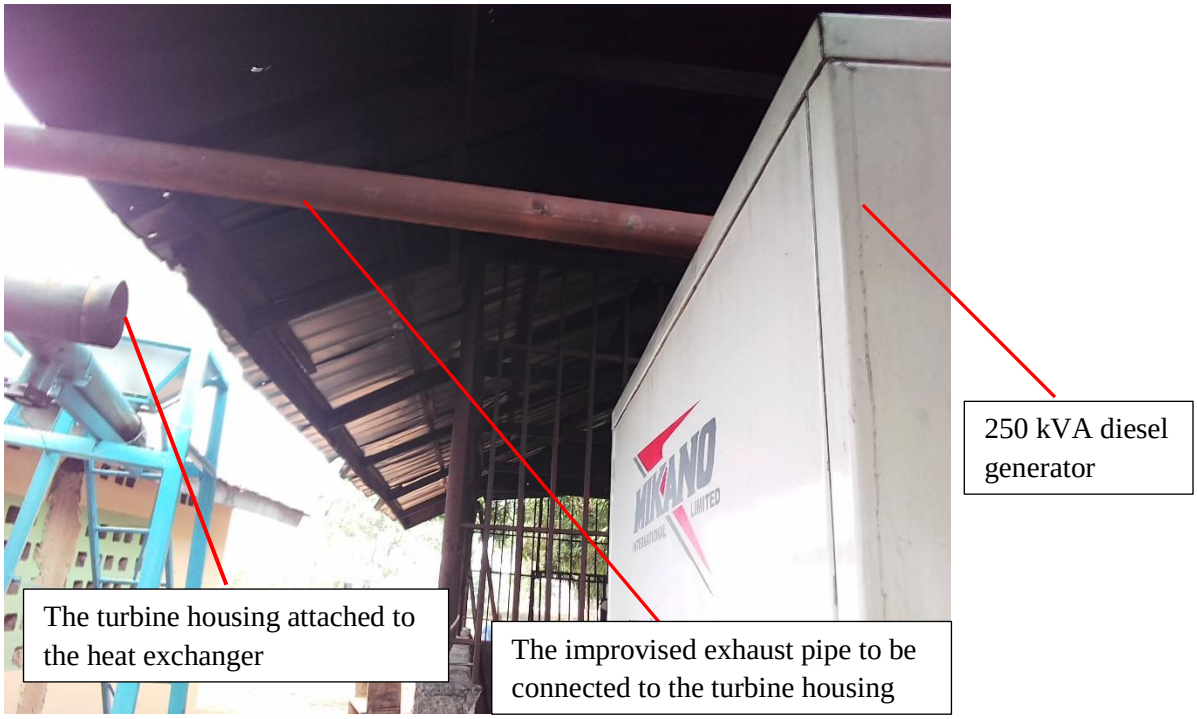

Plate 3.4: The point of connection of the turbine housing to the 250kVA generator set

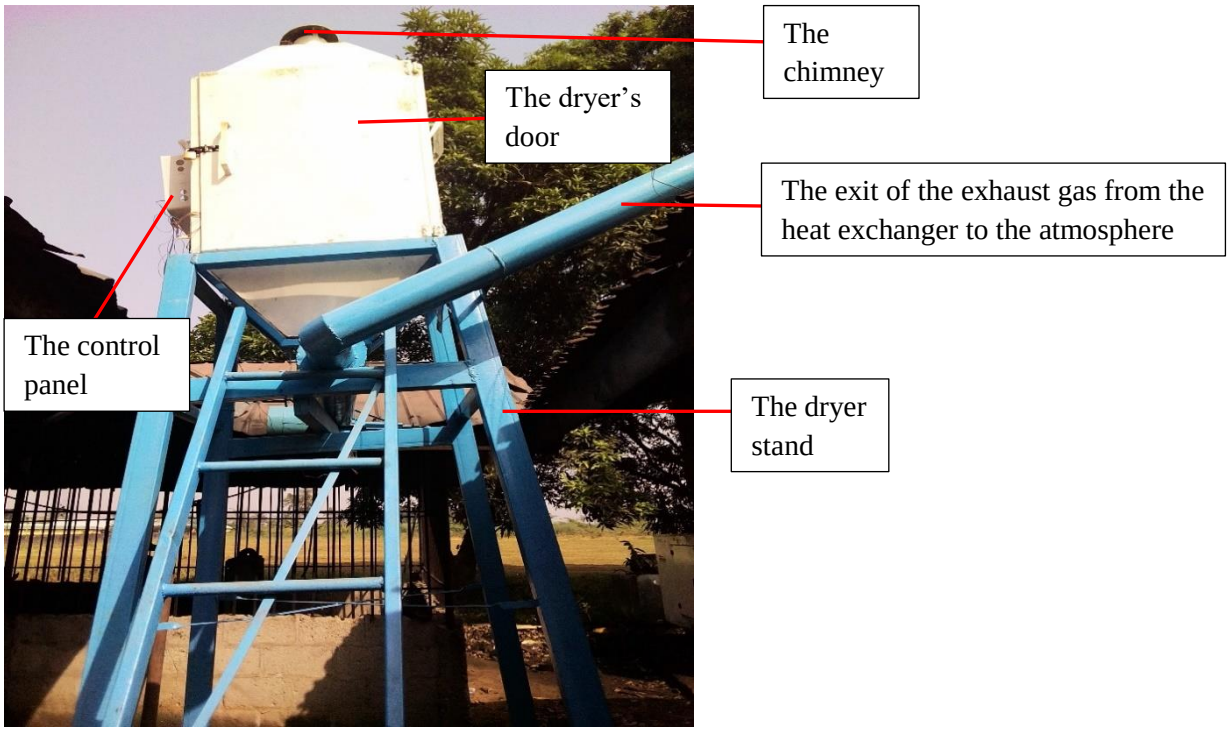

Plate 3.5: The front view of the waste heat recovery dryer.

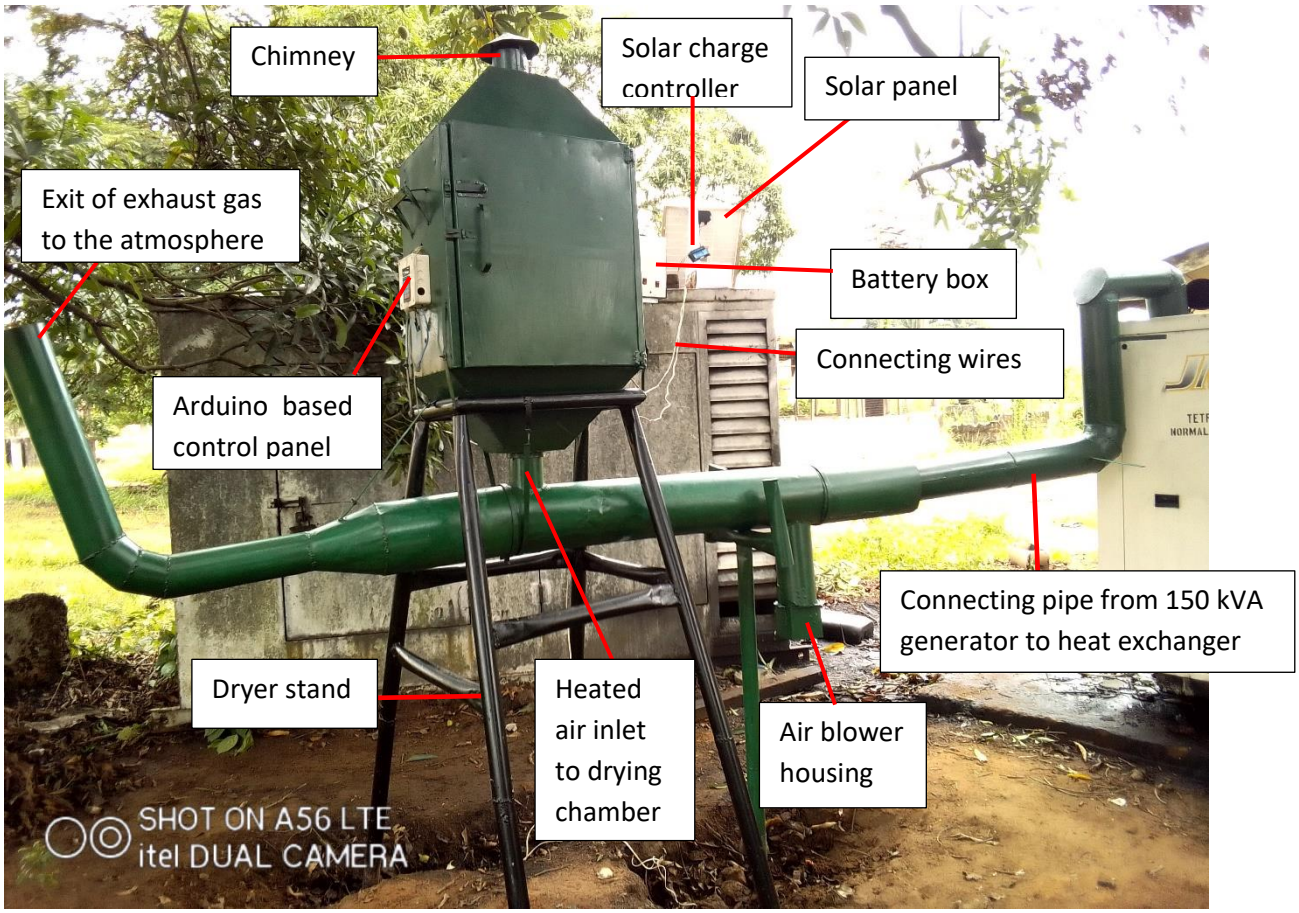

Plate 3.6: The tray dryer connected to a 150 kVA generator

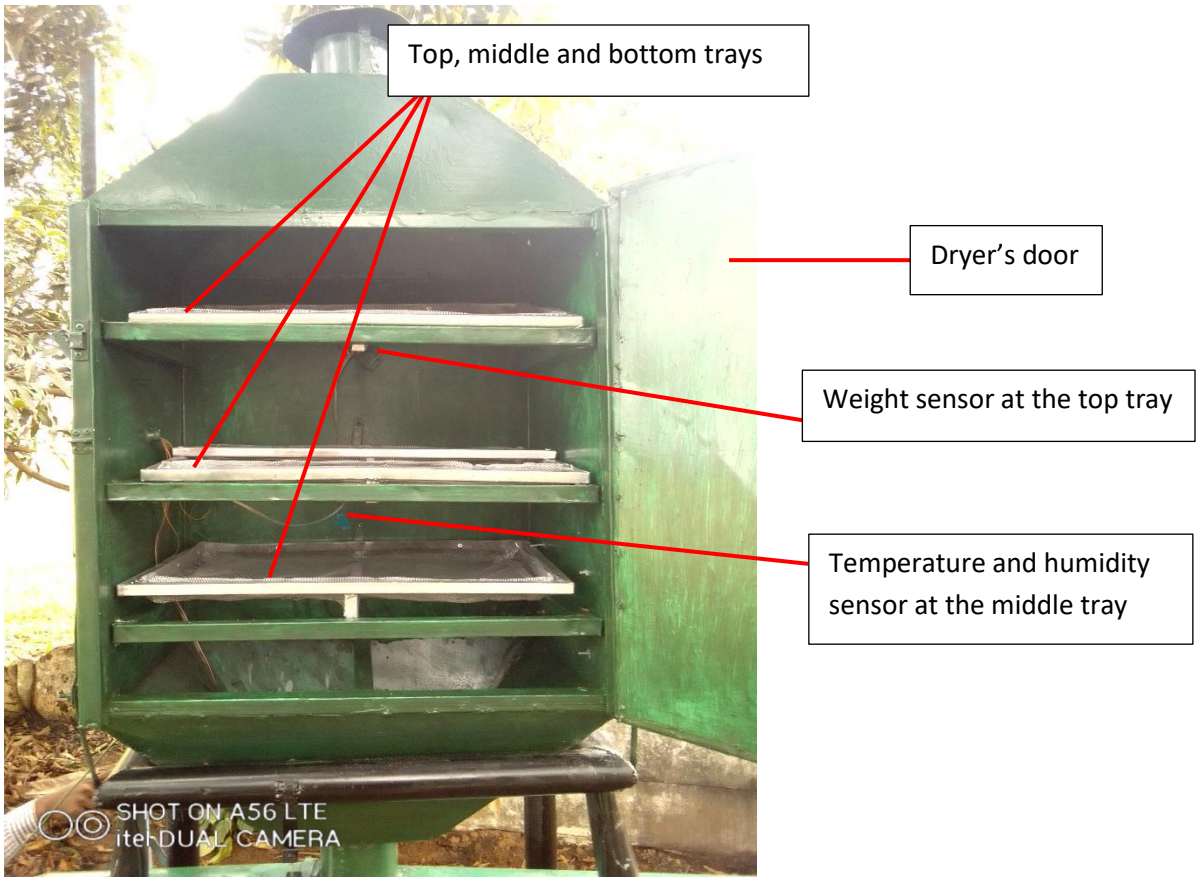

Plate 3.7. The interior of the dryer

Plate 3.8: Blanched yam slices in the tray before drying in the hot air tray dryer

Plate 3.9: Fresh maize grains during drying in the hot air tray dryer

3.2.10. Computer Programs for Processing and Analysis of the obtained Results

i. Design-Expert 11.0 version software was used to analyze the experimental data and to perform response surface/contour lines as well as to obtain three dimensional graphs of response.

ii. Microsoft Excel 2016 package, was used to plot some relevant graphs and to fit some known thin-layer drying models with the experimental data.

iii. MATLAB software will also be used for the analysis of the experimental results.

3.2.11. Experimental Procedure

During drying, the thermal conductivity of food products within the falling rate period is low, and for this reason, the heat transfer to the inner sections of the drying product by convective heating is limited, resulting in more energy consumption (Motevali, Minaei, Banakar, Ghobadian and Khoshtaghaza, 2014a). This high energy consumption problem was minimized by resorting to thin layer drying for the product samples as recommended by Ohanwe and Sule (2007), in order to improve the rate of heat transfer across the maize grains and yam slices to be dried; thus making the drying process more convenient and cost effective. Thus freshly harvested ears of yellow maize and

yam tubers were obtained from the Relief Market, Owerri. The maize husks were removed and the grains shelled using a kitchen knife. This operation was carefully carried out to avoid causing damage to the soft wet grains, and the grains were eventually cleaned of dirt. Uniform corn kernels of average radius of approximately 3.49 mm were used for the study. The yam tuber was washed, peeled, sliced into slabs of three different thicknesses, blanched, dewatered and stored in a refrigerator. Dry moisture can was procured and weighed. Then samples of both wet grains and yam slices were in turn placed in it and reweighed, and the weight of the samples were taken. Dry matters of 10g samples of the wet grains and yam slices were obtained separately by drying in an oven at 105°C for 24 hours to constant weight in accordance with standard methods (Ranganna, 1986; Kouadio *et al*., 2017). A table top Binatone oven (TT0-5800, China) was used to carry out this operation. This method was used to determine the initial moisture contents of the drying samples. Samples of the white yam slices of 1, 1.5 and 2cm, were prepared for the study using blanching water of 80^0 C and 30 minutes soaking time based on data from literature. Sanful *et al*. (2015) observed that fresh yam slices had higher activation energies than blanched yam slice samples during dehydration process for samples of the same thickness, indicating more ease of release of water in the blanched samples than in the fresh samples. Hence the reason for the application of blanching before drying of the yam slices. The prepared maize grains and yam slices for the drying experiment were preserved from decay and moisture loss by keeping them in sealed plastic bags and stored in a refrigerator at $4-8℃$. From the stored samples, 1500 g of maize and 2200g of yam slices were used in each drying experimental treatment. The samples were placed in a wire mesh tray of dimension: 66 cm x 47 cm and introduced into the drier. Pertinent information from the literature shows that maize is dried over a temperature range of 30-110°C (Nazmi and Esref, 2013; Zahra *et al*., 2014; Dagde and Iminabo, 2018); and yam, 50-95°C (Ramiro *et al*., 2011; Aasa *et al*., 2012 ; Sanful *et al*., 2015; Ajala and Abubakar, 2018; Akinola and Ezeorah, 2019). Thus before each drying experiment, the drier was allowed to run without load in order to achieve steady state conditions of the drying air at each of the pre-set temperatures:50, 55, 60, respectively for maize grains drying;

and 55, 65 and 75°C, respectively for the drying of yam slices. The drying air velocities investigated for both products were 1.0, 1.5 and 2.0 m/s, respectively. The maize grains were dried from the initial moisture content to 10% final moisture content (wet basis). While yam slices were dried from the initial moisture content to 12% safe final moisture content (wet basis). Drying experiments were conducted in triplicates and average data values were recorded for analysis. During the drying experiment in the convective dryer, the weight losses of the drying samples were monitored and recorded (every 30 minutes for maize grains, and 20 minutes for yam slices) with a strain gauge-balance beam load cell (Model: MLC 825, China) of 30mA, 5V and accuracy, ± 0.05 g attached to the tray. DHT11 temperature-humidity sensors of 20mA, 5V each were placed at the inlet of the hot air entering the dryer, at the drying tray, and at the exit of the hot air to measure the temperatures and humidities of the drying air at these designated positions. One sensor was also placed outside the dryer to record the ambient temperature and humidity. The speed of the drying air was measured using a speed meter (hot wire anemometer, model 20004 AHYK). The dryer consists of three trays. However, for the sake of experimental investigation, and to easily achieve an adequate control of the conditions of the drying air across the drying product in the chamber, only the tray at the middle was used for the drying experiments. During a no load test of the dryer, the temperature of the hot air at inlet to the drying chamber T_o, was measured. The temperatures of the topmost tray, T_1, middle tray T_2 and the bottom tray, T_3, would be measured to establish the temperature profile for the dryer for no load test.

3.2.12. Experimental Design

The experiments carried out were factorial in nature and conducted in a Completely Randomized Design (CRD). Two factors, viz: drying air temperature (T) and drying air velocity (V) are considered for the drying of maize; while for the drying of yam, three factors are considered viz: air temperature (T), air velocity (V), and slice thickness (X). The factors have three levels each: T_1, T_2 and T_3; v_1, v_2 and v_3, and X_1, X_2 and X_3, respectively. Their values are: 50, 55 and 60℃; 1.0, 1.5 and 2.0 m/s respectively for the drying of the maize grains; and 55, 65 and 75℃; 1.0, 1.5 and 2.0 m/s; 1cm, 1.5cm and 2.0cm respectively for the drying of yam slices. The experiments were

conducted in three replications, and the average data obtained were used for analysis. The maize grains has two factors T and v under consideration with three levels; and the treatment combinations of these Factors are given numerically as $3 \times 3 = 9$ which is a 3^2 factorial experiment for maize grain drying; while yam slice drying has three factors viz, T, V and X with three levels; and their treatment combinations are $3 \times 3 \times 3 = 27$ which is a 3^3 factorial experiment. Factorial experiments are presented in an exponential form, p^s where p is the size of the levels and s is the number of factors (Obi, 1995). However, since there are three replicates of the experiments, then the total number of data or experimental points (number of observations) becomes $3 \times 9 = 27$ for maize drying and $3 \times 27 = 81$ for yam slice drying. Tables 3.3 and 3.4 show the treatment combinations of the experiments in CRD whose interactions are to be studied. The average results for the experimental layout based on the replications shown in Tables 3.3 and 3.4 for the drying of maize grains and yam slices in terms of drying time and energy consumption are presented in Appendices F1 to F3.

Table.3.3. Experimental layout of the treatment combination for the drying of maize grains

Air velocity (m/s)	Drying air temperature T (℃)			Total	Mean
	$\mathbf{T_1}$	$\mathbf{T_2}$	$\mathbf{T_3}$		
$\mathbf{v_1}$	v_1T_1	v_1T_2	v_1T_3		
$\mathbf{v_2}$	v_2T_1	v_2T_2	v_2T_3		
$\mathbf{v_3}$	v_3T_1	v_3T_2	v_3T_3		
Total					
Mean					
$\mathbf{v_1}$	v_1T_1	v_1T_2	v_1T_3		
$\mathbf{v_2}$	v_2T_1	v_2T_2	v_2T_3		
$\mathbf{v_3}$	v_3T_1	v_3T_2	v_3T_3		
Total					
Mean					
$\mathbf{v_1}$	v_1T_1	v_1T_2	v_1T_3		
$\mathbf{v_2}$	v_2T_1	v_2T_2	v_2T_3		
$\mathbf{v_3}$	v_3T_1	v_3T_2	v_3T_3		
Total					
Mean					

Table.3.4. Experimental layout of the treatment combination for the drying of yam slices.

Thickness (cm)	Air velocity (m/s)	Drying air temperature T (℃)			Total	Mean
		$\mathbf{T_1}$	$\mathbf{T_2}$	$\mathbf{T_3}$		
	$\boldsymbol{v_1}$	$x_1v_1T_1$	$x_1v_1T_2$	$x_1v_1T_3$		
$\mathbf{x_1}$	$\boldsymbol{v_2}$	$x_1v_2T_1$	$x_1v_2T_2$	$x_1v_2T_3$		
	$\boldsymbol{v_3}$	$x_1v_3T_1$	$x_1v_3T_2$	$x_1v_3T_3$		
	Total					
	Mean					
	$\boldsymbol{v_1}$	$x_2v_1T_1$	$x_2v_1T_2$	$x_2v_1T_3$		
$\mathbf{x_2}$	$\boldsymbol{v_2}$	$x_2v_2T_1$	$x_2v_2T_2$	$x_2v_2T_3$		
	$\boldsymbol{v_3}$	$x_2v_3T_1$	$x_2v_3T_2$	$x_2v_3T_3$		
	Total					
	Mean					
	$\boldsymbol{v_1}$	$x_3v_1T_1$	$x_3v_1T_2$	$x_3v_1T_3$		
$\mathbf{x_3}$	$\boldsymbol{v_2}$	$x_3v_2T_1$	$x_3v_2T_2$	$x_3v_2T_3$		
	$\boldsymbol{v_3}$	$x_3v_3T_1$	$x_3v_3T_2$	$x_3v_2T_3$		
	Total					
	Mean					
	$\boldsymbol{v_1}$	$x_1v_1T_1$	$x_1v_1T_2$	$x_1v_1T_3$		
$\mathbf{x_1}$	$\boldsymbol{v_2}$	$x_1v_2T_1$	$x_1v_2T_2$	$x_1v_2T_3$		
	$\boldsymbol{v_3}$	$x_1v_3T_1$	$x_1v_3T_2$	$x_1v_3T_3$		
	Total					
	Mean					
	$\boldsymbol{v_1}$	$x_2v_1T_1$	$x_2v_1T_2$	$x_2v_1T_3$		
$\mathbf{x_2}$	$\boldsymbol{v_2}$	$x_2v_2T_1$	$x_2v_2T_2$	$x_2v_2T_3$		
	$\boldsymbol{v_3}$	$x_2v_3T_1$	$x_2v_3T_2$	$x_2v_3T_3$		
	Total					
	Mean					
	$\boldsymbol{v_1}$	$x_3v_1T_1$	$x_3v_1T_2$	$x_3v_1T_3$		
$\mathbf{x_3}$	$\boldsymbol{v_2}$	$x_3v_2T_1$	$x_3v_2T_2$	$x_3v_2T_3$		
	$\boldsymbol{v_3}$	$x_3v_3T_1$	$x_3v_3T_2$	$x_3v_2T_3$		
	Total					
	Mean					
	$\boldsymbol{v_1}$	$x_1v_1T_1$	$x_1v_1T_2$	$x_1v_1T_3$		
$\mathbf{x_1}$	$\boldsymbol{v_2}$	$x_1v_2T_1$	$x_1v_2T_2$	$x_1v_2T_3$		
	$\boldsymbol{v_3}$	$x_1v_3T_1$	$x_1v_3T_2$	$x_1v_3T_3$		
	Total					
	Mean					
	$\boldsymbol{v_1}$	$x_2v_1T_1$	$x_2v_1T_2$	$x_2v_1T_3$		
$\mathbf{x_2}$	$\boldsymbol{v_2}$	$x_2v_2T_1$	$x_2v_2T_2$	$x_2v_2T_3$		
	$\boldsymbol{v_3}$	$x_2v_3T_1$	$x_2v_3T_2$	$x_2v_3T_3$		
	Total					
	Mean					
	$\boldsymbol{v_1}$	$x_3v_1T_1$	$x_3v_1T_2$	$x_3v_1T_3$		
$\mathbf{x_3}$	$\boldsymbol{v_2}$	$x_3v_2T_1$	$x_3v_2T_2$	$x_3v_2T_3$		
	$\boldsymbol{v_3}$	$x_3v_3T_1$	$x_3v_3T_2$	$x_3v_2T_3$		
	Total					
	Mean					

3.2.13. Performance Evaluation

The performance evaluation of the tray dryer by experimentation with maize grains and yam slices as drying products was achieved by:

- Determining the thermal efficiency, effective moisture diffusivity, activation energy and energy consumption parameters for the thin-layer drying of the selected food crops.
- Optimizing the drying conditions and generate model equations for the operating parameters and their responses using Response Surface Methodology with Design Expert software.
- Studying the interactions between the factors and the responses, showing significant and non-significant interactions.
- Testing of some mathematical drying models used in describing the thin-layer drying kinetics of food crops; and determining the most appropriate among the models that are suitable for the drying of the selected food crops.

3.2.13.1. The Response Surface Methodology

The Response Surface Methodology (RSM) is a statistical tool used for studies on optimization of drying process parameters of food products, **among others**. It makes use of the quantitative data from suitable experimental designs to determine and at the same time, solve multivariate problems. It generates equations that describe the effect of independent variables on responses, determine interrelationships among dependent variables, and represent the combined effect of all dependent variables in any response. This procedure helps a researcher to make effective investigation of a process or system (Zafer and Filiz, 2009b). The optimization of processes in industries requires some response variables which measure the performance of the systems to be optimized. Since the variables are indices of performance, some were maximized while others were minimized. In many situations, the responses compete in the sense that an improvement in one response may have an inverse effect on another variable, thus making the situation to be more complicated (Zafer and Filiz, 2009b). The solution of this problem has witnessed the use of several approaches such as the constrained optimization procedure; the superimposition of the contour diagrams of the different

response variables; and the use of a desirability function combining all responses into one measurement (Eren and Kaymak-Ertekin, 2007). In this work, desirability functions were considered as the criteria for determining the minimum values of drying time and specific energy consumption, and the maximum thermal efficiency. The appropriateness (adequacy) of generated models is checked by the values of R^2, the adjusted R^2 (adj-R^2), the Predicted R^2 (pre-R^2), Adeq Precision, and the coefficient of variance (C.V). The adequacy of the models is such that $R^2 > 0.95$; Pre-$R^2 > 0.7$; (Adj-R^2–Pre-R^2) < 0.2; Adeq Precision > 4**;** and C.V < 10 (Myers and Montgomery, 2002). Design Expert statistical tool (Ver. 11.00) was employed for the optimization analysis of the drying process and the fitting of the 3-D response surface plots, which yields the following:

i) Model equations using the factors (drying air temperature, velocity, and also slice thickness for yam drying) as independent variables, and response variables such as drying time, specific energy consumption, and thermal efficiency.

ii) The effect of the interactions between the experimental factors and responses, showing significant and non-significant interactions.

iii) The graphical representation of the relationship between the dependent and independent variables using the response surface methodology.

3.2.13.2. **Determination of Kinetics of the Tray Dryer**

The variation in moisture ratio (MR) versus time (t) is highly required in thin layer drying equations. Hence, at the end of the drying experiments of the sample products, MR would be calculated at drying temperatures ranging from 50 ℃ to 60 ℃ for the maize grains; and 55 ℃ to 75 ℃ for the yam slices. According to Zafer and Filiz (2009a), statistical methods of regression and correlation analysis are usually required in the mathematical modelling of food crops drying. To determine the most applicable drying models for the sample products in the tray dryer, some constant values which indicate how suitable a model is must be determined. The constants are obtained by first of all plotting the values of MR against t followed by carrying out a regression analysis with some known thin layer drying mathematical models (selected from Eqns 2.15 to 2.23 and others from Table 2.5). However, the selection of the most suitable models for the description of the drying characteristics

of the dried products depends on some statistical indicators. These statistical indicators are the coefficient of determination (R^2) which provides information on the goodness of fit of the models; the sum of squares error (SSE) test and the root mean square error ($RMSE$) analysis, respectively. Higher values of $R^2$of any of the models show how more appropriate the model is in predicting the drying characteristics of the sample product. In a similar way, lower values of SSE and $RMSE$ of any model indicate how more appropriate the model is in predicting the drying behavior of the drying sample (Zafer and Filiz, 2009a; Kucuk *et al*., 2014). The expressions for the calculation of the values of R^2, SSE and $RMSE$ presented in Eqns (3.97 to 3.99) are used in this study (Zafer and Filiz, 2009a; Sanful *et al*., 2015).

$$R^2 = 1 - \left[\frac{\sum_{i=1}^{n}\left(MR_{pre,i} - MR_{exp,i}\right)^2}{\sum_{i=1}^{n}\left(\overline{MR_{pre,i}} - MR_{exp,i}\right)^2}\right] \qquad (3.97)$$

$$SSE = \sum_{i=1}^{N}(X_i - \bar{X})^2 \qquad (3.98)$$

$$RMSE = \left[\frac{1}{N}\sum_{i=1}^{N}\left(MR_{pre,i} - MR_{exp,i}\right)^2\right]^{1/2} \qquad (3.99)$$

where, *N* represents the number of observations, *n* is the total number of constants in the drying model, $MR_{pre,i}$ is the *i*th predicted moisture ratio values, $MR_{exp,i}$ is the *i*th experimental moisture ratio values, while $\overline{MR_{pre,i}}$ is the mean of the predicted moisture ratio. The values of the statistical model parameters and constants obtained from nonlinear regression of some selected thin layer drying models for corn and yam drying are presented in Appendices 4.5 to 4.11. Ten known thin-layer drying models were used to study the drying behavior of the maize grains, while six models were used in studying the drying characteristics of the yam slices.

3.2.13.3. **Determination of the effective moisture diffusivity (D_e).**

A complete drying profile comprises three stages, viz, the initial period, a constant-rate period, and a falling-rate period as show in the drying curve (Figure 2.28) in the previous chapter above. Drying of most food materials usually occurs within the falling rate period. This gives an indication that the transfer of moisture during drying is influenced by internal diffusion. Fick's second law of diffusion

is used to describe the internal diffusion that takes place in the falling rate period for most food products (Nwajinka, Nwuba, and Udoye, 2014; Onu *et al*., 2017) as seen in Eqn (3.100):

$$\frac{\delta M}{\delta t} = D\nabla^2 M \qquad (3.100)$$

where: M = moisture content (kg water/kg dry matter), t is the drying time, and D = diffusivity (m^2/s).

From the literature, Eqn (3.100) can be analytically solved with some pertinent assumptions as seen below (Zafer and Filiz, 2009a; Amira *et al*., 2014).

i. External resistance and shrinkage of the product during the process of drying were considered negligible;
ii. The yam slices are considered to be slab-shaped materials;
iii. The maize kernels are considered to be spherically-shaped materials
iv. Diffusivity and temperature throughout the drying process are constant;
v. The density of the drying air is constant while its velocity was uniformly distributed in the drying chamber.
vi. The drying product samples are isotropic and homogeneous;
vii. The pressure variations are neglected;
viii. Evaporation occurs only at the surface;
ix. Moisture distribution is uniform initially and symmetrical during the process;
x. The heat transfer within the product takes place by conduction and by convection externally.

Thus the analytical solution of the Fick's second law of diffusion (Eqn 3.100) as presented in (Amira *et al*., 2014; Beigi, 2016; Onu *et al*., 2017) for slab-shaped materials such as yam slices is:

$$MR = \frac{M_t - M_e}{M_0 - M_e} = \frac{8}{\pi^2}\sum_{n=0}^{\infty}\frac{1}{(2n+1)^2}exp\left[-\frac{(2n+1)^2\pi^2 D_e d_t}{4L^2}\right] \qquad (3.101)$$

where M_t is the moisture content at any given time (kg water/ kg dry matter); M_e is equilibrium moisture content (kg water/kg dry matter); M_0 is the initial moisture content; d_t is the drying time (min) and D_e is the effective diffusivity (m^2/s); n is the number of terms considered (say, 0,1,2,3…); MR is the moisture ratio as expressed in Eqn (2.11) while L is the half thickness of the slice (m) (Zafer and Filiz, 2009a).

The expansion series of Eqn (3.101) for values of n ranging from 0 to 2 yields Eqn (3.102) (Lopez, Iguaz, Esnoz, and Vireda, 2000; Onu *et al*., 2017):

$$MR = \frac{8}{\pi^2}\left\{\exp\left[-\left(\frac{\pi}{2L}\right)^2 D_e d_t\right] + \frac{1}{3^2}\exp\left[\left(\frac{3\pi}{2L}\right)^2 D_e d_t\right] + \frac{1}{5^2}\exp\left[-\left(\frac{5\pi}{2L}\right)^2 D_e d_t\right] + \cdots\right\} \quad (3.102)$$

Sacilik, (2007) observed that the first term of Eqn (3.102) has the tendency of dominating the other expansion series solution terms. Also, for long period of drying time, d_t is very large; and for this reason, the first-term alone of the series equation is found to be significant for values of $\frac{D_e d_t}{4L^2} > 0.02$ with error not up to 3% (Onu *et al*., 2017). Therefore, Eqn (3.102) is simplified thus:

$$MR = \frac{8}{\pi^2}\left\{\exp\left[-\left(\frac{\pi}{2L}\right)^2 D_e d_t\right]\right\} \quad (3.103)$$

Taking the natural logarithm of Eqn (3.103) produces a linear equation of the form: $y = mx + c$ as seen in Eqn (3.104):

$$\ln MR = \ln\frac{8}{\pi^2} - \left[\frac{\pi^2 D_e d_t}{4L^2}\right] \quad (3.104)$$

From the experimental data, plotting $\ln MR$ versus drying time gives a straight line graph; therefore, the term, $-\left[\frac{\pi^2 D_e}{4L^2}\right]$ in Eqn (3.104) represents the slope, k_0. Hence the calculation of the effective moisture diffusivity can be done using Eqn (3.105):

$$D_e = -\left[\frac{4L^2}{\pi^2}\right] \times k_0 \quad (3.105)$$

For spherically shaped materials such as maize kernels, Eqn (3.106) is used based on the analytical solution of Fick's second law of diffusion for spheres (Di Matteo *et al*., 2000; Abasi *et al*., 2017):

$$\ln MR = \ln\frac{6}{\pi^2} - \left[\frac{\pi^2 D_e d_t}{r^2}\right] \quad (3.106)$$

Therefore, the effective moisture diffusivity can be obtained using Eqn (3.107):

$$D_e = -\left[\frac{r^2}{\pi^2}\right] \times k_1 \quad (3.107)$$

where r is radius of sphere (m) and k_1 is the slope of the line.

3.2.13.4. Determination of the activation energy (E_A)

Activation energy in drying, is the minimum energy needed to initiate a drying process. For this to be obtained, D_e should be related with drying temperature as expressed in the Arrhenius equation as seen in Eqn (3.108) (Onu *et al*., 2017):

$$D_e = D_o exp\left[\frac{-E_A}{RT_a}\right] \quad (3.108)$$

where D_o(m^2/s) is the Arrhenius constant. D_o is the same as the diffusivity at infinitely high temperature. E_A is the energy of activation (kJ/ mol), R is the universal gas constant (8.314J/ mol K), and T_a is the absolute temperature (K). The natural logarithm of Eqn (3.108) gives a straight line graph as seen in Eqn (3.109) (Nwajinka *et al*, 2014; Onu *et al*., 2017):

$$\ln D_e = \ln D_0 - \frac{E_A}{RT_a} \quad (3.109)$$

Plotting the graph of $\ln D_e$ versus $\frac{1}{T_a}$, gives the slope, $-\frac{E_A}{R}$ which is used to determine the activation energy as seen in Eqn (3.110):

$$E_A = k_2 \times R \quad (3.110)$$

where k_2 is the slope of the line.

3.2.13.9. **Determination of the Specific power consumption**

Specific power consumption (SPC) is the ratio of the amount of electric power consumed to the mass of material to be dried, and is expressed as (Vieira, Estrella and Rocha, 2007; Motevali and Chayian, 2017):

$$\mathrm{SPC} = \frac{\mathrm{EPC}}{m_w} \qquad (3.111)$$

where EPC is the total electric power consumed during drying process, and m_w is the mass of material to be dried.

3.2.13.10. **Determination of the Specific energy consumption**

Specific energy consumption (SEC) values can be obtained using Eqn (3.112). It is defined as the ratio of the total energy consumed in each drying phase, E_T (kWh) to the mass of water removed from sample product, M_w(kg) (Motevali *et al.,* 2014a; Onu *et al*., 2017):

$$SEC = \frac{E_T}{M_w} \qquad (3.112)$$

But

$$E_T = E_{elec} + E_{th} \qquad (3.113)$$

where E_{elec} or EPC, is the electrical energy expended in driving the blower and other electrical devices in the dryer; and E_{th} is the thermal energy required; and can calculated using Eqn (3.114) (Motevali, Minaei, Banakar and Darvishi. 2014b; Beigi, 2016; Onu *et al*., 2017):

$$E_{th} = (v_a A_t \rho_a C_a \Delta T) d_t \qquad (3.114)$$

where v_a, ρ_a and ρ_a are the drying air velocity (m/s), the air density (kg/m^3) and the specific heat capacity of air (kJ/kgK); A_t is the area of drying tray; ΔT is the difference between the ambient and hot air temperatures (K), and d_t is the total drying time of sample product. The density, ρ_a was calculated using Eqn (3.115) (Naghavi, Moheb and Ziaei-Rad, 2010):

$$\rho_a = \frac{101.325}{0.287 T_a} \qquad (3.115)$$

while the specific heat capacity of air, C_a is obtained using Eq (3.116) (Aghbashlo, Mobli, Rafiee and Madadlou, 2012):

$$C_a = 1.04841 - \frac{3.83719T_a}{10^4} + \frac{9.45378{T_a}^2}{10^7} - \frac{5.49031{T_a}^3}{10^{10}} + \frac{7.92981{T_a}^4}{10^{14}} \quad (3.116)$$

3.2.13.11. **Thermal Efficiency of the drying process**

This shows the extent of energy conversion or transfer process in a device that makes use of thermal energy. However, in the field of drying, it is referred to as the ratio of latent heat of vaporization of moisture in a sample of wet product to the amount of energy needed to vaporize moisture from free water. Mathematically, it is expressed as seen in Eqn (3.117) (Hebbar, Vishwanathan and Ramesh, 2004; Singh, 1994):

$$\eta_{th} = \frac{A_t.P.h_{fg}.(M_0 - M_f)}{Q_r.t.(100 - M_f)} \quad (3.117)$$

where h_{fg} is the latent heat of vaporisation of water (kJ/ kg)**,** P is the loading density of sample (kg/ m^2), and Q_r is the capacity of heating source used or the heat transfer rate (kW) (Ehiem *et al*., 2009), respectively. M_0 is the initial moisture content (wb), M_f is the final moisture content (wb). From Rajput (2010), Q_r can be calculated using Eqn (3.118):

$$Q_r = hA_{he}(t_s - t_b) \quad (3.118)$$

where h is the heat transfer coefficient (W/m^2 ℃), A_{he} is the surface area of the heat exchanger (m^2), t_s is the surface temperature of the heat exchanger tube (℃), t_b is the mean bulk temperature (℃) which can obtained using Eqn (3.119):

$$t_b = \frac{(t_i + t_0)}{2} \quad (3.119)$$

where t_0 (t_a) is the inlet temperature of air into the heat exchanger, and t_0 is the drying air temperature. The heat transfer coefficient (h) can be obtained using Eqn (3.120) (Rajput, 2010):

$$h = \frac{N_u k}{D} \quad (3.120)$$

where N_u is the Nusselt number, D is the diameter of heat exchanger and k is the thermal conductivity of air evaluated at the mean bulk temperature. N_u is obtained using Eqn (3.121) which is the correlation of turbulent flows for heating of fluids in circular tubes (Rajput, 2010):

$$N_u = 0.023(R_e)^{0.8}(P_r)^{0.4} \quad (3.121)$$

where P_r is the Prandtle number, and R_e is the Reynolds number obtained using Eqn (3.122) (Rajput, 2010):

$$R_e = \frac{\rho_a v_a D}{\mu_s} \quad (3.122)$$

where all the properties of air were evaluated at the mean bulk temperature, t_b with the exception of the dynamic viscosity, μ_s (kg/ms) which was evaluated at the surface temperature, t_s. The latent heat of vaporisation, h_{fg} may be obtained using Eqns (3.123 and 3.124) (Aghbashlo *et al*., 2012):

$$h_{fg} = 2.503 \times 10^6 - 2.386 \times 10^6(T_{abs} - 273.16) \quad 273.16 \leq T_{abs}(°K) \leq 338.72 \quad (3.123)$$

$$h_{fg} = \left(7.33 \times 10^{12} - 1.60 \times 10^7 {T_{abs}}^2\right)^{0.5} \quad 338.72 \leq T_{abs}(°K) \leq 533.16 \quad (3.124)$$

3.2.13.12. **Average drying rate of agricultural products**

The average drying rate (d_A) of agro-products can be calculated using Eqn (3.125) (Dassin, Godi and Kingsley, 2015; Matuam, Edoun, and Kuitche, 2015):

$$d_A = \frac{M_w}{d_T} \quad (3.125)$$

where d_T is the total drying time per batch.

CHAPTER FOUR

RESULTS AND DISCUSSION

4.1. Results

The results of the no load test of the dryer as well as those of the drying experiments with fresh maize grains and blanched yam slices at varying drying conditions of the drying air are presented in this section. Bone dry mass of 10g sample of the wet grains dried in an oven at 100 ℃ for 12hrs gave an initial moisture content of 35.6%. Hence for a weight of 1500g of the same sample during drying, the bone dry mass would be 966g. In the same vein, the bone dry mass of 10g sample of the blanched slices dried in an oven at 100 ℃ for 12hrs gave an initial moisture content of 69.5%. Hence for the weight of 2200g of the same sample during drying, the bone dry mass would be 671g. However, it was intended to dry the fresh samples of the maize grains (for the main experimental investigation) to a final moisture content of 0.10 $g_{water}/g_{wet\ matter}$, *for a shelf life of 5years* (Brooker, 1973); and the blanched samples of the yam slices to a final moisture content of 0.12 $g_{water}/g_{wet\ matter}$ (wet basis). Hence, the drying experiments of the samples of maize grains and yam slices for the experimental treatments were monitored (albeit not strictly) in order to stop drying at the designated moisture contents to avoid unnecessary waste of energy. ***Plates 3.8 and 3.9 show the pictures of the wet maize grains and blanched yam slices before drying; while the pictures of the dried maize grains and yam slice samples in the tray of the dryer under study are shown in Appendices M1 and M2, respectively.*** The average results of the experiments for the stipulated drying treatments of each of the sample products are shown in Appendices D1 to D36. Here, the values of the moisture content (wet basis), MC_{wb} (kg water/ kg solids); moisture content (dry basis), MC_{db} (kg water/ kg solids); drying rate, d_R (g_{water}/min) and the dimensionless moisture ratio, MR were obtained using Eqs. 2.7, 2.10, 2.13 and 2.12, respectively.

4.1.1. Results of the Test Rig at No Load

This section considers the results of the test rig at no load as show in Figures 4.1 to 4.3

4.1.1.1. Temperature Profile of the Drying Chamber at No Load

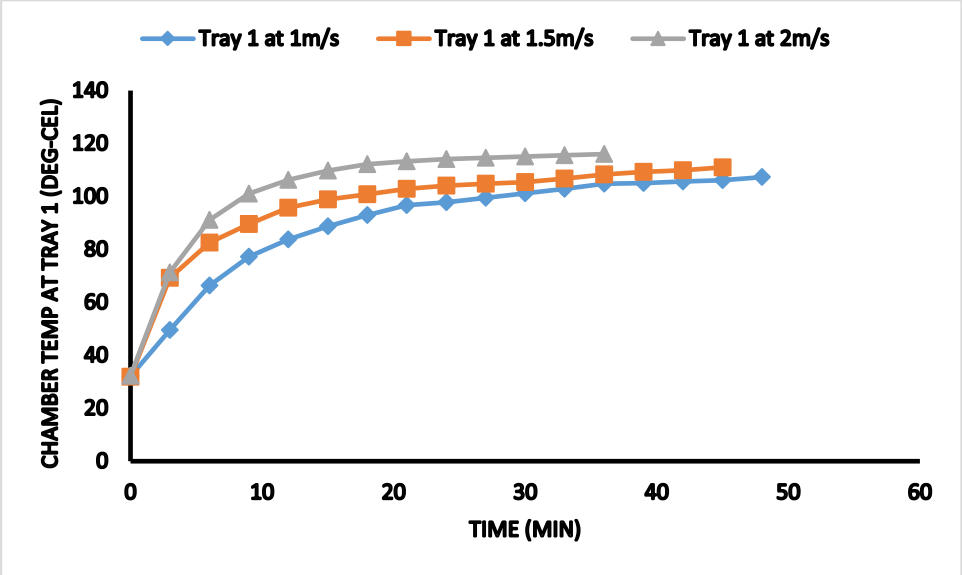

Figure 4.1: Temperature profile of the drying chamber at the topmost tray

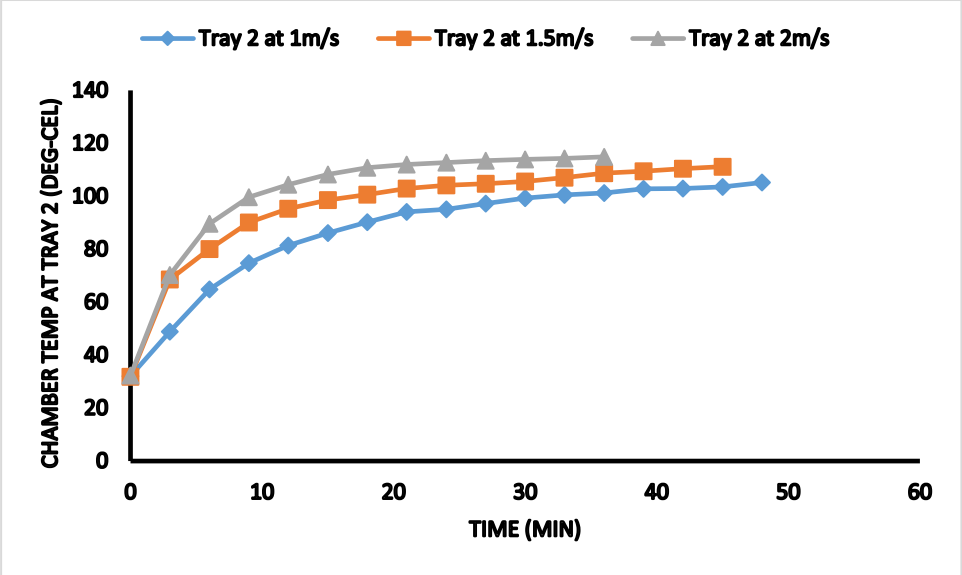

Figure 4.2: Temperature profile of the drying chamber at the middle tray

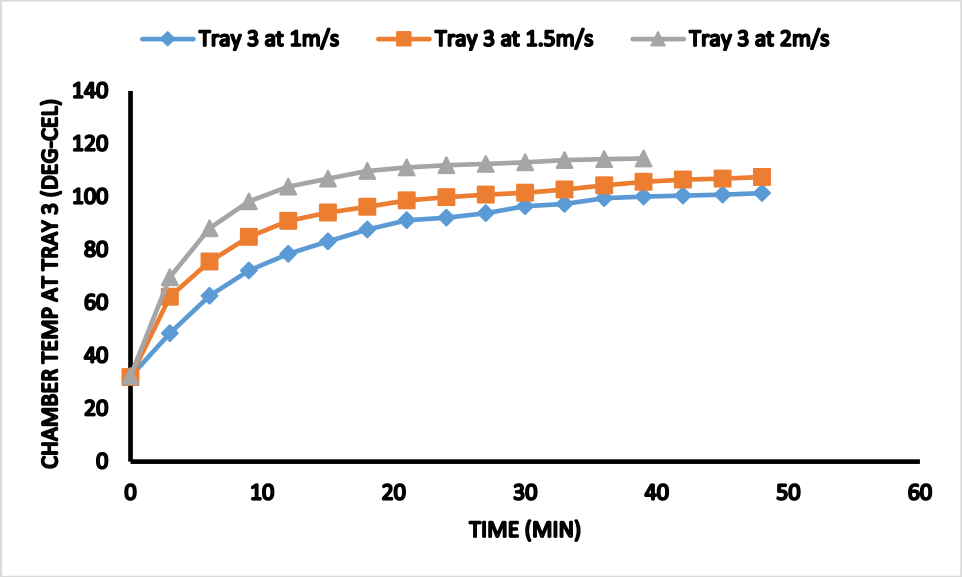

Figure 4.3: Temperature profile of the drying chamber at the bottom tray

4.1.2. Moisture Loss and Drying Time of the Product Samples

In this section, the results of the influence of the drying air temperature and velocity are presented as shown in Figures 4.4 to 4.8.

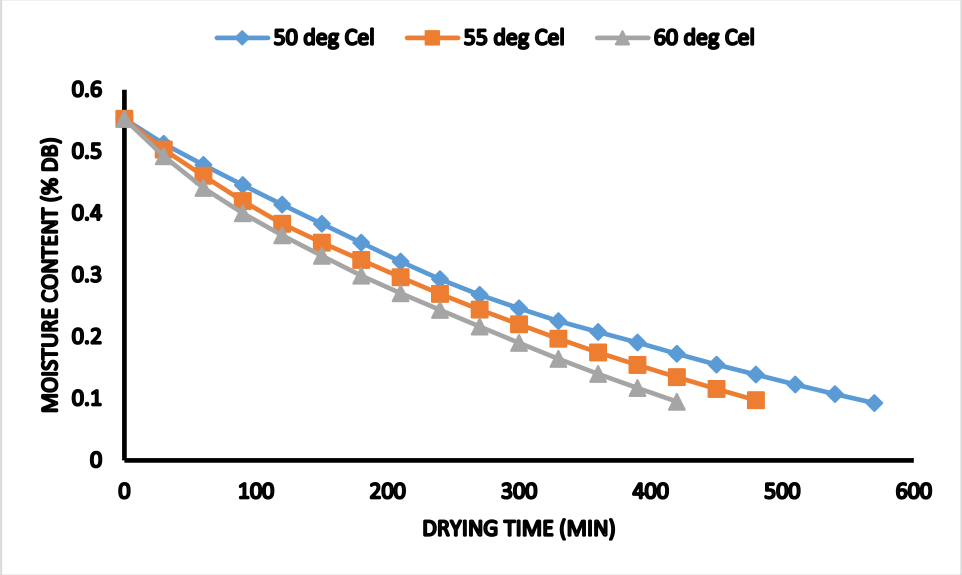

Figure 4.4: Moisture content against time for maize grain drying at an air velocity of 1m/s and varying air temperatures

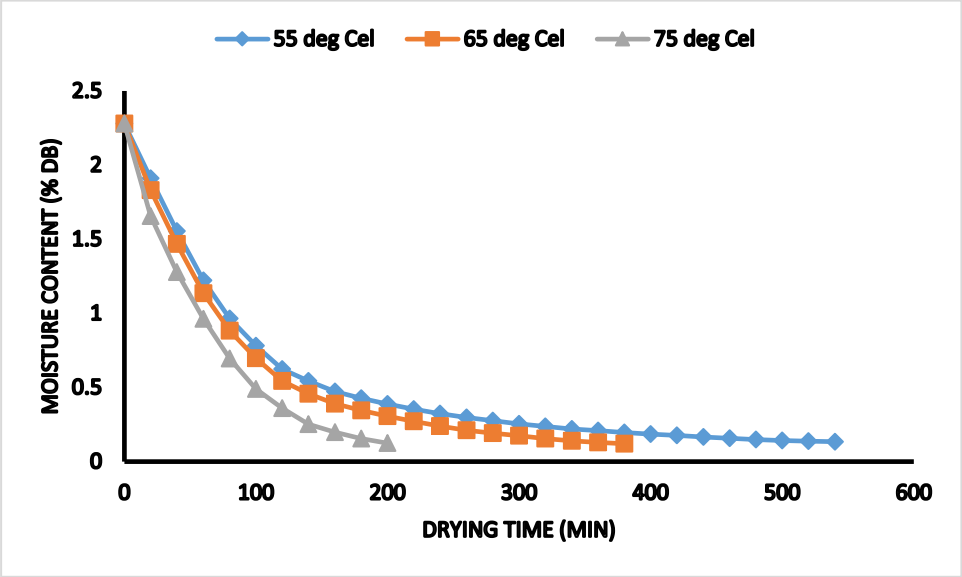

Figure 4.5: Moisture content against time of 1cm yam slices at 2m/s and varying air temperatures

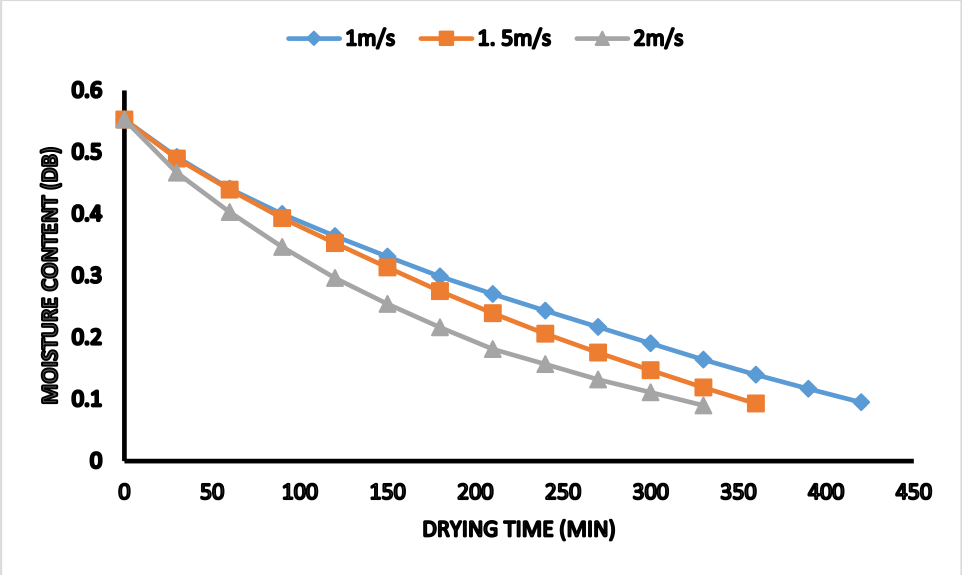

Figure 4.6: Moisture content against time for corn drying at air temperature of 60 ℃ and varying air velocities.

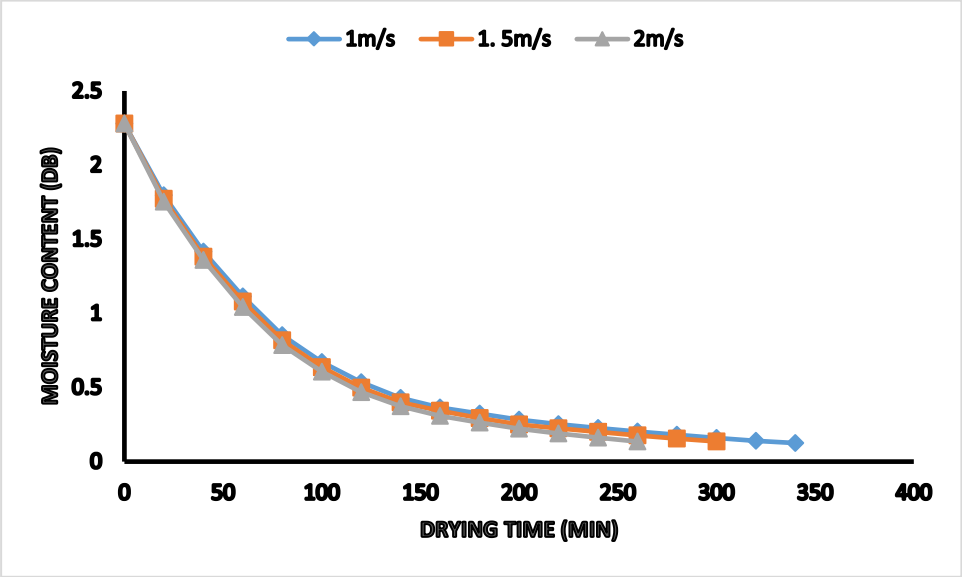

Figure 4.7: Moisture content against time for the drying of yam of 1.5cm slice thickness at an air temperature of 75 ℃ and varying air velocities.

4.1.3. Effect of Slice Thickness on Drying Time of the Yam Slices

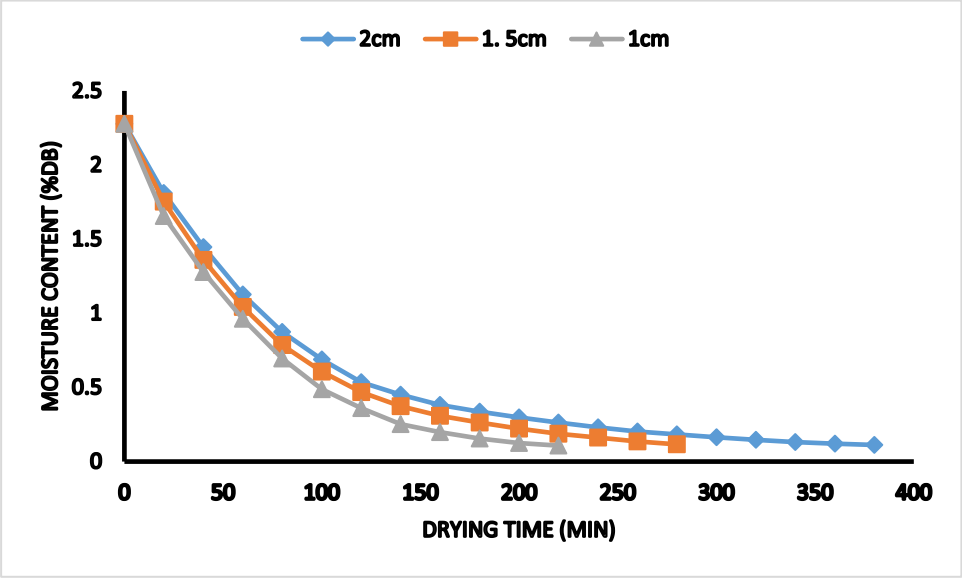

Figure 4.8: Moisture content against time of yam drying at 2m/s and 75℃ for varying slices thicknesses.

4.1.4. Drying Rate of the Product Samples

The results of the drying rates of the maize grains and yam slices are introduced in this section as shown in as shown in Figures 4.9 to 4.12

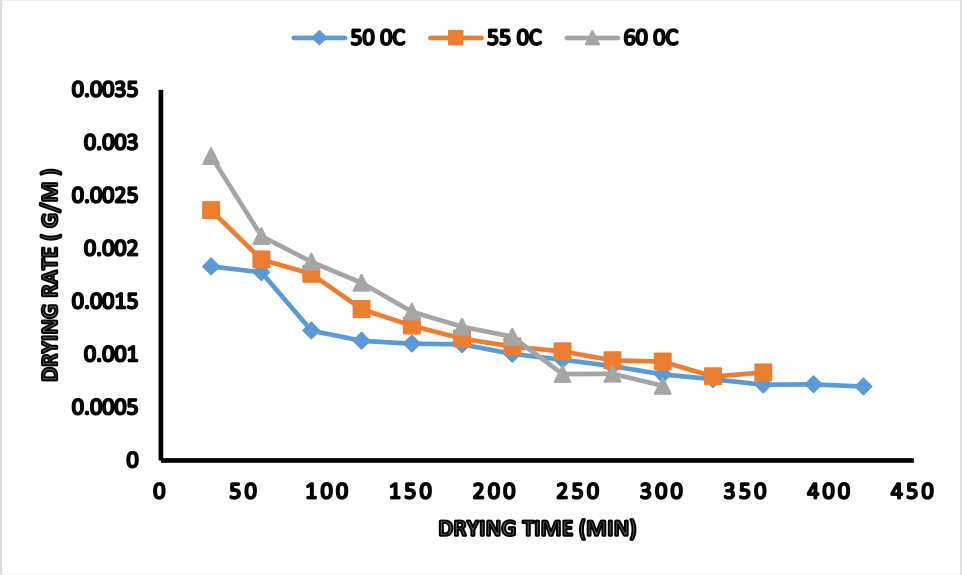

Figure 4.9: Drying rate of maize grains at 2m/s and varying air temperatures

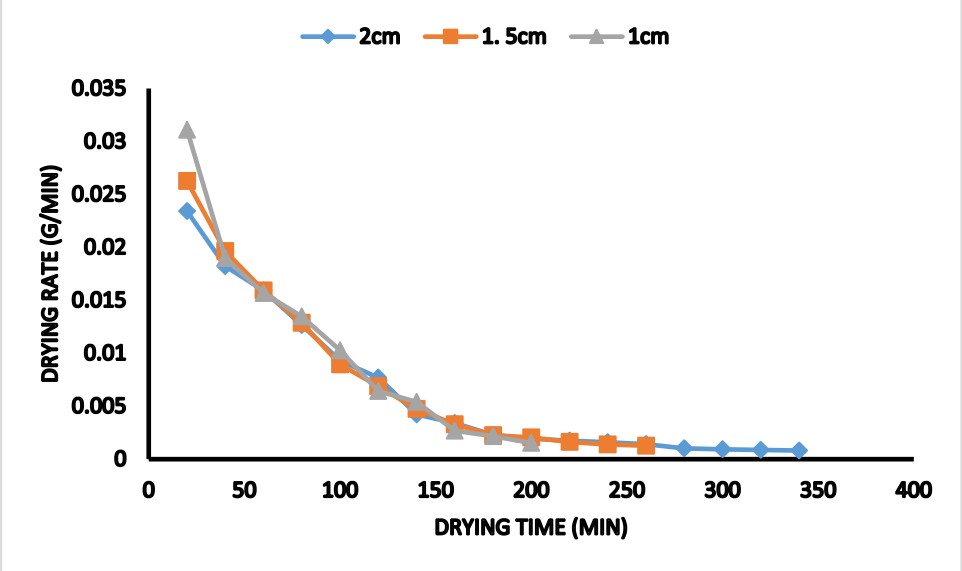

Figure 4.10: Drying rate curve of yam slices at 75℃ , 2. 0 m/s and varying thickness

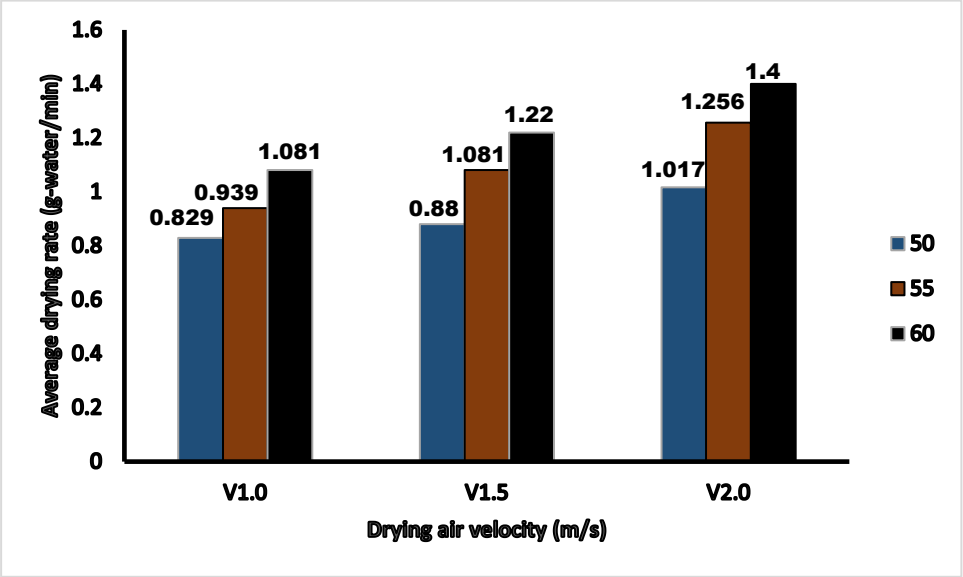

Figure 4.11: Average drying rate of the maize grains at varying air temperature and velocity

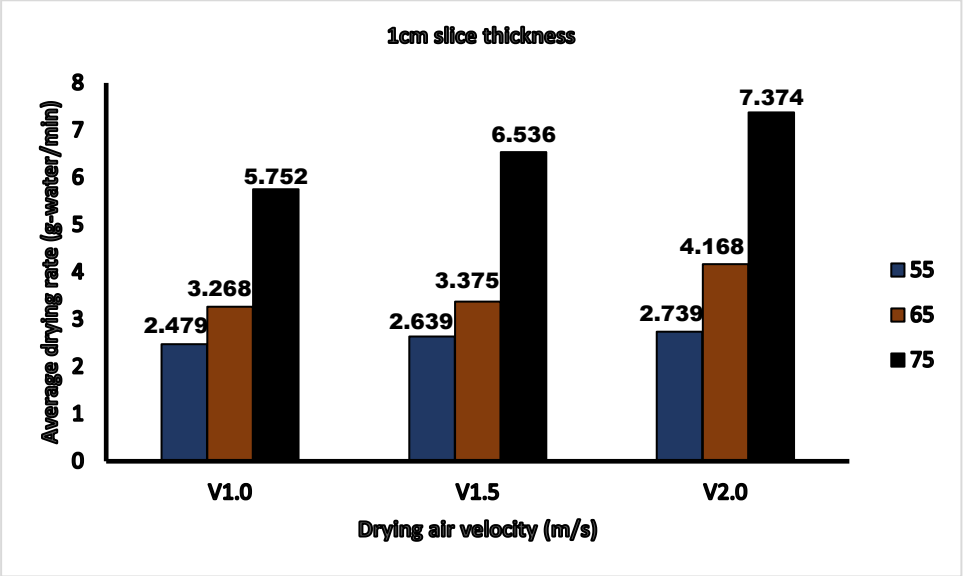

Figure 4.12: Average drying rate of the 1cm yam slices at varying air temperature and velocity

4.1.5. Thermal Efficiency of the Dryer for the Product Samples at varying air temperatures and velocities

The thermal efficiency results of the crop dryer are shown in Figures 4.13 to 4.16.

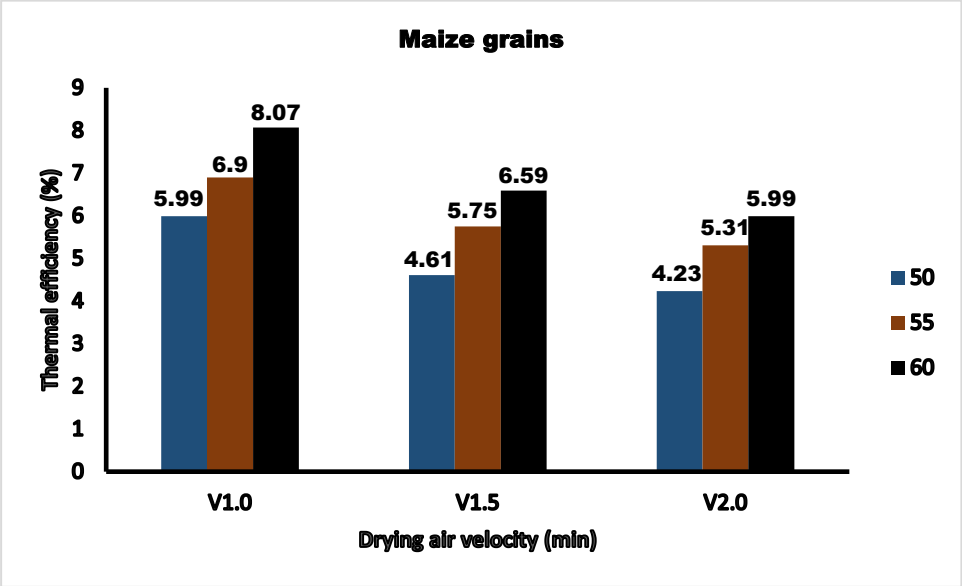

Figure 4.13: Thermal efficiency of maize grain drying

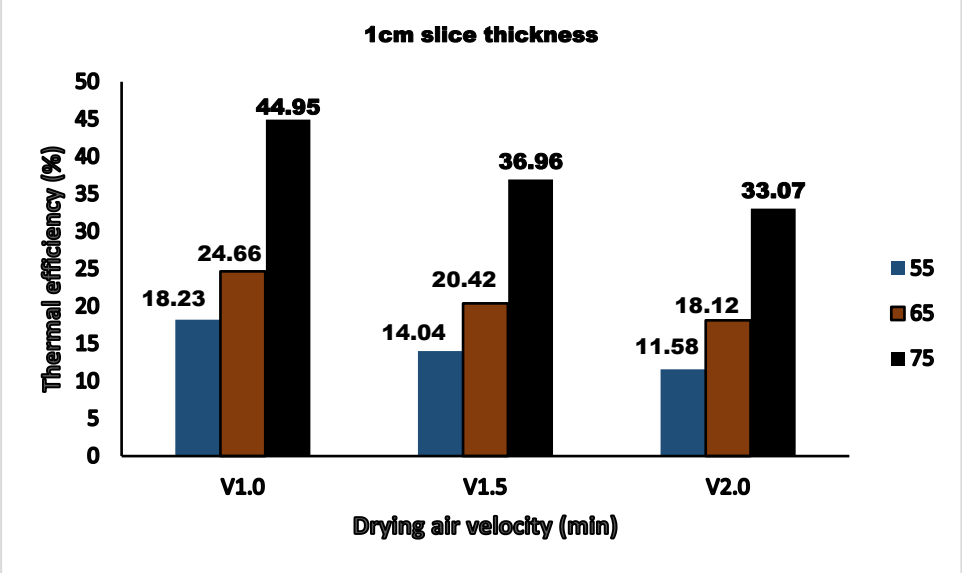

Figure 4.14: Thermal efficiency of 1cm yam slice drying

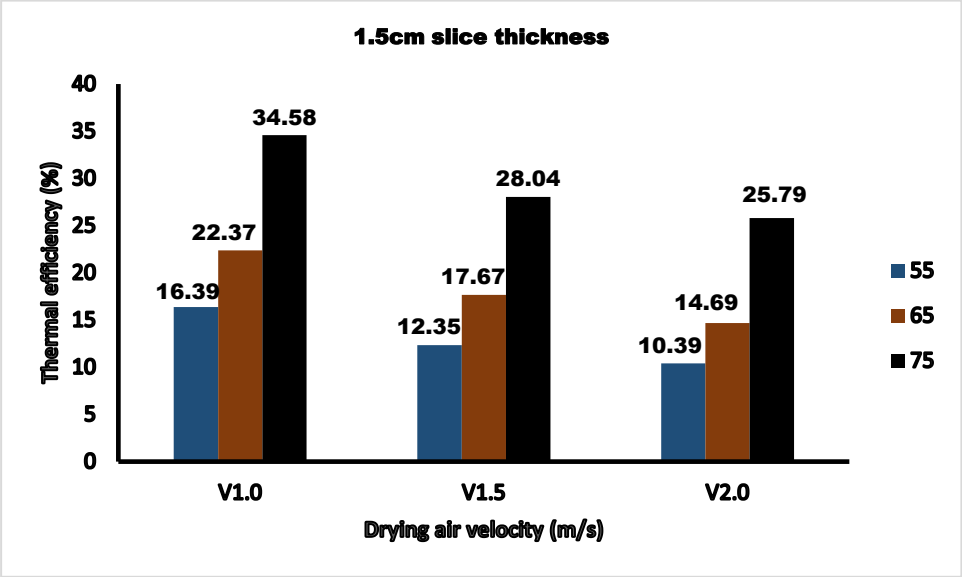

Figure 4.15: Thermal efficiency of 1.5cm yam slice drying

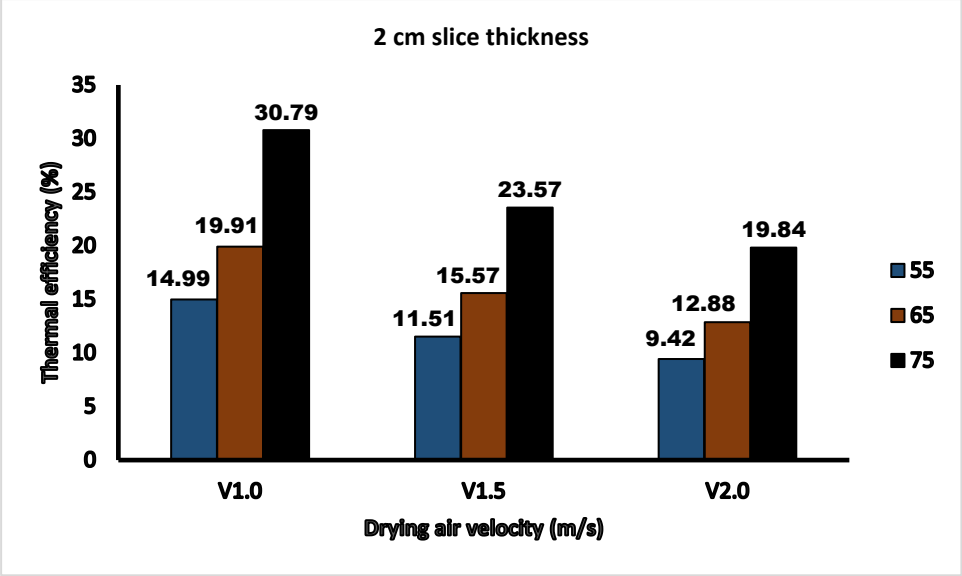

Figure 4.16: Thermal efficiency of 2cm yam slice drying

4.1.6. Energy consumption during drying of the products at varying air temperatures and Velocities

This section considers the energy consumption (both thermal and electrical) of the dryer for the crop samples as shown in Figures 4.17 to 4.23 and Tables 4.1 to 4.5.

4.1.6.1. Electric and thermal energy consumption during Drying of the Products at varying air temperatures and velocities

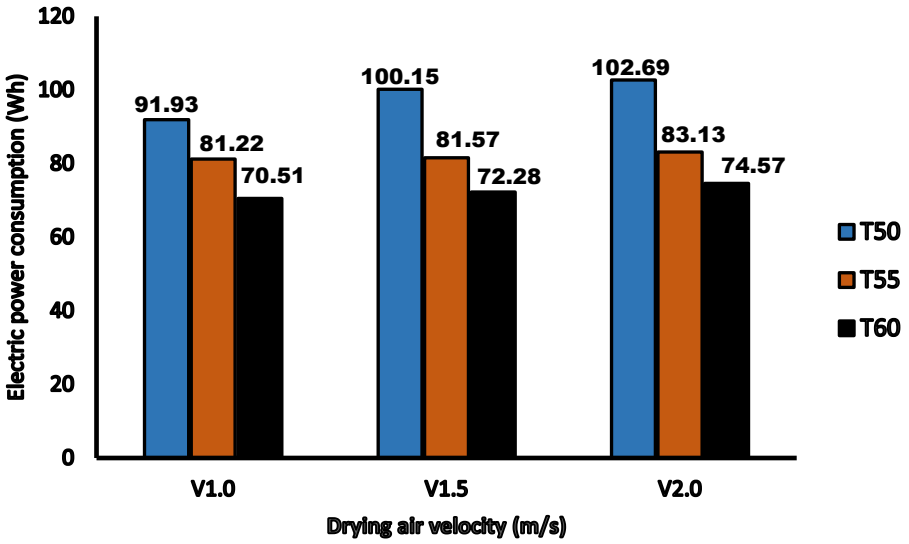

Figure 4.17: Electric power consumption for corn drying

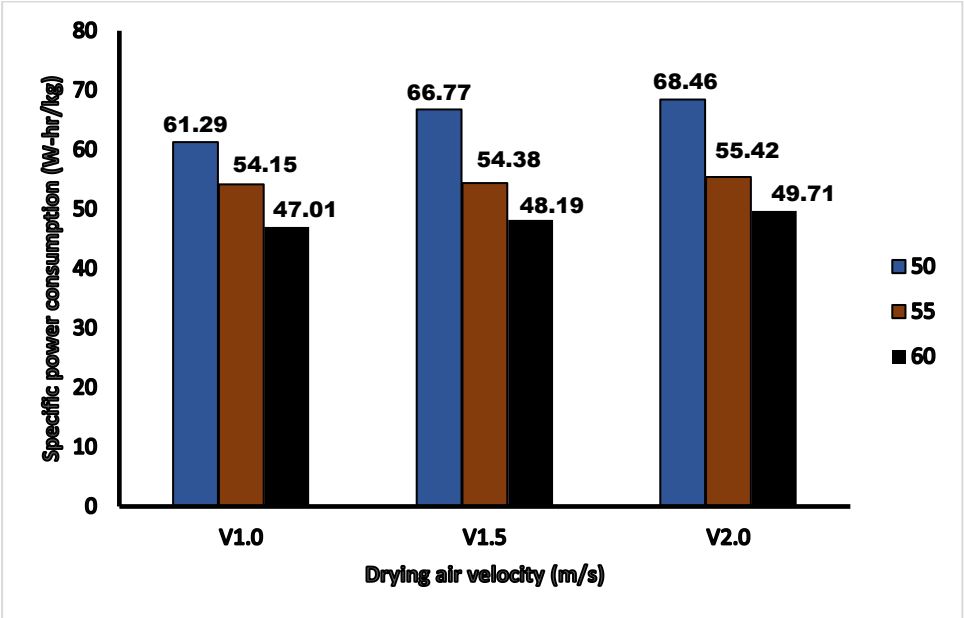

Figure 4.18: Specific Power Consumption for corn drying

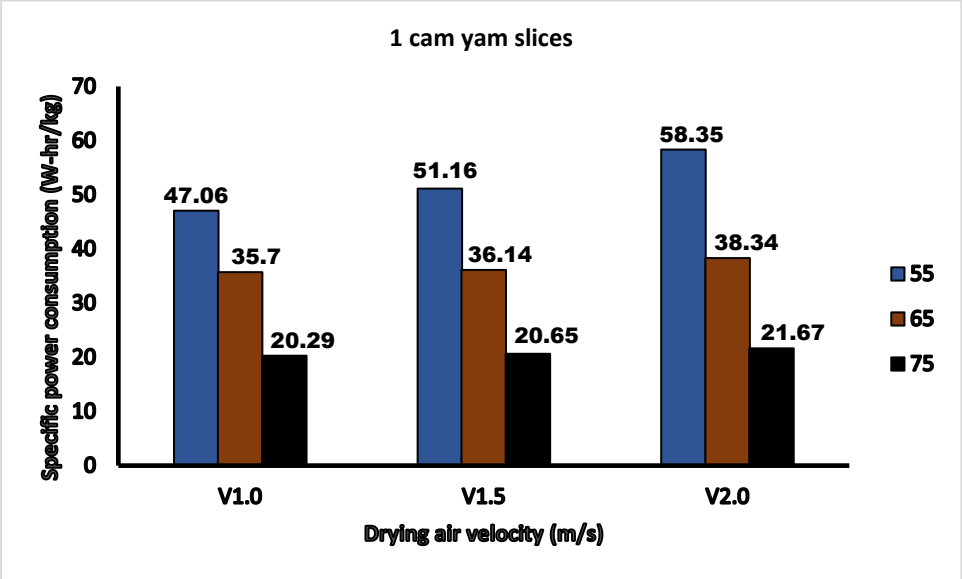

Figure 4.19: Specific Power Consumption for 1cm yam slice drying

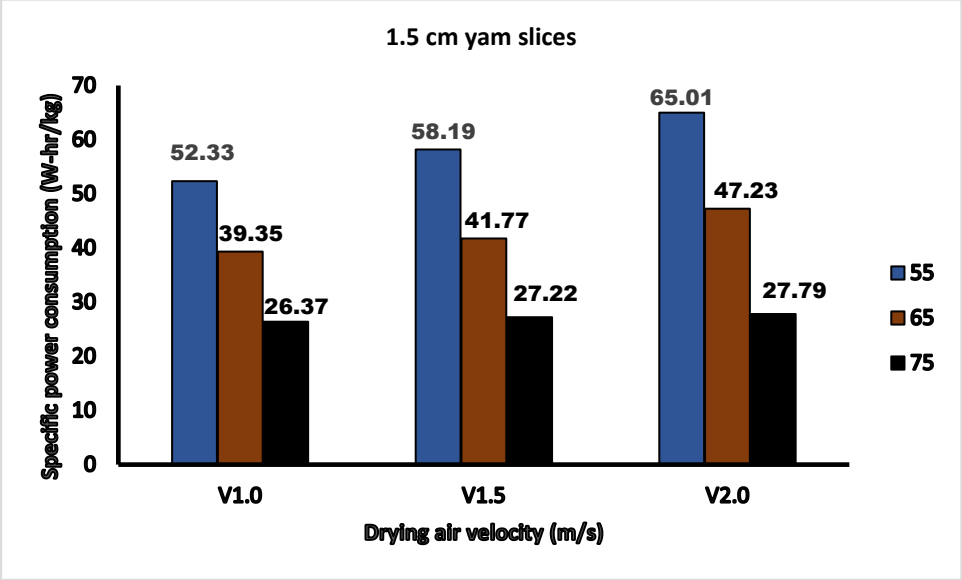

Figure 4.20: Specific Power Consumption for 1.5cm yam slice drying

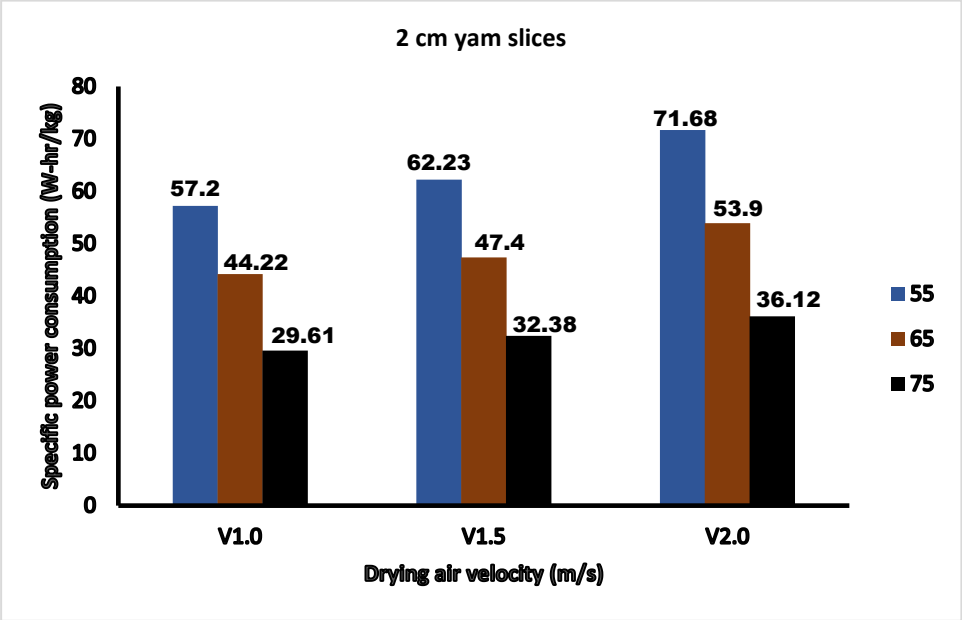

Figure 4.21: Specific power consumption for 2cm yam slice drying

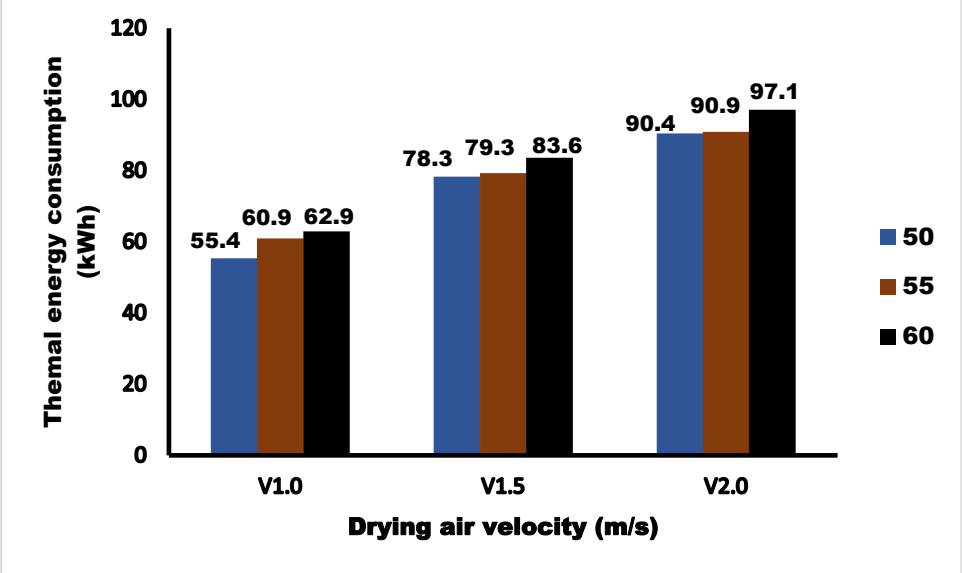

Figure 4.22: Thermal Energy Consumption for maize grain drying

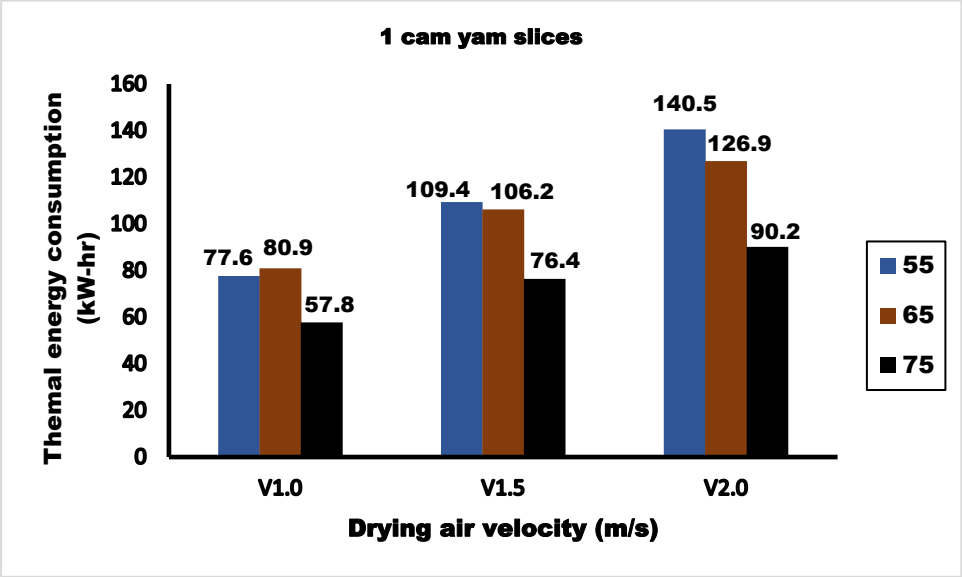

Figure 4.23: Thermal Energy Consumption for 1cm yam slice drying

Table 4.1: Measured values of electric current flow through the components of the dryer during operation.

S/N	Total number	Device	Status	Air velocity ($m\ s^{-1}$)	Current flow (mA)	Rated voltage (V)	Power consumed (W)
1	1	Air blower	Varying	1.0 1.5 2.0	480 620 810	12	5.76 7.44 9.72
2	1	Outlet fan	Constant	1.0 1.5 2.0	200 200 200	12	2.40 2.40 2.40
3	6	Temperature and humidity sensor	Constant	1.0 1.5 2.0	20 20 20	5	0.60 0.60 0.60
4	3	Weight sensor	Constant	1.0 1.5 2.0	30 30 30	5	0.45 0.45 0.45
5	1	Microcontroller	Constant	1.0 1.5 2.0	80 80 80	5	0.40 0.40 0.40
6	1	LCD	Constant	1.0 1.5 2.0	120 120 120	5	0.60 0.60 0.60
7	1	Other contents of the control panel	Constant	1.0 1.5 2.0	100 100 100	5	0.50 0.50 0.50

Table 4.2: Total electric power output of the components of the dryer at various air velocities

Air velocity ($m\ s^{-1}$)	Electric Power Output (W)
1.0	10.71
1.5	12.39
2.0	14.67

Table 4.3: Total drying times of the sample products at varying drying air temperatures and velocities.

T (℃)	v (m/s)	d_t (min)	T (℃)	v (m/s)	d_t (min)		
		Maize grains			Yam slices of 1cm	Yam slices of 1.5cm	Yam slices of 2cm
	1.0	515		1.0	580	645	705
50	1.5	485	**55**	1.5	545	620	665
	2.0	420		2.0	525	585	645
	1.0	455		1.0	440	485	545
55	1.5	395	**65**	1.5	385	445	505
	2.0	340		2.0	345	425	485
	1.0	395		1.0	250	325	365
60	1.5	350	**75**	1.5	220	290	345
	2.0	305		2.0	195	250	325

4.1.6.2. Total and Specific Energy Consumption during Drying of the Products

Table 4.4: Total Energy Consumption of the Product Samples

T (℃)	v (m/s)	E_t (kW-hr)	T (℃)	v (m/s)	E_t (kW-hr)		
		Maize grains			Yam slices of 1cm	Yam slices of 1.5cm	Yam slices of 2cm
	1.0	55.49		1.0	77.72	86.43	94.47
50	1.5	78.36	**55**	1.5	109.51	124.58	133.62
	2.0	90.46		2.0	140.64	156.71	172.78
	1.0	60.97		1.0	81.01	89.29	100.34
55	1.5	79.37	**65**	1.5	106.30	122.87	139.44
	2.0	91.09		2.0	127.00	156.45	178.54
	1.0	62.96		1.0	57.88	75.25	84.51
60	1.5	83.66	**75**	1.5	76.39	100.69	119.79
	2.0	97.19		2.0	90.28	115.74	150.46

Table 4.5: Specific Energy Consumption of the Product Samples

T (℃)	v (m/s)	SEC (kW-hr/kg)	T (℃)	v (m/s)	SEC (kW-hr/kg)		
		Maize grains			Yam slices of 1cm	Yam slices of 1.5cm	Yam slices of 2cm
50	**1.0**	129.95	**55**	**1.0**	54.05	60.10	65.69
	1.5	183.50		**1.5**	76.15	86.63	92.92
	2.0	211.85		**2.0**	97.80	108.98	120.16
55	**1.0**	142.78	**65**	**1.0**	56.34	62.09	69.78
	1.5	185.88		**1.5**	73.92	85.45	96.97
	2.0	213.30		**2.0**	88.32	108.79	124.16
60	**1.0**	147.45	**75**	**1.0**	40.25	52.33	58.77
	1.5	195.93		**1.5**	53.12	70.03	83.31
	2.0	227.63		**2.0**	62.78	80.49	104.63

4.1.7. Effective Moisture Diffusivity of the Sample Products

This section considers the moisture diffusion coefficient values as shown in Tables 4.6 to 4.7.

Table 4.6: Effective moisture diffusivity for maize grains at varying drying air temperature and velocity

T (℃)	v (m/s)	D_e (m^2/s)
50	**1.0**	5.77×10^{-11}
	1.5	6.38×10^{-11}
	2.0	7.62×10^{-11}
55	**1.0**	7.00×10^{-11}
	1.5	7.82×10^{-11}
	2.0	9.67×10^{-11}
60	**1.0**	8.23×10^{-11}
	1.5	1.01×10^{-10}
	2.0	1.11×10^{-10}

Table 4.7: Effective moisture diffusivity for yam slices at varying drying air temperature and velocity

T (℃)	v (m/s)	D_e (m^2/s)		
		Yam slices of 1cm	Yam slices of 1.5cm	Yam slices of 2cm
55	**1.0**	7.27×10^{-10}	1.44×10^{-9}	2.23×10^{-9}
	1.5	7.43×10^{-10}	1.48×10^{-9}	2.37×10^{-9}
	2.0	7.93×10^{-10}	1.56×10^{-9}	2.57×10^{-9}
65	**1.0**	1.01×10^{-9}	2.05×10^{-9}	3.03×10^{-9}
	1.5	1.18×10^{-9}	2.17×10^{-9}	3.32×10^{-9}
	2.0	1.33×10^{-9}	2.28×10^{-9}	3.52×10^{-9}
75	**1.0**	1.85×10^{-9}	1.44×10^{-9}	2.23×10^{-9}
	1.5	2.27×10^{-9}	1.48×10^{-9}	2.37×10^{-9}
	2.0	2.52×10^{-9}	1.56×10^{-9}	2.57×10^{-9}

4.1.8. Activation Energy of the Sample Products

Tables 4.8 to 4.9 present the activation energy values of the crop samples.

Table 4.8: Values of E_A and D_0 for maize grains at different air velocities

Air velocity (m/s)	E_A *(kJ/mol)*	D_0 *(m^2/s)*	R^2
1	31.75	7.89×10^{-6}	0.998
1.5	41.05	2.75×10^{-4}	0.995
2	33.66	2.15×10^{-5}	0.979

Table 4.9: Values of E_A and D_0 for yam slices at different air velocities.

Thickness	*Air velocity (m/s)*	E_A *(kJ/mol)*	D_0 *(m^2/s)*	R^2
	1	43.14	5.19×10^{-3}	0.994
1.0 cm	**1.5**	51.59	1.19×10^{-1}	0.987
	2	53.40	2.50×10^{-1}	0.967
	1	34.36	4.26×10^{-4}	0.986
1.5 cm	**1.5**	38.69	2.13×10^{-3}	0.997
	2	44.29	1.72×10^{-2}	0.999
	1	37.94	2.38×10^{-3}	0.979
2.0 cm	**1.5**	36.29	1.41×10^{-3}	0.993
	2	35.98	1.35×10^{-3}	0.988

4.1.9. Optimization of the process parameters using Response Surface Methodology (RSM)

Tables 4.10 to 4.21 show the results of optimization of the process parameters using RSM.

4.1.9.1. Results of the optimization of the process parameters for maize drying

Table 4.10: Solutions of the optimization of the variables for maize grain drying

S/N	T (^{0}C)	v (m/s)	d_t (min)	SEC	η_{th}	Desirability	
1	**60.000**	**1.000**	**395.000**	**150.882**	**8.012**	**0.762**	**Selected**
2	60.000	1.005	394.509	151.262	7.994	0.760	
3	60.000	1.017	393.272	152.221	7.949	0.757	
4	59.250	1.000	404.250	149.739	7.875	0.736	
5	59.045	1.000	406.783	149.426	7.837	0.729	

Table 4.11: The ANOVA for the drying time (d_t) of maize grain dehydration

Source	Sum of Squares	Df	Mean Square	F-value	p-value	
Model	37816.67	2	18908.33	136.14	< 0.0001	**Significant**
A-Temperature	22816.67	1	22816.67	164.28	< 0.0001	
B-Velocity	15000.00	1	15000.00	108.00	< 0.0001	
Residual	833.33	6	138.89			
Cor Total	38650.00	8				

Table 4.12: The ANOVA of the *SEC* for maize grain dehydration

Source	Sum of Squares	Df	Mean Square	F-value	p-value	
Model	9365.36	2	4682.68	117.11	< 0.0001	Significant
A-Temperature	348.23	1	348.23	8.71	0.0256	
B-Velocity	9017.13	1	9017.13	225.52	< 0.0001	
Residual	239.90	6	39.98			
Cor Total	9605.26	8				

Table 4.13: **The ANOVA of the thermal efficiency (η_{th}) for maize grain dehydration**

Source	Sum of Squares	Df	Mean Square	F-value	p-value	
Model	10.97	5	2.19	151.72	0.0008	Significant
A-Temperature	5.65	1	5.65	390.43	0.0003	
B-Velocity	4.91	1	4.91	339.86	0.0003	
AB	0.0256	1	0.0256	1.77	0.2754	
A^2	0.0108	1	0.0108	0.7439	0.4519	
B^2	0.3727	1	0.3727	25.77	0.0148	
Residual	0.0434	3	0.0145			
Cor Total	11.01	8				

Table 4.14: The final equations in terms of actual factors for the maize grains

Response variables and interaction between factors and their P-values								
Drying time (min)			SEC (kWh/kg)			Thermal efficiency (%)		
d_t	Factors and interactions	p-value	*SEC*	Factors and interactions	p-value	η_{th}	Factors and interactions	p-value
=			=			=		
+1235.0			-18.072			-9.884		
-12.333	T	< 0.0001	+1.523	T	0.0256	+0.565	T	0.0003
-100.0	V	< 0.0001	+77.533	V	< 0.0001	-5.230	V	0.0003
						-0.032	T * V	**0.2754**
						-0.0029	T^2	**0.4519**
						+1.7267	V^2	0.0148

Table 4. 15: Fit Statistics of the response variables for maize grain drying

Statistical parameters for the Response				**Corresponding R^2 and Adeq Precision values**			
	d_t	*SEC*	η_{th}		d_t	*SEC*	η_{th}
Std. Dev.	11.79	6.32	0.1202	R^2	0.9784	0.9750	0.9961
Mean	406.67	182.03	5.94	Adjusted R^2	0.9713	0.9667	0.9895
C.V. %	2.90	3.47	2.03	Predicted R^2	0.9571	0.9467	0.9545
				Adeq Precision	32.823	25.411	38.195

4.1.9.2. Results of optimization of the process parameters for yam slice drying

Table 4.16: Solutions of the optimization of the variables for yam slice dehydration

S/N	T (^{0}C)	v (m/s)	X (cm)	d_t (min)	SEC	η_{th}	Desirability	
1	75.000	1.000	1.000	255.741	39.520	43.018	0.941	Selected
2	75.000	1.011	1.000	255.041	39.843	42.846	0.940	
3	74.983	1.006	1.000	255.625	39.746	42.887	0.940	
4	75.000	1.000	1.006	256.425	39.651	42.926	0.940	
5	75.000	1.000	1.010	256.970	39.754	42.854	0.939	

Table 4.17: The ANOVA of the drying time for the yam slice dehydration

Source	Sum of Squares	df	Mean Square	F-value	p-value	
Model	5.681E+05	3	1.894E+05	3157.05	< 0.0001	Significant
A-Temperature	4.835E+05	1	4.835E+05	8060.03	< 0.0001	
B-Velocity	17422.22	1	17422.22	290.45	< 0.0001	
C-Thickness	67222.22	1	67222.22	1120.67	< 0.0001	
Residual	1379.63	23	59.98			
Cor Total	5.695E+05	26				

Table 4.18: The ANOVA of SEC for the yam slice dehydration

Source	Sum of Squares	df	Mean Square	F-value	p-value	
Model	12898.42	9	1433.16	381.56	< 0.0001	Significant
A-Temperature	1364.51	1	1364.51	363.28	< 0.0001	
B-Velocity	7881.82	1	7881.82	2098.42	< 0.0001	
C-Thickness	2536.14	1	2536.14	675.21	< 0.0001	
AB	213.36	1	213.36	56.80	< 0.0001	
AC	131.94	1	131.94	35.13	< 0.0001	
BC	265.55	1	265.55	70.70	< 0.0001	
A^2	494.44	1	494.44	131.64	< 0.0001	
B^2	8.51	1	8.51	2.27	0.1506	
C^2	2.14	1	2.14	0.5708	0.4603	
Residual	63.85	17	3.76			
Cor Total	12962.27	26				

Table 4.19: **The ANOVA for the thermal efficiency of yam slice dehydration**

Source	Sum of Squares	df	Mean Square	F-value	p-value	
Model	2099.53	9	233.28	195.82	< 0.0001	Significant
A-Temperature	1399.03	1	1399.03	1174.34	< 0.0001	
B-Velocity	280.77	1	280.77	235.67	< 0.0001	
C-Thickness	224.72	1	224.72	188.63	< 0.0001	
AB	14.96	1	14.96	12.56	0.0025	
AC	89.93	1	89.93	75.48	< 0.0001	
BC	0.1925	1	0.1925	0.1616	0.6927	
A^2	75.88	1	75.88	63.69	< 0.0001	
B^2	9.37	1	9.37	7.86	0.0122	
C^2	4.69	1	4.69	3.94	0.0635	
Residual	20.25	17	1.19			
Cor Total	2119.79	26				

Table 4.20: The final Equations in Terms of Actual Factors for yam slice drying

Response variables and interaction between factors and their P-values								
Drying time (min)			SEC (kWh/kg)			Thermal efficiency (%)		
d_t	Factors and interactions	p-value	*SEC*	Factors and interactions	p-value	η_{th}	Factors and interactions	p-value
=			=			=		
+1424.91			-330.38			+77.63		
-16.39	T	< 0.0001	+11.201	T	< 0.0001	-2.59	T	< 0.0001
-62.22	V	< 0.0001	+82.74	V	< 0.0001	-9.14	V	< 0.0001
+122.22	X	< 0.0001	-40.42	X	< 0.0001	+17.15	X	< 0.0001
-			-0.8433	T*v	< 0.0001	-0.223	T*v	0.0025
-			+0.663	T*X	< 0.0001	-0.55	T*X	< 0.0001
			+18.816	V*X	< 0.0001	+0.51	V*X	**0.6927**
			-0.0908	T^2	< 0.0001	+0.036	T^2	< 0.0001
			-4.764	v^2	**0.1506**	+4.99	v^2	0.0122
			-2.391	X^2	**0.4603**	+3.54	X^2	**0.0635**

Table 4.21: Fit Statistics of the response variables for yam slice drying

Statistical parameters for the Response				Corresponding R^2 and Adeq Precision values			
	d_t	*SEC*	η_{th}		d_t	*SEC*	η_{th}
Std. Dev.	7.74	1.94	1.09	R^2	0.9976	0.9951	0.9904
Mean	449.63	79.04	20.84	Adjusted R^2	0.9973	0.9925	0.9854
C.V. %	1.72	2.45	5.24	Predicted R^2	0.9966	0.9858	0.9734
				Adeq Precision	171.828	70.3746	49.3982

4.1.10. Thin-layer modelling of the drying processes for both maize and yam samples

Tables 4.22 to 4.55 present the results of the thin layer drying of the crop samples using some know mathematical drying models.

Table 4.22: Average values of statistical parameters of the selected models for maize grain drying at varying drying air temperature and constant air velocities of 1 m/s, 1.5 m/s and 2 m/s and the overall average

Model	Av. R^2	Av. SSE	Av. RMSE	Av. R^2	Av. SSE	Av. RMSE	Av. R^2	Av. SSE	Av. RMSE	Overall average		
		1 m/s			1.5 m/s			2 m/s		R^2	SSE	RMSE
Newton	0.9871	0.01453	0.02826	0.9853	0.01586	0.02991	0.9845	0.01509	0.03196	0.9856	0.01516	0.03004
Page	0.9947	0.00587	0.01765	0.9945	0.00594	0.01916	0.9935	0.00611	0.02134	0.9942	0.00597	0.01938
Henderson & Pabis	0.9886	0.01275	0.08125	0.9886	0.01233	0.02741	0.9880	0.01161	0.02931	0.9884	0.01223	0.04599
Wang & Singh	0.9975	0.00284	0.01231	0.9974	0.00273	0.01266	0.9946	0.00505	0.01832	0.9965	0.00354	0.01443
Demir *et al*	0.9897	0.01154	0.02381	0.9666	0.03570	0.04985	0.9880	0.01162	0.03189	0.9814	0.01962	0.03518
Weibull	0.9497	0.05619	0.04115	0.9558	0.04692	0.06944	0.9812	0.01675	0.03206	0.9622	0.03995	0.04755
Aghbashlo	0.9979	0.00225	0.01075	**0.9983**	**0.00187**	**0.01061**	**0.9972**	**0.00265**	**0.01417**	***0.9978***	***0.00226***	***0.01184***
Peleg	**0.9991**	**0.00099**	**0.00745**	0.9916	0.00906	0.01823	0.9959	0.00385	0.01377	0.99553	0.00463	0.01315
Hii *et al*	0.9985	0.00165	0.00948	0.9091	0.09841	0.09218	0.9926	0.00672	0.02311	0.96673	0.035593	0.04159
Verma *et al*	0.9898	0.01139	0.07748	0.9704	0.03325	0.03758	0.9845	0.01508	0.02161	0.98157	0.019907	0.045557

Table 4.23: Average values of statistical parameters of the selected models for 1cm yam slice drying at varying drying air temperature and constant air velocities of 1 m/s, 1.5 m/s and 2 m/s and the overall average.

Model	R^2	SSE	RMSE	R^2	SSE	RMSE	R^2	SSE	RMSE	Overall average		
		1 m/s			1.5 m/s			2 m/s		R^2	SSE	RMSE
Page	0.9823	0.01796	0.02605	0.98436	0.01509	0.02501	0.98633	0.01288	0.02345	0.9843	0.01531	0.02484
Wang & Singh	0.7937	0.20306	0.09298	0.83133	0.15968	0.08469	0.84373	0.14348	0.08201	0.8229	0.16874	0.08656
Aghbashlo	0.9936	0.00636	0.01601	**0.99353**	**0.00598**	**0.01696**	0.99413	0.00524	0.01624	***0.9938***	***0.00586***	***0.01640***
Peleg	0.9815	0.01752	0.02854	0.98057	0.01703	0.03006	0.98143	0.01564	0.02955	0.9812	0.01673	0.02938
Hii *et al*	**0.9998**	**0.00069**	**0.00343**	0.97776	0.02311	0.02535	0.97707	0.01473	0.02900	0.9849	0.01284	0.01926
Demir *et al*	0.9975	0.00260	0.00973	0.97463	0.02283	0.03161	**0.99740**	**0.00224**	**0.01159**	0.9898	0.00922	0.01764

Table 4.24: Average values of statistical parameters of the selected models for 1.5 cm yam slice drying at varying drying air temperature and constant air velocities of 1 m/s, 1.5 m/s and 2 m/s.

Model	R^2	SSE	RMSE	R^2	SSE	RMSE	R^2	SSE	RMSE	Overall average		
		1 m/s			1.5 m/s			2 m/s		**R^2**	**SSE**	**RMSE**
Page: $\boldsymbol{MR = \exp(-kt^n)}$	0.9776	0.02396	0.02961	0.9803	0.02032	0.02794	0.9822	0.01805	0.02618	0.9800	0.02078	0.02791
Wang & Singh: $\boldsymbol{MR = 1 + at + bt^2}$	0.751	0.2622	0.10047	0.7788	0.2224	0.0960	0.7947	0.20189	0.09286	0.7748	0.22883	0.09644
Aghbashlo: $\boldsymbol{MR = exp\left(\frac{k_1 t}{1+k_2 t}\right)}$	0.9924	0.00805	0.01748	0.9893	0.00703	0.01979	0.9936	0.00635	0.016	0.9918	0.00714	0.01775
Peleg: $\boldsymbol{MR = 1 - {t}/{(a + bt)}}$	0.9807	0.0196	0.02846	0.9814	0.01809	0.02834	0.9817	0.01734	0.02839	0.9813	0.01834	0.02839
Hii *et al*: $\boldsymbol{MR = a\,exp(-k_1 t^n) + b\,exp(-k_2 t^n)}$	0.9814	0.01805	0.02403	0.9902	0.00877	0.01881	**0.9978**	**0.00196**	**0.00814**	0.9898	0.00959	0.01699
Demir *et al*: $\boldsymbol{MR = a\,exp(-kt)^n + b}$	**0.9962**	**0.0042**	**0.01219**	**0.9969**	**0.00325**	**0.01104**	0.9974	0.00266	0.00989	***0.9968***	***0.00337***	***0.00698***

Table 4.25: Average values of statistical parameters of the selected models for 2 cm yam slice drying at varying drying air temperature and constant air velocities of 1 m/s, 1.5 m/s and 2 m/s.

Model	R^2	SSE	RMSE	R^2	SSE	RMSE	R^2	SSE	RMSE	Overall average		
		1 m/s			1.5 m/s			2 m/s		R^2	SSE	RMSE
Page: $\boldsymbol{MR = \exp(-kt^n)}$	0.9733	0.03044	0.03216	0.9763	0.02599	0.03047	0.9778	0.02374	0.02959	0.9758	0.02672	0.03074
Wang & Singh: $\boldsymbol{MR = 1 + at + bt^2}$	0.7063	0.33293	0.10743	0.7440	0.27983	0.10112	0.7537	0.26093	0.09977	0.7347	0.29123	0.10277
Aghbashlo: $\boldsymbol{MR = exp\left(\frac{k_1 t}{1+k_2 t}\right)}$	0.9911	0.01005	0.01888	0.9919	0.00876	0.01812	0.9924	0.00802	0.01759	0.9918	0.00894	0.01819
Peleg: $\boldsymbol{MR = 1 - t/(a + bt)}$	0.9791	0.02283	0.02935	0.9804	0.02064	0.02883	0.9809	0.01955	0.02849	0.9801	0.02101	0.02889
Hii *et al*: $\boldsymbol{MR = a\,exp(-k_1 t^n) + b\,exp(-k_2 t^n)}$	0.9751	0.03092	0.02404	0.9329	0.07034	0.05258	0.9952	0.00443	0.01408	0.9677	0.03523	0.03023
Demir *et al*: $\boldsymbol{MR = a\,exp(-kt)^n + b}$	**0.9947**	**0.00622**	**0.00937**	**0.9956**	**0.00495**	**0.01289**	**0.9961**	**0.00427**	**0.01553**	***0.9955***	***0.00515***	***0.01259***

4.2. Discussion

4.2.1. Performance of the Test Rig at No Load

During test, while the solar panel was disconnected, the turbine housing was connected to the tail pipe of a 250kVA generator (as shown in Plate 3.4) to test its performance when the pulleys to hold the dynamo had not yet been installed. Plate 3.1 shows the positions of the turbine shaft and the bearing holding it at the turbine housing. The test was carried out with only the energy recovery turbine to investigate its performance before the installation of the pulleys and the dynamo. The turbine blades (as shown in Plate 3.2) were made of a rigid mild steel material. The essence of the rigid material was to ensure the turbine does not lose pressure due to bending of its rotor blades when engaged with the exhaust gas moving out from the generator exhaust pipe during operation. Pressure losses due to pliability of blades would certainly impede the progress of the revolutions per minute (rpm) of the turbine. However, during the first sets of test, the turbine unit did not perform satisfactorily as the weight of the blades generated a lot of resistance causing a poor rotation of the blades. Thereafter, the mild steel blades were changed with an aluminium fan whose blades were reshaped to have the features of an axial turbine. The new blades were then subjected to test, and the rotational speed improved significantly; but the problem of flexibility of the blades was observed. The blades were not thick enough to resist the bending force to which they were subjected by the exhaust gases; causing the blades not to effectively utilize the gas pressure available to produce an appreciably high rpm required to drive the dynamo for electricity production. Another problem with the turbine unit was that of the stiffening of the turbine shaft over time during operation. The lubricant at the bearing holding the turbine shaft of the turbine housing was rendered ineffective due to its unrestrained exposure to high temperature exhaust gases. This eventually led to excessive friction resulting in the stalling of the turbine rotation due to poor lubrication. The major challenge faced here was the inability to provide constant lubrication of the moving parts

at the turbine unit during operation. Another major setback was the problem of providing adequate cooling for the part of the turbine shaft protruding beyond the turbine housing to be attached to the driving pulley. The undesirable situation here was the excessive conductive heat transfer to this part which would soon affect the pulley belt in the course of its operation if installed. The challenge here is that the exhaust gas travels axially through the direction of rotation of the blades. Therefore, the high temperature exhaust gases heat up the turbine shaft as they travel along the shaft length to the other end of the housing where the bearing is holding the shaft. And thereafter, the exhaust gases change their course into the heat exchanger. However, given the technical challenges associated with the turbine unit, the alternative source of electric power generation (the solar panel) was then used to provide the electricity required to drive the electrical components of the dryer.

The solar power-generating unit was connected to the battery for constant power supply while the possible things to be done to solve the problems associated with the turbine unit in respect of its lubrication were being considered. This time, the test rig was transferred to a 150 kVA generator with a smaller and shorter dryer stand for easier monitoring of the drying experiments (as shown in Plate 3.6). The 250 kVA generator, however, has a better flowrate to drive the turbine than the 150 kVA; **but since the turbine unit was suspended, it was decided that the smaller generator be used for the experiments. Interestingly, during test, the solar system functioned effectively.** Its performance was highly satisfactory during the tests, as it supplied constant electricity for continuous running of the drying equipment throughout the experiments.

4.2.1.1. Temperature Profile of the Drying Chamber at No Load

After its installation to the 150 kVA generator, the dryer was subjected to a test without load in order to ascertain the temperature profile across the trays of the dryer at varying drying air velocities. The resulting temperature profile as shown in Appendix B is such that the higher

the air velocity passing through the heat exchanger, the higher the heating effectiveness of the drying air. At higher velocities, more air was inducted into the heat exchanger resulting in more evacuation of heat from the exhaust gas at the heat exchanger. From Figures 4.1 to 4.3, it could be easily seen during the no load test that for each of the drying trays, it took the drying air the shortest time duration to reach the highest temperature at 2.0 m/s, while the longest duration of time was recorded for the lowest air speed of 1.0 m/s. This is in line with the temperature value obtained through calculation at the selection stage of the components of the dryer where the value of air velocity was $0.1026\, m/s$ for an air temperature of 85℃. Therefore, it can be surmised that higher air velocities in the heat exchanger would surely improve the rate of heating of the drying chamber. At the drying air velocity of 1m/s, the temperatures of the top tray ($\boldsymbol{T_1}$ **(**℃**)**), middle tray ($\boldsymbol{T_2}$ **(**℃**)**) and bottom tray ($\boldsymbol{T_3}$ **(**℃**)**) increased from the ambient temperature of 31℃ to 107.3, 105.2 and 101.4 ℃ in 48mins, respectively. At 1.5m/s; the values were 111.0, 111.3 and 107.5 ℃ in 48 mins. While for a velocity of 2m/s, the temperature values were 116.1, 114.9 and 114.5 ℃ in 39 mins, respectively as shown in Appendix B. Throughout the no load experiment for the various air velocities, the temperature of tray 3 (bottom tray) remained the least value among the temperatures of the three trays kept at different positions along the height of the drying chamber. Towards the end of the no load test for each drying air speed as seen in Appendix B, it was observed that the temperatures of the trays remained fairly constant. Thus, about the period of 42 minutes, the rate of heating of the chamber trays became very slow, thereby showing that the drying chamber had reasonably reached its peak temperature at the various air velocities. Furthermore, for each of the air velocities, it was observed that among the three trays, the tray closest to the heat source recorded the least temperature values (for the three air velocity levels), although it was initially believed to be the hottest. The reason might perhaps be as a result of convection current taking place in the drying chamber, causing hotter and lighter air to move up, and colder and heavier air to move down

the dryer. In addition, from Appendix B, the changes in temperature between trays 1 and 2 were irregular in the sense that at some points, the temperature of tray 1 was higher while that of tray 2 was lower and vice versa. The inlet temperature of the exhaust gas at the inlet of the heat exchanger was 305 ^{0}C, while the average temperature of the exhaust gas at the outlet of the heat exchanger for the three air velocity levels was 189 ^{0}C.

4.2.2. Moisture Loss and Drying Time of the Products

The maize grains were dried at the drying air temperatures of 50, 55, and 60℃, and velocities of 1.0, 1.5 and 2.0 m/s, respectively; while the yam slices were dehydrated at the drying air temperatures and velocities of 55, 65, and 75℃, and 1.0, 1.5 and 2.0 m/s, respectively. From Figure 4.4 (plotted with the data from Appendices D7, D8 and D9) and Figure 4.5 (plotted with the data from Appendices D10, D19 and D28) as well as Table 3, it is obvious that an increase in the drying air temperature from 50 to 60℃ (for the maize grains), and 55 to 75℃ (for the yam slices) at the given drying air velocities resulted in a reduction in the drying time of the sample products. This is because as the temperature increased, more moisture loss was recorded within a specified period showing agreement with what was reported in the literature that an increase in the drying temperature helps to expedite the attainment of equilibrium moisture content of drying products (Etoamaihe and Ibeawuchi, 2009; Onu *et al*., 2017). As the drying air temperature increases, the average kinetic energy of the moisture is enhanced, causing an increase in moisture diffusion out of the products as a result of an increase in the thermal gradient and the evaporation rate of the products (Mohammad *et al*, 2013; Onu *et al*., 2017). Thus the drying air temperature has a significant influence on the moisture content of a product sample, and hence impacts appreciably on the duration of its drying. Furthermore, Figure 4.6 (plotted using the data from Appendices D1, D4 and D7) and Figure 4.7 (plotted with the data from Appendices D31, D32 and D33) as well as Appendices G1 and G2, also show that at a given air temperature, an increase in the drying air velocity from 1 to 2m/s improved the

products moisture loss which resulted in a reduction in the drying time. Similar results were reported by Beigi (2016), and Onu *et al*. (2017) during the drying of apple and potato slices. According to Beigi (2016), higher drying air temperatures and velocities facilitate the heat transfer rate between the source of heat and the drying product leading to faster moisture evaporation and shorter drying time. Other factors that are capable of influencing the drying time of food products are the initial and final moisture contents of the product, and the method of drying used.

4.2.3. Effect of Slice Thickness on Drying Time of the Yam Slices

Apart from the drying air temperature and velocity, drying time is also affected by the thickness of the drying product. The effect of slice thickness of the yam samples during drying (plotted using the data from Appendices D28, D31 and D34) is shown in Figure 4.8. At the drying air temperature of 75 ℃ and 2m/s drying air velocity, the 1cm thick slices were dried to the desired moisture content faster than that observed in 1.5cm, while the 1.5cm thick slices dried faster than that observed in the 2cm thick yam slices. Hence, thicker slices of the yam products for all the experimental treatment combinations dried more slowly than thinner ones, showing that thin materials approach equilibrium moisture content in a shorter time period during drying than thick ones. This is in agreement with what was reported by Onu *et al*. (2017) during the dehydration of potato slices, that at small slice thicknesses, free moisture is easily removed from the surface of products than at large slice thicknesses.

4.2.4. Drying Rate of the Product Samples

The drying rate, d_R (g_{water}/min) was calculated using Eqn (2.13). The changes in its value with respect to the duration of drying at varying conditions of air temperature and velocity for some experimental treatments of the maize grains and yam slices are as shown in Appendices D1 to D36. It is obvious from the tables (Appendices D1 to D36) that the drying rates were higher from the beginning than those observed towards the end of the drying experiments. This shows

that the drying rate decreases with an increase in the drying time and a decrease in the moisture content. Hence, drying of the products occurred during the falling rate period which agrees well with the reports in the literature (Parry, 1985; Passamai and Saravia, 1997; Igbeka, 2013). Factors such as drying air temperature and speed as well as slice thickness of a drying sample significantly influence its drying rate. An increase in the value of the drying air temperature and velocity reduces the moisture content of a drying product, thus increasing the drying rate. Conversely, an increase in the slice thickness of a product sample reduces its drying rate. This is because, it takes a longer time for moisture particles to move from the inside of a thicker product to its surface due to a longer distance of travel. Figure 4.9 (plotted using the data from Appendices D1, D2 and D3) and Figure 4.10 (plotted with the data from Appendices D28, D31 and D34) show the drying rate of maize grains at 2m/s and varying temperatures; and of yam slices of varying slice thicknesses at the drying air temperature and velocity of 75℃ and $2.0\,m/s$, respectively. The values of the average drying rate, d_A (g_{water}/min) of the sample products for the various experimental treatments, were calculated using Eqn (3.125), and tabulated as shown in Appendices G1 and G2. Figures 4.11 and 4.12 show the relationship between the average drying rate of the maize grains and yam slices with drying air temperature and speed for different experimental treatments. Here, it can be easily observed that drying air temperature and speed had a significant impact on the drying rate of both products. For each of the figures, at a particular air speed, the highest drying rate was recorded at the highest drying air temperature. In the same vein, at a given temperature, the highest value of the drying rate occurred at the maximum drying air velocity. This is in agreement with what was reported in the literature that an increase in temperature and speed of the drying air, increases the drying rate of products (Mohamed and Christopher, 2013; Onu *et al*., 2017). Furthermore, a careful consideration of Figure 4.12, shows that the drying air temperature impacted more significantly on the drying rate of the dried yam slices than the drying air velocity. This agrees well with

what was reported in the literature with regard to the thin layer drying of Potato slices and cocoa bean (Ndukwu, 2014; Onu *et al*., 2017).

4.2.5. Thermal Efficiency of the Dryer for the Product Samples

The thermal efficiency (η_{th}) was calculated using Eqn (3.117), and the results obtained are presented in Appendix G1 for the maize grains, and Appendix G2 for the yam slices. The η_{th} indicates the degree of energy conversion in a device that makes use of thermal energy. According to Syahrul *et al*. (2002), the process of drying makes use of high energy in comparison to other production processes due to relatively low energy efficiency of dryers and high latent heat of evaporation of water. Hence, convective hot air dryers are generally associated with low thermal efficiency (Beigi, 2016). Considering Figures 4.13 to 4.16, and Appendices G1 and G2, it can be easily observed that an increment in the drying air temperature at a given air speed improved the value of η_{th}; whereas an increment in the drying air velocity at a particular temperature decreased its value. The reason for the low values of η_{th} at elevated drying air velocities might probably be due to the shorter residence time of the hot air in the drying chamber, as it likely caused an underutilization of the heat content of the hot air during the process of drying. The minimum value of η_{th} for the maize grains was 4.23 % achieved at the experimental treatment of 50 °C and 2 m/s, while a maximum value of 8.07%, was recorded at 60 °C and 1 m/s experimental treatment, respectively. For the yam slices, the minimum values of thermal efficiency were 11.58, 10.39 and 9.42 % for 1, 1.5 and 2cm slice thicknesses, achieved at 55 °C and 2 m/s; while the maximum values were 44.95, 34.58 and 30.79 % for 1, 1.5 and 2cm slice thicknesses, achieved at 75 °C and 1 m/s, respectively. Beigi (2016) reported similar results for the drying of apple slices in a convective hot air dryer, where the minimum thermal efficiency of 3.70% was obtained for the drying treatment of 50 °C and 2 m/s; whereas the maximum value of 9.44% was achieved at 70 °C and 1 m/s, respectively. Furthermore, it is

evident from Figures 4.14 to 4.16, that an increment in the slice thickness of the yam samples caused a reduction in the thermal efficiency of the product during drying.

4.2.6. Energy Consumption during Drying of the Products

In products drying, the energy consumption (W-hr) is usually a combination of both thermal and electrical energy. The thermal energy is responsible for raising the temperature of the dryer, while the electrical energy does the work of driving the air blower and other electrical components of the dryer. In conventional dryers, an increment in air temperature increases their energy requirement, since more kW-hr of energy will be supplied to the heating source of the drying system to raise the air temperature above ambient. In this work, the evaluation of the energy consumption during drying is considered in terms of the electrical energy consumed (EPC) and the thermal energy consumed (E_{th}). The electrical energy was utilized in the operation of the air blower and other instrumentation devices of the dryer such as the weight sensors, temperature and humidity sensors, Arduino-based control panel, etc. However, the thermal energy used to heat up the drying chamber was not supplied by the electrical system of the dryer; rather it was extracted from the exhaust gas waste heat of an electric generator.

4.2.6.1. Electric and thermal energy consumption during Drying of the Products at varying air temperatures and velocities

For the evaluation of the electric energy or power consumption (EPC), what was actually considered was the energy expended by the battery during the period of each drying batch. This was calculated by finding the product of the total electric power output of the components of the dryer for the three drying air velocity levels (Table 4.2) and the total drying time for each experimental treatment (Table 4.3) and presented in Appendices H1 to H4. Table 4.2 was derived as the sum total of the power output values of the components of the dryer across the three drying air velocity levels as shown in Table 4.1. The values of the EPC for corn drying as shown in Appendix H1, ranged from 70.51 to 102.69 W-hr. The minimum EPC was

achieved at a drying air temperature and velocity of 60 ℃ and 1.0 m/s, whereas a maximum value of 102.69 W-hr was obtained at the drying air temperature and velocity of 50 ℃ and 2.0 m/s, respectively. The same pattern of power consumption was also observed in the drying of yam slices of different thicknesses for the drying air temperatures of 65 to 75 ℃ and velocities of 1 to 2 m/s. The range of values of power consumption for the yam slices were from 44.63 to 128.36 W-hr, 58.01 to 143.03 W-hr and 65.15 to 157.70 W-hr, respectively for 1cm, 1.5cm and 2cm slice thicknesses as presented in Appendices H2 to H4. A similar trend was reported by Beigi (2016), where the minimum energy consumption was obtained at the highest air temperature of 70 ℃ and lowest air velocity of 1.0 m/s treatment; whereas the maximum electric energy consumption was achieved at the lowest air temperature of 50 ℃ and highest air velocity of 2.0 m/s treatment. This is because the lower the drying air temperature, the longer it takes to complete a drying phase leading to more electrical energy consumption. However, if the drying air temperature is increased, then the duration required to complete a given drying phase is reduced leading to lower electricity consumption, as the components of the dryer operate for a shorter time period. From Figure 4.17, it can be observed that at each drying air temperature, the electrical energy consumed increased with an increase in the drying air velocity. This is probably because for higher air velocities, more energy is required to drive the air blower. Conversely, at each level of the drying air velocity, the electric energy consumption decreased with an increase in air temperature. This observation is in line with what was reported in terms of energy consumption by Beigi (2016) for the drying of apple slices; Motevali *et al*. (2014a) for the drying of pomegranate; and Abbaszadeh, Motevali, Ghobadian, Khoshtaghaza and Minaei, (2012) for the drying of Russian olive.

The specific power consumption (SPC) was obtained using Eqn (3.117). Figures 4.18 to 4.21 show the relationship of specific power consumption with drying air temperature and velocity for the maize grain and yam slice drying. The minimum values obtained were 47.01 W-hr/kg

for the maize grains; 20.29, 26.37 and 29.61 W-hr/kg for the yam slices of 1.0, 1.5 and 2.0cm, respectively. Thus, these values are the minimum electrical power required to dry 1kg of the wet maize grains and blanched yam slices at their respective highest drying air temperatures and lowest drying air velocity (i.e. 60 ℃ and 1.0 m/s for the maize grains, and 75 ℃ and 1.0 m/s for the yam slices). The maximum values of SPC were 68.46 for the maize grains, 58.35, 65.01 and 71.68 W-hr/kg, respectively for 1.0, 1.5 and 2.0cm yam slice thicknesses. These values were achieved at the respective lowest drying air temperatures and highest drying air velocities (i.e. 50 ℃ and 1.0 m/s for the maize grains, and 55 ℃ and 1.0 m/s for the yam slices) of the drying products.

The thermal energy consumption (E_{th}) in kW-hr for the drying of the product samples was calculated using Eqn (3.114). The values of E_{th} did not follow exactly the pattern that was observed in the *EPC*. For maize grain drying, the higher the drying air temperature, the more the thermal energy consumed. The minimum value (55.40 kW-hr) was achieved at 50 ℃ and 1.0 m/s treatment, while the maximum thermal energy consumed (97.12 kW-hr) was achieved at 60 ℃ and 2.0 m/s experimental treatment. From Appendix H1, it could be easily observed that an increase in both drying air temperature and velocity for maize grain drying, increased the thermal energy consumed. For yam slice drying, the values of the minimum E_{th} obtained followed the same pattern as the values of *EPC* obained in the sense that the minimum values (57.88, 75.19 and 84.44 kW-hr for 1, 1.5 anc 2cm) were achieved at the maximum temperature (75℃) and minimum velocity (1.0 m/s). While the maximum values of E_{th} obtained were 140.64, 156.57 and 178.42 kW-hr, for the 1, 1.5 and 2cm yam slices. These maximum values of E_{th} obtained did not follow a definite pattern, since the maximum values obtained for both 1.0cm and 1.5cm yam slices occurred at the minimum air temperature (55℃) and maximum air velocity (2.0 m/s) as shown in Appendices H2 to H4. Whereas the maximum value of E_{th} for the 2cm yam slices (178.42) occurred at 65℃ as shown in Appendix G. Furthermore, from

Appendices H1 to H4, it is evident that the electric energy consumed is very small compared to the thermal energy consumption. This is because in convective hot air drying, the main portion of the energy is channeled to the heating of the drying air. From Figures 4.22 and 4.23, it is clear that the trend of thermal energy consumption is different for the two crops. The pattern followed by the maize grain drying is such that the higher the drying air temperature, the more the thermal energy consumption. Whereas, the drying air temperature had an inverse effect on the thermal energy consumption for the yam slice drying. This is because, there was better heat utilization by the yam slices during drying than by the maize grains as evidenced by the higher values of thermal efficiency obtained for the yam slice drying than for the maize grain drying. Thus causing a reduction in thermal energy losses, drying time.

4.2.6.2. Total and Specific Energy Consumption during Drying of the Products

The total energy consumption, E_T(kW-hr) is the sum of the thermal energy and electrical energy consumed Eqn (3.113). The values of E_T obtained were in the range of 55.49 to 97.19 kW-hr for maize grain drying as shown in Table 4.4. While for the yam slices drying, the values of E_T as also shown in Table 4.4 were in the range of 57.88 to 140.64 kW-hr, 75.25 to 156.71 kW-hr and 84.51 to 178.54 kW-hr, respectively for 1.0, 1.5 and 2.0cm yam slice thicknesses. The specific energy consumption, *SEC* (kW-hr/kg) is the ratio of the total energy consumption to the mass of water removed during a drying process as expressed in Eqn (3.112). The values of *SEC* for the sample products obtained are as presented Table 4.5. The values were in the range of 129.95 to 227.63 kW-hr/kg for maize grain drying; and 40.25 to 97.80 kW-hr/kg, 52.33 to 108.98 kW-hr/kg and 58.77 to 124.16 kW-hr/kg, respectively for 1.0, 1.5 and 2.0cm yam slice thicknesses. A comparative study of energy consumption of the two products dried revealed that the maize grain drying consumed more energy per kg of the product dried to a safe moisture content than the yam slices due to the more prolonged drying time per kg of the maize grains dried as shown in Appendix H5. The comparative analysis considered the drying

of the two products at 55℃ across the drying air velocity levels (1, 1.5 and 2 m/s). Appendix H5 was extracted from Table 4.5. From Appendix H5, it can be seen that the maize grains during drying consumed energy in the range of 55.86 %(at 55℃ 2 m/s) to 90.16 % (at 55℃ and 1m/s) more than the yam slices for the given treatment combinations. Thus, in terms of energy economy, the dryer is more suitable for the drying of yam slices than maize grains.

4.2.7. Effective Moisture Diffusivity of the Sample Products

For the given drying conditions, the values of the effective moisture diffusivity (D_e) were obtained using Eqn (3.107) for the maize grains and Eqn (3.105) for the yam slices; and the results were presented in Tables 4.3 and 4.4. The values of D_e obtained were in the range of 5.77×10^{-11} to $1.11 \times 10^{-10}\ m^2/s$ for maize grain drying. Similar results were reported by other researchers for the thin layer drying of maize kernels with D_e at the boarder of 10^{-11} to $10^{-10}\ m^2/s$ (Chayjan, Parian and Ashari, 2011; Abasi *et al*., 2017; Ajala and Abubakar, 2018). For yam slice drying, the value of D_e varied from 7.27×10^{-10} to 2.52×10^{-9}; 1.44×10^{-9} to 4.07×10^{-9}; and from 2.23×10^{-9} to 5.60×10^{-9} for 1cm, 1.5cm and 2cm yam slices, respectively. Similar results were reported in the literature. Kamal *et al*. (2020) reported D_e in the range of 2.01×10^{-10} to $4.25 \times 10^{-10}\ m^2/s$ for the drying of yam slices from 50 to 80℃. Sanful *et al*. (2015) reported a variation in the values of D_e for the dehydration of fresh yam slices in the range of 1.401×10^{-10} to 6.720×10^{-10} m^2/s from 50 to 70°C. Abano and Amoah (2015) reported D_e for hot water blanched samples of yam in the range of 8.81×10^{-9} to $1.53 \times 10^{-8}\ m^2/s$ for drying air temperatures of 70 to 90 °C. These values are within the range of values found in the literature for food materials (10^{-11} to 10^{-6}) (Olanipekun *et al*., 2014; Beigi, 2016). Appendices L1 and L2 show the graphs of ln MR against drying time for the evaluation of D_e for maize grains at 60℃ and 2 m/s, and 2cm yam slices at 75 °C and 1m/s. These two graphs and other graphs used for the evaluation of D_e at the rest of the drying

conditions and treatments for maize and yam slices were plotted with Excel program- version 2016 using the data from Appendices D1 and D36, respectively.

From Tables 4.3 and 4.4, it can be easily noticed that the value of D_e increased as the temperature increased. This is due to improvement in the internal mass transfer, because the energy of heating increases the activity of water molecules, thus leading to increased moisture diffusivity values during products drying. Similar results were reported in literature. Tulek (2011) reported D_e in the range of 9.619×10^{-10} to $1.556 \times 10^{-9}\ m^2/s$ for the drying of mushroom slice at 0.2 m/s air velocity and temperatures of 50, 60, and 70℃, respectively. Beigi, (2016) reported the values of D_e in the range of 6.75×10^{-10} to $1.28 \times 10^{-9}\ m^2/s$ for apple slice drying, from $50\ to\ 60$℃ and 1.0 to 2.0 m/s. Sanful *et al*. (2015) reported a variation in the values of D_e for the dehydration of fresh yam slices in the range of 1.401×10^{-10} to 6.720×10^{-10} m^2/s at drying air temperatures in the range of 50 to 70°C. Considering Tables 4.2 and 4.3, it is also evident that an increase in the air velocity and slice thickness increased the value of D_e. This is in agreement with what was reported in literature (Beigi, 2016; Onu *et al*., 2017). It is also interesting to note that the values of D_e obtained for the maize grains were less than the values for the yam slices. Ajala and Abubakar (2018) suggested that the small values of D_e for corn grains are as a result of their low moisture content, internal structure and thick outer coat.

4.2.8. Activation Energy of the Sample Products

For the evaluation of the activation energy, (E_A)**,** the graph of ln D_e versus $\frac{1}{T_a}$ was first plotted; and the values were calculated using Eqn (3.110). The values of E_A and the Arrhenius constant (D_0) for the dried products are tabulated as shown in Tables 4.5 and 4.6. For the maize grains, the obtained values of E_A were 31.75, 41.05, and 33.66 kJ/mol for the air velocities of 1, 1.5, and 2m/s as shown in Table 4.8. While the obtained values of E_A ranged from 43.14 to 53.40 kJ/mol for 1cm yam slice thickness, and 34.36 to 44.29 for 1.5cm yam slice thickness; whereas

for the 2cm yam slice thickness, the E_A values ranged from 35.98 to 37.94 kJ/mol, respectively for drying air velocities ranging from 1 to 2 m/s as shown in Table 4.9. These values are within the established range of activation energy for food products (1.2 to 110kJ/mol) (Aghbashlo, Kianmehr and Samimi-Akhijahani, 2008).

The R^2 values of the fitted lines with experimental data almost approached unity showing good correlation. Considering the influence of the drying air velocity on the activation energy of food products, different trends have been reported by different authors. Abasi et al. (2017) reported a trend that fairly agrees with the one observed in this work for the drying of corn. The report shows that for flow rates of 1, 1.4 and 1.8 kg/min, the values of activation energy for the drying of corn grains without the desiccant wheel were 14.293, 16.193 and 13.761 kJ/mol, respectively. Whereas with the desiccant unit operating for the same range of flow rates, the reported values of activation energy were 17.677, 14.638 and 14.874 kJ/mol, respectively. Thus showing no direct relationship between airflow and activation energy. Chayjan, Salari, Abedi, and Sabziparvar (2013) reported E_A values for the drying of squash seeds as 31.945, 3.394 and 34.487 kJ/mol at air velocities of 2.51, 4.01 and 5.32m/s, respectively; showing a direct relationship between air velocity and E_A (i.e, E_A increased as the air velocity increased). However, Onu et al. (2017) reported a different trend for the thin layer drying of potato slices, where the E_A decreased from 37.363 to 28.06 KJ/mol as the air velocity increased from 2.0 to 4.0 m/s showing an inverse relationship between the two variables.

A similar report was given by Abbaszadeh et al. (2012) for the drying of Russian olive, where E_A decreased from 63.83 to 48.18 kJ/mol as the air velocity increased from 0.5 to 1.5 m/s, showing an inverse relationship. These reports are in agreement with the values obtained here in the drying of the yam slices of 2cm thickness from 1m/s to 2m/s as shown in Table 4.9. However, for the drying of the 1cm yam slices, an opposite trend was observed; the activation energy increased as the velocity increased. Whereas, for the 1.5cm yam slices, the E_A increased

as the drying air velocity increased from 1 m/s to 1.5 m/s, and then decreased as the air velocity increased to 2 m/s.

Furthermore, considering the relationship between slice thickness and activation energy for the dried yam slices, it can be observed from Table 4.9 that the values of the activation energy decreased as the yam slice thickness increased from 1.0cm to 2.0cm. An exception to this occurred for yam slice thicknesses of 1.5 and 2.0cm at an air velocity of 1.0m/s, where the activation energy increased from 34.36 to 37.94 kJ/mol. However, the report published by Sanful et al. (2015), shows no definite pattern in terms of the relationship between yam slice thickness and activation energy. This is because the values of E_A were 28.42 and 30.33kJ/mol for the drying of fresh yam samples of thicknesses: 0.5cm and 1cm, whereas the values of E_A for the drying of boiled yam samples were 15.37 and 6.77kJ/mol for 0.5cm and 1.0cm slice thicknesses, respectively. Hence, it could be surmised that the E_A values have no definite relationship with the drying air velocity and slice thickness of products; and may possibly depend on the combination of some drying process factors and the nature of materials dried. Appendices L3 and L4 show the plots of In D_e against the reciprocal of absolute temperature ($^1/_T$) of maize grains with MATLAB program - version 2007 (using data from Table 4.6), and yam slices of 2cm thickness (using data from Table 4.7) for the evaluation of E_A.

4.2.9. Optimization of the process parameters using Response Surface Methodology

The Response Surface Methodology (RSM) statistical analysis was employed to investigate the main effects of the process variables (drying air temperature, drying air velocity, and slice thickness for yam) on the responses (drying time, specific energy consumption, and thermal efficiency) associated with the drying products. The experimental process (independent) variables and their levels were structured using a Completely Randomized Design (CRD) layout as shown in Tables 3.6 and 3.7. The results of different runs for the drying experimental treatments are as shown in Appendices I1 and I2. The resulting experimental data were

analyzed using response surface methodology (RSM), and the regression coefficients obtained were used to determine the optimum drying conditions for the drying of both crops.

4.2.9.1. Results of the optimization of the process parameters for maize drying

Optimization of the drying process parameters for maize grain drying gave the optimum drying conditions as 60^0C and 1 m/s. The predicted responses (d_t, SEC and η_{th}) for the optimized combination of the drying air temperature and velocity for the maize grain drying were 395 min, 150.882 kWh/kg and 8.012%, respectively with a desirability factor of 0.762. The five solutions found are as presented in Table 4.10. The Design Expert tool suggested linear polynomials as the most appropriate models of the response variables for maize grain drying (based on the P-values) for both the drying time (d_t) and specific energy consumption (*SEC*); whereas it suggested a quadratic polynomial for the thermal efficiency (η_{th}). The ANOVA for the three Response variables, d_t, *SEC* and η_{th} are presented in Tables 4.8 to 4.10. The **Models F-values** obtained (136.14, 117.11 and 151.72) showed that the models are significant; and there is only a 0.01 % probability that the F-values as large as the values obtained for the drying time and SEC, as well as 0.08% probability that the values obtained for the η_{th} could occur due to noise. **P-values** less than 0.0500 indicate that model terms are significant. Hence, only A and B are the significant model terms for both d_t and *SEC*, while A, B and B^2 are the only significant model terms for the η_{th}. Values greater than 0.1000 indicate the model terms are not significant, therefore, the model terms whose **P-values** are more than 0.1 are discarded to simplify the models. The final Equations for the response variables (d_t, *SEC* and η_{th}) in terms of Actual Factors for the maize grains are presented in Table 4.14. The model equations show that there are no significant interactions between the independent variables. From Table 4.14, the model equations for the response variables are as shown in Eqns 4.1 to 4.3:

$$d_t = 1235 - 12.33\mathrm{T} - 100\mathrm{v} \quad (4.1)$$

$$SEC = -18.07167 + 1.52367\mathrm{T} + 77.533\mathrm{v} \quad (4.2)$$

$$\eta_{th} = 0.564667\mathrm{T} - 5.23\mathrm{v} - 0.032\mathrm{vT} - 0.002933T^2 + 1.72667v^2 - 9.88444 \quad (4.3)$$

However, the model terms corresponding to the p-values in bold font style (T*v and T^2) for the thermal efficiency are insignificant, hence the equation for η_{th} is finally reduced to Eqn 4.4:

$$\eta_{th} = 0.564667\mathrm{T} - 5.23\mathrm{v} + 1.72667v^2 - 9.88444 \quad (4.4)$$

These equations in terms of actual factors are suitable for making predictions about the responses only for the given levels of each factor used in this work.

From Table 4.15, the **Predicted R^2 values of** of 0.9571, 0.9467 and 0.9545 are in reasonable agreement with the **Adjusted R^2 values** of 0.9713, 0.9667 and 0.9895 for the dependent variables d_t, *SEC* and η_{th}; i.e. the difference is less than 0.2. The Adeq Precision measures the signal to noise ratio. The obtained ratios of 32.823, 25.411 and 38.195 for d_t, *SEC* and η_{th} indicate an adequate signal, as a ratio greater than 4 is desirable. Appendices N1 to N3 show the comparison between the experimental and predicted values of the response variables (d_t, *SEC* and η_{th}). In these figures, it is obvious that the values of the individual response variables are in close alignment with the predicted values, as the straight lines are approximately at an angle of 45^0. Thus showing that the relationship between the factors and responses of the models are reliable. Appendices N4 to N6 show the 3-D response surface graphs for the independent variables versus the experimental factors of maize grain drying.

4.2.9.2. Results of optimization of the process parameters for yam slice drying

For the yam slice drying, the optimization of the drying process parameters gave the optimum drying conditions as 75 ^{0}C, 1.0 m/s and 1.0 cm. While the predicted responses for the optimized combination of the factors were 255.74 min, 39.52 kWh/kg and 43.02 %, respectively with the desirability factor of 0.941. Five of the solutions found are as presented in Table 4.16. The

Design Expert program suggested the most appropriate models for the response variables based on the p-values. It generated a linear polynomial for drying time, and quadratic polynomials for both *SEC* and η_{th}, respectively. The ANOVA for the three response variables, d_t, *SEC* and η_{th} are presented in Tables 4.14 to 4.16. The **Models F-values** obtained (3157.05, 381.56 and 195.82) showed that the models are significant; and there is only a 0.01 % probability that the F-values as large as the values obtained for the drying time, SEC and thermal efficiency could occur due to noise. **P-values** less than 0.0500 indicate that the model terms are significant. Hence, A, B and C are significant model terms for the drying time; A, B, C, AB, AC, BC and A^2 are significant model terms for the *SEC*; while A, B, C, AB, AC, A^2, B^2 are significant model terms for the η_{th}. Values greater than 0.1000 indicate the model terms are not significant, therefore, the model terms whose **p-values** are more than 0.1 are discarded to improve the models. The final Equations of the response variables (d_t, *SEC* and η_{th}) in terms of Actual Factors are as presented in Table 4.20. The model equations for yam slice drying show that there are significant interactions between the independent variables (SEC and η_{th}), except for the drying time, d_t. From Table 4.20, it can be observed that the interaction between the drying air velocity and slice thickness (v*X) for the thermal efficiency (η_{th}) is insignificant since its p-value (0.6927) is greater than 0.05. From Table 4.20, the model equations for the response variables are as shown in Eqns. 4.5 to 4.7:

$$d_t = 122.22\mathrm{X} - 16.39\mathrm{T} - 62.22\mathrm{v} + 1424.91 \qquad (4.5)$$

$$SEC = 11.2T + 82.74v - 40.42X - 0.84T * v + 0.66T * X + 18.82v * X - 0.091T^2 - 4.76v^2 - 2.39X^2 - 330.38 \qquad (4.6)$$

$$\eta_{th} = 17.15\mathrm{X} - 2.59\mathrm{T} - 9.14\mathrm{v} - 0.22\mathrm{T} * \mathrm{v} - 0.55\mathrm{T} * \mathrm{X} + 0.51\mathrm{v} * \mathrm{X} + 0.04T^2 + 4.99v^2 + 3.54X^2 + 77.63 \qquad (4.7)$$

However, the model terms corresponding to the p-values in bold style (v^2 and X^2) for *SEC*, and (V*X and X^2) for η_{th} are not significant, hence the Eqns (4.6 and 4.7) are further reduced to Eqns (4.8) and (4.9):

$$SEC = 11.2T + 82.74v - 40.42X - 0.84T * v + 0.66T * X + 18.82v * X - 0.091T^2 - 330.38 \quad (4.8)$$

$$\eta_{th} = 17.15X - 2.59T - 9.14v - 0.223T * v - 0.55T * X + 0.036T^2 + 4.99v^2 + 77.63 \quad (4.9)$$

From Table 4.21, the **Predicted R^2 values** of 0.9966, 0.9858 and 0.9734 are in reasonable agreement with the **Adjusted R^2 values** of 0.9973, 0.9925 and 0.9854 for the dependent variables d_t, *SEC* and η_{th}; i.e. the difference is less than 0.2. The Adeq Precision measures the signal to noise ratio. The obtained ratios of 171.828, 70.375 and 49.398 for d_t, *SEC* and η_{th} indicate an adequate signal, as a ratio greater than 4 is desirable. Appendices N7 to N9 show the comparison between the experimental and predicted values of the response variables (d_t, *SEC* and η_{th}) for the drying of yam slices. In these Figures, it is obvious that the values of the individual response variables are in close alignment with the predicted values, as the straight lines are approximately at an angle of 45^0. Thus showing that the relationship between the factors and responses of the models are reliable. Appendices N10 to N12 show the 3-D response surface graphs for the independent variables versus the experimental factors.

4.2.10. Thin-layer modelling of the drying processes for both maize and yam samples

Ten known thin-layer mathematical drying models (Newton (El-Beltagy et al., 2007), Page (1949), Henderson and Pabis (1961), Wang and Singh (1978), Demir *et al* (2007), Weibull (Tzempelikos et al., 2014), Aghbashlo (2009), Peleg (Da Silva et al., 2013), Hii *et al* (2009) and Verma *et al*. (1985)) were employed in studying the drying behaviour of the maize grains, while six models (Page (1949), Wang & Singh (1978), Demir *et al* (2007), Aghbashlo (2009),

Peleg (Da Silva et al., 2013), and Hii *et al* (2009)) were used in studying the drying characteristics of the yam slices. This aspect of study was achieved by fitting the experimental dimensionless moisture ratio (*MR*) versus drying time to the listed semi-theoretical models (with MATLAB program-version 2007 using the data from Appendices D1 to D36); and determining the goodness of fit of the models using the generated statistical parameters. The generated statistical indicators are the coefficient of determination (R^2), the sum of squares error (*SSE*) test, and the root mean square error (*RMSE*) analysis, as expressed in Eqs 3.90, 3.91 and 3.92, respectively. The average values of the statistical parameters (R^2, *SSE* and *RMSE*) of the selected models for maize grain drying at varying drying air temperatures (50, 55 and 60 ^{0}C) for constant air velocities of 1 m/s, 1.5 m/s and 2 m/s are presented in Table 4.22. Whereas the average values of R^2, *SSE* and *RMSE* for the dried yam slices of the thicknesses: 1cm, 1.5cm and 2cm, at varying drying air temperatures of 55, 65 and 75 ^{0}C, and constant drying air velocities of 1 m/s, 1.5 m/s and 2 m/s are shown in Tables 4.20, 4.21 and 4.22, respectively. The R^2 values of the models for all the drying conditions of the maize grains were above 0.92; except for the Hii *et al* model of R^2 (0.8473) at 55℃ and 1.5 m/s; and Weibull model of R^2 (0.8506) at 60℃ and 1 m/s as shown in Appendix J1. Furthermore, the R^2 values of the selected models for all the drying conditions of the yam slices were above 0.92, except for the Wang and Singh model whose R^2 values ranged from 0.7063 to 0.84373 as shown in Appendices J2 to J4. Thus indicating that the Wang and Singh model is not at all suitable for describing the thin-layer drying behaviour of the yam slices since its R^2 values are well below unity (1). The fitting curves for the validation of the selected thin-layer drying models were generated by MATLAB 2007 using the data from Appendices D1 to D36. However, only the curve fitting graphs generated using the data from Appendices D3, D11, D22 and D35 are presented as shown in Appendices K1, K2, K3 and K4, respectively.

From Table 4.22, the results obtained showed that at a constant drying air velocity of 1 m/s across the three drying air temperature levels for the maize grain drying, the Peleg model was the most suitable drying model for describing the thin-layer drying behavior of the maize grains due to its highest average R^2 value of 0.9991; and lowest average *SSE* and *RMSE* values of 0.00099 and 0.00745, respectively. Whereas the Aghbashlo model was the best suited model for the description of the thin-layer drying characteristics of the maize grains at constant velocities of 1.5 and 2 m/s, on account of its highest average R^2 values of 0.9983 and 0.9972; lowest average *SSE* values of 0.00187 and 0.00265; and lowest average *RMSE* values of 0.01061 and 0.01417, respectively. The results contained in Table 4.23 revealed that at a constant drying air velocity of 1 m/s across the drying air temperature levels (55, 65 and 75^0C) for 1 cm yam slice drying, the Hii *et al* model was the most suitable drying model for describing the thin-layer drying behavior of the yam slices due to its highest average R^2 value of **0.9998**; and lowest average *SSE* and *RMSE* values of **0.00069** and **0.00343**, respectively. For 1.5 m/s air velocity of the same slice thickness, the Aghbashlo model was the best with the average R^2 value of **0.99353**, *SSE* of **0.00598**, and *RMSE* of **0.01696,** respectively. While for 2 m/s air velocity of the same 1 cm slice thickness, the Demir *et al* model was the best with the highest R^2 value of **0.99740**; and lowest average SSE and *RMSE* values of **0.00224** and **0.01159**, respectively. For 1 m/s and 1.5 m/s of 1.5cm yam slices (Table 4.24), the Demir *et al* model was the best model with the average R^2 values of **0.9962 and 0.9969;** while the average values of *SSE* were **0.00420** and**0.00325**, and the average *RMSE* values were **0.01219** and **0.01104,** respectively. Whereas for the 2 m/s drying air velocity of 1.5cm yam slices, the Hii *et al* model was the most suitable model with an average R^2 value of **0.9978**; and the average *SSE* and *RMSE* values of **0.00196** and **0.00814,** respectively. However, for the 2cm yam slice drying, the Demir *et al* model was the best for all the levels of the constant drying air velocity treatments (1 m/s, 1.5 m/s and 2 m/s) at varying air temperatures as shown in Table 4.25. The

average R^2 values were **0.9947, 0.9956** and **0.9961;** and the average *SSE* values were **0.00622, 0.00495** and **0.00427;** while the average *RMSE* values were **0.00937**, **0.01289** and **0.01553**, respectively. The values of the model constants obtained from the nonlinear regression of the ten selected drying models for the maize grain drying are shown in Appendices J5 to J7. However, for the modelling of the thin-layer drying of yam slices, the model constants of the best three among the six selected thin-layer drying models for 1 cm yam slices at varying drying air temperatures and velocities are shown in Appendices J8 to J10.

The overall average values of the statistical indicators as presented in Tables 4.19 to 4.22, showed that the Aghbashlo model was the most suitable drying model for describing the thin-layer drying behavior of the maize grains due to its highest overall average R^2 value of 0.9978; and lowest *SSE* and *RMSE* values of 0.00226 and 0.01184, respectively. The Aghbashlo model also proved to be the best drying model for describing the thin-layer drying characteristics of the 1cm yam slices due to its highest average R^2 value of **0.9938**; and lowest average *SSE* and *RMSE* values of **0.00586** and **0.01640**, respectively. Furthermore, for the drying of the 1.5cm and 2cm yam slices, the Demir *et al* model was the best suited model for predicting the drying behavior of the yam slices, on account of its highest overall average R^2 values of 0.9968 and 0.9955; lowest *SSE* values of 0.00337 and 0.00515; and lowest *RMSE* values of 0.00698 and 0.01259, respectively.

CHAPTER FIVE
CONCLUSION AND RECOMMENDATIONS

5.1. Conclusion

The sizing, development and performance evaluation of a convective hot air dryer powered by a diesel generator exhaust gas waste heat for food crops drying have been carried out. The sizing of the components of the equipment was achieved using known design principles. The concept was geared towards the recovery and utilization of the waste heat of a diesel generator, thereby reducing the quantity of pollutants released into the environment. The recovered energy was applied to the drying of agro-products, instead of resorting to the burning of fresh fuels to do the same work. The essence of this work (recovery and application of the waste energy to drying) is to reduce the demand on depleting fossil fuel reserves in order to save a considerable amount of primary fuel; help farmers to minimize the amount of agricultural product losses usually incurred during postharvest periods; assist food processing industries to save some portion of the thermal energy waste incurred daily and apply it meaningfully. This is evidenced by the success achieved in the drying of maize grains and yam slices for safe preservation. Thus showing that the application of recovered exhaust gas waste heat to drying of farm produce will help to improve the value and profit margin of both farmers and owners of food processing industries. This method will also prevent the environment from experiencing excessive damage due to the impact of global warming. This is because the burning of fresh fuels to operate dryers (which will surely generate more pollutants) can be substituted with the use of available waste heat from exhaust gases. The performance evaluation of the waste heat recovery tray dryer was investigated with no load, and with load using maize grains and yam slices as drying products. Given the results obtained, the following conclusions are hereby drawn:

a. At no load, an increase in the velocity of air inlet to the heat exchanger, improved the rate of heating of the drying chamber.

b. The drying air temperature and velocity substantially influenced the moisture content reduction which grossly diminished the drying duration. Higher rates of drying were obtained as a result of increased drying air temperature and velocity for both product samples.

c. The average drying rate for the maize grains was in the order of 0.83 to 1.4 g/min; and the drying duration ranged from 305 to 515 minutes. Whereas the average drying rates for the yam slices ranged from 2.48 to 7.37, 2.23 to 5.75, and 2.04 to 4.43; while the drying time was in the range of 195 to 580, 250 to 645, and 325 to 705 minutes for 1cm, 1.5cm and 2cm samples, respectively.

d. An increase in the drying air conditions (temperature and velocity) improved the moisture diffusion coefficient (D_e), which varied between 5.77 $x10^{-11}$ and 1.11 x 10^{-10} m^2/s for the maize grains. Whereas for the 1cm, 1.5cm and 2cm yam slices, the D_e values were in the order of 7.27 $x10^{-10}$ to 2.52 x 10^{-9}, 1.44 $x10^{-9}$ to 4.07 x 10^{-9}, and 2.23 $x10^{-9}$ to 5.60 x 10^{-9} m^2/s, respectively.

e. The activation energy exhibited no definite relationship with the air velocity. Its values varied between 31.75 and 41.05 kJ/mol for the maize grains; whereas the values for the 1cm, 1.5cm and 2cm yam slices ranged from 43.14 to 53.40, 34.36 to 44.29, and 35.98 to 37.94 kJ/mol, respectively.

f. The thermal efficiency had a direct relationship with the drying air temperature, and an inverse relationship with the drying air velocity. The minimum value of thermal efficiency for the maize grains was 4.23 % achieved at the experimental treatment of 50 °C and 2 m/s, while the maximum value was 8.07%, achieved at 60 °C and 1 m/s experimental treatment. For the yam slices, the minimum values of thermal efficiency were 11.58, 10.39 and 9.42 % for 1, 1.5 and 2cm slices, achieved at 55 °C and 2 m/s; while the maximum values were 44.95, 34.58 and 30.79 % for 1, 1.5 and 2cm slices,

achieved at 75 °C and 1 m/s, respectively. This shows that the maximum values of the thermal efficiency were obtained at the maximum drying air temperatures and minimum air velocity; whereas its minimum values were obtained at the minimum drying air temperature and maximum drying air velocity.

g. The total energy consumption of the drying process varied with both the drying air velocity and temperature. The maximum value of 97.19 kWh was obtained at 50^{o}C and 2 m/s; whereas the minimum energy value of 55.49 kWh corresponded with the 60^{o}C air temperature and 1.0 m/s air velocity for the maize grains. While for the yam slices, its values ranged from 57.84 to 140.51, 75.19 to 156.57, and 84.44 to 178.42kWh for 1cm, 1.5cm and 2cm yam slice samples, respectively.

h. The specific power consumed (*SPC*) per batch of the drying sample showed an increasing trend with air velocity at constant air temperature, whereas increasing the drying air temperature caused a reduction in the specific power consumption at constant air velocity. The SPC obtained were 47.01 W-hr/kg for the maize grains; 20.29, 26.37 and 29.61 W-hr/kg for yam slice thicknesses of 1.0, 1.5 and 2.0cm, respectively. These values are the minimum electric power required to dry 1kg of the wet maize grains at the drying air temperature and velocity combinations of 60 ℃ and 1.0 m/s; and at 75 ℃ and 1.0 m/s for the yam slices. The maximum values of *SPC* were 68.46 W-hr/kg for the maize grains at 50 ℃ and 2 m/s; and 58.35, 65.01 and 71.68 W-hr/kg, respectively for 1.0, 1.5 and 2.0cm yam slices at 55 ℃ and 2,0 m/s.

i. The minimum and maximum thermal energy values were obtained as 55.4 and 97.12kW-hr for the maize grains; while for the yam slices, the values were 57.84 and 140.51, 75.19 and 156.57, and 84.44 and 178.42kWh for 1cm, 1.5cm and 2cm yam slice samples, respectively.

j. The specific energy consumption (*SEC*) per batch of the drying process, which varied between 129.95 and 227.63 kWh/kg increased with increasing air temperature and velocity for the maize grains. While its values which varied from 40.25 to 97.80, 52.33 to 108.98, and 58.77 to 124.16 kWh/kg (for 1cm, 1.5cm and 2cm yam slice samples) did not follow the same trend as the values obtained for the maize grain samples. Here, the drying air temperature had an inverse effect on the values of the SEC of the dryer system at constant air velocity; whereas its values increased as the drying air velocity increased at constant air temperature.

k. The comparative study of the two products at the drying air velocities of 1 to 2 m/s and 55℃, showed that the maize grains consumed more energy per kg of the product dried to a safe moisture content in the range of 55.86 to 90.16 % than the yam slices. Thus revealing that the dryer is more suitable for the drying of yam slices than maize grains.

l. The results obtained for the optimization of the drying process parameters showed that the optimum drying conditions are 60^0C and 1 m/s for the maize grains; and 75 ^{0}C, 1.0 m/s and 1.0 cm for the yam slices. The predicted response variables for the suggested optimum drying conditions of the maize grains were 395 min, 150.882 kWh/kg and 8.012% with desirability factor of 0.762. While the predicted response variables for the suggested optimum drying conditions of the yam slices were 255.74 min, 39.52 kWh/kg and 43.02 %, respectively with desirability factor of 0.941.

m. For the description of the thin-layer drying behaviour of the maize grains, the Aghbashlo model proved to be the most suitable drying model due to its highest overall average R^2 value of 0.9978; and lowest *SSE* and *RMSE* values of 0.00226 and 0.01184, respectively.

n. Aghbashlo model was also the best drying model for describing the thin-layer drying characteristics of the 1cm yam slices due to its highest overall average R^2 value of

0.9938; and lowest overall average *SSE* and *RMSE* values of 0.00586 and 0.01640, respectively.

o. For the drying of the 1.5cm and 2cm yam slices, the Demir *et al* model was the best-suited model for predicting the drying behaviour of the yam slices, on account of its highest overall average R^2 values of 0.9968 and 0.9955; lowest overall average *SSE* values of 0.00337 and 0.00515, and lowest overall average *RMSE* values of 0.00698 and 0.01259, respectively.

p. The results obtained in terms of thermal energy and electric power consumption showed that the dryer is more efficient for yam slice drying than maize grain drying.

q. The overall results also showed that the dryer has a great potential to solve the problem of the huge cost associated with the burning of fuels experienced in conventional dryers as it is powered by the waste heat of exhaust gases, thus preventing the expenses that would have been incurred if conventional drying systems were used.

r. The dryer is also very useful in solving most of the problems encountered with open sun drying such as crop contamination by dust, insect infestation, attacks by rodents, etc.

s. This novel application technique of waste heat to drying will help for the achievement of drying of agro-products in the context of global warming, environmental protection, and economic improvement strategies.

t. The results presented in this study will come in handy for future development of waste heat crop dryers, as well as the analysis and optimization of their process parameters.

u. Heat recovery with the turbine for the production of electricity to run the electrically operated components of the dryer was not achieved when the turbine was subjected to test; hence, the electricity for the operation of the electrical components of the dryer was generated solely by the solar panel throughout the period of experiment.

5.2. Recommendations for further studies

Future studies may consider the following:

1. Considering the appreciably high thermal profiles of the dryer during the no-load test, it is obvious that the dryer can be successfully scaled up to a much larger waste heat recovery drying equipment that may be useful in food processing industries.
2. In view of the technical problems associated with the turbine unit in respect of its lubrication, efforts should be made towards their solution; for any success achieved in resolving these may be useful in other aspects of mechanical engineering research and development.
3. The optimization of the specific energy demand and process conditions of different indigenous grains, tubers and other crops is of great importance.
4. Studies on the economic and environmental sustainability analyses of the convective dryer is essential.
5. During drying, when the drying air temperature in the drying chamber exceeds the pre-set temperature of the drying product, the blower is automatically switched off during which time the heat recovery stops, it is recommended that the exhaust gas be channelled to other applications such as space heating for the purpose of incubation, etc.
6. The results achieved in this work may be useful to agro/food industries in conserving some portions of the waste heat usually encountered during food processing operations which may be applied optimally to meet the drying energy demands with reduced cost.

Contributions to knowledge

The results of the process parameters on the energy indices of maize and yam convective drying using generator exhaust gas waste heat have contributed to existing knowledge. They may gain relevance in the drying of other crops of indigenous and exotic origins, as well as in the design of energy-efficient and environment-friendly commercial crop dryers. The ways by which this work has made contributions to knowledge are as follows:

a. The successful development of an eco-friendly and economically viable convective hot air drying system powered by generator exhaust gas waste heat has been achieved. Thus providing a suitable means of cost saving in the field of drying which may have a significant impact in the area of economic development and environmental protection.
b. This study has shown that the enormous heat of the exhaust gas of combustion engines, which is directly dumped into the environment, could still be harnessed to serve some useful and economic purpose, even in other unreported areas of research that may not be related to drying.
c. It was discovered that the higher the thickness of yam slices, the lower the values of the thermal efficiency during drying. This trend is a contribution in the drying of agro-products.
d. The optimization of the drying process parameters for maize grains and yam slices in a convective hot air dryer powered by a generator exhaust gas waste heat is also a contribution to the existing knowledge.

REFERENCES

Aasa, S. A., Ajayi, O. O., & Omotosho, O. A. (2012). Design optimization of hot air dryer for yam flour chunk. *Asian Journal of Scientific Research*.; 3, 143–152.

Abano, E. E., & Amoah, R. S. (2015). Microwave and blanch-assisted drying of white yam (Dioscorea rotundata). *Food Science & Nutrition*, 3(6): 586–596. doi:10.1002/fsn3.249.

Abasi, S., Minaei, S., & Khoshtaghaza, M. H. (2017). Effect of desiccant system on thin layer drying kinetics of corn. *J Food Sci Technol*. DOI 10.1007/s13197-017-2914-z.

Abbaszadeh, A., Motevali, A., Ghobadian, B., Khoshtaghaza, M. H., & Minaei, S. (2012) Effect of air velocity and temperature on energy and effective moisture diffusivity for Russian olive (Elaeugnusan gastifolial) in thin-layer drying. *Iran journal of chemistry and chemical engineering*, 31(1): 75-79.

Adejumo, B. A., Okundare, R. O., Afolayan, O. I., & Balogun, S. A. (2013). Quality attributes of yam flour (elubo) as affected by blanching water temperature and soaking time. *IJES*. 2(1), 216-221.

Ade-Omowaye, B.I.O., Rastogi, N.K. Angersbach, A., & Knorr, D. (2002). Osmotic dehydration behaviour of red paprika (Capsicum annuum 400 L.). *Journal of Food Science*. 67 (5), 1790–1796.

Adzimah, K. S. & Seckley, E. (2009). Improvement on the Design of a Cabinet Grain Dryer. American J. of Engineering and Applied Sciences 2 (1): 217-228, 2009. ISSN 1941-7020.

Aghbashlo, M., Mobli, H., Rafiee, S., & Madadlou, A. (2012). Energy and exergy analyses of the spray drying process of fish oil microencapsulation. Biosystems Engineering, 111(2), 229-241. http:// dx.doi.org/10.1016/j.biosystemseng.2011.12.001.

Aghbashlo, M., Kianmehr, M. H., & Samimi-Akhijahani, H. (2008). Influence of drying conditions on the effective moisture diffusivity, energy of activation and energy consumption during the thin-layer drying of beriberi fruit (Beriberidaceae). Energy Conversion and Management, 49 (10) : 2865-2871.

Aghbashlo, M., Mobli, H., Rafiee, S., & Madadlou, A. (2013). A review on exergy analysis of drying processes and systems. *Renewable & Sustainable Energy Reviews*, 22, 1-22. http://dx.doi.org/10.1016/j. rser.2013.01.015.

Ajala, A. S. & Abubakar, M. A. (2018). Study of drying kinetics and quality attributes of fermented corn grains as affected by drying temperatures and velocities. *J Nutr Health Food Eng*, 8(2):205–212. DOI: 10.15406/jnhfe.2018.08.00270.

Ajala, A. S., Ngoddy, P. O., & Olajide, J. O. (2015). Design and Construction of a Tunnel Dryer for Food Crops. *International Multidisciplinary Research Journal*.. doi: 10.25081/imrj.2018.v8.3449.

Akinola, A. A. & Ezeorah, S. N. (2019). Moisture Diffusivity and Activation Energy Estimation of White Yam *(Dioscorea rotundata)* Slices Using Drying Data from a Refractance WindowTM Dryer. *FUOYE Journal of Engineering and Technology*, Vol 4, Issue 1, March 2019 ISSN: 2579-0625.

Akpinar, E., Midilli, A., & Bicer, Y. (2003) Single layer drying behaviour of potato slices in a convective cyclone dryer and mathematical modeling. *Energy Conversion Management*. 44: 1689–1705.

Akpinar, E. K., Bicer, Y., & Cetinkaya, F. (2006). Modelling of thin layer drying of parsley leaves in a convective dryer and under open sun. *Journal of Food Engineering*. **75**:308–315.

Ali, A. & Mohammad, R. V. (2015). Waste Heat Recovery Power Generation Systems for Cement Production Process. *IEEE Transactions on Industry Applications*, VOL. 51, 1-6.

Aminu, S. M. (2013). Design and construction of a Vegetable Drier. *The International Journal of Engineering And Science* (IJES). Volume 2: 88-94. ISSN(e): 2319 – 1813 ISSN(p): 2319 – 1805.

Amira, T. Saber, C., & Fethi, Z. (2014). Moisture Diffusivity and Shrinkage of Fruit and Cladode of *Opuntia ficus-indica* during Infrared Drying. *Journal of Food Processing* 2014, Article ID 175402, 9 pages http://dx.doi.org/10.1155/2014/175402.

Antwi, K.N. (2007). Comparative Study of Hybrid Solar-Gas Crop Dryer. *Unpublished M.Sc.Thesis*. University of Cape Coast, Ghana. Pp. 10-25.

Babiæ, L. J. Radojèin, M., Pavkov, I., Babiæ1, J. Turan1, M. Zoranoviæ1, & Stanišiæ, S. (2013). Physical properties and compression loading behaviour of corn seed. *Int. Agrophys*, 27, 119-126 doi: 10.2478/v10247-012-0076-9

Baker, C.G.J. (1997). Preface. In**:** Industrial Drying of Foods. Baker, C.G.J. Eds., *Chapman & Hall*, London.

Baker, C. & Shi, L. (2012). Experimental and Modeling Study of Heat Exchanger Concept for Thermoelectric Waste Heat Recovery from Diesel Exhaust", *SAE Technical Paper* 2012-01-0411, doi: 10.4271/2012-01-0411.

Barbosa-Canovas, G. V. and Vega-Mercado, H. (1996). Dehydration of Foods. USA: *Chapman and Hall*. 330 p.

BCS, Engineering Scoping Study, pp. 4-16, 2006.

Beigi, M. (2016). Energy efficiency and moisture diffusivity of apple slices during convective drying. *Food Sci. Technol, Campinas*, 36(1): 145-150, DOI: 10.1590/1678-457X.0068.

Bergmeier, M. (2003). The history of waste energy recovery in Germany since 1920. *Energy, 28*(13), 1359-1374. doi: 10.1016/s0360-5442(03)00114-2.

Brennan, J. G. (2006). Food Processing Handbook, *John Wiley and Sons*, pp-88-107

Brooker, F.H. (1973). Drying Cereal Grain. 2nd Edn., *John Wiley and Sons*, New York.

Bureau of Energy Efficiency (2014). Waste Heat Recovery: Classification, Advantages and applications, Commercially viable waste heat recovery devices, Saving potential. www.em-ea.org>book-2. Accessed 8 May 2015.

Cal, K. and Solohub, K. (2009). Spray drying technique: II. Current applications in pharmaceutical technology. *Journal of Pharmaceutical Sciences* ; 99(2):587-97.

Cao, G. Z., Tan, R., & Zhang, R. (2004). Case study based on TRIZ: Speedy cutting off valve. Retrieved from http://www.triz-journal.com/ archives/ 2004/ 07/ 03.pdf 414k 08/Jul/2009.

Caparino, O. A., Tang, J., Nindo C.I., Sablani, S.S., Powers, J.R. and Fellman, J.K. (2012) Effect of drying methods on the physical properties and microstructures of mango (Philippine 'Carabao' var.) powder J*ournal of Food Engineering* 111 , 1 , 135-148.

Carbon Trust. (2017). Food and drink – Energy efficiency and carbon saving advice for the food and drink sector, *Carbon Trust , London*.

Chayjan, R. A. , Parian J. A. and Ashari, M. E. (2011). Modeling of moisture diffusivity, activation energy and specific energy consumption of high moisture corn in a fixed and fluidized bed convective dryer. *Spanish Journal of Agricultural Research*, 9(1): 28-40.

Chayjan, R. A., Salari, K., Abedi, Q. and Sabziparvar, A. A. (2013). Modeling moisture diffusivity, activation energy and specific energy consumption of squash seeds in a semi fluidized and fluidized bed drying. *J Food Sci Technol*, 50(4): 667–677 DOI 10.1007/s13197-011-0399-8.

Chandra, P.K. and Singh, R.P. (1995). Applied Numerical Methods for Food and Agricultural Engineers. pp. 163–167. *CRC Press*, Boca Raton, FL.

Chen, H. (2011). *Converting Low-Grade Heat into Electrical Power*. [Internet document, accessed 8 August 2011]. Available at http://www.eng.usf.edu/~ hchen4/index.htm.

Claussen, I. C. Ustad, T. S. Strommen, I. and Walde. P. M.(2007.) Atmospheric Freeze Drying-A Review. *Drying Technology: An International Journal* Volume **25**, Issue 6, DOI: 10.1080/07373930701394845.

Cortez, A. and Wild-Altamirano, C. (1972). Contributions to the lime treated corn flour technology, In: *Nutritional Improvement of* Maize, Eds. Bressani, R., Braham, J.E. and Behar, INCAP pub. L4 , pp. 99-106.

Dagde, K. K. and Iminabo, J. T. (2018). Determination of kinetic parameters for thin layer drying of corn. *International Research Journal of Advanced Engineering and Science*, Volume 3, Issue 4, pp. 119-124, 2018. ISSN (Online): 2455-9024.

Danilo, M. (2003). Maize Post-Harvest Operation. *Food and Agriculture Organization of the United Nations* (FAO), AGST.

Da Silva, W. P., Silva, C. M. D., De Sousa, J. A. R., and Farias, V. S. O. (2013). Empirical and diffusion models to describe water transport into chickpea (*Cicer arietinum L*.). *Intl J Food Sci Technol*, 48(2):267–73. doi:10.1111/j.1365-2621.2012.03183.x.

Dassin, D. Y., Godi, N. Y., and Kingsley, O. C., (2015). Experimental investigation of the performance of passive solar food dryer tested in Yola-Nigeria. *International journal of energy*.

Di Matteo, M., Cinquanta, L., Galiero, G., and Crescitelli, S. (2000). Effect of a novel physical pretreatment process on the drying kinetics of seedless grapes. *Journal of Food Engineering*, 46: 83–89.

Donald, G. M. (2012). A basic guide to drying fruits and vegetables. Department of Food Science University of Guelph Ontario, Canada. https://es.scribd.com (2012). Accessed 19 February 2018.

Doymaz, I. and Pala, M. (2003). The thin-layer drying characteristics of corn. *Journal of Food Engineering* 60, 125–130.

Earle, R. L. (1992). Unit operations in food processing 2nd Edition Pargaution Press 101. Pp.79.

Eastop, T. D. & MacConkey, A. (1999). Applied Thermodynamics for Engineering Technologists. *Pearson Education Ltd*. 5th edn. 11, (pp. 366-379). Panchsheel Park, New Delhi, India

Ehiem, J.C., Irtwange, S.V. and Obetta, S.E. (2009). Design and development of an industrial fruit and vegetable dryer. *Research Journal of Applied Sciences, Engineering and Technology*, 1(2), 44 –53.

Ekechukwu, O.V. (1999). Review of solar-energy drying systems I: an overview of drying principles and theory. Energy Conversion & Management, 40: 593-613.

El-Beltagy A., Gamea, G. R., and Essa, A. H. A. (2007). Solar drying characteristics of strawberry. *J Food Engr*, 78:456–64. doi:10.1016/j.jfoodeng.2005.10.015.

Elikhani, Z. (1990). Zeolites as particulate medium for contact heating and drying of corn. The thesis submitted to the Faculty of Graduate Studies and Research of McGill University, Québec, Canada.

Woolley, E., Yang, L. and Alessandro, S. (2018). Industrial waste heat recovery: A systematic approach. *Sustainable Energy Technologies and Assessments, (29) 50–59.*

Eran, K. and Yalçin C. (2007). Moisture Dependent Physical Properties of Dry Sweet Corn Kernels. *International Journal of Food Properties, Taylor & Francis Group*, LLC, (10) 549–560.

Eren, I. and Kaymak-Ertekin, F. (2007). Optimization of osmotic dehydration of potato using response surface methodology. *Journal of Food Engineering*, (79), 344–352.

Etoamaihe, U. J. and Ibeawuchi, K. O. (2010) Prediction of the drying rates of cassava slices during oven drying. *Journal of Eng and Applied sciences,* 5(4), 308-311.

FAO., (1992). Food loss prevention in perishable crops. *Food and Agriculture Organization of the United Nations*.

Farkas, D. and Lazar, M.G. (1969). Osmotic dehydration of apple pieces. *Food Technology*, 196 23:688-690.

Fashina, A. B., Akande, F. B., Ibrahim, S. O. and Sanusi, B. A. (2013). Design parameters for a small- scale batch in-bin maize dryer. Vol.4, No.5B, 90-95 (2013) *Agricultural Sciences* doi:10.4236/as.2013.45B017.

Feldman, M. (1984). Heat Recovery for Canadian Food and Beverage Industries, *Minister of Supply and Services Canada, Ottawa.*

Goswami, D. Y. (1998). Solar thermal power technology: Present status and ideas. *Energy Sources,* vol. 20, p. 137.

Greszler, A. (2008). Diesel Turbo-compound Technology", presented at ICCT/NESCCAF Workshop, USA, February 20th.

Gunnar, L. (2013). Waste Heat Recovery from Combustion Engines based on the Rankine Cycle. Thesis for Licentiate of Engineering, Department of Applied Mechanics, Chalmers University of Technology Gothenburg, Sweden. no 04, 2013: P. 21-26, ISSN: 1652-8565.

Gürsoy, S, Choudhary, R, Watson, D. G. (2013). Microwave drying kinetics and quality characteristics of corn. *Int J Agric & Biol Eng*, 6(1): 90－99.

Hatazawa, M., Sugita, H., Ogawa, T. and Seo, Y.(2004). Performance of a thermoacoustic sound wave generator driven with waste heat of automobile gasoline engine". *Transactions of the Japan Society of Mechanical Engineers*;70(689):292–9.

Hebbar, H. U., Vishwanathan, K. H., & Ramesh, M. N. (2004). Development of combined infrared and hot air dryer for vegetables. *Journal of Food Engineering*, 65(4), 557-563. http://dx.doi.org/10.1016/j. jfoodeng.2004.02.020.

Henderson, S.M., and Pabis, S. (1961). Grain drying theory I: Temperature effect on drying coefficient. *Journal of Agricultural Engineering Research*. **6**:169–174.

Henry, C. J. K. (1997). New food processing technologies: from foraging to farming to food technology. *Proceedings of the Nutrition Society* **56**, 855-863.

Herter, U. and Burris, J. S. (1989). Preconditioning reduces the susceptibility to drying incury in corn seed. *Canadian Journal of Plant Science*; 69: 775-789.

Heywood, J. B. (2011). Internal Combustion Engine Fundamental," *Tata McGraw Hill Education Private Limited*, Edition, pp 249-250.

Holman, J.P. (1998). Heat Transfer. 9th Edn. *McGraw Hill*, New York.

Hugues, L. and Talom, A. B. (2009), "Heat recovery from automotive engine" *Applied Thermal Engineering*, 29: 439–444.

Hussain, Q. E., Brigham, D. R. and Maranville, C. W. (2009). "Thermoelectric Exhaust Heat Recovery for Hybrid Vehicles", *SAE Int. J. Engines* 2(1):1132-1142, doi: 10.4271/2009-01-0327.

Jin, Z.H. (2014). Thermal stresses in a multilayered thin film thermoelectric structure. Microelectron. Reliab, (54), 1363–1368.

Jouhara, H., Navid, K., Sulaiman, A., Bertrand D., Amisha C., Savvas, A. T. (2018). Waste heat recovery technologies and applications. *Thermal Science and Engineering Progress 6 (2018) 268–289.*

Ingram, G. (2009). Basic Concepts in Turbomachinery. *Ventus Publishing APS*. ISBN: 978-87-7681-435-9.

Ismail, Y., Durrieu, D., Menegazzi, P., Chesse, P. and Chalet, D (2012). Potential of Exhaust Heat Recovery by Turbocompounding, *SAE Technical Paper* 01-1603, doi: 10.4271/2012-01-1603.

Jadhao, J. S. and Thombare, D. G. (2013). Review on Exhaust Gas Heat Recovery for I.C. Engine. *International Journal of Engineering and Innovative Technology (IJEIT)* Volume 2, Issue 12, June 2013. ISSN: 2277-3754.

Jiangzhou, S. R., Wang, Z., Lu, Y.Z., Xu, Y.X., Wu, J.Y. and Li, Z.H. (2003). Locomotive driver cabin adsorption air-conditioner," *Renewable Energy* 28 (2003) 1659–1670.

Karthik, S.K., Mahesh, T.,Sumanth, B. Tanmay, M. (2017). Study of Physical and Engineering Properties of Corn (*Zea mays*). *Bull. Env. Pharmacol.* Life Sci., Vol 6 Special issue [1] 2017: 404-409.

Katiyar, A. and Sudhakar, K. (2013). A review on the Tray Dryer System for Agricultural Products. Conference Paper: *Energy Centre*, Maulana Azad National Institute of Technology, Bhopal (M.P) 462051, India.

Keey, R. B. (1972). Introduction. In: Drying Principles and Practice. pp. 1–18. Keey, R.B. Eds., *Pergamon Press, Oxford*.

Khurmi, R. S. and Gupta, J. K. (2005). A text book on Machine Design. *Eurasia Publishing House* (PVT.) Ltd. Ram Nagar, New Delhi-110 055.

Kouadio, C. J., Ghislaine, D. N. K., Assoi, Y.D., Kouamé, L. P. and Kamenan, A. (2017). Biochemical and Functional Properties of Yam Flour during the Post-harvest Conservation of Dioscorea alata Cultivar « Azaguié ». *Current Journal of Applied Science and Technology*, 21(6): 1-10, 2017; Article no.CJAST.32404.

Kucuk, H., Midilli, A., Kilic, A. and Dincer, I. (2014). A review on thin-layer drying-curve equations. *Drying Technol* 32(7):757–73. doi:10.1080/07373937.2013.873047.

Kudra, T., and Mujumdar, A.S. (2002). Part I. General Discussion: Conventional and Novel Drying Concepts. In: *Advanced Drying Technologies*. pp. 1–26.

Kushwaha, S. (2012). Physical and Nutritional Quality of Onion Stalk. Asian J. *exp. biol. SCI*. Vol **3**(3): 531- 535.

Law, L.C and Mujumdar, A.S. (2006), Fluidized bed drying, Handbook of industrial drying, Chap 8. ©*Taylor & Francis Group LLC*.

Lee, M.Y., Seo, J.H., Lee, H.S. and Garud, K.S.(2020). Power generation, efficiency and thermal stress of thermoelectric module with leg geometry, material, segmentation and two-stage arrangement. *Symmetry*, 12, 786.

Legros, A., Guillaume, L., Diny, M., Zaïdi, H. and Lemort, V. (2014). Comparison and Impact of Waste Heat Recovery Technologies on Passenger Car Fuel Consumption in a Normalized Driving Cycle. *Energies*, 7, 5273-5290;ISSN 1996-1073. www.mdpi.com/journal/energies.

Lewis, W.K. (1921). The rate of drying of solid materials. I&EC-Symposium of Drying, 3(5):42.

Lopez, A., Iguaz, A., Esnoz, A. and Vireda, P. (2000): Thin-layer drying behavior of vegetable waste from wholesale market. *Drying Technology*, 18: 995–1006.

Ma, Q., Fang, H., & Zhang, M. (2017). Theoretical analysis and design optimization of thermoelectric generator. *Appl. Therm. Eng*., (127), 758–764

Makanjuola, G. A., Abimbola, T. O. and Anazodo, U. G. (1991). Agricultural mechanization policies and strategies in Nigeria. *Proceedings of a workshop on agriculture, mechanical and strategies in Africa*. 1991; 99–120.

Marinos-Kouris, D., and Maroulis, Z.B. (1995). Transport Properties in the Drying of Solids. In:Handbook of Industrial Drying. pp. 113–160.

Marques, L. G., Silveira, A. M., and José, T. (2006). Freire Freeze-Drying Characteristics of Tropical Fruits. *Drying Technology: An International Journal* Volume 24, Issue 4, pages 457-463 DOI:10.1080/07373930600611919.

Martin, N., Worrell, E., Ruth, M., Price, L., Elliott, R. N., & Shipley, A. M. (2000). *Emerging energy-efficient industrial technologie*. Retrieved from http:// Gerdau. escholarship.org/uc/item/5jr2m969.

Matuam, B., Edoun, M., Kuitche, A. (2015). Zeghmati Belkacem Experimental Evaluation of the Thermal Performance of Dryer Airflow Configuration. *International Journal of Energy Engineering*, 5(4): 80-86 DOI: 10.5923/j.ijee.20150504.03.

Minasyan, A., Bradshaw, J., and Pesyridis, A. (2018). Design and Performance Evaluation of an Axial Inflow Turbocharger Turbine. *Energies*, 11: 278.

Minxing, S. (2011). The feasibility of waste heat recovery and energy efficiency assessment in a steel plant. A Master Degree thesis, Clayton H. Riddell Faculty of Environment, Earth and Resources, Natural Resources Institute University of Manitoba Winnipeg, Manitoba-R3T 2N2.

Misha, S., Mat, S., Ruslan, M. H., Sopian, K.and Salleh, E. (2013).Review on the Application of a Tray Dryer System for Agricultural Products. *World Applied Sciences Journal* 22 (3): 424-433, 2013, ISSN 1818- 4952.

Mlcak, H.A. (1996). An Introduction to the Kalina Cycle. Vol. 30, *Proceedings of the International Joint Power Generation Conference*. Book No. H01077.

Mohammad, Z., Seyed, H. S. and Barat, G. (2013) Kinetic drying and mathematical modeling of Apple slices in dehydration process. *Journal of food process and technology*. 4, (7) : 1-4.

Mohamed, S. P. and Christopher D. (2013). Design of Exhaust Heat Recovery Power Generation System Using Thermo-Electric Generator. *International Journal of Science and Research (IJSR)* ISSN (Online): 2319-7064.

Mojtaba, T. , Saeed J. and Mojtaba B. (2013). A comprehensive study on waste heat recovery from internal combustion engines using organic Rankine cycle . *Thermal Science*, 17(2): 611-624.

Montross, M. D., Bakker-Arkema, F. W.and Hines, R. E. (1999). Moisture content variation and grain quality of corn dried in different high-temperature dryers. *Transactions of the ASAE*; 42(2): 427-433.

Mori, M., Yamagami, T., Oda, N., Hattori, M. *et al*. (2009). Current Possibilities of Thermoelectric Technology Relative to Fuel Economy," *SAE Technical Paper* -01-0170, 2009, doi: 10.4271/2009-01-0170.

Motevali, A. and Chayjan, R. A. (2017). Effect of various drying bed on thermodynamic characteristics. *Case Studies in Thermal Engineering; Elsevier Ltd*: 10 (2017) 399–406.

Motevali, A., S. Minaei, A. Banakar, B. Ghobadian, and M. Khoshtaghaza. (2014a). Comparison of energy parameters invarious dryers. *Energy Conversion and Management*, 87(87):711-725.

Motevali, A., S. Minaei, A., Banakar, B. G. and H. Darvishi. (2014b). Energy analysis and drying of chamomile leaves in microwave-convective dryer. *Journal of the Saudi Society of Agricultural Sciences*, 26(2):179-187

Mujumdar, A. S. (2004) Research and Development in Drying: Recent Trends and Future Prospects, Drying Technology: *An International Journal*, **22(**1-2): 1-26, DOI: 10.1081/DRT-12002820.

Myers, R. H., Montgomery, D. C. (2002). Response Surface Methodology: Process and Product Optimization Using Designed Experiments, 2nd ed.; John Wiley & Sons: New York, 328–335.

Nadaf, S. L and Gangavati, P. B. (2014). A Review on Waste Heat Recovery and Utilization from Diesel Engines. *International Journal of Advanced Engineering Technology*, Vol. V/Issue IV/Oct.-Dec.,2014/31-39.

Naghavi, Z., Moheb, A., & Ziaei-Rad, S. (2010). Numerical simulation of rough rice drying in a deep-bed dryer using non-equilibrium model. *Energy Conversion and Management*, 51(2), 258-264. http:// dx.doi.org/10.1016/j.enconman.2009.09.019.

Nagpurwala, Q. H. (2010). Design of Axial Flow Turbine. M. S. *Ramaiah School of Advanced Studies*, Bengalaru.

Nazmi, I. and Esref, I. (2013). Batch drying characteristics of dent corn (*Zea mays* var. *indentata* Sturt). *Journal of Food, Agriculture & Environment*, 11 (1): 2 5 9 - 2 6 3.

Ndukwu, M. C. (2009) Effect of Drying Temperature and Drying Air velocity on the Drying rate and Drying constant of cocoabean. Agricultural Engineering international: *the CIGR Ejournal. Manuscript* 1091 (11): 1 – 7.

Nguyen, N.-H., Lee, D.-Y., Garud, K.S. & Lee, M.-Y. (2021). Energy Saving Economic Evaluations of Exhaust Waste Heat Recovery Hot Water Supply System for Resort. *Symmetry*, 13, 624. https://doi.org/ 10.3390/sym13040624.

Nwakuba, N.R. (2018). Experimental and Numerical Study of the Drying Process and Energy Requirements of a Hybrid Convective Vegetable Crop Dryer. Unpublished PhD thesis, Department of Agricultural and Bioresources Engineering, Federal University of Technology Owerri, Imo state, Nigeria.

Nwajinka, C.O., Nwuba, E.I.U., & Udoye, B.O. (2014) Moisture diffusivity and activation energy of drying of melon seeds. *International Journal of Applied science and Engineering*, 2 (2), 37-43.

Obi, I. U. (2001). Introduction to Factorial Experiments for Agricultural, Biological and Social Sciences Research. *Optimal International Ltd*. 113 Agbani Road, Enugu, Nigeria. 2nd Ed. ISBN: 978 2039 68 3.

Odigboh, E. U. (1991). Continuing controversies on tillage mechanization in Nigeria. *Journal of Agricultural Science and Technology*, 1: 41–49.

Oetjen, G.H., Haseley, P. (2004). Freeze Drying, completely revised edition. *Wiley VCH*.

Ojediran, J. O., Okonkwo, C. E., Adeyi, A.J., Adeyi, O., Olaniran, A. F., George, N. E, and Olayanju, A. T. (2020). Drying characteristics of yam slices (Dioscorea rotundata) in a convective hot air dryer: application of ANFIS in the prediction of drying kinetics. *Heliyon*, 6: 1-13. DOI: 10.1016/j.heliyon.2020.e03555.

Olanipekun, B. F., Tunde-Akintunde, T. Y., Oyelade, O. J., Adebisi, M. G., & Adenaya, T. A. (2015). Mathematical modelling of thin-layer pineapple drying. *Journal of Food Processing and Preservation*. 39**,** 1431–1441 (2015). DOI:10.1111/JFPP.12362.

Oni, R. and Mazlan, M. (2021). A review of Industrial Waste Heat Recovery System for Power Generation with Organic Rankine Cycle : Recent Challenges and Future Outlook. Journal of Cleaner Production. Vol 287. https://doi.org/10.1016/j.jclepro.2020.125070

Onu, C. E., Igbokwe P. K. and Nwabanne J. T. (2017). Effective Moisture Diffusivity, Activation Energy and Specific Energy Consumption in the Thin-Layer Drying of Potato. *International Journal of Novel Research in Engineering and Science*, 3(2): 10-22.

Onwude, D.I., Hashim N., Janius, R.B., Nawi, N.M. and Abdan K. (2016).Modeling the Thin-Layer Drying of Fruits and Vegetables: A Review. *Comprehensive Reviews in Food Science and Food Safety*, 15: 599-618. doi: 10.1111/1541-4337.12196.

Oomori, H.; Ogino, S. (1993). Waste heat recovery of passenger car using a combination of rankine bottoming cycle and evaporative engine cooling system. *SAE Technical Paper* 1993, doi:10.4271/930880.

Otegbayo, B.O., Samuel, F.O., Kehinde, A.L., Sangoyomi, T.E., & Okonkwo, C.C. (2010) Perception of food quality in yam by some Nigerian farmers. *Afr J Food Sci*. 4(8), 541-549.

Overhults, D. G., White, G.M., Hamilton, H.E., and Ross, I.J. (1973). Drying soybeans with heated air. *Trans. ASAE*, 16:112–113.

Oyewole, S. N., Olaoye, S. O. (2013). Effect of Drying and Blanching Parameters on Drying Rate of 'Poundo' Yam. International Journal of Scientific & Engineering Research, 4: Issue 1, January-2013 ISSN 2229-5518,IJSER © 2013. http://www.ijser.org.

O'zdemir, M., and Devres, Y.O. (1999). The thin layer drying characteristics of hazelnuts during roasting. *Journal of Food Engineering*. 42:225–233.

Page, G.E. (1949). Factors ınfluencing the maximum rate of air drying of shelled corn in thin-layers. M.S.Thesis, Purdue University, West Lafayette, Indiana.

Parry, J. L. (1985). Mathematical modeling and computer simulation of heat and mass transfer in agricultural grain drying. *Journal of Agricultural Engineering Research*. **54**:339–352.

Parti, M. (1993). Selection of mathematical models for drying in thin layers. *Journal of Agricultural Engineering Research*. **54**:339–352.

Passamai, V. and Saravia, L. (1997): Relationship between a solar drying model of red pepper and the kinetics of pure water evaporation. II. *Drying Technology*, **15**: 1433–1457.

Patel, P.S. & Doyle, E.F. (1976). Compounding the truck diesel engine with an organic rankine cycle system. *In Proceedings of Automotive Engineering Congress and Exposition*, Detroit, MI, USA.

Patil, M.S. Seo, J.H. & Lee, M.Y. (2018). Numerical Study on Geometric Parameter effects of Power Generation Performances for Segmented Thermoelectric Generator. *Int. J. Air-Cond. Refrig*. 26, 1850004.

Paulsen, M. R., Hofing, S. L. Hill, L. D. and Eckhoff, S. R. (1996). Corn quality characteristics for Japan markets. *Applied Engineering in Agriculture*; 12(6): 731-738.

Pradip, G. K. and Hole, J. A. (2015). A review on waste heat recovery and utilization from exhaust gas of I.C engine. *International Journal for Scientific Research & Development*, 3: 1321–1325.

Pua, C. K., Hamid, N. S. A., Tan, C. P., Mirhosseini, H., Rahman, R. B. A. and Rusul, G. (2010). Optimization of drum drying processing parameters for production of jackfruit (*Artocarpus heterophyllus*) powder using response surface methodology. *LWT-Food Science and Technology*, **43**: 343-349.

Rahman, M. S. (2006). Handbook of food preservation. *First Indian Reprint*, ©Marcel Dekker, Inc. pp 187-192.

Rajput, R.K. (2010). Heat and Mass Transfer in S. I. Units. 3rd Ed. *S. Chand and Company Ltd*. Ram Nagar, New Delhi-110 055, pp. 454-626.

Ramiro, T., Everaldo, J., Ricardo, D. A. Omar A. P. and Hugo T. (2012). Drying Kinetics of Two Yam (*Dioscorea alata)* Varieties. Dyna, year 79, Nro. 171, pp. 175-182. *Medellin*. ISSN 0012-7353.

Ranganna, S. (1986). Handbook of Analysis and Quality Control for Fruit and Vegetable Products. 2nd edn. P 4. *Tata McGraw-Hill Publishing Limited*, New Delhi.

Rankine, W. J. M. (1859). A Manual of the Steam Engine and Other Prime Movers. Richard Griffin and Company, Publisher to the University of Glasgow, Scotland.

Rastogi, N., Raghavarao, K., Niranjan K. and Knorr, D. (2002). Recent developments in osmotic dehydration: methods to enhance mass transfer. *Trends in food science and technology*,**13**:48 59.

Ratti, C and Crapiste, G.H. (1992). A generalized curve for shrinking food materials. In: *Drying'*92. Mujumdar A.S. Ed. Amsterdam: *Elsevier Science*, pp 864-873.

Robert, H. P. and Don, W. S. (1997). Perry's Chemical Handbook. 7th Edn. McGraw Hill, New.

Rowe, D. M. (1995). "CRC Handbook of Thermoelectrics", *CRC Press*, Florida, USA, ISBN: 978-0-8493 -0146-9.

Sablani, S. S. (2006). Drying of Fruits and Vegetables: Retention of Nutritional/Functional Quality, *Drying Technology: An International Journal*, 24:2, 123-135.

Sacilik, K. (2007). Effect of drying methods on thin-layer drying characteristics of hull less seed pumpkin (*Cucurbita pepo* L.). *J. Food Eng*, 79: 23-30.

Saidur, R. (2012). Technologies to recover exhaust heat from internal combustion engines. *Renewable and Sustainable Energy Reviews* 16, 2012, 5649–5659.

Sanful, R., Addo, A., Oduro I. and Ellis, W. (2015). Air Drying Characteristics of Aerial Yam (*Dioscorea bulbifera*). *Sch. J. Eng. Tech*., 3(8):693-700.

Siddiqui, A. S., Marnay, C., Firestone, R. M., & Zhou, N. (2007). Distributed generation with heat recovery and storage. *Journal of Energy Engineering*, *133*(3), 181-210.

Singham, P. and Birwal, P. (2012). Technological Revolution in Drying of Fruit and Vegetables. *International Journal of Science and Research* (IJSR) ISSN (Online): 2319-7064.

Stabler, F. (2002). Automotive applications of high efficiency thermoelectrics, in DARPA/ONR program review and DOE high efficiency thermoelectric workshop: San Diego.

Stobart, R., Wijewardane, A. and Allen, C. (2010). The Potential for Thermo-Electric Devices in Passenger Vehicle Applications", *SAE Technical Paper* 2010-01-0833, doi: 10.4271/2010-01-0833.

Syahrul, S., Hamdullahpur, F., & Dincer, I. (2002). Exergy analysis of fluidized bed drying of moist particles. *Exergy International Journal*, 2(2): 87-98. http://dx.doi.org/10.1016/S1164-0235(01)00044-9.

Talbi, M. and Agnew, B. (2002). Energy recovery from diesel engine exhaust gases for performance enhancement and air conditioning," *Applied Thermal Engineering*, 22: 693–702.

Timothy, J. (1990). Chemical ecology & origin of human diet and medicine. *University of Arizona Press*. pp **82**-84.

Tiwari, G. N. (2012.). Solar Energy Fundamentals, Design, Modeling and Application. *Narosa Publishing House PVT Ltd*., New Delhi; Pp. 203 – 250.

Toom, R. (2007). Waste heat regeneration systems for internal combustion engines. In Proceedings of Global Powertrain Congress, Berlin, Germany.

Turner, W. & Doty, S. (2006). Energy Management Handbook. *US DOE EIA, Annual Energy Review*.

Turns, S. R. (2006). Thermodynamics: Concepts and Applications, *Cambridge University Press*, UK, ISBN 978-0521850421.

Tzempelikos, D. A., Vouros, A. P., Bardakas, A. V., Filios, A. E., and Margaris, D. P. (2014). Case studies on the effect of the air drying conditions on the convective drying of quinces. *Case Stud Thermal Engr*, 3:79–85. doi:10.1016/j.csite.2014.05.001.

Valdimarsson, P. (2003). ORC and Kalina Analysis and Experience. Lecture material.

Van Arsdel, W. B. and Copley, M. J. (1963). Food Dehydration, Vol.1, *The AVI Publishing Company*, pp 85.

Vieira, M. G. A., Estrella, L., Rocha, S. C. S. (2007). Energy efficiency and drying kinetics of recycled paper pulp. *Dry. Technol*, 25: 1639–1648.

Vijayaraghavan, S. and Goswami, D.Y. (2006). A combined power and cooling cycle modified to improve resource utilization efficiency using a distillation stage, *Energy*, 31: 1177-1196.

Wall, J. S., James, C. and Donaldson, G. L. (1975). Corn proteins: Chemical and physical changes during drying of corn. *Cereal Chemistry*; 52 (6): 779-790.

Wang, R. Z. & Wu, D. W. (2006). Combined cooling, heating and power: A review. *Progress in Energy and Combustion Science,* 32: 459–495.

Watkins, A. E and Maier, D. E. (1997). Thin layer drying rates and stress cracking of white food corn hybrids. *ASAE Paper,* No. 97-6065.

White, G. M., Bridges, T. C., Loewer, O. J., and Ross, I. J. (1978). Seed coat damage in thin layer drying of soybeans as affected by drying conditions. *ASAE paper* no. 3052.

Wilhelm, L. R., Suter, D. A. and Brusewitz, G. H. (2004). Food and Process Engineering Technology, *American Society of Agricultural Engineers (ASAE)*, USA, pp. 213-235.

Yagcioglu, A., Degirmencioglu, A., and Cagatay, F. (1999). Drying characteristics of laurel leaves under different conditions. Proceedings of the 7th international congress on agricultural mechanization and energy, ICAME'99, pp. 565–569, Adana, Turkey.

Yamaguchi, H., Zhang, X. R., Fujima, K., Enomoto, M. and Sawada, N. (2006). Solar energy powered Rankine cycle using supercritical CO2. Applied Thermal Engineering 26, 2345–2354.

Yilbas, B.S., Hussain,M.M., and Dincer, I. (2003). Heat and moisture diffusion in slab products to convective boundary conditions. *Heat and Mass Transfer*. 39:471–476.

Zafer, E. and Filiz, I. (2009a). A Review of Thin Layer Drying of Foods: Theory, Modeling, and Experimental Results. Critical Reviews in Food Science and Nutrition, 50:441–464. *Taylor and Francis Group, LLC*; DOI: 10.1080/10408390802437063.

Zafer, E. & Filiz, I. (2009b): Optimization of Drying of Olive Leaves in a Pilot-Scale Heat Pump Dryer, *Drying Technology: An International Journal*, 27:3, 416-427.

Zahra, N., Mohammad, J. S., Seyyed, M. S. and Mohammad, E .K. F. (2014). Analysis of Laboratory Model of Corn Reservoir Dryer with Fixed Bed. *International Journal of Farming and Allied Sciences*. 3-10/1049-1053, ISSN 2322-4134.

Zamfirescu, C. & Dincer, I. (2008). Thermodynamic analysis of a novel ammonia– water trilateral Rankine cycle. *Thermochimica Acta,* 477: 7–15.

APPENDICES

Appendix A: Properties of some common food products

Crop	Freezing point (°C)	Percent water	Specific heat above freezing (kJ kg^{-1}°C^{-1})	Specific heat below freezing (kJ kg^{-1}°C^{-1})	Latent heat of fusion (kJ kg^{-1})
Apples	-2	84	3.60	1.88	280
Bananas	-2	75	3.35	1.76	255
Grapefruit	-2	89	3.81	1.93	293
Peaches	-2	87	3.78	1.93	289
Pineapples	-2	85	3.68	1.88	285
Watermelons	-2	92	4.06	2.01	306
Vegetables					
Asparagus	-1	93	3.93	2.01	310
Beans (green)	-1	89	3.81	1.97	297
Cabbage	-1	92	3.93	1.97	306
Carrots	-1	88	3.60	1.88	293
Corn	-1	76	3.35	1.80	251
Peas	-1	74	3.31	1.76	247
Tomatoes	-1	95	3.98	2.01	310
Meat					
Bacon	-2	20	2.09	1.26	71
Beef	-2	75	3.22	1.67	255
Fish	-2	70	3.18	1.67	276
Lamb	-2	70	3.18	1.67	276
Pork	-2	60	2.85	1.59	197
Veal	-2	63	2.97	1.67	209
Miscellaneous					
Beer	-2	92	4.19	2.01	301
Bread	-2	32-37	2.93	1.42	109-121
Eggs	-3		3.2	1.67	276
Ice cream	-3 to -18	58-66	3.3	1.88	222
Milk	-1	87.5	3.9	2.05	289
Water	0	100	4.19	2.05	335

Based on extracts, by permission, from *ASHRAE Guide and Data Books*.

Appendix B: Average values of temperature profile for no load test of the dryer for the three drying trays at varying air velocities

- Average ambient temperature – 32.1℃
- Average humidity -52%

Time (min)	Air velocity (m/s)								
	1.0			**1.5**			**2.0**		
	T_1 (℃)	T_2 (℃)	T_3 (℃)	T_1 (℃)	T_2 (℃)	T_3 (℃)	T_1 (℃)	T_2 (℃)	T_3 (℃)
0	32.1	32.1	32.1	31.9	31.9	31.9	32.3	32.3	32.3
3	49.6	48.9	48.5	69.3	68.6	62.2	71.3	70.3	69.6
6	66.4	64.8	62.6	82.5	80.1	75.6	91.1	89.6	88.1
9	77.2	74.8	72.2	89.6	90.1	84.8	101.1	99.7	98.3
12	83.8	81.4	78.5	95.7	95.3	90.9	106.2	104.4	103.8
15	88.7	86.1	83.2	98.9	98.6	94.1	109.8	108.3	106.9
18	92.9	90.3	87.6	100.8	100.6	96.2	112.2	110.8	109.8
21	96.7	94.1	91.1	102.9	103.0	98.6	113.3	112.0	111.1
24	97.8	95.1	92.1	104.1	104.2	99.9	114.1	112.8	112.0
27	99.5	97.3	93.8	104.8	104.8	100.8	114.6	113.5	112.4
30	101.2	99.3	96.5	105.4	105.6	101.6	115.1	113.9	113.0
33	102.9	100.5	97.3	106.8	107.1	102.8	115.6	114.3	113.9
36	104.8	101.2	99.5	108.3	108.7	104.3	116.0	114.9	114.3
39	105.1	102.8	100.1	109.3	109.5	105.6	116.1	114.9	114.5
42	105.7	103.0	100.4	109.9	110.5	106.5	116.1	114.9	114.5
45	106.1	103.5	100.8	111.0	111.2	106.9	116.1	114.9	114.5
48	107.3	105.2	101.4	111.0	111.3	107.5	116.1	114.9	114.5

Appendix C: Bill of Engineering Measurement and Evaluation (BEME)

S/N	Material /Description	Capacity	Quantity	Unit price(rate) (N)	Total Amount (N)
FOR THE FABRICATION OF HEAT RECOVERY TURBINE					
1	Impeller/ propeller shaft			800	800
3	Bearing		2	300	600
4	Pulley		2	1,500	3,000
5	Belt		2	200	400
6	Half gauge 16 sheet			5000	5,000
7	Galvanized pipe			2000	2,000
8	Bolt/nuts			200	200
9	Labour			5000	5,000
10	Transportation			3000	3,000
11	Subtotal			18,800	**20,800**
12	Labour			5000	5,000
13	Total				**25,800**
FOR THE FABRICATION OF THE HEAT EXCHANGER					
14	Galvanized pipes				10,000
15	Half gauge 16 sheet			5000	5,000
16	Electrodes			1000	1,000
17	Paint			1,500	1,500
18	Blower	10 watt	1	3500	3,500
19	Frame pipes		5	1200	6,000
20	Thermal insulating material		2kg	1000	2,000
21	Diesel		10 litres	200	2,000
22	Subtotal				**38,000**
23	Labour			10,000	10,000
24	Total				**48,000**
FOR THE FABRICATION OF THE DRYER					
26	2.5 sheets (16 gauge)			25,000	25,000
27	Pipes for frames		3	2000	6,000
28	Electrodes			3000	3,000
39	Pyrometer		1	12000	12,000
30	Thermometers		2	1000	2,000
40	Abrasive			800	800
41	Pop rivets			2000	2,000
42	Fibre glass			5000	5,000
43	4” pipe			7,600	7,600
44	Pipe bends		6	600	3,600
33	Cutting discs			2000	2000
34	Wire gauge			3000	3,000

35	Quarter rods		9	500	4,500
36	Temperature control valves		2	3000	6,000
37	Bimetallic strip		1	2500	2,500
38	Diesel			3000	3,000
39	Subtotal				**88, 000**
40	Labour				15,000
41	Total				**103,000**
Grand Total = N176,800					

Appendix D

D1: Drying Data for Maize Grains at 60℃ and 2.0 m/s

Time (mins)	Sample weight (g)	Moisture Content (wb)	Moisture Content (db)	Weight Loss (%)	Drying Rate (g/min)	Moisture Ratio
0	1500	0.356	0.552795	0.00000	0.00000	1.00000
30	1416.72	0.318143	0.466584	5.552	0.002874	0.844045
60	1355.34	0.287264	0.403043	9.644	0.002118	0.729101
90	1301.01	0.2575	0.346801	13.266	0.001875	0.62736
120	1252.38	0.228669	0.29646	16.508	0.001678	0.536292
150	1211.65	0.20274	0.254296	19.22333	0.001405	0.460019
180	1175.08	0.177928	0.216439	21.66133	0.001262	0.391536
210	1141.18	0.153508	0.181346	23.92133	0.00117	0.328052
240	1117.52	0.135586	0.156853	25.49867	0.000816	0.283745
270	1093.78	0.116824	0.132277	27.08133	0.000819	0.239288
300	1073.34	0.100006	0.111118	28.444	0.000705	0.201011
330	1053.05	0.082665	0.090114	29.79667	0.0007	0.163015
360	1032.875	0.064746	0.069229	31.14167	0.000696	0.125234
390	1013.48	0.046848	0.049151	32.43467	0.000669	0.088914
420	998.76	0.032801	0.033913	33.416	0.000508	0.061348
450	989.45	0.0237	0.024275	34.03667	0.000415	0.043914

D2: Drying Data for Maize Grains at 55℃ and $2.0\ m/s$

Time (mins)	Sample weight (g)	Moisture Content (wb)	Moisture Content (db)	Weight Loss (%)	Drying Rate (g/min)	Moisture Ratio
0	1500	0.356	0.552795	0.00000	0.00000	1.00000
30	1431.55	0.325207	0.481936	4.563333	0.002362	0.871816
60	1376.51	0.298225	0.424959	8.232667	0.001899	0.768745
90	1325.47	0.271202	0.372122	11.63533	0.001761	0.673165
120	1284.065	0.247702	0.32926	14.39567	0.001429	0.595627
150	1247.18	0.225453	0.291077	16.85467	0.001273	0.526554
180	1213.84	0.204178	0.256563	19.07733	0.00115	0.46412
210	1182.67	0.183204	0.224296	21.15533	0.001076	0.405749
240	1152.84	0.162069	0.193416	23.144	0.001029	0.349888
270	1125.42	0.141654	0.165031	24.972	0.000946	0.298539
300	1098.34	0.120491	0.136998	26.77733	0.000934	0.247828
330	1075.35	0.101688	0.113199	28.31	0.000793	0.204775
360	1051.31	0.081146	0.088313	29.91267	0.00083	0.159757
390	1030.01	0.062145	0.066263	31.33267	0.000735	0.119869
420	1010.345	0.043891	0.045906	32.64367	0.000679	0.083043
450	998.18	0.032239	0.033313	33.45467	0.00042	0.060262
480	990.98	0.025207	0.025859	33.93467	0.000248	0.046779

D3: Drying Data for Maize Grains at 50℃ and 2.0 m/s

Time (mins)	Sample weight (g)	Moisture Content (wb)	Moisture Content (db)	Weight Loss (%)	Drying Rate (g/min)	Moisture Ratio
0	1500	0.356	0.552795	0.00000	0.00000	1.00000
30	1446.91	0.33237	0.497836	3.539333	0.001832	0.900581
60	1395.41	0.30773	0.444524	6.972667	0.001777	0.804139
90	1359.87	0.289638	0.407733	9.342	0.001226	0.737584
120	1327.16	0.27213	0.373872	11.52267	0.001129	0.67633
150	1295.23	0.254187	0.340818	13.65133	0.001102	0.616536
180	1263.42	0.235409	0.307888	15.772	0.001098	0.556966
210	1234.28	0.217357	0.277723	17.71467	0.001006	0.502397
240	1206.73	0.19949	0.249203	19.55133	0.000951	0.450805
270	1180.88	0.181966	0.222443	21.27467	0.000892	0.402397
300	1157.37	0.165349	0.198106	22.842	0.000811	0.358371
330	1135.17	0.149026	0.175124	24.322	0.000766	0.316798
360	1114.43	0.133189	0.153654	25.70467	0.000716	0.277959
390	1093.57	0.116655	0.13206	27.09533	0.00072	0.238895
420	1073.34	0.100006	0.111118	28.444	0.000698	0.201011
450	1054.67	0.084074	0.091791	29.68867	0.000644	0.166049
480	1036.96	0.068431	0.073458	30.86933	0.000611	0.132884
510	1022.54	0.055294	0.05853	31.83067	0.000498	0.10588
540	1009.91	0.043479	0.045455	32.67267	0.000436	0.082228
570	1002.43	0.036342	0.037712	33.17133	0.000258	0.068221

D4: Drying Data for Maize Grains at 60℃ and $1.5\ m/s$

Time (mins)	Sample weight (g)	Moisture Content (wb)	Moisture Content (db)	Weight Loss (%)	Drying Rate (g/min)	Moisture Ratio
0	1500	0.356	0.552795	0.00000	0.00000	1.00000
30	1439.15	0.32877	0.489803	4.056667	0.0021	0.886049
60	1390.43	0.305251	0.439369	7.304667	0.001681	0.794813
90	1345.78	0.282201	0.393147	10.28133	0.001541	0.711199
120	1306.57	0.26066	0.352557	12.89533	0.001353	0.637772
150	1268.51	0.238477	0.313157	15.43267	0.001313	0.566498
180	1231.62	0.215667	0.274969	17.892	0.001273	0.497416
210	1197.18	0.193104	0.239317	20.188	0.001188	0.432921
240	1165.24	0.170986	0.206253	22.31733	0.001102	0.373109
270	1135.51	0.149281	0.175476	24.29933	0.001026	0.317434
300	1107.93	0.128104	0.146925	26.138	0.000952	0.265787
330	1081.01	0.106391	0.119058	27.93267	0.000929	0.215375
360	1055.87	0.085115	0.093033	29.60867	0.000867	0.168296
390	1035.35	0.066982	0.071791	30.97667	0.000708	0.129869
420	1020.53	0.053433	0.056449	31.96467	0.000511	0.102116
450	1008.005	0.041671	0.043483	32.79967	0.000432	0.078661
480	998.92	0.032956	0.034079	33.40533	0.000313	0.061648

D5: Drying Data for Maize Grains at 55℃ and $1.5\ m/s$

Time (min)	Sample weight (g)	Moisture Content (wb)	Moisture Content (db)	Weight Loss (%)	Drying Rate (g/min)	Moisture Ratio
0	1500	0.356	0.552795	0.00000	0.00000	1.00000
30	1442.34	0.330255	0.493106	3.844	0.00199	0.892022
60	1393.94	0.307	0.443002	7.070667	0.00167	0.801386
90	1353.51	0.2863	0.401149	9.766	0.001395	0.725674
120	1317.75	0.266932	0.36413	12.15	0.001234	0.658708
150	1286.85	0.24933	0.332143	14.21	0.001066	0.600843
180	1256.86	0.231418	0.301097	16.20933	0.001035	0.544682
210	1228.29	0.213541	0.271522	18.114	0.000986	0.49118
240	1201.16	0.195777	0.243437	19.92267	0.000936	0.440375
270	1174.25	0.177347	0.21558	21.71667	0.000929	0.389981
300	1148.96	0.15924	0.1894	23.40267	0.000873	0.342622
330	1124.73	0.141127	0.164317	25.018	0.000836	0.297247
360	1101.45	0.122974	0.140217	26.57	0.000803	0.253652
390	1078.57	0.10437	0.116532	28.09533	0.00079	0.210805
420	1058.835	0.087677	0.096102	29.411	0.000681	0.173848
450	1041.07	0.072109	0.077712	30.59533	0.000613	0.140581
480	1028.6	0.060859	0.064803	31.42667	0.00043	0.117228
510	1018.37	0.051425	0.054213	32.10867	0.000353	0.098071
540	1010.65	0.044179	0.046222	32.62333	0.000266	0.083614

D6: Drying Data for Maize Grains at 50℃ and 1.5 m/s

Time (mins)	Sample weight (g)	Moisture Content (wb)	Moisture Content (db)	Weight Loss (%)	Drying Rate (g/min)	Moisture Ratio
0	1500	0.356	0.552795	0.00000	0.00000	1.00000
30	1450.83	0.334174	0.501894	3.27800	0.001697	0.907921
60	1410.17	0.314976	0.459803	5.988667	0.001403	0.831779
90	1369.87	0.294824	0.418085	8.675333	0.001391	0.756311
120	1338.13	0.278097	0.385228	10.79133	0.001095	0.696873
150	1306.62	0.260688	0.352609	12.89200	0.001087	0.637865
180	1280.06	0.245348	0.325114	14.66267	0.000916	0.588127
210	1254.34	0.229874	0.298489	16.37733	0.000888	0.539963
240	1229.12	0.214072	0.272381	18.05867	0.000870	0.492734
270	1204.85	0.19824	0.247257	19.67667	0.000837	0.447285
300	1181.68	0.18252	0.223271	21.22133	0.000800	0.403895
330	1160.47	0.167579	0.201315	22.63533	0.000732	0.364176
360	1140.91	0.153307	0.181066	23.93933	0.000675	0.327547
390	1123.15	0.139919	0.162681	25.12333	0.000613	0.294288
420	1106.48	0.126961	0.145424	26.23467	0.000575	0.263071
450	1091.45	0.114939	0.129865	27.23667	0.000519	0.234925
480	1077.005	0.103068	0.114912	28.19967	0.000498	0.207875
510	1062.73	0.09102	0.100135	29.15133	0.000493	0.181142
540	1048.83	0.078974	0.085745	30.078	0.000480	0.155112
570	1035.45	0.067072	0.071894	30.97	0.000462	0.130056

D7: Drying Data for Maize Grains at 60℃ and $1.0\ m/s$

Time (mins)	Sample weight (g)	Moisture Content (wb)	Moisture Content (db)	Weight Loss (%)	Drying Rate (g/min)	Moisture Ratio
0	1500	0.35600	0.552795	0.00000	0.00000	1.00000
30	1441.46	0.329846	0.492195	3.902667	0.00202	0.890375
60	1391.95	0.30601	0.440942	7.203333	0.001708	0.797659
90	1352.42	0.285725	0.400021	9.838667	0.001364	0.723633
120	1317.71	0.266910	0.364089	12.15267	0.001198	0.658633
150	1285.78	0.248705	0.331035	14.28133	0.001102	0.598839
180	1254.97	0.230260	0.299141	16.33533	0.001063	0.541142
210	1227.35	0.212938	0.270549	18.17667	0.000953	0.489419
240	1201.28	0.195858	0.243561	19.91467	0.000900	0.440599
270	1175.43	0.178173	0.216801	21.638	0.000892	0.392191
300	1149.92	0.159942	0.190393	23.33867	0.000880	0.344419
330	1124.72	0.14112	0.164306	25.01867	0.000870	0.297228
360	1100.98	0.1226	0.139731	26.60133	0.000819	0.252772
390	1079.12	0.104826	0.117101	28.05867	0.000754	0.211835
420	1057.87	0.086844	0.095104	29.47533	0.000733	0.172041
450	1040.22	0.07135	0.076832	30.652	0.000609	0.138989
480	1024.51	0.05711	0.060569	31.69933	0.000542	0.109569
510	1013.55	0.046914	0.049224	32.43	0.000378	0.089045
540	1006.46	0.0402	0.041884	32.90267	0.000245	0.075768

D8: Drying Data for Maize Grains at 55℃ and $1.0\ m/s$

Time (min)	Sample weight (g)	Moisture Content (wb)	Moisture Content (db)	Weight Loss (%)	Drying Rate (g/min)	Moisture Ratio
0	1500.00	0.35600	0.552795	0.00000	0.00000	1.00000
30	1452.24	0.334821	0.503354	3.184	0.001648	0.910562
60	1411.29	0.31552	0.460963	5.914	0.001413	0.833876
90	1371.6	0.295713	0.419876	8.56	0.00137	0.759551
120	1336.17	0.277038	0.383199	10.922	0.001223	0.693202
150	1306.68	0.260722	0.352671	12.888	0.001018	0.637978
180	1279.26	0.244876	0.324286	14.716	0.000946	0.586629
210	1252.34	0.228644	0.296418	16.51067	0.000929	0.536217
240	1226.12	0.212149	0.269275	18.25867	0.000905	0.487116
270	1201.83	0.196226	0.24413	19.87800	0.000838	0.441629
300	1178.68	0.180439	0.220166	21.42133	0.000799	0.398277
330	1156.34	0.164606	0.197039	22.91067	0.000771	0.356442
360	1134.78	0.148734	0.17472	24.34800	0.000744	0.316067
390	1115.23	0.133811	0.154482	25.65133	0.000675	0.279457
420	1096.43	0.118959	0.135021	26.90467	0.000649	0.244251
450	1077.81	0.103738	0.115745	28.14600	0.000643	0.209382
480	1060.05	0.088722	0.09736	29.33000	0.000613	0.176124
510	1042.53	0.073408	0.079224	30.49800	0.000605	0.143315
540	1029.73	0.061890	0.065973	31.35133	0.000442	0.119345
570	1024.654	0.057243	0.060718	31.68973	0.000175	0.109839

D9: Drying Data for Maize Grains at 50℃ and $1.0\ m/s$

Time (mins)	Sample weight (g)	Moisture Content (wb)	Moisture Content (db)	Weight Loss (%)	Drying Rate (g/min)	Moisture Ratio
0	1500.00	0.35600	0.552795	0.00000	0.00000	1.00000
30	1461.32	0.338954	0.512754	2.578667	0.001335	0.927566
60	1428.29	0.323667	0.478561	4.780667	0.00114	0.865712
90	1396.6	0.308320	0.445756	6.893333	0.001094	0.806367
120	1366.17	0.292914	0.414255	8.922000	0.00105	0.749382
150	1335.92	0.276903	0.38294	10.93867	0.001044	0.692734
180	1306.26	0.260484	0.352236	12.91600	0.001023	0.637191
210	1276.89	0.243474	0.321832	14.87400	0.001013	0.582191
240	1249.43	0.226847	0.293406	16.70467	0.000948	0.530768
270	1224.91	0.211371	0.268023	18.33933	0.000846	0.48485
300	1203.68	0.197461	0.246046	19.75467	0.000733	0.445094
330	1183.98	0.184108	0.225652	21.06800	0.00068	0.408202
360	1166.74	0.172052	0.207805	22.21733	0.000595	0.375918
390	1150.23	0.160168	0.190714	23.31800	0.00057	0.345
420	1132.49	0.147012	0.17235	24.50067	0.000612	0.311779
450	1115.81	0.134261	0.155083	25.61267	0.000576	0.280543
480	1100.25	0.122018	0.138975	26.65000	0.000537	0.251404
510	1084.87	0.109571	0.123054	27.67533	0.000531	0.222603
540	1069.73	0.096968	0.107381	28.68467	0.000522	0.194251
570	1055.67	0.084941	0.092826	29.62200	0.000485	0.167921
600	1045.654	0.076176	0.082458	30.28973	0.000346	0.149165

D10: Drying Data for yam slices at 55℃ , 2.0 m/s and 1cm

Time (min)	Sample weight (g)	Moisture Content (wb)	Moisture Content (wb)	Weight Loss (%)	Drying Rate (g/min)	Moisture Ratio
0	2200	0.695	2.278689			
20	1952.46	0.656331	1.909776	11.25182	0.018446	0.838103
40	1713.54	0.608413	1.553711	22.11182	0.017803	0.681844
60	1490.8	0.549906	1.221759	32.23636	0.016598	0.536167
80	1319.01	0.491285	0.965738	40.045	0.012801	0.423813
100	1195.66	0.438804	0.781908	45.65182	0.009192	0.343139
120	1090.11	0.384466	0.624605	50.44955	0.007865	0.274107
140	1035.76	0.352167	0.543607	52.92	0.00405	0.238561
160	988.65	0.321297	0.473398	55.06136	0.00351	0.20775
180	956.96	0.298821	0.42617	56.50182	0.002361	0.187024
200	932.01	0.280051	0.388987	57.63591	0.001859	0.170706
220	908.68	0.261566	0.354218	58.69636	0.001738	0.155448
240	888.12	0.244471	0.323577	59.63091	0.001532	0.142001
260	870.9	0.229533	0.297914	60.41364	0.001283	0.130739
280	855.77	0.215911	0.275365	61.10136	0.001127	0.120844
300	841.01	0.20215	0.253368	61.77227	0.0011	0.11119
320	829.46	0.19104	0.236155	62.29727	0.000861	0.103636
340	818.58	0.180288	0.21994	62.79182	0.000811	0.096521
360	810.8	0.172422	0.208346	63.14545	0.00058	0.091432
380	802.8	0.164175	0.196423	63.50909	0.000596	0.0862
400	795.61	0.156622	0.185708	63.83591	0.000536	0.081498
420	788.95	0.149503	0.175782	64.13864	0.000496	0.077142
440	781.91	0.141845	0.165291	64.45864	0.000525	0.072538
460	775.91	0.135209	0.156349	64.73136	0.000447	0.068613
480	770.47	0.129103	0.148241	64.97864	0.000405	0.065056
500	765.76	0.123746	0.141222	65.19273	0.000351	0.061975
520	763.2	0.120807	0.137407	65.30909	0.000191	0.060301
540	761.09	0.11837	0.134262	65.405	0.000157	0.058921

D11: Drying Data for yam slices at 55℃, $1.5\ m/s$ and 1cm

Time (min)	Sample weight (g)	Moisture Content (wb)	Moisture Content (wb)	Weight Loss (%)	Drying Rate (g/min)	Moisture Ratio
0	2200	0.695	2.278689			
20	1960.89	0.657808	1.92234	10.86864	0.017817	0.843617
40	1721.97	0.61033	1.566274	21.72864	0.017803	0.687358
60	1499.23	0.552437	1.234322	31.85318	0.016598	0.541681
80	1327.44	0.494516	0.978301	39.66182	0.012801	0.429326
100	1204.09	0.442733	0.794471	45.26864	0.009192	0.348653
120	1098.54	0.389189	0.637168	50.06636	0.007865	0.279621
140	1044.19	0.357397	0.55617	52.53682	0.00405	0.244075
160	997.08	0.327035	0.485961	54.67818	0.00351	0.213264
180	965.39	0.304944	0.438733	56.11864	0.002361	0.192538
200	940.44	0.286504	0.40155	57.25273	0.001859	0.17622
220	917.11	0.268354	0.366781	58.31318	0.001738	0.160961
240	896.55	0.251575	0.33614	59.24773	0.001532	0.147515
260	879.33	0.236919	0.310477	60.03045	0.001283	0.136252
280	864.2	0.223559	0.287928	60.71818	0.001127	0.126357
300	849.44	0.210068	0.265931	61.38909	0.0011	0.116704
320	837.89	0.199179	0.248718	61.91409	0.000861	0.10915
340	827.01	0.188643	0.232504	62.40864	0.000811	0.102034
360	819.23	0.180938	0.220909	62.76227	0.00058	0.096946
380	811.23	0.172861	0.208987	63.12591	0.000596	0.091714
400	804.04	0.165464	0.198271	63.45273	0.000536	0.087011
420	797.38	0.158494	0.188346	63.75545	0.000496	0.082655
440	790.34	0.150998	0.177854	64.07545	0.000525	0.078051
460	784.34	0.144504	0.168912	64.34818	0.000447	0.074127
480	778.29	0.137853	0.159896	64.62318	0.000451	0.07017
500	775.19	0.134406	0.155276	64.76409	0.000231	0.068143
520	770.63	0.129284	0.14848	64.97136	0.00034	0.06516
540	766.52	0.124615	0.142355	65.15818	0.000306	0.062472
560	762.48	0.119977	0.136334	65.34182	0.000301	0.05983

D12: Drying Data for yam slices at 55℃ , 1 m/s and 1cm

Time (min)	Sample weight (g)	Moisture Content (wb)	Moisture Content (wb)	Weight Loss (%)	Drying Rate (g/min)	Moisture Ratio
0	2200	0.695	2.278689			
20	1973.21	0.659945	1.9407	10.30864	0.016899	0.851674
40	1734.29	0.613098	1.584635	21.16864	0.017803	0.695415
60	1511.55	0.556085	1.252683	31.29318	0.016598	0.549738
80	1339.76	0.499164	0.996662	39.10182	0.012801	0.437384
100	1216.41	0.448377	0.812832	44.70864	0.009192	0.35671
120	1110.86	0.395963	0.655529	49.50636	0.007865	0.287678
140	1056.51	0.36489	0.574531	51.97682	0.00405	0.252132
160	1009.4	0.335249	0.504322	54.11818	0.00351	0.221321
180	977.71	0.313702	0.457094	55.55864	0.002361	0.200595
200	952.76	0.29573	0.419911	56.69273	0.001859	0.184277
220	929.43	0.278052	0.385142	57.75318	0.001738	0.169019
240	908.87	0.261721	0.354501	58.68773	0.001532	0.155572
260	891.65	0.247463	0.328838	59.47045	0.001283	0.14431
280	876.52	0.234473	0.306289	60.15818	0.001127	0.134415
300	858.76	0.218641	0.279821	60.96545	0.001323	0.122799
320	848.21	0.208922	0.264098	61.445	0.000786	0.115899
340	836.33	0.197685	0.246393	61.985	0.000885	0.108129
360	826.55	0.188192	0.231818	62.42955	0.000729	0.101733
380	817.55	0.179255	0.218405	62.83864	0.000671	0.095847
400	816.36	0.178059	0.216632	62.89273	8.87E-05	0.095069
420	809.17	0.170755	0.205917	63.21955	0.000536	0.090366
440	802.66	0.16403	0.196215	63.51545	0.000485	0.086109
460	796.66	0.157734	0.187273	63.78818	0.000447	0.082184
480	790.61	0.151288	0.178256	64.06318	0.000451	0.078228
500	784.51	0.144689	0.169165	64.34045	0.000455	0.074238
520	776.95	0.136367	0.157899	64.68409	0.000563	0.069294
540	771.84	0.130649	0.150283	64.91636	0.000381	0.065952
560	766.43	0.124512	0.142221	65.16227	0.000403	0.062413
580	762.51	0.120012	0.136379	65.34045	0.000292	0.05985
600	759.38	0.116384	0.131714	65.48273	0.000233	0.057802

D13: Drying Data for yam slices at 55℃, 2 m/s and 1.5 cm

Time (min)	Sample weight (g)	Moisture Content (wb)	Moisture Content (wb)	Weight Loss (%)	Drying Rate (g/min)	Moisture Ratio
0	2200	0.695	2.278689			
20	1975.74	0.66038	1.944471	10.19364	0.016711	0.853329
40	1736.82	0.613662	1.588405	21.05364	0.017803	0.69707
60	1514.08	0.556827	1.256453	31.17818	0.016598	0.551393
80	1342.29	0.500108	1.000432	38.98682	0.012801	0.439039
100	1218.94	0.449522	0.816602	44.59364	0.009192	0.358365
120	1113.39	0.397336	0.6593	49.39136	0.007865	0.289333
140	1059.04	0.366407	0.578301	51.86182	0.00405	0.253787
160	1011.93	0.336911	0.508092	54.00318	0.00351	0.222976
180	980.24	0.315474	0.460864	55.44364	0.002361	0.20225
200	955.29	0.297595	0.423681	56.57773	0.001859	0.185932
220	931.96	0.280012	0.388912	57.63818	0.001738	0.170674
240	911.4	0.26377	0.358271	58.57273	0.001532	0.157227
260	894.18	0.249592	0.332608	59.35545	0.001283	0.145965
280	879.05	0.236676	0.31006	60.04318	0.001127	0.136069
300	861.29	0.220936	0.283592	60.85045	0.001323	0.124454
320	850.74	0.211275	0.267869	61.33	0.000786	0.117554
340	838.86	0.200105	0.250164	61.87	0.000885	0.109784
360	829.08	0.190669	0.235589	62.31455	0.000729	0.103388
380	820.08	0.181787	0.222176	62.72364	0.000671	0.097502
400	812.89	0.17455	0.211461	63.05045	0.000536	0.092799
420	805.37	0.166843	0.200253	63.39227	0.00056	0.087881
440	800.19	0.161449	0.192534	63.62773	0.000386	0.084493
460	795.19	0.156177	0.185082	63.855	0.000373	0.081223
480	790.14	0.150783	0.177556	64.08455	0.000376	0.07792
500	784.04	0.144176	0.168465	64.36182	0.000455	0.073931
520	779.48	0.13917	0.161669	64.56909	0.00034	0.070948
540	774.37	0.133489	0.154054	64.80136	0.000381	0.067606
560	768.96	0.127393	0.145991	65.04727	0.000403	0.064068
580	765.04	0.122922	0.140149	65.22545	0.000292	0.061504
600	761.91	0.119319	0.135484	65.36773	0.000233	0.059457

D14: Drying Data for yam slices at 55℃, $1.5\ m/s$ and 1.5 cm

Time (min)	Sample weight (g)	Moisture Content (wb)	Moisture Content (wb)	Weight Loss (%)	Drying Rate (g/min)	Moisture Ratio
0	2200	0.695	2.278689			
20	1984.17	0.661823	1.957034	9.810455	0.016083	0.858842
40	1745.25	0.615528	1.600969	20.67045	0.017803	0.702583
60	1522.51	0.55928	1.269016	30.795	0.016598	0.556906
80	1350.72	0.503228	1.012996	38.60364	0.012801	0.444552
100	1227.37	0.453303	0.829165	44.21045	0.009192	0.363878
120	1121.82	0.401865	0.671863	49.00818	0.007865	0.294846
140	1067.47	0.371411	0.590864	51.47864	0.00405	0.2593
160	1020.36	0.342389	0.520656	53.62	0.00351	0.228489
180	988.67	0.32131	0.473428	55.06045	0.002361	0.207763
200	963.72	0.30374	0.436244	56.19455	0.001859	0.191445
220	940.39	0.286466	0.401475	57.255	0.001738	0.176187
240	919.83	0.270517	0.370835	58.18955	0.001532	0.16274
260	902.61	0.2566	0.345171	58.97227	0.001283	0.151478
280	887.48	0.243927	0.322623	59.66	0.001127	0.141583
300	869.72	0.228487	0.296155	60.46727	0.001323	0.129967
320	859.17	0.219014	0.280432	60.94682	0.000786	0.123067
340	847.29	0.208063	0.262727	61.48682	0.000885	0.115298
360	837.51	0.198816	0.248152	61.93136	0.000729	0.108901
380	828.51	0.190112	0.234739	62.34045	0.000671	0.103015
400	821.32	0.183022	0.224024	62.66727	0.000536	0.098313
420	813.8	0.175473	0.212817	63.00909	0.00056	0.093394
440	806.62	0.168134	0.202116	63.33545	0.000535	0.088698
460	800.62	0.1619	0.193174	63.60818	0.000447	0.084774
480	794.57	0.155518	0.184158	63.88318	0.000451	0.080818
500	789.47	0.150063	0.176557	64.115	0.00038	0.077482
520	784.91	0.145125	0.169762	64.32227	0.00034	0.0745
540	779.82	0.139545	0.162176	64.55364	0.000379	0.071171
560	774.39	0.133512	0.154083	64.80045	0.000405	0.067619
580	770.47	0.129103	0.148241	64.97864	0.000292	0.065056
600	766.53	0.124627	0.14237	65.15773	0.000294	0.062479
620	762.52	0.120023	0.136393	65.34	0.000299	0.059856

D15: Drying Data for yam slices at 55℃, $1m/s$ and 1.5 cm

Time (min)	Sample weight (g)	Moisture Content (wb)	Moisture Content (wb)	Weight Loss (%)	Drying Rate (g/min)	Moisture Ratio
0	2200	0.695	2.278689			
20	1994.49	0.663573	1.972414	9.341364	0.015314	0.865592
40	1755.57	0.617788	1.616349	20.20136	0.017803	0.709333
60	1532.83	0.562248	1.284396	30.32591	0.016598	0.563656
80	1361.04	0.506995	1.028376	38.13455	0.012801	0.451302
100	1237.69	0.457861	0.844545	43.74136	0.009192	0.370628
120	1132.14	0.407317	0.687243	48.53909	0.007865	0.301596
140	1077.79	0.37743	0.606244	51.00955	0.00405	0.26605
160	1030.68	0.348973	0.536036	53.15091	0.00351	0.235239
180	998.99	0.328322	0.488808	54.59136	0.002361	0.214513
200	974.04	0.311117	0.451624	55.72545	0.001859	0.198195
220	950.71	0.294212	0.416855	56.78591	0.001738	0.182937
240	930.15	0.278611	0.386215	57.72045	0.001532	0.16949
260	912.93	0.265004	0.360551	58.50318	0.001283	0.158228
280	897.8	0.252618	0.338003	59.19091	0.001127	0.148332
300	880.04	0.237535	0.311535	59.99818	0.001323	0.136717
320	869.49	0.228283	0.295812	60.47773	0.000786	0.129817
340	857.61	0.217593	0.278107	61.01773	0.000885	0.122047
360	847.83	0.208568	0.263532	61.46227	0.000729	0.115651
380	838.83	0.200076	0.250119	61.87136	0.000671	0.109765
400	830.64	0.192189	0.237914	62.24364	0.00061	0.104408
420	822.12	0.183817	0.225216	62.63091	0.000635	0.098836
440	815.94	0.177636	0.216006	62.91182	0.000461	0.094794
460	809.94	0.171544	0.207064	63.18455	0.000447	0.09087
480	803.89	0.165309	0.198048	63.45955	0.000451	0.086913
500	796.79	0.157871	0.187466	63.78227	0.000529	0.082269
520	791.23	0.151953	0.17918	64.035	0.000414	0.078633
540	786.14	0.146462	0.171595	64.26636	0.000379	0.075304
560	781.71	0.141625	0.164993	64.46773	0.00033	0.072407
580	776.79	0.136189	0.15766	64.69136	0.000367	0.069189
600	772.85	0.131785	0.151788	64.87045	0.000294	0.066612
620	768.34	0.126689	0.145067	65.07545	0.000336	0.063663
640	764.67	0.122497	0.139598	65.24227	0.000273	0.061262
660	760.34	0.1175	0.133145	65.43909	0.000323	0.05843

D16: Drying Data for yam slices at 55℃, $2.0\ m/s$ and 2cm

Time (min)	Sample weight (g)	Moisture Content (wb)	Moisture Content (wb)	Weight Loss (%)	Drying Rate (g/min)	Moisture Ratio
0	2200	0.695	2.278689			
20	1992.95	0.663313	1.970119	9.411364	0.015428	0.864585
40	1754.03	0.617452	1.614054	20.27136	0.017803	0.708326
60	1531.29	0.561807	1.282101	30.39591	0.016598	0.562649
80	1359.5	0.506436	1.02608	38.20455	0.012801	0.450294
100	1236.15	0.457186	0.84225	43.81136	0.009192	0.369621
120	1130.6	0.40651	0.684948	48.60909	0.007865	0.300589
140	1076.25	0.376539	0.603949	51.07955	0.00405	0.265043
160	1029.14	0.347999	0.533741	53.22091	0.00351	0.234232
180	997.45	0.327285	0.486513	54.66136	0.002361	0.213506
200	972.5	0.310026	0.449329	55.79545	0.001859	0.197188
220	949.17	0.293067	0.41456	56.85591	0.001738	0.181929
240	928.61	0.277415	0.38392	57.79045	0.001532	0.168483
260	911.39	0.263762	0.358256	58.57318	0.001283	0.15722
280	896.26	0.251333	0.335708	59.26091	0.001127	0.147325
300	878.5	0.236198	0.30924	60.06818	0.001323	0.13571
320	867.95	0.226914	0.293517	60.54773	0.000786	0.12881
340	856.07	0.216186	0.275812	61.08773	0.000885	0.12104
360	846.29	0.207128	0.261237	61.53227	0.000729	0.114644
380	837.29	0.198605	0.247824	61.94136	0.000671	0.108757
400	829.1	0.190689	0.235618	62.31364	0.00061	0.103401
420	820.58	0.182286	0.222921	62.70091	0.000635	0.097829
440	814.4	0.176081	0.213711	62.98182	0.000461	0.093787
460	808.4	0.169965	0.204769	63.25455	0.000447	0.089863
480	802.35	0.163707	0.195753	63.52955	0.000451	0.085906
500	795.25	0.15624	0.185171	63.85227	0.000529	0.081262
520	789.69	0.150299	0.176885	64.105	0.000414	0.077626
540	784.6	0.144787	0.1693	64.33636	0.000379	0.074297
560	780.17	0.139931	0.162697	64.53773	0.00033	0.0714
580	775.25	0.134473	0.155365	64.76136	0.000367	0.068182
600	771.31	0.130051	0.149493	64.94045	0.000294	0.065605
620	766.8	0.124935	0.142772	65.14545	0.000336	0.062655
640	763.13	0.120726	0.137303	65.31227	0.000273	0.060255
660	758.8	0.115709	0.130849	65.50909	0.000323	0.057423

D17: Drying Data for yam slices at 55℃, $1.5\ m/s$ and 2cm

Time (min)	Sample weight (g)	Moisture Content (wb)	Moisture Content (wb)	Weight Loss (%)	Drying Rate (g/min)	Moisture Ratio
0	2200	0.695	2.278689			
20	2001.4	0.664735	1.982712	9.027273	0.014799	0.870111
40	1762.48	0.619286	1.626647	19.88727	0.017803	0.713852
60	1539.74	0.564212	1.294694	30.01182	0.016598	0.568175
80	1367.95	0.509485	1.038674	37.82045	0.012801	0.455821
100	1244.6	0.460871	0.854844	43.42727	0.009192	0.375147
120	1139.05	0.410913	0.697541	48.225	0.007865	0.306115
140	1084.7	0.381396	0.616542	50.69545	0.00405	0.270569
160	1037.59	0.353309	0.546334	52.83682	0.00351	0.239758
180	1005.9	0.332936	0.499106	54.27727	0.002361	0.219032
200	980.95	0.315969	0.461923	55.41136	0.001859	0.202714
220	957.62	0.299305	0.427154	56.47182	0.001738	0.187456
240	937.06	0.283931	0.396513	57.40636	0.001532	0.174009
260	919.84	0.270525	0.370849	58.18909	0.001283	0.162747
280	904.71	0.258326	0.348301	58.87682	0.001127	0.152852
300	886.95	0.243475	0.321833	59.68409	0.001323	0.141236
320	876.4	0.234368	0.30611	60.16364	0.000786	0.134336
340	864.52	0.223847	0.288405	60.70364	0.000885	0.126566
360	854.74	0.214966	0.27383	61.14818	0.000729	0.12017
380	845.74	0.206612	0.260417	61.55727	0.000671	0.114284
400	837.55	0.198854	0.248212	61.92955	0.00061	0.108927
420	829.03	0.19062	0.235514	62.31682	0.000635	0.103355
440	822.85	0.184542	0.226304	62.59773	0.000461	0.099313
460	816.85	0.178552	0.217362	62.87045	0.000447	0.095389
480	810.8	0.172422	0.208346	63.14545	0.000451	0.091432
500	803.7	0.165111	0.197765	63.46818	0.000529	0.086789
520	797.14	0.158241	0.187988	63.76636	0.000489	0.082498
540	791.05	0.15176	0.178912	64.04318	0.000454	0.078515
560	785.62	0.145898	0.17082	64.29	0.000405	0.074964
580	780.17	0.139931	0.162697	64.53773	0.000406	0.0714
600	775.76	0.135042	0.156125	64.73818	0.000329	0.068515
620	770.25	0.128854	0.147914	64.98864	0.000411	0.064912
640	766.58	0.124684	0.142444	65.15545	0.000273	0.062511
660	764.52	0.122325	0.139374	65.24909	0.000154	0.061164
680	762.25	0.119711	0.135991	65.35227	0.000169	0.05968

D18: Drying Data for yam slices at 55℃, $1.0\ m/s$ and 2cm

Time (min)	Sample weight (g)	Moisture Content (wb)	Moisture Content (wb)	Weight Loss (%)	Drying Rate (g/min)	Moisture Ratio
0	2200	0.695	2.278689			
20	2012.94	0.666657	1.999911	8.502727	0.013939	0.877659
40	1774.02	0.621763	1.643845	19.36273	0.017803	0.7214
60	1551.28	0.567454	1.311893	29.48727	0.016598	0.575723
80	1379.49	0.513588	1.055872	37.29591	0.012801	0.463368
100	1256.14	0.465824	0.872042	42.90273	0.009192	0.382695
120	1150.59	0.416821	0.714739	47.70045	0.007865	0.313663
140	1096.24	0.387908	0.633741	50.17091	0.00405	0.278116
160	1049.13	0.360422	0.563532	52.31227	0.00351	0.247305
180	1017.44	0.340502	0.516304	53.75273	0.002361	0.226579
200	992.49	0.323923	0.479121	54.88682	0.001859	0.210262
220	969.16	0.307648	0.444352	55.94727	0.001738	0.195003
240	948.6	0.292642	0.413711	56.88182	0.001532	0.181557
260	931.38	0.279564	0.388048	57.66455	0.001283	0.170294
280	916.25	0.267667	0.365499	58.35227	0.001127	0.160399
300	898.49	0.253191	0.339031	59.15955	0.001323	0.148784
320	887.94	0.244318	0.323308	59.63909	0.000786	0.141884
340	876.06	0.234071	0.305604	60.17909	0.000885	0.134114
360	866.28	0.225424	0.291028	60.62364	0.000729	0.127717
380	857.28	0.217292	0.277615	61.03273	0.000671	0.121831
400	849.09	0.209742	0.26541	61.405	0.00061	0.116475
420	840.57	0.201732	0.252712	61.79227	0.000635	0.110903
440	834.39	0.19582	0.243502	62.07318	0.000461	0.106861
460	828.39	0.189995	0.23456	62.34591	0.000447	0.102937
480	822.34	0.184036	0.225544	62.62091	0.000451	0.09898
500	815.24	0.176929	0.214963	62.94364	0.000529	0.094336
520	808.68	0.170253	0.205186	63.24182	0.000489	0.090046
540	802.59	0.163957	0.19611	63.51864	0.000454	0.086063
560	796.16	0.157205	0.186528	63.81091	0.000479	0.081857
580	790.71	0.151396	0.178405	64.05864	0.000406	0.078293
600	785.3	0.145549	0.170343	64.30455	0.000403	0.074755
620	780.69	0.140504	0.163472	64.51409	0.000344	0.07174
640	775.12	0.134328	0.155171	64.76727	0.000415	0.068097
660	770.06	0.128639	0.14763	64.99727	0.000377	0.064787
680	766.39	0.124467	0.142161	65.16409	0.000273	0.062387
700	763.06	0.120646	0.137198	65.31545	0.000248	0.060209
720	760.73	0.117952	0.133726	65.42136	0.000174	0.058685

D19: Drying Data for yam slices at 65℃ , 2.0 m/s and 1cm

Time (min)	Sample weight (g)	Moisture Content (wb)	Moisture Content (wb)	Weight Loss (%)	Drying Rate (g/min)	Moisture Ratio
0	2200	0.695	2.278689	0.00000	0.00000	1.00000
20	1899.39	0.646729	1.830686	13.66409	0.0224	0.803394
40	1655.25	0.594623	1.466841	24.76136	0.018192	0.643721
60	1433.11	0.531788	1.135782	34.85864	0.016553	0.498437
80	1263.18	0.468801	0.882534	42.58273	0.012662	0.387299
100	1138.44	0.410597	0.696632	48.25273	0.009295	0.305716
120	1035.13	0.351772	0.542668	52.94864	0.007698	0.238149
140	978.59	0.31432	0.458405	55.51864	0.004213	0.201171
160	933.06	0.280861	0.390551	57.58818	0.003393	0.171393
180	902.5	0.25651	0.345007	58.97727	0.002277	0.151406
200	876.69	0.234621	0.306542	60.15045	0.001923	0.134526
220	853.36	0.213696	0.271773	61.21091	0.001738	0.119267
240	832.15	0.193655	0.240164	62.175	0.00158	0.105396
260	813.31	0.174976	0.212086	63.03136	0.001404	0.093074
280	799.48	0.160704	0.191475	63.66	0.001031	0.084029
300	787.89	0.148358	0.174203	64.18682	0.000864	0.076449
320	775.26	0.134484	0.15538	64.76091	0.000941	0.068188
340	764.34	0.122118	0.139106	65.25727	0.000814	0.061046
360	757.51	0.114203	0.128927	65.56773	0.000509	0.056579
380	751.95	0.107653	0.120641	65.82045	0.000414	0.052943

D20: Drying Data for yam slices at 65℃, $1.5\ m/s$ and 1cm

Time (min)	Sample weight (g)	Moisture Content (wb)	Moisture Content (wb)	Weight Loss (%)	Drying Rate (g/min)	Moisture Ratio
0	2200	0.695	2.278689	0.00000	0.00000	1.00000
20	1909.67	0.64863	1.846006	13.19682	0.021634	0.810118
40	1665.53	0.597125	1.482161	24.29409	0.018192	0.650445
60	1443.39	0.535122	1.151103	34.39136	0.016553	0.50516
80	1273.46	0.473089	0.897854	42.11545	0.012662	0.394022
100	1148.72	0.415872	0.711952	47.78545	0.009295	0.31244
120	1045.41	0.358147	0.557988	52.48136	0.007698	0.244872
140	988.87	0.321448	0.473726	55.05136	0.004213	0.207894
160	943.34	0.288698	0.405872	57.12091	0.003393	0.178116
180	912.78	0.264883	0.360328	58.51	0.002277	0.158129
200	886.97	0.243492	0.321863	59.68318	0.001923	0.141249
220	863.64	0.223056	0.287094	60.74364	0.001738	0.125991
240	842.43	0.203495	0.255484	61.70773	0.00158	0.112119
260	823.59	0.185274	0.227407	62.56409	0.001404	0.099797
280	809.76	0.171359	0.206796	63.19273	0.001031	0.090752
300	798.17	0.159327	0.189523	63.71955	0.000864	0.083172
320	785.54	0.145811	0.1707	64.29364	0.000941	0.074912
340	774.62	0.133769	0.154426	64.79	0.000814	0.06777
360	767.79	0.126063	0.144247	65.10045	0.000509	0.063303
380	762.89	0.12045	0.136945	65.32318	0.000365	0.060098
400	759.23	0.11621	0.13149	65.48955	0.000273	0.057704

D21: Drying Data for yam slices at 65℃ , 1 m/s and 1cm

Time (min)	Sample weight (g)	Moisture Content (wb)	Moisture Content (wb)	Weight Loss (%)	Drying Rate (g/min)	Moisture Ratio
0	2200	0.695	2.278689	0.00000	0.00000	1.00000
20	1919.43	0.650417	1.860551	12.75318	0.020907	0.816501
40	1676.29	0.599711	1.498197	23.805	0.018118	0.657482
60	1453.15	0.538245	1.165648	33.94773	0.016627	0.511543
80	1284.22	0.477504	0.91389	41.62636	0.012588	0.40106
100	1159.48	0.421292	0.727988	47.29636	0.009295	0.319477
120	1056.17	0.364686	0.574024	51.99227	0.007698	0.25191
140	997.63	0.327406	0.486781	54.65318	0.004362	0.213623
160	953.81	0.296506	0.421475	56.645	0.003265	0.184964
180	921.54	0.271871	0.373383	58.11182	0.002405	0.163859
200	896.73	0.251726	0.336408	59.23955	0.001849	0.147632
220	873.54	0.231861	0.301848	60.29364	0.001728	0.132466
240	852.69	0.213079	0.270775	61.24136	0.001554	0.118829
260	833.35	0.194816	0.241952	62.12045	0.001441	0.106181
280	819.52	0.181228	0.221341	62.74909	0.001031	0.097135
300	806.93	0.168453	0.202578	63.32136	0.000938	0.088901
320	795.3	0.156293	0.185246	63.85	0.000867	0.081295
340	787.38	0.147807	0.173443	64.21	0.00059	0.076115
360	779.55	0.139247	0.161773	64.56591	0.000583	0.070994
380	772.65	0.13156	0.15149	64.87955	0.000514	0.066481
400	767.54	0.125778	0.143875	65.11182	0.000381	0.063139
420	762.75	0.120288	0.136736	65.32955	0.000357	0.060007
440	757.99	0.114764	0.129642	65.54591	0.000355	0.056893

D22: Drying Data for yam slices at 65℃, 2 m/s and 1.5 cm

Time (min)	Sample weight (g)	Moisture Content (wb)	Moisture Content (wb)	Weight Loss (%)	Drying Rate (g/min)	Moisture Ratio
0	2200	0.695	2.278689	0.00000	0.00000	1.00000
20	1916.32	0.64985	1.855917	12.89455	0.021139	0.814467
40	1675.18	0.599446	1.496542	23.85545	0.017969	0.656756
60	1452.04	0.537892	1.163994	33.99818	0.016627	0.510818
80	1283.11	0.477052	0.912235	41.67682	0.012588	0.400334
100	1159.37	0.421237	0.727824	47.30136	0.009221	0.319405
120	1054.06	0.363414	0.570879	52.08818	0.007847	0.25053
140	997.52	0.327332	0.486617	54.65818	0.004213	0.213551
160	954.47	0.296992	0.422459	56.615	0.003208	0.185396
180	923.43	0.273361	0.3762	58.02591	0.002313	0.165095
200	898.62	0.2533	0.339225	59.15364	0.001849	0.148869
220	875.43	0.23352	0.304665	60.20773	0.001728	0.133702
240	854.58	0.214819	0.273592	61.15545	0.001554	0.120065
260	835.24	0.196638	0.244769	62.03455	0.001441	0.107417
280	821.41	0.183112	0.224158	62.66318	0.001031	0.098371
300	808.82	0.170396	0.205395	63.23545	0.000938	0.090137
320	797.19	0.158294	0.188063	63.76409	0.000867	0.082531
340	789.27	0.149847	0.176259	64.12409	0.00059	0.077351
360	781.44	0.141329	0.16459	64.48	0.000583	0.07223
380	774.54	0.133679	0.154307	64.79364	0.000514	0.067717
400	768.11	0.126427	0.144724	65.08591	0.000479	0.063512
420	762.64	0.120162	0.136572	65.33455	0.000408	0.059935
440	758.88	0.115802	0.130969	65.50545	0.00028	0.057475

D23: Drying Data for yam slices at 65℃, $1.5\ m/s$ and 1.5 cm

Time (min)	Sample weight (g)	Moisture Content (wb)	Moisture Content (wb)	Weight Loss (%)	Drying Rate (g/min)	Moisture Ratio
0	2200	0.695	2.278689	0.00000	0.00000	1.00000
20	1928.83	0.652121	1.87456	12.32591	0.020206	0.822649
40	1685.69	0.601943	1.512206	23.37773	0.018118	0.66363
60	1462.55	0.541212	1.179657	33.52045	0.016627	0.517691
80	1293.62	0.481301	0.927899	41.19909	0.012588	0.407207
100	1168.88	0.425946	0.741997	46.86909	0.009295	0.325625
120	1063.57	0.369106	0.585052	51.65591	0.007847	0.25675
140	1009.03	0.335005	0.50377	54.135	0.004064	0.221079
160	962.5	0.302857	0.434426	56.25	0.003467	0.190647
180	931.94	0.279997	0.388882	57.63909	0.002277	0.170661
200	906.13	0.259488	0.350417	58.81227	0.001923	0.15378
220	882.8	0.239918	0.315648	59.87273	0.001738	0.138522
240	861.59	0.221207	0.284039	60.83682	0.00158	0.12465
260	842.75	0.203797	0.255961	61.69318	0.001404	0.112328
280	828.92	0.190513	0.23535	62.32182	0.001031	0.103283
300	817.33	0.179034	0.218077	62.84864	0.000864	0.095703
320	804.7	0.166149	0.199255	63.42273	0.000941	0.087443
340	793.78	0.154678	0.182981	63.91909	0.000814	0.080301
360	783.95	0.144078	0.168331	64.36591	0.000732	0.073872
380	776.05	0.135365	0.156557	64.725	0.000589	0.068705
400	770.16	0.128752	0.147779	64.99273	0.000439	0.064853
420	765.23	0.123139	0.140432	65.21682	0.000367	0.061629
440	762.54	0.120046	0.136423	65.33909	0.0002	0.059869
460	760.67	0.117883	0.133636	65.42409	0.000139	0.058646

D24: Drying Data for yam slices at 65℃, $1m/s$ and 1.5 cm

Time (min)	Sample weight (g)	Moisture Content (wb)	Moisture Content (wb)	Weight Loss (%)	Drying Rate (g/min)	Moisture Ratio
0	2200	0.695	2.278689	0.00000	0.00000	1.00000
20	1940.18	0.654156	1.891475	11.81	0.019361	0.830072
40	1699.04	0.605071	1.532101	22.77091	0.017969	0.672361
60	1476.9	0.54567	1.201043	32.86818	0.016553	0.527077
80	1304.97	0.485812	0.944814	40.68318	0.012811	0.41463
100	1180.23	0.431467	0.758912	46.35318	0.009295	0.333048
120	1074.92	0.375767	0.601967	51.14	0.007847	0.264173
140	1020.38	0.342402	0.520686	53.61909	0.004064	0.228502
160	973.85	0.310982	0.451341	55.73409	0.003467	0.198071
180	941.29	0.287148	0.402817	57.21409	0.002426	0.176776
200	916.48	0.267851	0.365842	58.34182	0.001849	0.160549
220	893.15	0.248726	0.331073	59.40227	0.001738	0.145291
240	872.94	0.231333	0.300954	60.32091	0.001506	0.132073
260	855.41	0.215581	0.274829	61.11773	0.001306	0.120608
280	840.27	0.201447	0.252265	61.80591	0.001128	0.110706
300	825.68	0.187336	0.230522	62.46909	0.001087	0.101164
320	814.05	0.175726	0.213189	62.99773	0.000867	0.093558
340	804.13	0.165558	0.198405	63.44864	0.000739	0.08707
360	795.23	0.156219	0.185142	63.85318	0.000663	0.081249
380	787.44	0.147872	0.173532	64.20727	0.00058	0.076154
400	780.51	0.140306	0.163204	64.52227	0.000516	0.071622
420	776.58	0.135955	0.157347	64.70091	0.000293	0.069052
440	772.89	0.13183	0.151848	64.86864	0.000275	0.066638
460	768.98	0.127416	0.146021	65.04636	0.000291	0.064081
480	765.34	0.123265	0.140596	65.21182	0.000271	0.0617
500	762.02	0.119446	0.135648	65.36273	0.000247	0.059529

D25: Drying Data for yam slices at 65℃, 2.0 m/s and 2cm

Time (min)	Sample weight (g)	Moisture Content (wb)	Moisture Content (wb)	Weight Loss (%)	Drying Rate (g/min)	Moisture Ratio
0	2200	0.695	2.278689	0.00000	0.00000	1.00000
20	1938.23	0.653808	1.888569	11.89864	0.019506	0.828797
40	1697.31	0.604669	1.529523	22.84955	0.017952	0.67123
60	1474.57	0.544952	1.197571	32.97409	0.016598	0.525553
80	1302.78	0.484948	0.94155	40.78273	0.012801	0.413198
100	1179.43	0.431081	0.75772	46.38955	0.009192	0.332525
120	1073.88	0.375163	0.600417	51.18727	0.007865	0.263492
140	1019.53	0.341854	0.519419	53.65773	0.00405	0.227946
160	972.42	0.309969	0.44921	55.79909	0.00351	0.197135
180	940.73	0.286724	0.401982	57.23955	0.002361	0.176409
200	915.78	0.267291	0.364799	58.37364	0.001859	0.160092
220	892.45	0.248137	0.33003	59.43409	0.001738	0.144833
240	871.89	0.230408	0.299389	60.36864	0.001532	0.131387
260	854.67	0.214902	0.273726	61.15136	0.001283	0.120124
280	839.54	0.200753	0.251177	61.83909	0.001127	0.110229
300	824.78	0.18645	0.22918	62.51	0.0011	0.100576
320	813.23	0.174895	0.211967	63.035	0.000861	0.093022
340	802.35	0.163707	0.195753	63.52955	0.000811	0.085906
360	794.57	0.155518	0.184158	63.88318	0.00058	0.080818
380	786.57	0.146929	0.172235	64.24682	0.000596	0.075585
400	781.38	0.141263	0.164501	64.48273	0.000387	0.072191
420	775.72	0.134997	0.156066	64.74	0.000422	0.068489
440	770.68	0.12934	0.148554	64.96909	0.000376	0.065193
460	766.68	0.124798	0.142593	65.15091	0.000298	0.062577
480	763.24	0.120853	0.137466	65.30727	0.000256	0.060327
500	760.82	0.118057	0.13386	65.41727	0.00018	0.058744

D26: Drying Data for yam slices at 65℃, $1.5\ m/s$ and 2cm

Time (min)	Sample weight (g)	Moisture Content (wb)	Moisture Content (wb)	Weight Loss (%)	Drying Rate (g/min)	Moisture Ratio
0	2200	0.695	2.278689	0.00000	0.00000	1.00000
20	1947.57	0.655468	1.902489	11.47409	0.01881	0.834905
40	1706.65	0.606832	1.543443	22.425	0.017952	0.677338
60	1483.91	0.547816	1.21149	32.54955	0.016598	0.531661
80	1312.12	0.488614	0.955469	40.35818	0.012801	0.419307
100	1188.77	0.435551	0.771639	45.965	0.009192	0.338633
120	1083.22	0.380551	0.614337	50.76273	0.007865	0.269601
140	1028.87	0.347828	0.533338	53.23318	0.00405	0.234055
160	981.76	0.316534	0.46313	55.37455	0.00351	0.203244
180	950.07	0.293736	0.415902	56.815	0.002361	0.182518
200	925.12	0.274689	0.378718	57.94909	0.001859	0.1662
220	901.79	0.255924	0.343949	59.00955	0.001738	0.150942
240	881.23	0.238564	0.313308	59.94409	0.001532	0.137495
260	864.01	0.223389	0.287645	60.72682	0.001283	0.126233
280	848.88	0.209547	0.265097	61.41455	0.001127	0.116337
300	834.12	0.195559	0.2431	62.08545	0.0011	0.106684
320	822.57	0.184264	0.225887	62.61045	0.000861	0.09913
340	811.69	0.17333	0.209672	63.105	0.000811	0.092014
360	803.91	0.165329	0.198077	63.45864	0.00058	0.086926
380	795.91	0.15694	0.186155	63.82227	0.000596	0.081694
400	788.72	0.149254	0.17544	64.14909	0.000536	0.076991
420	782.06	0.14201	0.165514	64.45182	0.000496	0.072636
440	776.02	0.135332	0.156513	64.72636	0.00045	0.068685
460	771.02	0.129724	0.149061	64.95364	0.000373	0.065415
480	766.58	0.124684	0.142444	65.15545	0.000331	0.062511
500	762.87	0.120427	0.136915	65.32409	0.000276	0.060085
520	759.26	0.116245	0.131535	65.48818	0.000269	0.057724

D27: Drying Data for yam slices at 65℃, $1.0\ m/s$ and 2cm

Time (min)	Sample weight (g)	Moisture Content (wb)	Moisture Content (wb)	Weight Loss (%)	Drying Rate (g/min)	Moisture Ratio
0	2200	0.695	2.278689	0.00000	0.00000	1.00000
20	1957.93	0.657291	1.917928	11.00318	0.018038	0.841681
40	1717.01	0.609204	1.558882	21.95409	0.017952	0.684114
60	1494.27	0.550951	1.22693	32.07864	0.016598	0.538437
80	1322.48	0.49262	0.970909	39.88727	0.012801	0.426082
100	1199.13	0.440428	0.787079	45.49409	0.009192	0.345409
120	1093.58	0.386419	0.629776	50.29182	0.007865	0.276377
140	1039.23	0.35433	0.548778	52.76227	0.00405	0.240831
160	992.12	0.323671	0.478569	54.90364	0.00351	0.21002
180	960.43	0.301355	0.431341	56.34409	0.002361	0.189294
200	935.48	0.282721	0.394158	57.47818	0.001859	0.172976
220	912.15	0.264375	0.359389	58.53864	0.001738	0.157717
240	891.59	0.247412	0.328748	59.47318	0.001532	0.144271
260	874.37	0.23259	0.303085	60.25591	0.001283	0.133009
280	859.24	0.219077	0.280537	60.94364	0.001127	0.123113
300	844.48	0.205428	0.258539	61.61455	0.00110	0.11346
320	832.93	0.19441	0.241326	62.13955	0.000861	0.105906
340	822.05	0.183748	0.225112	62.63409	0.000811	0.09879
360	814.27	0.175949	0.213517	62.98773	0.00058	0.093702
380	806.27	0.167773	0.201595	63.35136	0.000596	0.08847
400	799.08	0.160284	0.190879	63.67818	0.000536	0.083767
420	792.42	0.153227	0.180954	63.98091	0.000496	0.079411
440	785.38	0.145637	0.170462	64.30091	0.000525	0.074807
460	779.38	0.139059	0.16152	64.57364	0.000447	0.070883
480	773.94	0.133008	0.153413	64.82091	0.000405	0.067325
500	769.23	0.127699	0.146393	65.035	0.000351	0.064245
520	766.67	0.124786	0.142578	65.15136	0.000191	0.06257
540	764.56	0.122371	0.139434	65.24727	0.000157	0.06119
560	761.52	0.118868	0.134903	65.38545	0.000227	0.059202

D28: Drying Data for yam slices at 75℃ , $2.0\ m/s$ and 1cm

Time (mins)	Sample weight (g)	Moisture Content (wb)	Moisture Content (db)	Weight Loss (%)	Drying Rate (g/min)	Moisture Ratio
0	2200	0.695	2.278689	0.00000	0.00000	1.000000
20	1782.62	0.623588	1.656662	18.97182	0.031101	0.727024
40	1527.78	0.560801	1.27687	30.55545	0.01899	0.560353
60	1317.56	0.490725	0.963577	40.11091	0.015665	0.422865
80	1136.67	0.409679	0.693994	48.33318	0.013479	0.304559
100	998.89	0.328254	0.488659	54.59591	0.010267	0.214447
120	912.67	0.264795	0.360164	58.515	0.006425	0.158058
140	840.15	0.201333	0.252086	61.81136	0.005404	0.110628
160	804.19	0.16562	0.198495	63.44591	0.00268	0.087109
180	774.89	0.134071	0.154829	64.77773	0.002183	0.067946
200	754.44	0.110599	0.124352	65.70727	0.001524	0.054572
220	743.22	0.097172	0.10763	66.21727	0.000836	0.047233
240	738.75	0.091709	0.100969	66.42045	0.000333	0.04431
260	735.89	0.088179	0.096706	66.55045	0.000213	0.04244
280	735.25	0.087385	0.095753	66.57955	4.77E-05	0.042021

D29: Drying Data for yam slices at 75℃, $1.5\ m/s$ and 1cm

Time (mins)	Sample weight (g)	Moisture Content (wb)	Moisture Content (db)	Weight Loss (%)	Drying Rate (g/min)	Moisture Ratio
0	2200	0.695	2.278689	0.00000	0.00000	1.000000
20	1810.91	0.629468	1.698823	17.68591	0.028993	0.745526
40	1563.48	0.570829	1.330075	28.93273	0.018437	0.583702
60	1350.67	0.50321	1.012921	38.60591	0.015858	0.444519
80	1168.45	0.425735	0.741356	46.88864	0.013578	0.325343
100	1019.89	0.342086	0.519955	53.64136	0.01107	0.228182
120	933.87	0.281485	0.391759	57.55136	0.00641	0.171923
140	874.32	0.232546	0.30301	60.25818	0.004437	0.132976
160	835.85	0.197224	0.245678	62.00682	0.002867	0.107816
180	799.39	0.16061	0.191341	63.66409	0.002717	0.08397
200	772.43	0.131313	0.151162	64.88955	0.002009	0.066337
220	754.87	0.111105	0.124993	65.68773	0.001308	0.054853
240	746.75	0.10144	0.112891	66.05682	0.000605	0.049542
260	741.89	0.095553	0.105648	66.27773	0.000362	0.046364
280	738.25	0.091094	0.100224	66.44318	0.000271	0.043983
300	736.67	0.089144	0.097869	66.515	0.000118	0.04295

D30: Drying Data for yam slices at 75℃, 1 m/s and 1cm

Time (mins)	Sample weight (g)	Moisture Content (wb)	Moisture Content (db)	Weight Loss (%)	Drying Rate (g/min)	Moisture Ratio
0	2200	0.695	2.278689	0.00000	0.00000	1.000000
20	1845.43	0.636399	1.750268	16.11682	0.026421	0.768103
40	1582.05	0.575867	1.35775	28.08864	0.019626	0.595847
60	1369.43	0.510015	1.040879	37.75318	0.015844	0.456789
80	1196.86	0.439366	0.783696	45.59727	0.012859	0.343924
100	1075.78	0.376267	0.603249	51.10091	0.009022	0.264735
120	982.23	0.316861	0.46383	55.35318	0.006971	0.203551
140	919.74	0.270446	0.3707	58.19364	0.004656	0.162681
160	876.56	0.234508	0.306349	60.15636	0.003218	0.134441
180	843.42	0.20443	0.25696	61.66273	0.002469	0.112767
200	818.45	0.180158	0.219747	62.79773	0.001861	0.096436
220	796.43	0.15749	0.18693	63.79864	0.001641	0.082034
240	776.12	0.135443	0.156662	64.72182	0.001513	0.068751
260	758.76	0.115662	0.13079	65.51091	0.001294	0.057397
280	746.87	0.101584	0.11307	66.05136	0.000886	0.049621
300	741.76	0.095395	0.105455	66.28364	0.000381	0.046279
320	738.89	0.091881	0.101177	66.41409	0.000214	0.044402
340	737.12	0.0897	0.098539	66.49455	0.000132	0.043244

D31:Drying Data for yam slices at 75℃, 2 m/s and 1.5 cm

Time (mins)	Sample weight (g)	Moisture Content (wb)	Moisture Content (db)	Weight Loss (%)	Drying Rate (g/min)	Moisture Ratio
0	2200	0.69500	2.278689	0.00000	0.00000	1.000000
20	1847.52	0.63681	1.753383	16.02182	0.026265	0.76947
40	1584.11	0.576418	1.36082	27.995	0.019628	0.597194
60	1370.44	0.510376	1.042385	37.70727	0.015922	0.457449
80	1197.79	0.439802	0.785082	45.555	0.012865	0.344532
100	1077.76	0.377412	0.60620	51.01091	0.008944	0.26603
120	985.31	0.318996	0.46842	55.21318	0.006889	0.205566
140	921.67	0.271974	0.373577	58.10591	0.004742	0.163944
160	877.61	0.235423	0.307914	60.10864	0.003283	0.135128
180	847.12	0.207904	0.262474	61.49455	0.002272	0.115186
200	819.46	0.181168	0.221252	62.75182	0.002061	0.097096
220	797.52	0.158642	0.188554	63.74909	0.001635	0.082747
240	778.81	0.138429	0.160671	64.59955	0.001394	0.07051
260	761.69	0.119064	0.135156	65.37773	0.001276	0.059313
280	748.85	0.103959	0.116021	65.96136	0.000957	0.050916
300	742.13	0.095846	0.106006	66.26682	0.000501	0.046521
320	739.34	0.092434	0.101848	66.39364	0.000208	0.044696
340	738.13	0.090946	0.100045	66.44864	9.02E-05	0.043905

D32:Drying Data for yam slices at 75℃, $1.5\ m/s$ and 1.5 cm

Time (mins)	Sample weight (g)	Moisture Content (wb)	Moisture Content (db)	Weight Loss (%)	Drying Rate (g/min)	Moisture Ratio
0	2200	0.69500	2.278689	0.00000	0.00000	1.000000
20	1859.63	0.639176	1.771431	15.47136	0.025363	0.77739
40	1597.32	0.579921	1.380507	27.39455	0.019546	0.605834
60	1395.44	0.519148	1.079642	36.57091	0.015043	0.4738
80	1219.19	0.449635	0.816975	44.58227	0.013133	0.358528
100	1098.54	0.389189	0.637168	50.06636	0.00899	0.279621
120	1005.39	0.332597	0.498346	54.30045	0.006941	0.218698
140	939.24	0.285593	0.399762	57.30727	0.004929	0.175435
160	901.58	0.255751	0.343636	59.01909	0.002806	0.150804
180	867.27	0.226308	0.292504	60.57864	0.002557	0.128365
200	839.46	0.200677	0.251058	61.84273	0.002072	0.110177
220	821.52	0.183221	0.224322	62.65818	0.001337	0.098443
240	805.57	0.167049	0.200551	63.38318	0.001189	0.088012
260	789.69	0.150299	0.176885	64.105	0.001183	0.077626
280	774.85	0.134026	0.154769	64.77955	0.001106	0.06792
300	762.13	0.119573	0.135812	65.35773	0.000948	0.059601
320	753.34	0.1093	0.122712	65.75727	0.000655	0.053852
340	746.97	0.101704	0.113219	66.04682	0.000475	0.049686
360	740.86	0.094296	0.104113	66.32455	0.000455	0.04569

D33: Drying Data for yam slices at 75℃, $1m/s$ and 1.5 cm

Time (mins)	Sample weight (g)	Moisture Content (wb)	Moisture Content (db)	Weight Loss (%)	Drying Rate (g/min)	Moisture Ratio
0	2200	0.69500	2.278689	0.00000	0.00000	1.000000
20	1876.34	0.642389	1.796334	14.71182	0.024118	0.788319
40	1620.76	0.585997	1.41544	26.32909	0.019045	0.621164
60	1417.61	0.526668	1.112683	35.56318	0.015138	0.4883
80	1243.53	0.460407	0.853249	43.47591	0.012972	0.374447
100	1120.64	0.401235	0.670104	49.06182	0.009157	0.294075
120	1029.37	0.348145	0.534083	53.21045	0.006801	0.234382
140	958.41	0.299882	0.428331	56.43591	0.005288	0.187973
160	915.48	0.267051	0.364352	58.38727	0.003199	0.159895
180	887.75	0.244157	0.323025	59.64773	0.002066	0.141759
200	860.46	0.220185	0.282355	60.88818	0.002034	0.123911
220	839.52	0.200734	0.251148	61.8400	0.00156	0.110216
240	822.23	0.183927	0.22538	62.62591	0.001288	0.098908
260	806.69	0.168206	0.202221	63.33227	0.001158	0.088744
280	791.85	0.152617	0.180104	64.00682	0.001106	0.079039
300	778.16	0.137709	0.159702	64.62909	0.00102	0.070085
320	765.12	0.123013	0.140268	65.22182	0.000972	0.061557
340	754.97	0.111223	0.125142	65.68318	0.000756	0.054918
360	747.86	0.102773	0.114545	66.00636	0.00053	0.050268
380	743.42	0.097415	0.107928	66.20818	0.000331	0.047364

D34: Drying Data for yam slices at 75℃ , $2.0\ m/s$ and 2cm

Time (min)	Sample weight (g)	Moisture Content (wb)	Moisture Content (wb)	Weight Loss (%)	Drying Rate (g/min)	Moisture Ratio
0	2200	0.69500	2.278689	0.00000	0.00000	1.000000
20	1885.62	0.644149	1.810164	14.2900	0.023426	0.794388
40	1641.18	0.591148	1.445872	25.40091	0.018215	0.634519
60	1427.39	0.529911	1.127258	35.11864	0.015931	0.494696
80	1257.46	0.466385	0.874009	42.84273	0.012662	0.383558
100	1132.72	0.407621	0.688107	48.51273	0.009295	0.301975
120	1029.41	0.34817	0.534143	53.20864	0.007698	0.234408
140	972.87	0.310288	0.449881	55.77864	0.004213	0.19743
160	927.34	0.276425	0.382027	57.84818	0.003393	0.167652
180	896.78	0.251767	0.336483	59.23727	0.002277	0.147665
200	870.97	0.229595	0.298018	60.41045	0.001923	0.130785
220	847.64	0.20839	0.263249	61.47091	0.001738	0.115526
240	826.43	0.188074	0.231639	62.435	0.00158	0.101655
260	807.59	0.169133	0.203562	63.29136	0.001404	0.089333
280	793.76	0.154656	0.182951	63.9200	0.001031	0.080288
300	781.28	0.141153	0.164352	64.48727	0.00093	0.072126
320	769.54	0.128051	0.146855	65.02091	0.000875	0.064447
340	758.62	0.115499	0.130581	65.51727	0.000814	0.057305
360	751.79	0.107464	0.120402	65.82773	0.000509	0.052838
380	746.23	0.100813	0.112116	66.08045	0.000414	0.049202

D35: Drying Data for yam slices at 75℃ , $1.5\ m/s$ and 2cm

Time (min)	Sample weight (g)	Moisture Content (wb)	Moisture Content (wb)	Weight Loss (%)	Drying Rate (g/min)	Moisture Ratio
0	2200	0.69500	2.278689	0.00000	0.00000	1.000000
20	1910.45	0.648774	1.847168	13.16136	0.021576	0.810628
40	1661.87	0.596238	1.476706	24.46045	0.018523	0.648051
60	1449.31	0.537021	1.159925	34.12227	0.015839	0.509032
80	1273.54	0.473122	0.897973	42.11182	0.013098	0.394075
100	1147.53	0.415266	0.710179	47.83955	0.00939	0.311661
120	1059.32	0.366575	0.578718	51.84909	0.006573	0.25397
140	982.67	0.317166	0.464486	55.33318	0.005712	0.203839
160	942.52	0.288079	0.40465	57.15818	0.002992	0.17758
180	912.56	0.264706	0.36000	58.5200	0.002232	0.157986
200	883.61	0.240615	0.316855	59.83591	0.002157	0.139052
220	856.52	0.216597	0.276483	61.06727	0.002019	0.121334
240	829.78	0.191352	0.236632	62.28273	0.001993	0.103846
260	807.67	0.169215	0.203681	63.28773	0.001648	0.089385
280	792.31	0.153109	0.18079	63.98591	0.001145	0.079339
300	781.63	0.141538	0.164873	64.47136	0.000796	0.072354
320	774.46	0.13359	0.154188	64.79727	0.000534	0.067665
340	767.34	0.125551	0.143577	65.12091	0.000531	0.063009
360	760.86	0.118103	0.13392	65.41545	0.000483	0.05877
285	754.89	0.111129	0.125022	65.68682	-0.00012	0.054866
300	749.65	0.104916	0.117213	65.9250	0.000521	0.051439

D36: Drying Data for yam slices at 75℃ , $1.0\ m/s$ and 2cm

Time (min)	Sample weight (g)	Moisture Content (wb)	Moisture Content (wb)	Weight Loss (%)	Drying Rate (g/min)	Moisture Ratio
0	2200	0.695	2.278689	0.00000	0.00000	1.000000
20	1927.38	0.651859	1.872399	12.39182	0.020314	0.82170046
40	1671.52	0.598569	1.491088	24.02182	0.019066	0.65436233
60	1453.65	0.538403	1.166393	33.9250	0.016235	0.5118705
80	1276.82	0.474476	0.902861	41.96273	0.013177	0.39621975
100	1156.59	0.419846	0.723681	47.42773	0.008959	0.31758666
120	1061.45	0.367846	0.581893	51.75227	0.007089	0.25536298
140	994.76	0.325465	0.482504	54.78364	0.004969	0.21174624
160	948.35	0.292455	0.413338	56.89318	0.003458	0.18139307
180	911.57	0.263907	0.358525	58.5650	0.002741	0.15733813
200	884.41	0.241302	0.318048	59.79955	0.002024	0.13957489
220	859.74	0.219531	0.281282	60.92091	0.001838	0.12344016
240	838.48	0.199742	0.249598	61.88727	0.001584	0.10953564
260	819.67	0.181378	0.221565	62.74227	0.001402	0.09723349
280	802.43	0.16379	0.195872	63.52591	0.001285	0.08595814
300	786.63	0.146994	0.172325	64.24409	0.001177	0.07562459
320	777.86	0.137377	0.159255	64.64273	0.000654	0.06988882
340	771.34	0.130085	0.149538	64.93909	0.000486	0.06562459
360	765.38	0.123311	0.140656	65.2100	0.000444	0.06172662
380	759.59	0.116629	0.132027	65.47318	0.000431	0.05793983
400	754.56	0.11074	0.124531	65.70182	0.000375	0.0546501
420	749.76	0.105047	0.117377	65.9200	0.000358	0.05151079
440	745.86	0.100367	0.111565	66.09727	0.000291	0.0489601

Appendix E: Average drying time for maize grains drying

Air vel (m/s)	Drying air Temperature (℃)			Total drying time (min)	Mean drying time (min))
	50	55	60		
1	515	455	395	1365	455
1.5	485	395	350	1230	410
2	420	340	305	1065	355

Appendix F

F 1: Average total energy consumption for maize grain drying

Air vel (m/s)	Drying air Temperature (℃)			Total Energy Consumption (kW-hr)	Mean Energy Consumption (kW-hr)
	50	55	60		
1	55.49	60.97	62.96	179.42	59.81
1.5	78.36	79.37	83.66	241.39	80.46
2	90.46	91.09	97.19	278.74	92.91

F2: Average total energy consumption for yam drying

Air vel (m/s)	Slice thickness (cm)	Drying air Temperature (℃) 55	65	75	Total Energy Consumption (kW-hr)	Mean Energy Consumption (kW-hr)
	1	77.72	81.01	57.88	216.61	72.20
1	1.5	86.43	89.29	75.25	250.97	83.67
	2	94.47	100.34	84.51	279.32	93.11
	1	109.51	106.30	76.39	292.20	97.40
1.5	1.5	124.58	122.87	100.69	348.14	116.05
	2	133.62	139.44	119.79	392.85	130.95
	1	140.64	127.00	90.28	357.92	119.31
2	1.5	156.71	156.45	115.74	428.9	142.97
	2	172.78	178.54	150.46	501.78	167.26

F3: Average drying time for yam drying

Air vel (m/s)	Slice thickness (cm)	Drying air Temperature (℃)			Total drying time (min)	Mean drying time (min))
		55	65	75		
	1	580	440	250	1270	423.33
1	1.5	645	485	325	1455	485.00
	2	705	545	365	1615	538.33
	1	545	385	220	1150	383.33
1.5	1.5	620	445	290	1355	451.67
	2	665	505	345	1515	505.00
	1	525	345	195	1065	355.00
2	1.5	585	425	250	1260	420.00
	2	645	485	325	1455	485.00

Appendix G

G1: Drying kinetics parameters for maize grains at varying drying air temperature and velocity.

T (℃)	$v\ (m/s)$	d_t (min)	d_A (g_{water}/min)	$D_e\ (m^2/s)$	η_{th} (%)
	1.0	515	0.829	5.77×10^{-11}	5.99
50	1.5	485	0.880	6.38×10^{-11}	4.61
	2.0	420	1.017	7.62×10^{-11}	4.23
	1.0	455	0.939	7.00×10^{-11}	6.90
55	1.5	395	1.081	7.82×10^{-11}	5.75
	2.0	340	1.256	9.67×10^{-11}	5.31
	1.0	395	1.081	8.23×10^{-11}	8.07
60	1.5	350	1.220	1.01×10^{-10}	6.59
	2.0	305	1.400	1.11×10^{-10}	5.99

G2: Drying kinetics parameters for yam slices at varying drying air temperature and velocity.

T (℃)	v (m/s)	d_t (min)	d_A (g_{water}/min)	D_e (m^2/s)	η_{th} (%)	d_t (min)	d_A (g_{water}/min)	D_e (m^2/s)	η_{th} (%)	d_t (min)	d_A (g_{water}/min)	D_e (m^2/s)	η_{th} (%)
		1 cm slice thickness				1.5 cm slice thickness				2 cm slice thickness			
55	1.0	580	2.479	7.27×10^{-10}	18.23	645	2.229	1.44×10^{-9}	16.39	705	2.039	2.23×10^{-9}	14.99
	1.5	545	2.639	7.43×10^{-10}	14.04	620	2.319	1.48×10^{-9}	12.35	665	2.169	2.37×10^{-9}	11.51
	2.0	525	2.739	7.93×10^{-10}	11.58	585	2458	1.56×10^{-9}	10.39	645	2.229	2.57×10^{-9}	9.42
65	1.0	440	3.268	1.01×10^{-9}	24.66	485	2.965	2.05×10^{-9}	22.37	545	2.638	3.03×10^{-9}	19.91
	1.5	385	3.375	1.18×10^{-9}	20.42	445	3.231	2.17×10^{-9}	17.67	505	2.848	3.32×10^{-9}	15.57
	2.0	345	4.168	1.33×10^{-9}	18.12	425	3.384	2.28×10^{-9}	14.69	485	2.965	3.52×10^{-9}	12.88
75	1.0	250	5.752	1.85×10^{-9}	44.95	325	4.425	3.03×10^{-9}	34.58	365	3.939	5.07×10^{-9}	30.79
	1.5	220	6.536	2.27×10^{-9}	36.96	290	4.959	3.42×10^{-9}	28.04	345	4.168	5.20×10^{-9}	23.57
	2.0	195	7.374	2.52×10^{-9}	33.07	250	5.752	4.07×10^{-9}	25.79	325	4.425	5.60×10^{-9}	19.84

Appendix H

H1: Energy parameters for maize grains drying at different drying air temperatures and velocities.

T (℃)	v (m/s)	d_t (min)	Q_r (W)	EPC (W-hr)	SPC (W-hr/kg)	E_{th} (kW-hr)	E_t (kW-hr)	SEC (kW-hr/kg)
50	1.0	515	519.45	91.93	61.29	55.40	55.49	129.95
	1.5	485	717.75	100.15	66.77	78.25	78.36	183.50
	2.0	420	904.19	102.69	68.46	90.35	90.46	211.85
55	1.0	455	511.26	81.22	54.15	60.89	60.97	142.78
	1.5	395	706.17	81.57	54.38	79.29	79.37	185.88
	2.0	340	889.37	83.13	55.42	90.99	91.09	213.30
60	1.0	395	503.11	70.51	47.01	62.89	62.96	147.45
	1.5	350	695.72	72.28	48.19	83.59	83.66	195.93
	2.0	305	877.81	74.57	49.71	97.12	97.19	227.63

H2: Energy parameters for yam slices of 1cm at different drying air temperatures and velocities.

T (℃)	V (m/s)	d_t (min)	Q_r (W)	EPC (W-hr)	SPC (W-hr/kg)	E_{th} (kW-hr)	E_t (kW-hr)	SEC (kW-hr/kg)
	1.0	580	511.26	103.53	47.06	77.62	77.72	54.05
55	1.5	545	706.17	112.54	51.16	109.39	109.51	76.15
	2.0	525	889.37	128.36	58.35	140.51	140.64	97.80
	1.0	440	498.13	78.54	35.70	80.93	81.01	56.34
65	1.5	385	687.39	79.50	36.14	106.22	106.30	73.92
	2.0	345	865.23	84.35	38.34	126.92	127.00	88.32
	1.0	250	480.99	44.63	20.29	57.84	57.88	40.25
75	1.5	220	664.66	45.43	20.65	76.35	76.39	53.12
	2.0	195	838.19	47.68	21.67	90.22	90.28	62.78

H3: Energy parameters for yam slices of 1.5cm at different drying air temperatures and velocities.

T (℃)	v (m/s)	d_t (min)	Q_r (W)	EPC (W-hr)	SPC (W-hr/kg)	E_{th} (kW-hr)	E_t (kW-hr)	SEC (kW-hr/kg)
	1.0	645	511.26	115.13	52.33	86.31	86.43	60.10
55	1.5	620	706.17	128.03	58.19	124.45	124.58	86.63
	2.0	585	889.37	143.03	65.01	156.57	156.71	108.98
	1.0	485	498.13	86.57	39.35	89.21	89.29	62.09
65	1.5	445	687.39	91.89	41.77	122.78	122.87	85.45
	2.0	425	865.23	103.91	47.23	156.35	156.45	108.79
	1.0	325	480.99	58.01	26.37	75.19	75.25	52.33
75	1.5	290	664.66	59.89	27.22	100.64	100.69	70.03
	2.0	250	838.19	61.13	27.79	115.68	115.74	80.49

H4: Energy parameters for yam slices of 2cm at different drying air temperatures and velocities.

T (℃)	v (m/ s)	d_t (min)	Q_r (W)	EPC (W-hr)	SPC (W-hr/kg)	E_{th} (kW-hr)	E_t (kW-hr)	SEC (kW-hr/kg)
	1.0	705	511.26	125.84	57.20	94.34	94.47	65.69
55	1.5	665	706.17	136.91	62.23	133.48	133.62	92.92
	2.0	645	889.37	157.70	71.68	172.63	172.78	120.16
	1.0	545	498.13	97.28	44.22	100.25	100.34	69.78
65	1.5	505	687.39	104.28	47.40	139.33	139.44	96.97
	2.0	485	865.23	118.58	53.90	178.42	178.54	124.16
	1.0	365	480.99	65.15	29.61	84.44	84.51	58.77
75	1.5	345	664.66	71.24	32.38	119.75	119.79	83.31
	2.0	325	838.19	79.46	36.12	150.38	150.46	104.63

H5: Comparative consideration of energy consumption of maize grain and yam slice drying

Temperature (℃)	Velocity (m/s)	Specific energy consumption, SEC (kW-hr/kg)			
		Maize grains	1cm yam slices	1.5cm yam slices	2cm yam slices
	1	142.78	54.05	60.10	65.69
55	1.5	185.88	76.15	86.63	92.92
	2	213.30	97.80	108.98	120.16

Appendix I

I1: Average data of the experimental runs of maize drying for d_t, *SEC and* η_{th}

STD	RUN	Factor 1 A: Temperature	Factor2 B: Velocity	Response1 d_t (min)	Response2 *SEC* (kWh/kg)	Response3 η_{th} (%)
4	1	50	1.5	485	183.50	4.61
5	2	60	1.5	350	195.93	6.59
1	3	50	1	515	129.95	5.99
7	4	55	2	340	213.3	5.31
3	5	60	1	395	147.45	8.07
9	6	55	1.5	395	185.88	5.75
2	7	55	1	455	142.78	6.9
8	8	60	2	305	227.63	5.99
6	9	50	2	420	211.85	4.23

I2: Average data of the experimental runs of yam drying for d_t, *SEC and* η_{th}

STD	RUN	Factor 1 A: Temperature	Factor2 B: Velocity	Factor 3 C: Thickness	Response1 d_t (min)	Response2 *SEC* (kWh/kg)	Response3 η_{th} (%)
2	1	65	1	1	440	56.34	24.66
3	2	75	1	1	250	40.25	44.95
8	3	65	2	1	345	88.32	18.12
16	4	55	2	1.5	585	108.98	10.39
5	5	65	1.5	1	385	73.92	20.42
24	6	75	1.5	2	345	83.31	23.57
9	7	75	2	1	195	62.78	33.07
7	8	55	2	1	525	97.8	11.58
4	9	55	1.5	1	545	76.15	14.04
27	10	75	2	2	325	104.63	19.84
18	11	75	2	1.5	250	80.49	25.79
26	12	65	2	2	485	124.16	12.88
22	13	55	1.5	2	665	92.92	11.51
6	14	75	1.5	1	220	53.12	36.96
11	15	65	1	1.5	485	62.09	22.37
15	16	75	1.5	1.5	290	70.03	28.04
19	17	55	1	2	705	65.69	14.99
17	18	65	2	1.5	425	108.79	14.69
13	19	55	1.5	1.5	620	86.63	12.35
10	20	55	1	1.5	645	60.1	16.39
1	21	55	1	1	580	54.05	18.23
12	22	75	1	1.5	325	52.38	34.58
14	23	65	1.5	1.5	445	85.45	17.67
20	24	65	1	2	545	69.78	19.91
23	25	65	1.5	2	505	96.97	15.52
25	26	55	2	2	645	120.16	9.42
21	27	75	1	2	365	58.77	30.79

Appendix J

J1: Values of Statistical model parameters for the dried maize grains

Model	T (^{0}C)	R^2			SSE			RMSE		
		1.0 m/s	1.5 m/s	2.0 m/s	1.0 m/s	1.5 m/s	2.0 m/s	1.0 m/s	1.5 m/s	2.0 m/s
Newton $MR = \exp(-kt)$	50	0.9912	0.9949	0.9931	0.009885	0.00519	0.006122	0.02281	0.01698	0.02091
	55	0.9874	0.9846	0.9824	0.01422	0.01702	0.01808	0.02811	0.03164	0.03472
	60	0.9826	0.9764	0.9779	0.01947	0.02538	0.02106	0.03385	0.04113	0.04025
Page $MR = \exp(-kt^n)$	50	0.9987	0.9973	0.9954	0.001457	0.00275	0.00403	0.008998	0.01271	0.0176
	55	0.9947	0.9926	0.9913	0.005925	0.008231	0.008871	0.01867	0.02268	0.02517
	60	0.9908	0.9936	0.9938	0.01023	0.00684	0.005421	0.02529	0.0221.	0.02126
Henderson & Pabis $MR = aexp(-kt)$	50	0.9912	0.9956	0.9936	0.009885	0.00453	0.005616	0.02281	0.01632	0.02079
	55	0.990	0.9869	0.9853	0.01129	0.01455	0.015074	0.02577	0.03015	0.032813
	60	0.9847	0.9833	0.9851	0.01708	0.0179	0.01413	0.03267	0.03576	0.03432
Wang & Singh $MR = 1 + at + bt^2$	50	0.9993	0.9968	0.9896	0.000757	0.00324	0.00919	0.006487	0.01381	0.02659
	55	0.9975	0.9964	0.9953	0.002826	0.003963	0.004808	0.01289	0.01574	0.018533
	60	0.9956	0.9991	0.9988	0.004933	0.000995	0.001165	0.01756	0.008432	0.009854
Demir *et al* $MR = a\,exp(-kt)^n + b$	50	0.999	0.9681	0.9936	0.000927	0.03216	0.00563	0.007613	0.04361	0.02263
	55	0.9874	0.9567	0.9853	0.01422	0.04798	0.015076	0.02892	0.05854	0.035444
	60	0.9826	0.9749	0.9851	0.01947	0.02697	0.01415	0.03489	0.04741	0.03761
Weibull $MR = \alpha - bexp(-k_0 t^n)$	50	0.9988	0.9678	0.9502	0.001377	0.03214	0.04397	0.00928	0.05672	0.06322
	55	0.9997	0.9716	0.9986	0.000386	0.03124	0.001419	0.00507	0.0713	0.01088
	60	0.8506	0.928	0.9949	0.1668	0.07739	0.004874	0.1091	0.08031	0.02208
Aghbashlo $MR = exp\left(\frac{k_1 t}{1 + k_2 t}\right)$	50	0.9996	0.9988	0.9974	0.000435	0.001233	0.00227	0.004913	0.008515	0.01321
	55	0.9981	0.9971	0.9964	0.002083	0.003194	0.003463	0.01107	0.01413	0.01573
	60	0.9962	0.9989	0.9977	0.004228	0.001184	0.002211	0.01626	0.009196	0.01357

Peleg $MR = 1 - {}^{t}/_{(a+bt)}$	50	0.9994	0.9997	0.9996	0.000674	0.000229	0.000222	0.006119	0.003676	0.004129
	55	0.9995	0.9986	0.9992	0.000589	0.001564	0.000796	0.005883	0.009887	0.007539
	60	0.9985	0.9764	0.9889	0.001718	0.02538	0.01054	0.01036	0.04113	0.02964
Hii *et al* $MR = a\,exp(-k_1 t^n) + b\,exp(-k_2 t^n)$	50	0.9993	0.9437	0.9831	0.000751	0.05767	0.01487	0.007074	0.06418	0.03856
	55	0.9998	0.8473	0.9959	0.000206	0.1692	0.004132	0.00384	0.1141	0.019380
	60	0.9964	0.9364	0.9988	0.00399	0.06837	0.001166	0.01752	0.09828	0.01138
Verma *et al* $MR = a\,exp(-kt) + (1-a)\exp(-gt)$	50	0.9912	0.9567	0.9931	0.009894	0.01654	0.006122	0.02412	0.04321	0.02091
	55	0.9957	0.9713	0.9824	0.004804	0.0653	0.018079	0.01733	0.03242	0.037293
	60	0.9826	0.9833	0.9779	0.01948	0.0179	0.02106	0.03603	0.03711	0.006623

J2: Results of statistical analysis on the model fitting of moisture ratio versus drying time for 1cm yam slices

Model	Air temp (℃)	R^2			SSE			RMSE		
		1.0 m/s	1.5 m/s	2.0 m/s	1.0 m/s	1.5 m/s	2.0 m/s	1.0 m/s	1.5 m/s	2.0 m/s
Page $MR = \exp(-kt^n)$	55	0.9685	0.9712	0.974	0.03501	0.03056	0.02703	0.03536	0.03429	0.03288
	65	0.9829	0.9863	0.9889	0.01554	0.01172	0.0092	0.02787	0.02551	0.02326
	75	0.9955	0.9956	0.9961	0.003338	0.003018	0.002418	0.01492	0.01524	0.0142
Wang & Singh $MR = 1 + at + bt^2$	55	0.6734	0.7114	0.7295	0.3629	0.3063	0.281	0.1138	0.1085	0.106
	65	0.8231	0.861	0.8757	0.161	0.1191	0.1031	0.08973	0.08136	0.07787
	75	0.8847	0.9213	0.926	0.08528	0.05364	0.04635	0.0754	0.06423	0.06215
Aghbashlo $MR = exp\left(\frac{k_1 t}{1 + k_2 t}\right)$	55	0.9898	0.9904	0.9911	0.01129	0.01024	0.009285	0.02008	0.01984	0.01927
	65	0.9932	0.9941	0.995	0.006198	0.00503	0.004133	0.0176	0.01672	0.01559
	75	0.9978	0.9961	0.9963	0.001603	0.002667	0.002301	0.01034	0.01432	0.01385
Peleg $MR = 1 - {}^{t}/_{(a + bt)}$	55	0.9779	0.978	0.9787	0.02457	0.02331	0.02214	0.02962	0.02994	0.02976
	65	0.9807	0.9825	0.9839	0.01755	0.01497	0.01335	0.02962	0.02884	0.02802
	75	0.9859	0.9812	0.9817	0.01043	0.01282	0.01144	0.02637	0.0314	0.03088
Hii *et al* $MR = a\,exp(-k_1 t^n) + b\,exp(-k_2 t^n)$	55	0.9996	0.940	0.9997	0.000402	0.06366	0.000311	0.004009	0.05261	0.003762
	65	0.9998	0.9936	0.9954	0.000185	0.005468	0.003833	0.003295	0.01909	0.01655
	75	0.9999	0.9997	0.9361	0.000108	0.000188	0.04003	0.002994	0.004334	0.0667
Demir *et al* $MR = a\,exp(-kt)^n + b$	55	0.9946	0.9818	0.9963	0.00596	0.01928	0.00385	0.01514	0.02835	0.01294
	65	0.9983	0.9444	0.9986	0.001539	0.04765	0.001163	0.009246	0.05457	0.008805
	75	0.9996	0.9977	0.9973	0.000301	0.00156	0.001699	0.004814	0.01191	0.01303

J3: Results of statistical analysis on the model fitting of moisture ratio versus drying time for 1.5cm yam slices

Model	Air temp (℃)	R^2			SSE			RMSE		
		1.0 m/s	1.5 m/s	2.0 m/s	1.0 m/s	1.5 m/s	2.0 m/s	1.0 m/s	1.5 m/s	2.0 m/s
Page $MR = \exp(-kt^n)$	55	0.9646	0.9669	0.9687	0.04205	0.03776	0.03494	0.03683	0.03609	0.03532
	65	0.9772	0.9813	0.9825	0.02258	0.01756	0.01577	0.03133	0.02892	0.02808
	75	0.9909	0.9926	0.9953	0.007261	0.005668	0.003442	0.02067	0.01882	0.01515
Wang & Singh $MR = 1 + at + bt^2$	55	0.6265	0.6641	0.6798	0.4435	0.3832	0.3572	0.1196	0.1150	0.1129
	65	0.7696	0.8068	0.819	0.2283	0.1817	0.1635	0.09963	0.09302	0.0904
	75	0.8569	0.8655	0.8852	0.1148	0.1023	0.08498	0.08218	0.07998	0.07527
Aghbashlo $MR = exp\left(\frac{k_1 t}{1 + k_2 t}\right)$	55	0.9891	0.978	0.9899	0.01298	0.012	0.01127	0.02046	0.0294	0.02006
	65	0.9916	0.9928	0.9932	0.008334	0.006787	0.006171	0.01904	0.01798	0.01756
	75	0.9965	0.997	0.9978	0.002843	0.002305	0.001619	0.01293	0.012	0.01039
Peleg $MR = 1 - {}^{t}/_{(a + bt)}$	55	0.978	0.978	0.9781	0.02608	0.02507	0.02445	0.029	0.0294	0.02955
	65	0.9786	0.9805	0.9809	0.02118	0.01834	0.01722	0.03034	0.02955	0.02934
	75	0.9856	0.9857	0.986	0.01154	0.01087	0.01035	0.02605	0.02607	0.02627
Hii *et al* $MR = a\,exp(-k_1 t^n) + b\,exp(-k_2 t^n)$	55	0.9996	0.9996	0.9996	0.000449	0.000436	0.000445	0.004004	0.004093	0.00422
	65	0.9508	0.9785	0.994	0.0488	0.02022	0.005377	0.0494	0.03351	0.01779
	75	0.9939	0.9926	0.9999	0.004896	0.005668	0.000071	0.0187	0.01882	0.002437
Demir *et al* $MR = a\,exp(-kt)^n + b$	55	0.9923	0.9938	0.9946	0.009177	0.007088	0.005988	0.01779	0.0162	0.01518
	65	0.9975	0.9978	0.9981	0.002488	0.002055	0.001705	0.01088	0.0104	0.009733
	75	0.9988	0.9992	0.9996	0.000935	0.000596	0.000295	0.007896	0.006522	0.004764

J4: Results of statistical analysis on the model fitting of moisture ratio versus drying time for 2cm yam slices

Model	Air temp (℃)	R^2			SSE			RMSE		
		1.0 m/s	1.5 m/s	2.0 m/s	1.0 m/s	1.5 m/s	2.0 m/s	1.0 m/s	1.5 m/s	2.0 m/s
Page $MR = \exp(-kt^n)$	55	0.9603	0.9632	0.9651	0.04981	0.04459	0.04146	0.03828	0.03733	0.03657
	65	0.9722	0.9758	0.9777	0.02949	0.02462	0.02209	0.03368	0.03203	0.03099
	75	0.9873	0.990	0.9906	0.01201	0.008759	0.007656	0.02451	0.02206	0.02122
Wang & Singh $MR = 1 + at + bt^2$	55	0.5739	0.6099	0.6248	0.535	0.4727	0.4454	0.1254	0.1215	0.1199
	65	0.7083	0.7494	0.7673	0.3096	0.2548	0.2302	0.1091	0.103	0.1000
	75	0.8367	0.8727	0.8691	0.1542	0.112	0.1072	0.08779	0.07887	0.0794
Aghbashlo $MR = exp\left(\frac{k_1 t}{1 + k_2 t}\right)$	55	0.988	0.9887	0.9892	0.01505	0.01368	0.01279	0.02104	0.02067	0.02031
	65	0.9907	0.9914	0.9918	0.009923	0.008741	0.00807	0.01954	0.01908	0.01873
	75	0.9945	0.9956	0.9961	0.005166	0.003843	0.003208	0.01607	0.01461	0.01374
Peleg $MR = 1 - {t}/{(a + bt)}$	55	0.9779	0.9781	0.9782	0.02774	0.02658	0.02592	0.02856	0.02882	0.02892
	65	0.978	0.9789	0.979	0.02331	0.02145	0.02078	0.02994	0.0299	0.03006
	75	0.9815	0.9842	0.9854	0.01745	0.01389	0.01194	0.02954	0.02778	0.0265
Hii *et al* $MR = a\,exp(-k_1 t^n) + b\,exp(-k_2 t^n)$	55	0.9293	0.9	0.9996	0.08879	0.1211	0.000443	0.05352	0.06463	0.003977
	65	0.9997	0.9925	0.9915	0.000369	0.007598	0.008422	0.004009	0.01902	0.02052
	75	0.9962	0.9064	0.9946	0.003614	0.08233	0.00441	0.01458	0.07409	0.01775
Demir *et al* $MR = a\,exp(-kt)^n + b$	55	0.9893	0.9912	0.9923	0.01342	0.01065	0.009177	0.02048	0.01884	0.01779
	65	0.996	0.9968	0.9974	0.004197	0.003279	0.002549	0.01322	0.01221	0.01102
	75	0.9989	0.9989	0.9987	0.001044	0.000934	0.001088	0.007616	0.007638	0.008516

J5: Values of model constants obtained from the nonlinear regression of some selected thin layer drying models for maize at 50℃

Model	Air vel (m/s)	Model constants and coefficients for the various treatments of maize grains at 50℃								
		k	k_1	k_2	a	b	k_0	n	g	α
Newton $MR = \exp(-kt)$	1.0	0.002753								
	1.5	0.00312								
	2.0	0.005424								
Page $MR = \exp(-kt^n)$	1.0	0.001234						1.138		
	1.5	0.00205						1.074		
	2.0	0.003673						1.073		
Henderson & Pabis $MR = aexp(-kt)$	1.0	0.002753			1					
	1.5	0.00319			1.019					
	2.0	0.005552			1.022					
Wang & Singh $MR = 1 + at + bt^2$	1.0				-0.00226	1.434E-6				
	1.5				-0.0026	1.928E-6				
	2.0				-0.00419	4.745E-6				
Demir *et al* $MR = a\,exp(-kt)^n + b$	1.0	0.05757			1.155	-0.13		0.04024		
	1.5									
	2.0	0.02863			1.022	0.000142		0.1939		
Weibull $MR = \alpha - bexp(-k_0 t^n)$	1.0					-1.97	0.00489	0.7603		-0.9001
	1.5									
	2.0					-0.7319	-1.959	-0.06567		-2.598
Aghbashlo $MR = exp\left(\frac{k_1 t}{1 + k_2 t}\right)$	1.0		-0.00233	-0.00042						
	1.5		-0.00279	-0.00031						
	2.0		-0.00483	-0.00046						
Peleg	1.0				398.9	0.5019				
	1.5				330.8	0.5719				

$MR = 1 - {}^{t}/_{(a+bt)}$	2.0				181.8	0.6378	
Hii *et al*	1.0		2.287	0.000768	-4.082	0.9676	1.212
MR	1.5		-0.2056	-0.1853	-4.789	5.511	0.2986
$= a\ exp(-k_1 t^n)$	2.0		3.235	0.01571	-0.00246	1.177	0.8264
$+ b\ exp(-k_2 t^n)$							
Verma *et al*	1.0	0.002729			0.6681		0.002805
MR	1.5						
$= a\ exp(-kt)$	2.0	0.007265			4.323		0.008008
$+ (1-a)\exp(-gt)$							

J6: Values of model constants obtained from the nonlinear regression of some selected thin layer drying models for maize at 55℃

Model	Air vel (m/s)	Model constants and coefficients for the various treatments of maize grains at 55℃								
		k	k_1	k_2	a	b	k_0	n	g	α
Newton $MR = \exp(-kt)$	1.0	0.003245								
	1.5	0.00375								
	2.0	0.004691								
Page $MR = \exp(-kt^n)$	1.0	0.001475						1.138		
	1.5	0.001663						1.144		
	2.0	0.002023						1.154		
Henderson & Pabis $MR = aexp(-kt)$	1.0	0.00339			1.041					
	1.5	0.003916			1.04					
	2.0	0.00494			1.05					
Wang & Singh $MR = 1 + at + bt^2$	1.0				-0.00258	1.80E-6				
	1.5				-0.00293	2.295E-6				
	2.0				-0.00357	3.341E-6				
Demir *et al* $MR = a\,exp(-kt)^n + b$	1.0	0.05691			1	7.751E-7			0.05701	
	1.5	1.055			0.8893	0.09475			0.00421	
	2.0	0.2152			1.05	1.253E-5			0.02295	
Weibull $MR = \alpha - bexp(-k_0 t^n)$	1.0					-1.492	0.00295	0.9075		-0.4898
	1.5									
	2.0					-5.338	0.00795	0.5505		-4.186
Aghbashlo $MR = exp\left(\frac{k_1 t}{1 + k_2 t}\right)$	1.0		-0.00268	-0.00052						
	1.5		-0.00305	-0.00059						
	2.0		-0.00376	-0.00074						
Peleg	1.0				340.7	0.512				
	1.5				293.7	0.529				

$MR = 1 - {}^{t}/_{(a+bt)}$	2.0			233.3	0.5487		
Hii *et al*	1.0		2.584E-5	0.000386	0.7488	0.1971	1.771
$MR = a\,exp(-k_1 t^n) + b\,exp(-k_2 t^n)$	1.5		-2.689	-0.01884	-0.00102	0.6989	0.1384
	2.0		2.519	0.000484	-271.7	0.8956	1.391
Verma *et al*	1.0	0.005203			-9.024		0.004943
$MR = a\,exp(-kt) + (1-a)\exp(-gt)$	1.5						
	2.0	0.02352			1.70E-5		0.004691

J7: Values of model constants obtained from nonlinear regression of some selected thin layer drying models for maize at 60℃

Model	Air vel (m/s)	Model constants and coefficient for the various treatments of maize grains at 60℃								
		k	k_1	k_2	a	b	k_0	n	g	α
Newton $MR = \exp(-kt)$	1.0	0.003769								
	1.5	0.004373								
	2.0	0.005424								
Page $MR = \exp(-kt^n)$	1.0	0.001637						1.148		
	1.5	0.001254						1.227		
	2.0	0.003673						1.073		
Henderson & Pabis $MR = aexp(-kt)$	1.0	0.003934			1.039					
	1.5	0.004733			1.076					
	2.0	0.00549			1.011					
Wang & Singh $MR = 1 + at + bt^2$	1.0				-0.00292	2.253E-6				
	1.5				-0.00332	2.836E-6				
	2.0				-0.00419	4.745E-6				
Demir *et al* $MR = a\,exp(-kt)^n + b$	1.0	0.2701			1	2.22E-14		0.01395		
	1.5	1.195			1.036	0.0412		0.00429		
	2.0	0.6813			0.9534	0.0673		0.00944		
Weibull $MR = \alpha - bexp(-k_0 t^n)$	1.0					74.51	0.06395	-0.3791		74.28
	1.5					-0.5209	-2.485	-0.03439		-3.747
	2.0					-0.6331	-1.985	-0.178		4.217
Aghbashlo $MR = exp\left(\frac{k_1 t}{1 + k_2 t}\right)$	1.0		-0.00303	-0.00063						
	1.5		-0.00330	-0.00089						
	2.0		-0.00483	-0.00046						

Peleg $MR = 1 - {}^{t}/_{(a+bt)}$	1.0				295	0.5207	
	1.5				227.3	0.5639	
	2.0				181.8	0.6378	
Hii *et al* $MR = a\,exp(-k_1 t^n) + b\,exp(-k_2 t^n)$	1.0		1.782	0.00034	-781.2	0.896	1.402
	1.5		0.2342	0.2448	33.69	-32.25	0.4496
	2.0		0.00602	0.00044	0.193	0.8046	1.421
Verma *et al* $MR = a\,exp(-kt) + (1-a)\exp(-gt)$	1.0	0.003769			1		0.0197
	1.5	0.004734			1.076		1.152
	2.0	0.007265			4.323		0.00801

J8: Values of the model constants obtained from the nonlinear regression of the best three thin layer drying models for 1 cm yam slices at 1 m/s.

Model	Temp ℃	Model constants and coefficients for the various treatments of 1 cm yam slices at 1 m/s					
		k	k_1	k_2	a	b	n
Aghbashlo $MR = exp\left(\frac{k_1 t}{1 + k_2 t}\right)$	55		-0.01215	0.0024			
	65		-0.0129	0.0018			
	75		-0.01423	0.0010			
Hii *et al* $MR = a\,exp(-k_1 t^n) + b\,exp(-k_2 t^n)$	55		0.00512	0.0005	0.7778	0.2319	1.246
	65		0.00048	0.0039	0.2191	0.738	1.317
	75		0.0011	0.0056	0.1799	0.7515	1.241
Demir *et al*: $MR = a\,exp(-kt)^n + b$	55	0.1109			0.9697	0.0806	0.1078
	65	0.0349			0.9809	0.0664	0.3791
	75	0.1897			0.9839	0.0360	0.07601

J9: Values of the model constants obtained from the nonlinear regression of the best three thin layer drying models for 1 cm yam slices at 1.5 m/s.

Model	**Temp ℃**	**Model constants and coefficients for the various treatments of 1 cm yam slices at 1.5 m/s**					
		k	k_1	k_2	a	b	n
Aghbashlo $MR = exp\left(\frac{k_1 t}{1 + k_2 t}\right)$	55		0.00235	0.00235			
	65		-0.01292	0.00164			
	75		-0.0145	0.00042			
Hii *et al* $MR = a\,exp(-k_1 t^n) + b\,exp(-k_2 t^n)$	55		7.872	2.627	14040	43.81	0.1353
	65		0.2823	0.2791	-101.2	102.5	0.4803
	75		0.0003		0.0879	0.781	0.0027
Demir *et al*: $MR = a\,exp(-kt)^n + b$	55	-0.0019			0.9024	0.1075	-6.627
	65	-3.226			0.859	0.1405	-0.0048
	75	0.0818			1.002	0.0239	0.1868

J10: Values of the model constants obtained from the nonlinear regression of the best three thin layer drying models for 1 cm yam slices at 2 m/s.

Model	Temp ℃	Model constants and coefficients for the various treatments of 1cm yam slices at 2 m/s					
		k	k_1	k_2	a	b	n
Aghbashlo $MR = exp\left(\frac{k_1 t}{1 + k_2 t}\right)$	55		-0.01244	0.00225			
	65		-0.01301	0.001476			
	75		-0.01529	-0.01529			
Hii *et al* $MR = a\,exp(-k_1 t^n) + b\,exp(-k_2 t^n)$	55		0.0044	0.00047	0.7606	0.2264	1.28
	65		1.256	0.6596	-14.57	7.935	0.3395
	75		0.0552	0.0558	-3.717	4.694	0.6951
Demir *et al*: $MR = a\,exp(-kt)^n + b$	55	0.1108			0.9741	0.0751	0.1119
	65	0.1164			0.9836	0.0577	0.1159
	75	0.1058			0.9952	0.0178	0.1498

Appendix K

K1: Plot of moisture ratio versus drying time for the modelling of the thin-layer drying of maize grains at 50 ºC and 2 m/s.

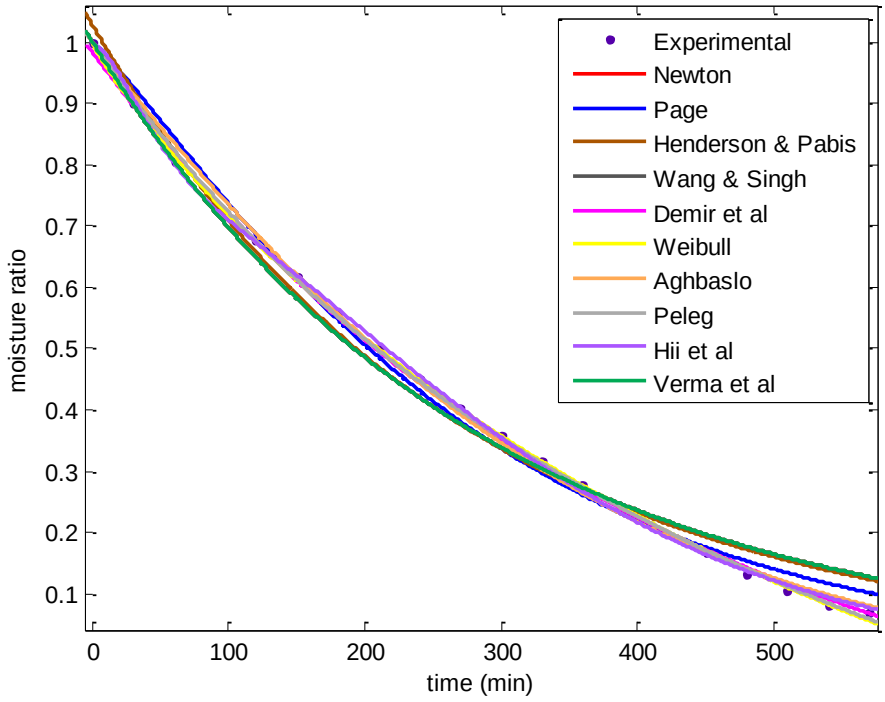

K2: Plot of moisture ratio versus drying time for the modelling of the thin-layer drying of yam slice at 55℃, $1.5\ m/s$ and 1cm

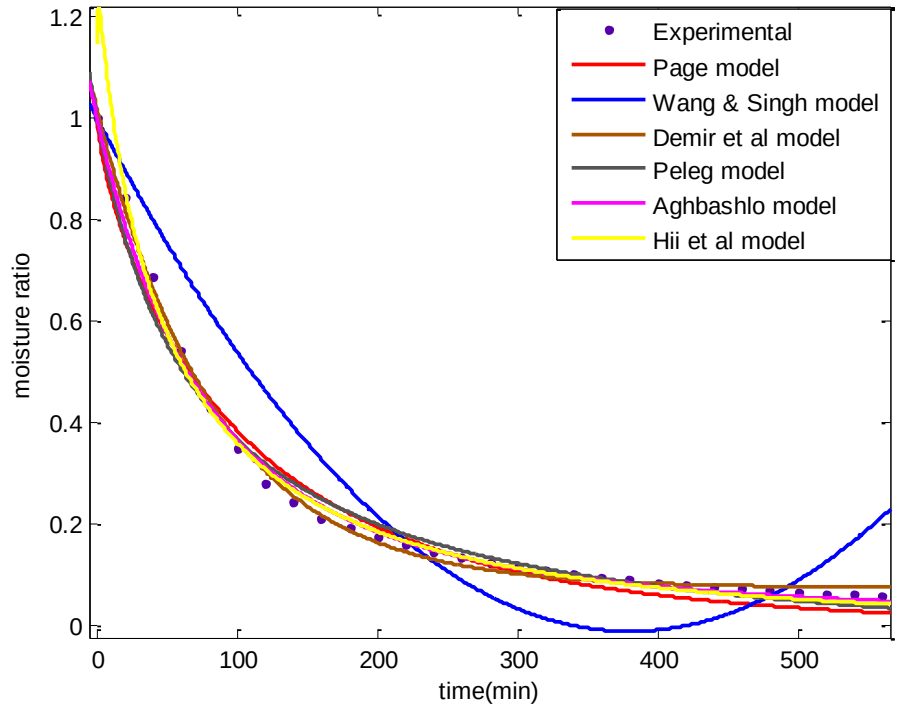

K3: Plot of moisture ratio versus drying time for modelling of the thin-layer drying of yam slices at 65℃, 2 m/s and 1.5 cm.

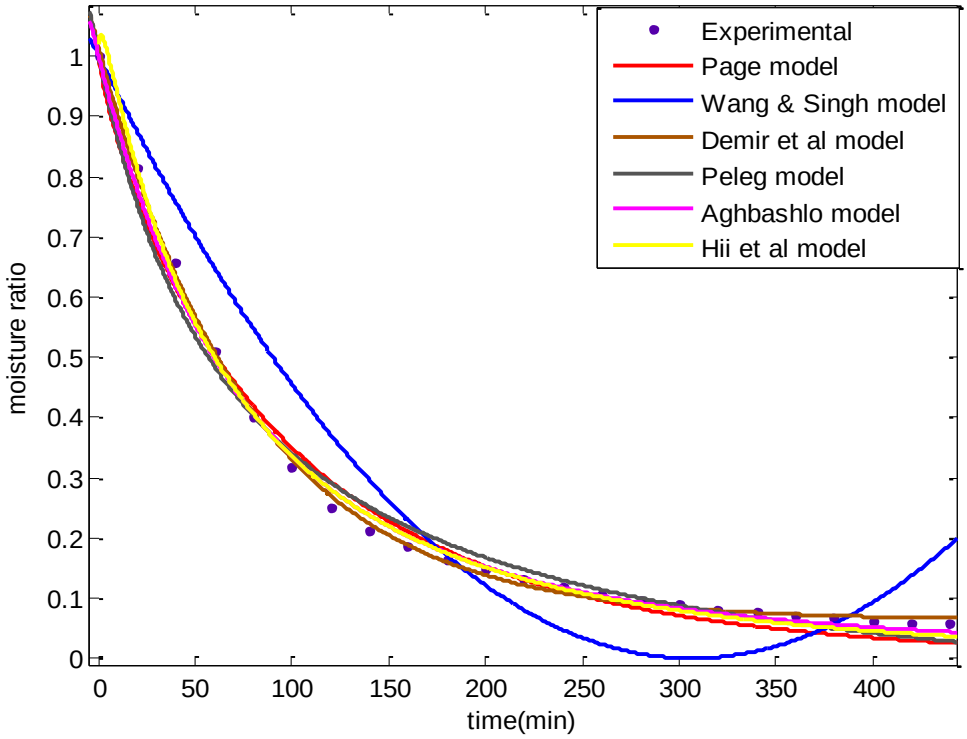

K4: Plot of moisture ratio versus drying time for the modelling of the thin-layer drying of yam slice at 75℃ , 1. 5 m/s and 2cm.

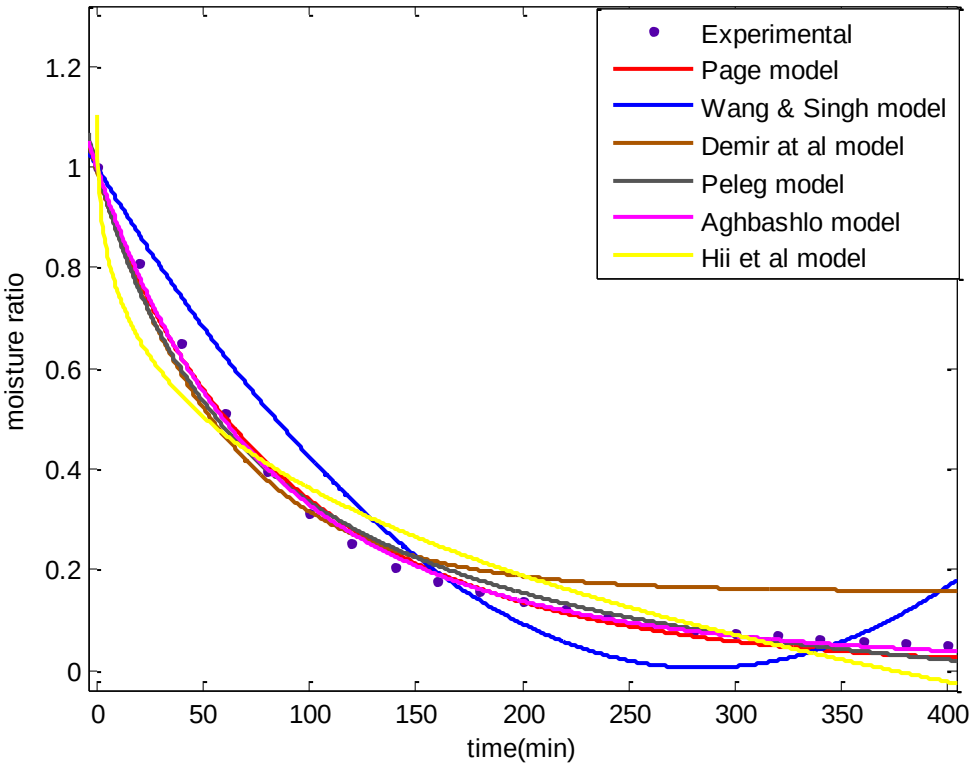

Appendix L

L1: ln MR versus drying time for maize grains at 60°C and 2 m/s

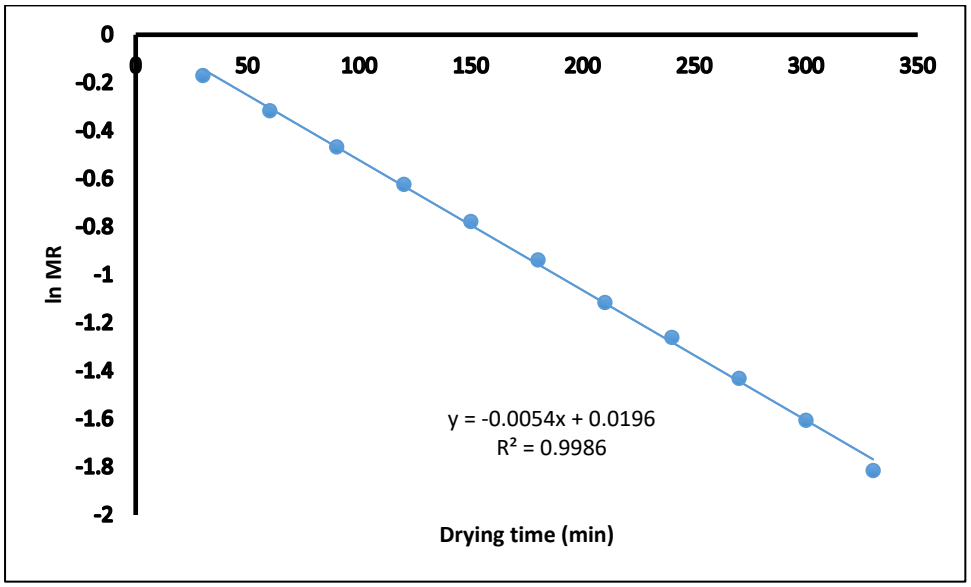

L2: ln MR versus drying time (min) for 2cm yam slices at 75 °C and 1m/s

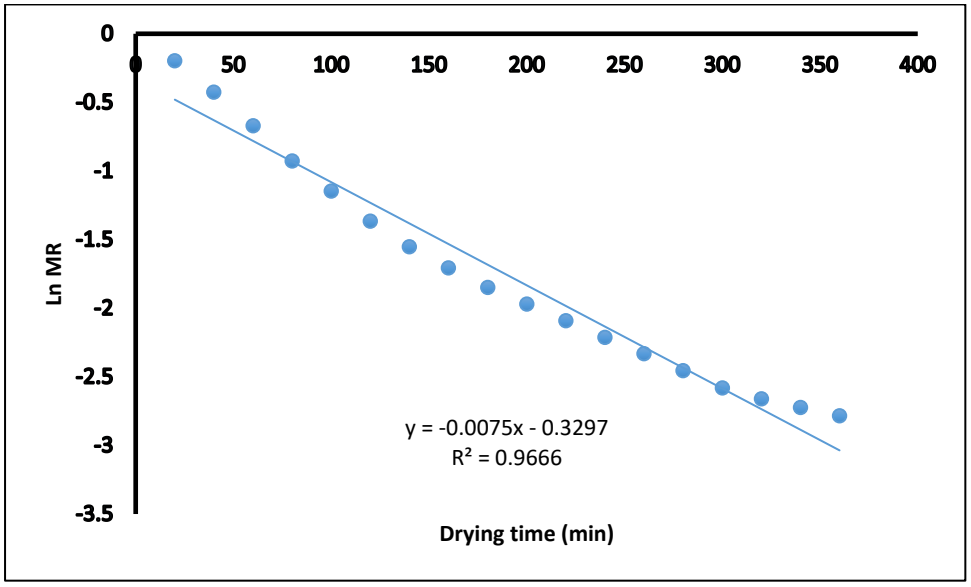

L3: ln D_e versus reciprocal of absolute temperature for corn drying at varying air velocity

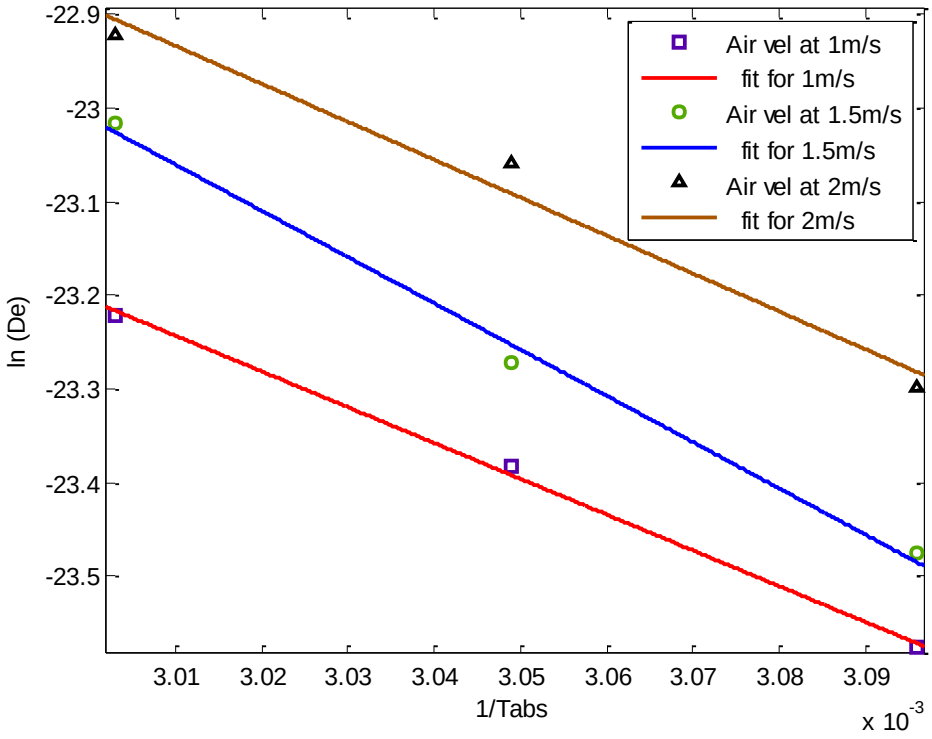

L4: ln D_e versus reciprocal of absolute temperature for 2cm yam slices at varying air velocity

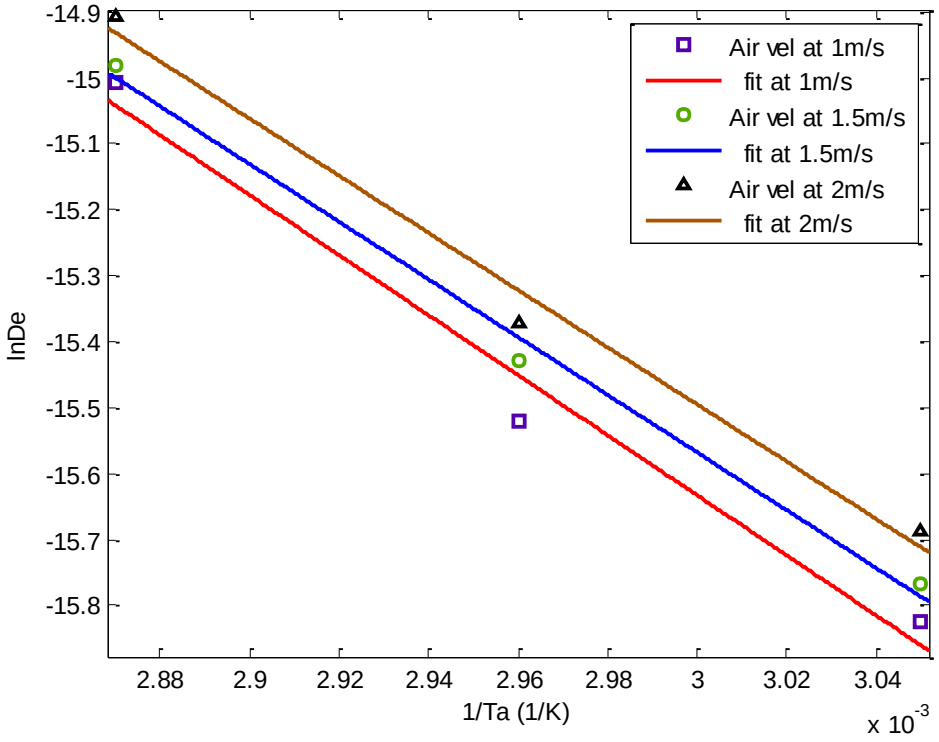

Appendix M

M1: Blanched yam slices in the tray after drying in the hot air tray dryer

M2: Maize grains in the tray after drying in the hot air tray dryer

Appendix N

N1: The experimental and predicted values of drying time for maize drying

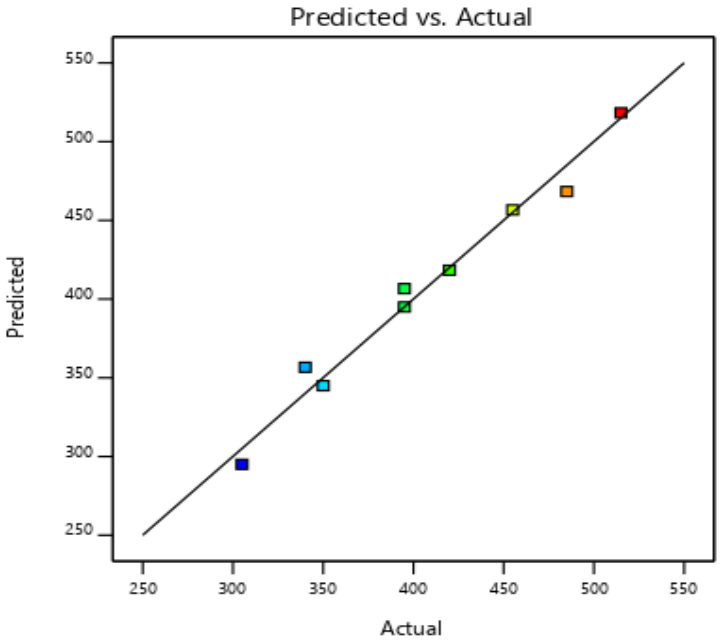

N2: The experimental and predicted values of *SEC* for maize drying

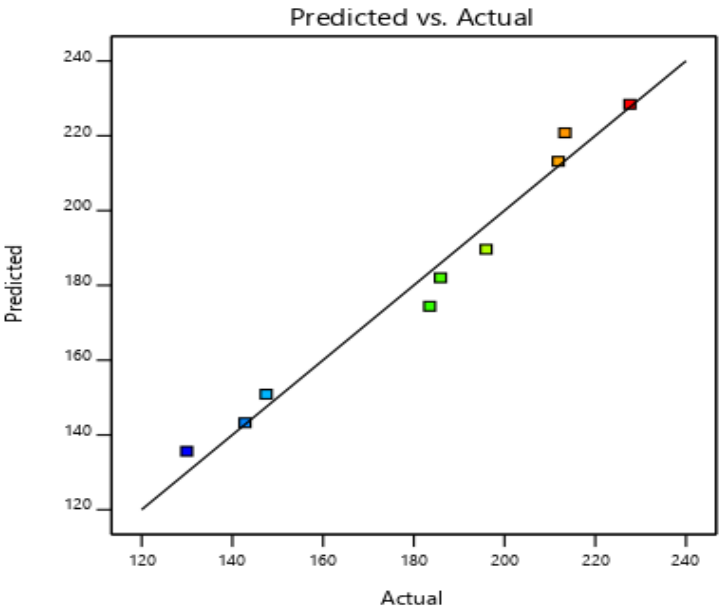

N3: The experimental and predicted values of thermal efficiency for maize drying

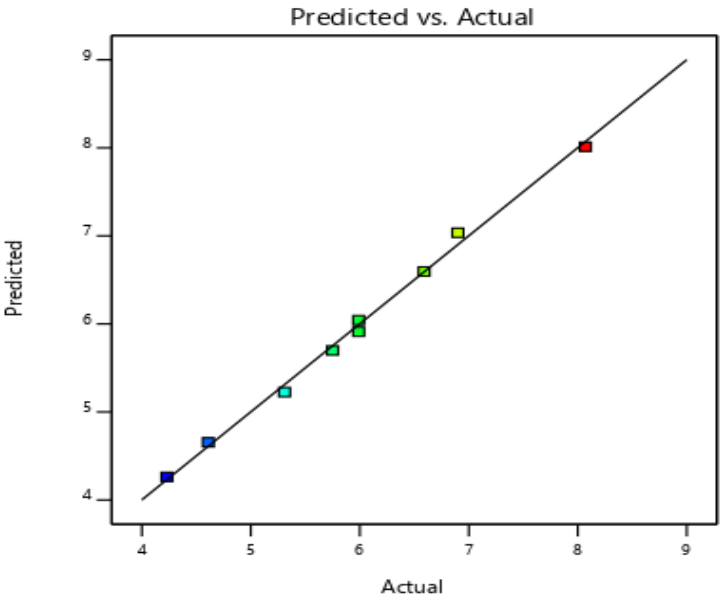

N4: Response surface plot of t (min) at varying air velocity and temperature

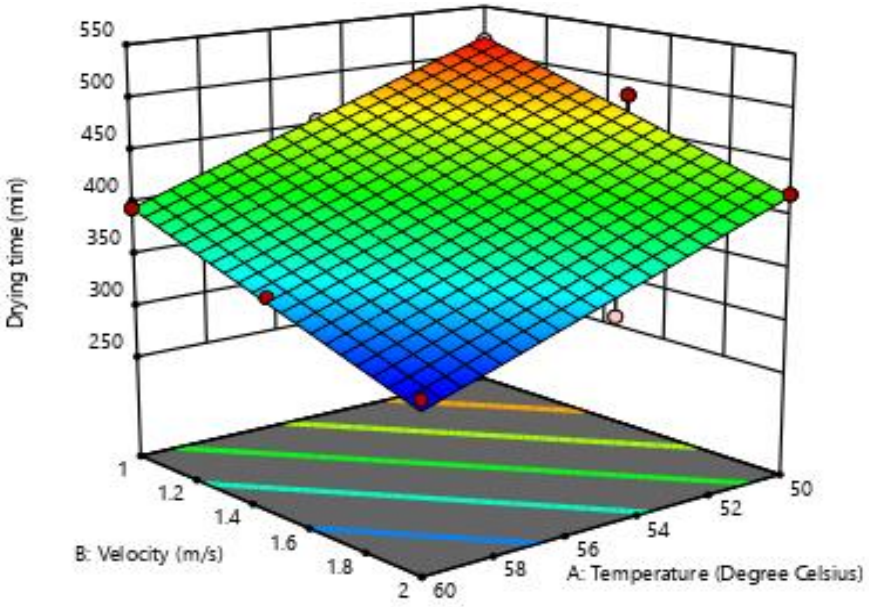

N5: Response surface plot of *SEC* at varying air velocity and temperature

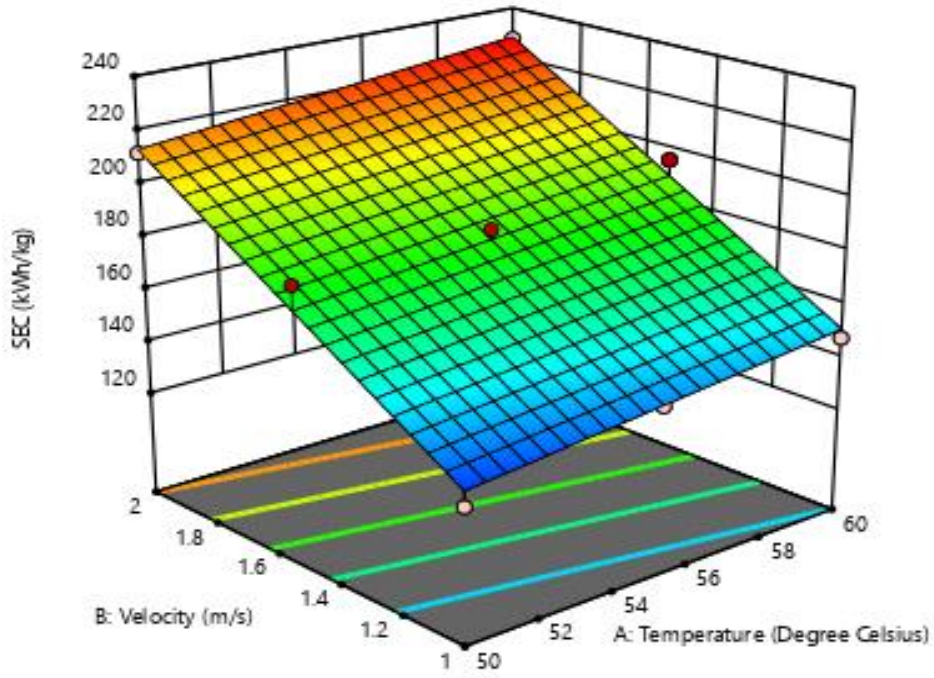

N6: Response surface plot of thermal efficiency at varying air velocity and temperature

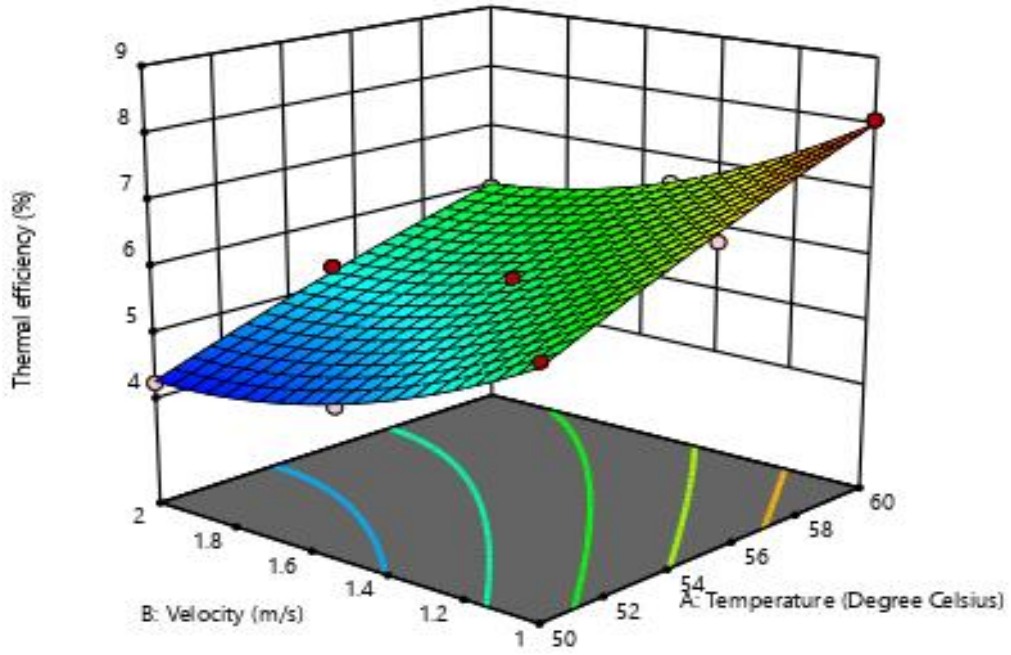

N7: The experimental and predicted values of drying time for yam slices

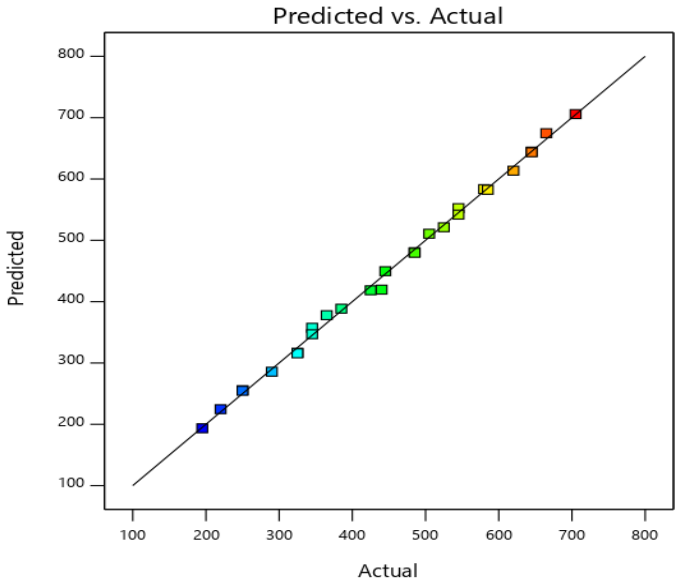

N8: The experimental and predicted values of *SEC* for yam slices

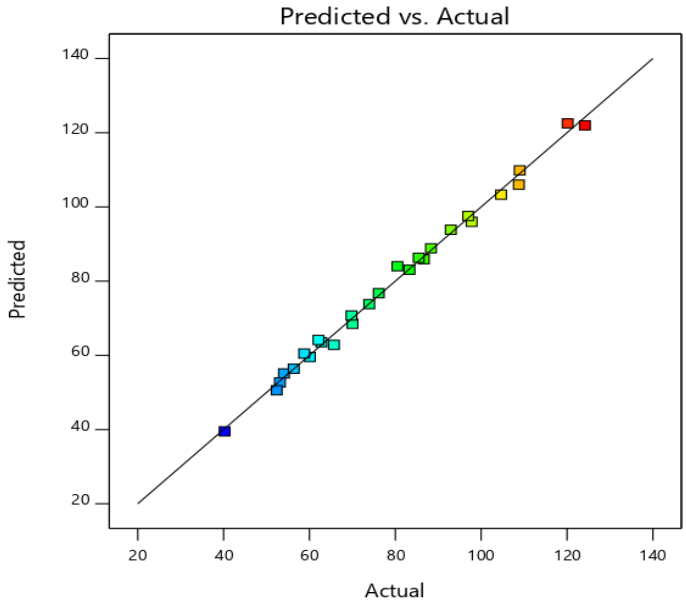

N9: The experimental and predicted values of thermal efficiency for yam slices

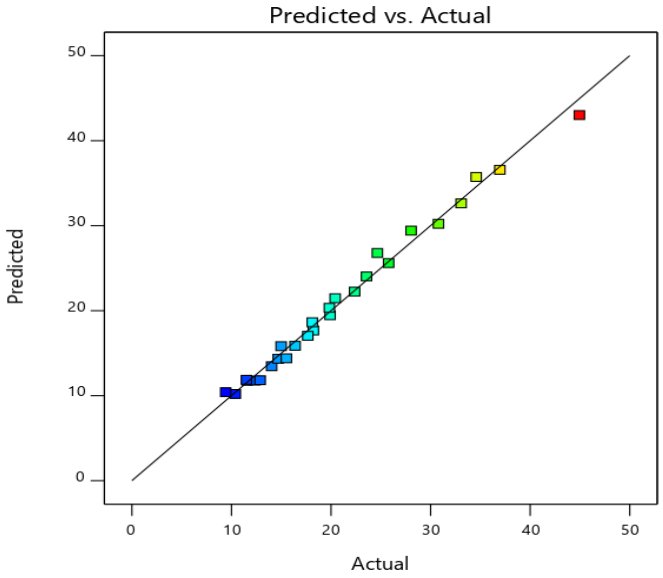

N10: Response surface plot of time (min) at varying air temperature and thickness

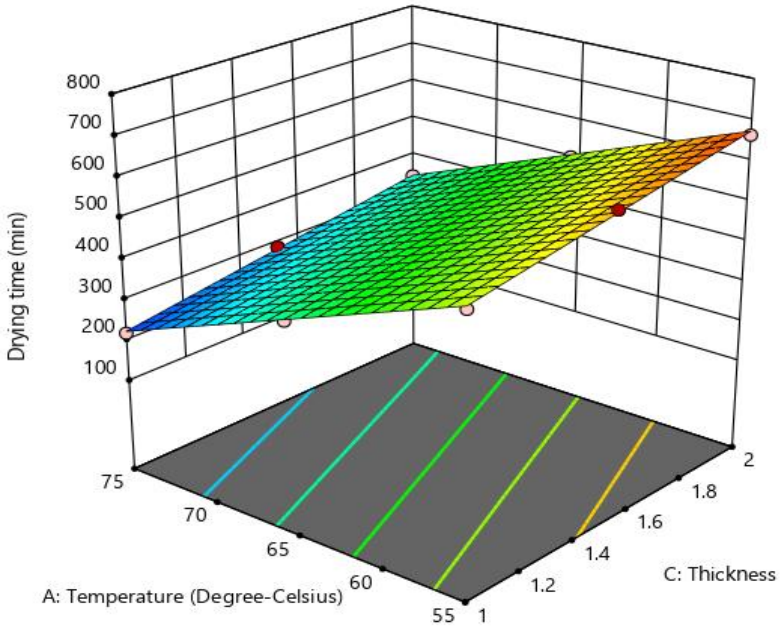

N11: Response surface plot of *SEC* at varying air temperature and thickness

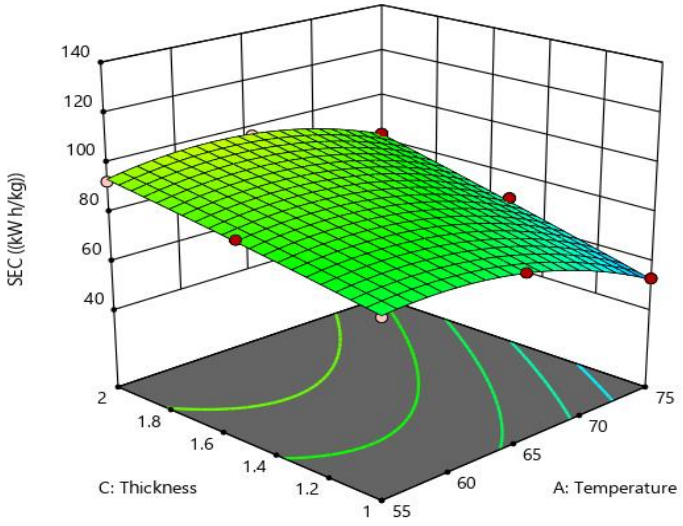

N12: Response surface plot of thermal efficiency at varying air velocity and thickness

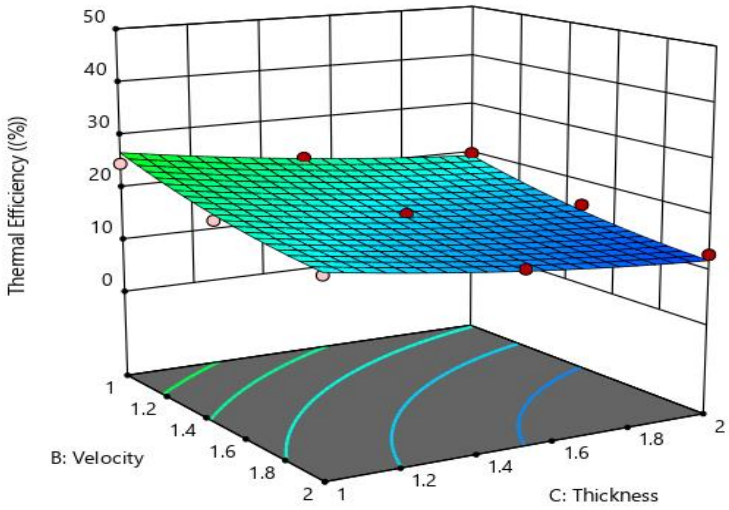

Appendix O

O1: Nusselt number calculation

t_o	t_b	R_{ev1}	R_{ev2}	R_{ev3}	P_{rv1}	C	$(Re_{v1})^{0.8}$	$(Re_{v2})^{0.8}$	$(Re_{v3})^{0.8}$	$(Pr_{v1})^{0.4}$	Nu_{v1}	Nu_{v2}
50	40.5	4.06E+03	6.09E+03	8.13E+03	1.05	0.023	7.71E+02	1.07E+03	1.34E+03	1.01970775	1.81E+01	2.50E+01
55	43	4.02E+03	6.04E+03	8.05E+03	1.04	0.023	7.65E+02	1.06E+03	1.33E+03	1.01581199	1.79E+01	2.47E+01
60	45.5	4.00E+03	6.00E+03	8.00E+03	1.03	0.023	7.61E+02	1.05E+03	1.33E+03	1.0118937	1.77E+01	2.45E+01
65	48	3.96E+03	5.94E+03	7.92E+03	1.03	0.023	7.55E+02	1.04E+03	1.32E+03	1.0118937	1.76E+01	2.43E+01
75	53	3.90E+03	5.85E+03	7.80E+03	1.01	0.023	7.46E+02	1.03E+03	1.30E+03	1.00398806	1.72E+01	2.38E+01

O2: Heat transfer coefficient calculation

Air temp, t_o	t_s	t_b	k W/K	D	Nu_{v1}	Nu_{v2}	Nu_{v3}	h_{v1}	h_{v2}	h_{v3}
50	254.5	40.5	0.02662	0.1	1.81E+01	2.50E+01	3.15E+01	4.82E+00	6.66E+00	8.39E+00
55	254.5	40.5	0.02684	0.1	1.79E+01	2.47E+01	3.11E+01	4.80E+00	6.63E+00	8.35E+00
60	254.5	40.5	0.02699	0.1	1.77E+01	2.45E+01	3.09E+01	4.78E+00	6.61E+00	8.34E+00
65	254.5	40.5	0.02719	0.1	1.76E+01	2.43E+01	3.06E+01	4.79E+00	6.61E+00	8.32E+00
75	254.5	40.5	0.02753	0.1	1.72E+01	2.38E+01	3.00E+01	4.74E+00	6.55E+00	8.26E+00

O3: Heat transfer rate calculation

Air temp, t_o	t_s	t_b	A_{he}	h_{v1}	h_{v2}	h_{v3}	Qr_{v1}	Qr_{v2}	Qr_{v3}
50	254.5	40.5	0.5036	4.82E+00	6.66E+00	8.39E+00	519.45333	717.75086	904.19366
55	254.5	43	0.5036	4.80E+00	6.63E+00	8.35E+00	511.25472	706.17058	889.37019
60	254.5	45.5	0.5036	4.78E+00	6.61E+00	8.34E+00	503.10647	695.71836	877.80502
65	254.5	48	0.5036	4.79E+00	6.61E+00	8.32E+00	498.12839	687.39637	865.22509
75	254.5	53	0.5036	4.74E+00	6.55E+00	8.26E+00	480.9934	664.66387	838.1868